2014 / Volume 52 / Number 3
ISSN 1641-4640

Folia NEUROPATHOLOGICA

www.folianeuro.termedia.pl

Official Journal of Mossakowski Medical Research Centre Polish Academy of Sciences
and
Polish Association of Neuropathologists

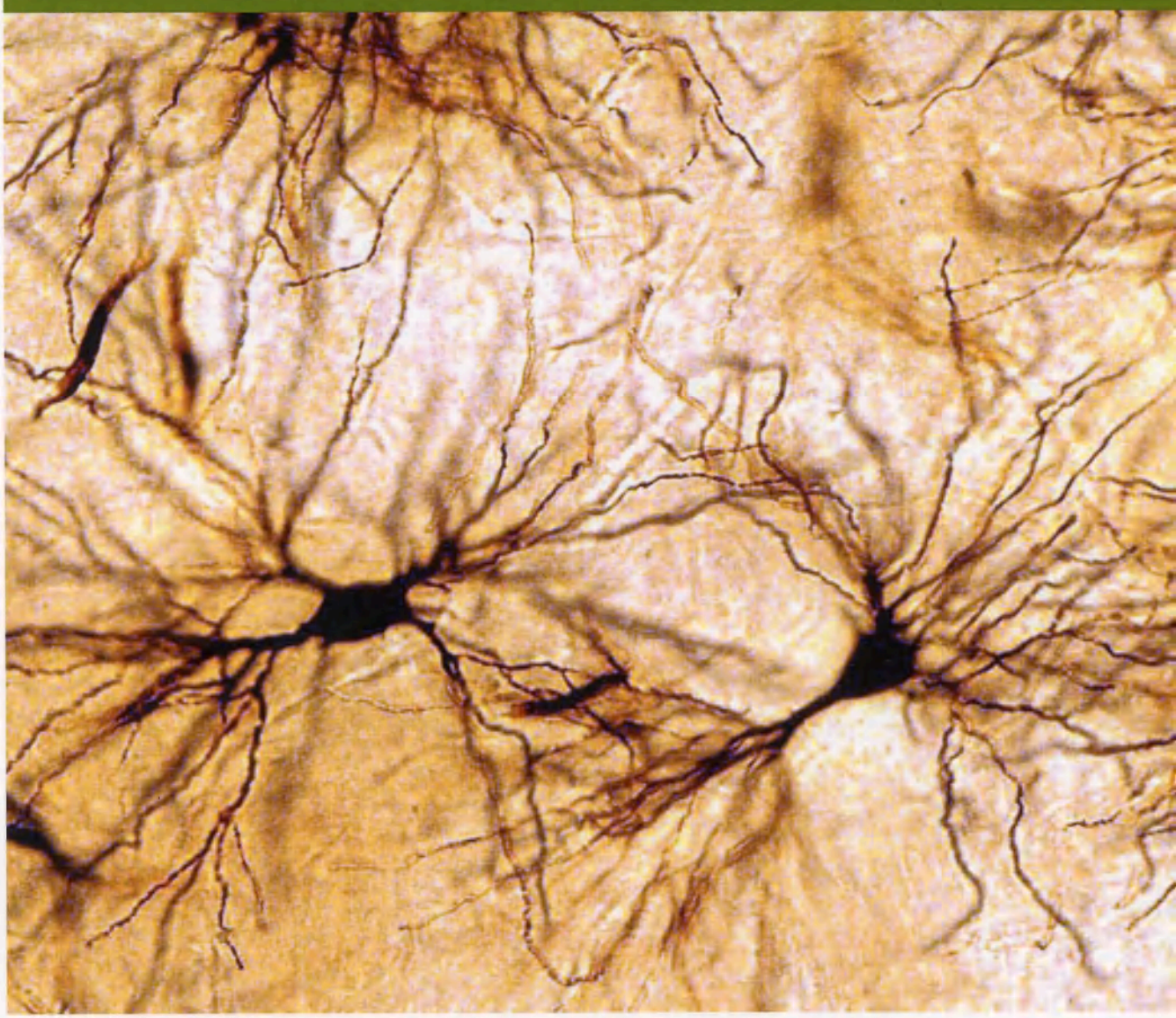

ISSN 1641-4640

Folia Neuropathologica

TERMEDIA Publishing House

Folia
Neuropathologica
former *Neuropatologia Polska*

Official Journal of Mossakowski Medical Research Centre Polish Academy of Sciences and Polish Association of Neuropathologists

The journal is partly financially supported by the Ministry of Science and Higher Education

termedia

Termedia Publishing House
Kleeberga 2, 61-615 Poznan, Poland
phone/fax: +48 61 822 77 81
e-mail: termedia@termedia.pl
www.termedia.pl
www.folianeuro.termedia.pl

Warsaw office
phone/fax: +48 22 827 75 14
e-mail: biuro.warszawa@termedia.pl

president of the management board
editor-in-chief of the Publishing House, director
Janusz Michalak
e-mail: j.michalak@termedia.pl

director of the Publishing House
Andrzej Kordas
e-mail: a.kordas@termedia.pl

Marketing and Advertising Department
Renata Dolata
phone: +48 61 822 77 81 ext. 508
e-mail: r.dolata@termedia.pl

Distribution Subscription Department
Jolanta Jankowiak
phone: +48 61 656 22 00
e-mail: prenumerata@termedia.pl

Impact Factor for Folia Neuropathologica equals 1.667
MNiSW score for Folia Neuropathologica equals 15.00
Index Copernicus score (2011) for Folia Neuropathologica equals 18.13
Position in Index Copernicus ranking systems available at http://www.indexcopernicus.pl

Abstracted and indexed in Index Medicus/MEDLINE, Neuroscience Citation Index, SciSearch, Research Alert, Chemical Abstracts, EMBASE/Excerpta Medica, Polish Medical Bibiography, Index Copernicus

The journal is financially supported by the Ministry of Sciences and Higher Education.

Print run: 450 copies

Folia
Neuropathologica
2014: 52/3: 211-376

Contents

Review paper

Folia Neuropathologica

A critical analysis of the 'amyloid cascade hypothesis'

Richard A. Armstrong

Vision Sciences, Aston University, Birmingham, UK

Folia Neuropathol 2014; 52 (3): 211-225 DOI: 10.5114/fn.2014.45562

Abstract

The 'amyloid cascade hypothesis' (ACH) is the most influential model of the pathogenesis of Alzheimer's disease (AD). The hypothesis proposes that the deposition of β-amyloid (Aβ) is the initial pathological event in AD, leading to the formation of extracellular senile plaques (SP), tau-immunoreactive neurofibrillary tangles (NFT), neuronal loss, and ultimately, clinical dementia. Ever since the formulation of the ACH, however, there have been questions regarding whether it completely describes AD pathogenesis. This review critically examines various aspects of the ACH including its origin and development, the role of amyloid precursor protein (APP), whether SP and NFT are related to the development of clinical dementia, whether Aβ and tau are 'reactive' proteins, and whether there is a pathogenic relationship between SP and NFT. The results of transgenic experiments and treatments for AD designed on the basis of the ACH are also reviewed. It was concluded: (1) Aβ and tau could be the products rather than the cause of neurodegeneration in AD, (2) it is doubtful whether there is a direct causal link between Aβ and tau, and (3) SP and NFT may not be directly related to the development of dementia, (4) transgenic models involving APP alone do not completely replicate AD pathology, and (5) treatments based on the ACH have been unsuccessful. Hence, a modification of the ACH is proposed which may provide a more complete explanation of the pathogenesis of AD.

Key words: *Alzheimer's disease, amyloid cascade hypothesis, β-amyloid, neurofibrillary tangles, disease pathogenesis.*

Introduction

The 'amyloid cascade hypothesis' (ACH) [57] is the most influential model of the pathology of Alzheimer's disease (AD) proposed over the last 25 years. As a result, numerous studies of AD pathogenesis have been carried out [6,8] and potential treatments proposed and tested based on the ACH [69,113].

It was the discovery of β-amyloid (Aβ), the most important molecular constituent of senile plaques (SP) [49], and mutations of the amyloid precursor protein (APP) gene linked to early-onset familial AD (FAD) [27,50], which led to the original formulation of the hypothesis [57]. The ACH proposed first, a direct relationship between the development of Aβ, in the form of senile plaques (SP), and neurofibrillary tangles (NFT) and second, between these lesions and clinical dementia. Hence, deposition of Aβ is the initial pathological event in AD, leading to the formation of SP, tau-immunoreactive NFT, neuronal loss, and ultimately clinical dementia. The ACH is often regarded as the 'conclusive model' of the aetiology of early-onset FAD, and sporadic AD (SAD), a more complex disorder caused by a variety of factors, but resulting from essentially the same pathological cascade [42,127].

Communicating author:

Dr Richard A. Armstrong, Vision Sciences, Aston University, Birmingham B4 7ET, UK, phone: 0121-204-4102, fax: 0121-204-4048, e-mail: R.A.Armstrong@aston.ac.uk

Since its publication there have been observations difficult to reconcile with the ACH and concerns whether it completely describes AD pathogenesis [11,90]. First, transgenic mice, in which genes overexpress amyloid precursor protein (APP), do not reproduce the predicted cascade [39,90]. Second, SP and NFT are separated in brain both spatially [11] and temporally [39,82] questioning the pathogenic link between them. Third, Aβ and tau could be the reactive products of neurodegeneration rather than their cause, arising as a consequence of oxidative stress [126]. Fourth, study of various neuronal injury biomarkers does not support a central pathological role for Aβ, especially in late-onset SAD [28]. These observations suggest a more complex relationship between Aβ, tau, and AD pathogenesis than suggested by the ACH. In addition, concentration on the ACH may have been to the detriment to the study of other possible aetiologies including: (1) perturbation of vesicular trafficking, (2) disruption of the cytoskeletal network, and (3) disturbance of membrane cholesterol [37]. These views are supported by a critique of the ACH by Teplow [133] who argues that 'insufficient rigour' has been applied to studies of Aβ in AD based on the ACH and 'confusion not clarity' has been the result.

This review critically examines various aspects of the ACH including its origin and development, the role of amyloid precursor protein (APP), whether SP and NFT are related to the development of clinical dementia, whether Aβ and tau are 'reactive' peptides, and whether there is a pathogenic relationship between SP and NFT. The results of transgenic experiments and treatments for AD designed on the basis of the ACH are also reviewed. Finally, a modified scheme based on the ACH is proposed which may provide a more complete description of the pathogenesis of all forms of AD.

Key observations in the development of the amyloid cascade hypothesis

The original formulation of the ACH as proposed by Hardy and Higgins [57] is shown in Figure 1. A number of key observations resulted in the formulation and subsequent development of the hypothesis:

1. Aβ was discovered as the most important molecular constituent of SP [49], emphasising the importance of amyloid peptides in AD.

2. Altered proteolytic processing of APP and its accumulation were shown to be early events in AD and were followed by microglial activation, astrocytosis, and dystrophic neurites (DN) [105].

3. Mutations of *APP* gene [27,50] were linked to early-onset FAD, the presence of point mutations in *APP* evidence that amyloid deposition was the causative factor [56]. Three main groups of APP mutations have been identified, i.e., those which act at: (a) the beta APP cleaving enzyme 1 (βACE1) site, (b) the gamma APP cleaving enzyme site, and (c) the mid-domain of the Aβ region.

4. Formation of Aβ peptides was directly linked to APP processing with two events being necessary to generate Aβ [116]: (a) cleavage by βACE1 which cleaves APP on the amino side of Aβ resulting in a large secreted derivative and an Aβ membrane-associated C-terminal derivative (CTFβ) and (b) cleavage by γ-secretase which cleaves CTFβ to release the Aβ peptide [63]. A variety of Aβ peptides can be formed as a result of cleavage of APP [54], the most common being $Aβ_{42}$ [131], found largely in discrete Aβ deposits [139], and the more soluble $Aβ_{40}$, also found in association with blood vessels [86], and which may develop later in the disease [35]. In addition, $Aβ_{43}$ may be formed and has a particularly potent amyloidogenicity [115]. Mutations of *APP* within the Aβ coding region can also result in the deposition of $Aβ_{38}$ in vessel walls, especially in those

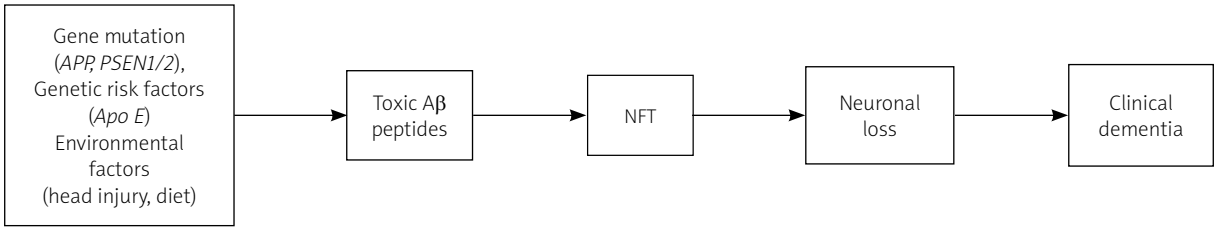

Aβ – β-amyloid, Apo E – apolipoprotein E, APP – amyloid precursor protein, PSEN1/2 – presenilin genes 1 and 2, NFT – neurofibrillary tangles

Fig. 1. The amyloid cascade hypothesis (ACH) in its original form.

cases with extensive cerebral amyloid angiopathy (CAA) [88]. Early toxic soluble oligomers could also be involved, which vary with a type of mutant, thus providing a genetic basis for variations in pathogenesis observed among FAD cases [46,48].

5. Subsequently, the most common form of early-onset FAD was linked to mutations of *presenilin* (*PSEN)* genes *PSEN1* [123] and *PSEN2* [78]. Full length PSEN protein is composed of nine trans-membrane domains located on the endoplasmic reticulum membrane. Endoproteolytic cleavage of PSEN and assembly into γ-secretase complex is followed by transport to the cell surface, thus potentially influencing APP processing [61]. Hence, mutant *PSEN1* could enhance 42-specific-γ-secretase cleavage of normal APP resulting in increased deposition of amyloid-forming species [129]. Alternatively, deficiency of PSEN1 may inhibit the normal cleavage of APP [34,141]. *PSEN1* also appears to alter the ratio of Aβ species, the ratio of $A\beta_{40/42}$ being lower and the ratio of $A\beta_{42/40}$ higher in *PSEN1* cases compared with SAD [60].

6. Studies of FAD cases caused by APP_{717} (valine–isoleucine) mutation showed them to have significant numbers of tau-immunoreactive NFT supporting a link between APP and degeneration of the cytoskeleton [75].

7. Early experiments using transgenic mice expressing high levels of APP resulted in Aβ deposition, synaptic loss, and gliosis [44].

8. In Down's syndrome (DS), which replicates many of the features of AD pathology [5,9], water soluble peptides ending in residue 42 precede the formation of SP and also increase with age [114].

9. Aβ peptides are toxic and can induce cell death depending on cell type [55], Aβ toxicity being mediated by the necrotic rather than the apoptotic pathway [20,76].

10. Aβ may induce the phosphorylation of tau by: (a) directly interacting with a domain of APP (714-723) [47,125], (b) by inducing tau protein kinase I and subsequently, tau proteins recognised by the antibody Alz-50 [132], (c) as a result of synergisms between Aβ and tau [100,101], or (d) by directly altering the phosphorylated state of tau [23].

11. Senile plaques and NFT acquire several 'secondary' constituents (Table I) which may be involved in the maturation of Aβ deposits into SP [7] including silicon and aluminium [82], acute-phase proteins such as α-antichymotrypsin and α_2-macroglobulin [40,81,136] and their mediator interleukin-6 (IL-6) [122], intercellular adhesion molecules such as cell adhesion molecule 1 (CAM1) [40], apolipoprotein E (Apo E) which is present in the earliest stages of SP formation [145], apolipoprotein D (Apo D) [36], the heterodimeric glycoprotein clusterin, vibronectin, the complement proteins C1q, C_4, and C_3 [137], blood proteins such as amyloid-P (especially in classic 'cored' SP) [67,68], cathepsins B/D [124], and the

Table I. Molecular composition of senile plaques (SP) and neurofibrillary tangles (NFT) in Alzheimer's disease (AD) (From: Armstrong [7])

Pathology	Molecular composition
Diffuse SP	APP (lacking C terminus), Aβ oligomers, especially $A\beta_{42/43}$, apolipoprotein E, α_1-antichymotrypsin, HSPG, complement proteins (C1q, C_3, C_4), amyloid-P, may contain neuronal and astrocytic markers
Primitive SP	APP (N & C-terminal), $A\beta_{42/43}$, free ubiquitin, conjugated ubiquitin, PHF-antigen, phosphorylated tau, chromogranin-A, bFGF, apolipoprotein E, interleukin-6, acetylcholinesterase, cholinergic, somatostatin, GABA, neuropeptide-Y, parvalbumin, and catecholamine immunoreactive neurites
Classic SP	$A\beta_{42/43}$ ('core'), a-synuclein ('ring'), $A\beta_{40}$, actin, tubulin, phosphorylated tau, NF-protein, CAM, chromogranin-A ('ring'), α_2-macroglobulin, complement proteins ('core'), immunoglobulins ('core'), amyloid-P, α_1-antichymotrypsin, antitrypsin, antithrombin III, apolipoprotein E and D ('core'), DOPPEL, bFGF, PrP, may contain acetylcholinesterase, cholinergic, somatostatin, GABA, neuropeptide-Y, parvalbumin, and catecholamine + neurites ('ring'), silicon/aluminium ('core'), interleukin-6 ('ring')
Intracellular NFT	Phosphorylated 3R/4R tau (C & N terminal), ubiquitin (C & N termini), MAP, NF-protein, apolipoprotein E, synaptophysin, bFGF, HSPG
Extracellular NFT	Degraded tau (lacking N/C termini), GFAP, Aβ, ubiquitin (lacking N-terminus), amyloid-P, Apo E

Aβ – β-amyloid, APP – amyloid precursor protein, bFGF – basic fibroblast growth factor, CAM – cell adhesion molecule, GFAP – glial fibrillary acidic protein, HSPG – heparan sulfate proteoglycan, MAP – microtubule associated proteins, NF-protein – neurofilament protein, PHF – paired helical filament, PrP – prion protein

sulphated glycosaminoglycans such as heparan sulphate proteoglycan (HSPG). Many of these proteins may act as molecular 'chaperones' enhancing Aβ aggregation, ultimately forming a growing SP [7]. In addition, the molecular composition of NFT varies markedly depending on whether they are intracellular NFT (I-NFT) or extracellular NFT (E-NFT). Unlike I-NFT, E-NFT are immunoreactive for glial fibrillary acidic protein (GFAP) and Aβ [144], and also contain significant amounts of amyloid-P [104] and ubiquitin [17]; these proteins likely to have been acquired after degeneration of NFT-containing neurons.

These observations suggest that in early-onset FAD, Aβ within SP is the residue of the effects of a pathogenic gene mutation which, via the accumulation of toxic and insoluble Aβ oligomers, leads to the formation of NFT, cell death, and dementia. Since the pathological phenotype of FAD is similar, apart from age of onset, to that of the more common SAD [13,59,97], similar mechanisms, via additional genetic risk factors and/or environmental factors, are assumed to be involved in the pathogenesis of all types of AD [128]. A more fully developed version of the ACH incorporating these various features is shown in Figure 2.

Problems and limitations of the amyloid cascade hypothesis

Formation, structure and function of amyloid precursor protein

There are a number of questions regarding APP and Aβ which have implications for the ACH. First, little is known of the normal functioning of APP [37], which remains a 'current enigma' [93]. Amyloid precursor protein has been implicated in various brain functions including development, learning, memory, and synaptic plasticity, and it may also be secreted as a neuroprotectant [62,93]. Second, the detailed structure of APP does not appear to explain how aggregated peptides such as Aβ are formed [73]. One possibility is that excess APP overwhelms the normal degradation pathway leading to the formation of Aβ, as in DS. Third, some mutations of APP, e.g., amino acid changes at codon 717, appear to shed little light on its mechanism of action in AD [91]. Hence, amino acid substitutions at codon 717 in APP_{717} cases are not incorporated into amyloid deposits and hence, mutant Aβ may have additional metabolic effects which determine pathogenesis [79]. Fourth, secretion of Aβ requires cleavage at both the N and C-ter-

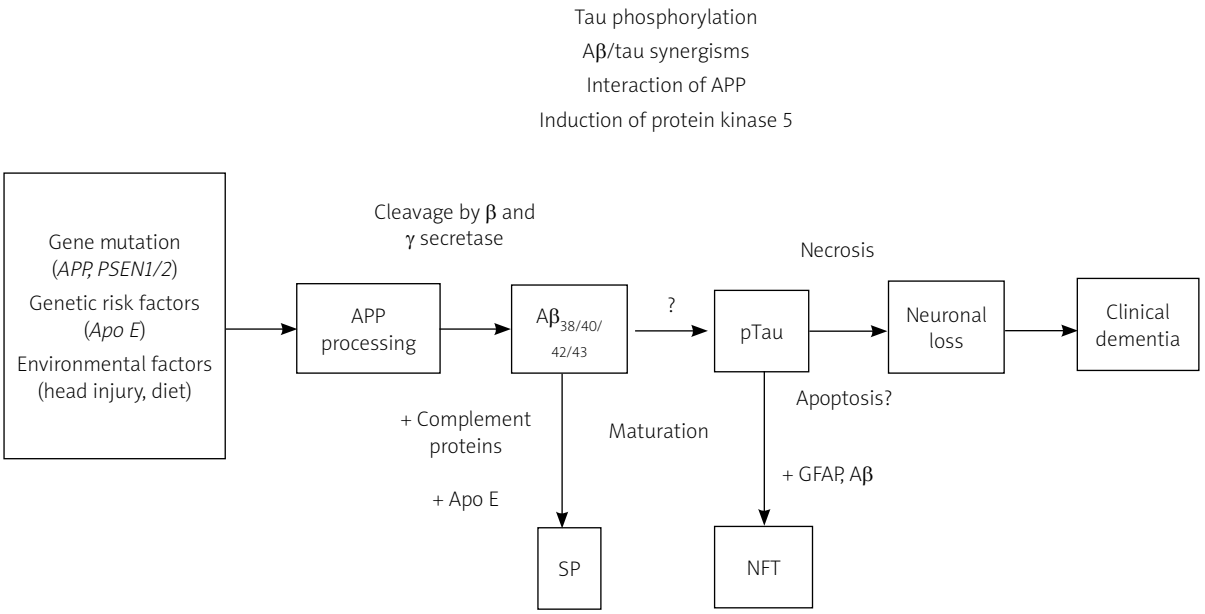

Aβ – β-amyloid, Apo E – apolipoprotein E, APP – amyloid precursor protein, GFAP – glial fibrillary acidic protein, PSEN1/2 – presenilin genes 1 and 2, NFT – neurofibrillary tangles, pTau – hyperphosphorylated tau, SP – senile plaques

Fig. 2. The amyloid cascade hypothesis (ACH) in a more fully developed form.

minal sites [83] and therefore, membrane damage may be necessary before Aβ can be formed [140], i.e., neuronal degeneration may precede Aβ formation. Fifth, Aβ toxicity requires micromolar concentrations of Aβ whereas levels in brain are frequently in the picomolar range [84]. Hence, AD may be caused by inflammatory reactions associated with activated microglia rather than by Aβ directly [84]. Moreover, in toxicity experiments, Aβ may not induce neuronal loss directly but may act to increase the risk of death of neurons from other causes [17,76,142].

Correlation of classical pathology with clinical dementia

If the ACH is an accurate description of AD pathology, then there should be a correlation between the abundance of SP and/or NFT and clinical dementia. However, the link between these lesions and cognitive impairment is often complex both in humans [106] and in rodent models of AD [44]. Several studies have attempted to correlate the numerical density of SP and NFT in AD brain with patient age and duration or degree of dementia [19,117,140]. Hence, significant correlations have been reported between: (1) the quantity of Aβ in entorhinal cortex and degree of cognition [30], (2) density and surface area of Aβ and months of severe dementia [19], (3) NFT counts and dementia in sectors CA1, CA4 and the subiculum [117], and (4) between neuritic SP and NFT and degree of dementia [140].

By contrast, Hyman *et al*. [65] found no quantitative measure of Aβ correlated with age in control patients, or with disease duration in AD, and suggested that Aβ did not accumulate in the brain throughout the course of the disease. That the relationship between SP and NFT and dementia is more complex was also emphasised by Bennett *et al*. [21]. No change in SP or NFT density was found from biopsy to autopsy suggesting that the pathology was well advanced before development of overt clinical symptoms. In a further study of 97 elderly cases with no symptoms of dementia, AD-type pathology was observed in 20-40% of cases, and although NFT were age-related there was no correlation between Aβ load and age [106]. Similarly, a significant correlation was observed between neuronal loss, NFT, and disease progression but not with Aβ [51]. In addition, some studies report that SP density declines with advancing AD, possibly as a result of the removal of Aβ deposits by glial cells [10]. A similar conclusion was reported by McKenzie *et al*. [85] who found that neither mean nor maximum SP density increased with age. Hence, SP may not progressively accumulate over the course of the disease but develop over a limited period of time and then stabilise to a constant level or even decline. These results question whether there is a direct or simple association between the formation and abundance of SP and NFT and developing dementia in AD as suggested by the ACH.

Is the formation of Aβ and tau a reactive process?

In survivors of head injury, enhanced levels of APP are found in neuronal perikarya and in DN surrounding Aβ deposits, similar pathological features to AD [45]. The processing of APP into Aβ in these cases occurs within the synaptic terminal fold of the axons, the presence of glial cells not being necessary for the conversion. Hence, APP formation may be a response to neuronal injury in AD [45]. Subsequently, it was shown that specific neurons in medial temporal lobe secreted large quantities of APP and that there were more APP-immunoreactive neurons in these areas in head injury patients [85]. Hence, increased expression of APP in head trauma may be an acute-phase response to neuronal injury [112], overexpression of APP leading to Aβ deposition. This conclusion is supported by the localisation of several acute-phase proteins within the different morphological types of Aβ deposit including diffuse, primitive, and classic deposits, e.g., amyloid-P, complement factors, and α-antichymotrypsin [7] (Table I). Furthermore, Regland and Gottfries [108] proposed that APP is involved in AD secondarily to maintain cell function. APP may therefore, maintain neuronal growth and survival and its putative neurotrophic action is also suggested by the observation that it shares structural features with the precursor for epidermal growth factor [108]. Furthermore, NFT may be part of the neurons response to injury [109].

Animal experiments also suggest that the formation of Aβ may be a reaction to brain damage. Hence, experimental lesions that damage the nucleus basalis in rat brain elevate APP synthesis in the cerebral cortex suggesting APP production is a specific response to loss of functional innervation of the cortex [138]. Chemically induced lesions of the brain

produce similar results. For example, lesions of the nucleus basalis using N-methyl D-aspartate (NMDA) elevate APP synthesis in cortical polysomes [138] and, in areas of brain damaged by kainite [70], APP was recorded in dystrophic neurites adjacent to the lesion. In addition, intrathecal or intraparenchymal injections of a toxin induced the formation of APP in hippocampal neurons subsequent to neuronal damage [68].

Lesion experiments can also induce pathological changes implicated in NFT formation. Hence, denervation of the dopamine pathways and septal lesions affecting both the cholinergic system and γ-aminobutyric acid (GABA) neurons which project to the dentate gyrus, result in a loss of dendritic microtubule associated protein 2 (MAP2) and the appearance of tau-immunoreactive dentate gyrus granule cells [134]. Hence, denervation of these pathways may cause transsynaptic changes in dentate gyrus neurons and these changes could represent a precursor stage to NFT formation.

These observations suggest that Aβ and tau may be the consequence of neuronal degeneration and not its cause and therefore, do not initiate the pathological cascade in AD. Hence, Aβ and NFT formation may occur 'downstream' of the 'real' causative events in AD but once formed, could initiate a secondary phase of degeneration.

Is the formation of neurofibrillary tangles related to Aβ?

Several attempts have been made to explain how Aβ may lead to NFT, as proposed by the ACH, but none have become universally accepted [23,47,100,101]. Alzheimer's disease was first recognised as a distinct disease entity in 1910 and was named after Alzheimer by Kraepelin based on the clinical and pathological description of the original cases [52]. Of the two original cases described by Alzheimer [2], however, both had numerous SP but only one of the cases had significant numbers of NFT [52], thus creating a controversy as to the relationship between the two 'signature' pathological features [58,72,87]. In addition, SP and NFT can develop alone in different disorders, e.g., NFT in tangle-only dementia [143] and Aβ in hereditary cerebral haemorrhage with amyloidosis of the Dutch type (HCHA-D) [64]. These observations suggest a more complex relationship between Aβ and tau formation than suggested by the ACH.

Studies also suggest that SP and NFT exhibit distinct but independently distributed topographic patterns in the cerebral cortex in AD [12,64]. Braak and Braak [22] showed that tau pathology occurred first in entorhinal cortex, often in the absence of SP, whereas the subsequent spread and distribution of Aβ was more variable. Studies of the spatial patterns of SP and NFT also show them to be clustered, the clusters often being regularly distributed relative to the pia mater [3]. Clusters of SP and NFT, however, are not spatially correlated, which would not support a direct pathogenic link between them. Perez *et al*. [103], however, showed that $A\beta_{25-35}$ could result in tau aggregation and that a decrease in Aβ aggregation was induced by tau peptides. Hence, aggregation of tau may be correlated with disassembly of Aβ which could explain the lack of spatial correlation [12]. In addition, SP and NFT may be temporally separated in the brain [82]. In entorhinal cortex [39] and in sector CA1 of the hippocampus [43], for example, NFT may precede the appearance of SP against the prediction of the ACH. In sector CA1, it is possible that Aβ is present in neurons before NFT are formed but not easily detectable by conventional methods [43].

Disconnection between the processes of Aβ and tau formation does not invalidate other features of the ACH. Hence, Aβ deposition may be the earliest lesion detectable in AD while tau formation occurs later by an independent process [66]. It is also possible that Aβ and tau formation are different consequences of degeneration of the same neurons, SP forming on the axonal terminals of NFT-containing neurons [3,31,102], which could also explain the spatial separation of SP and NFT within the brain.

Evidence from transgenic experiments

Based on the ACH, a variety of transgenic rodent models have been developed in an attempt to replicate AD pathology, including those based on single, double, and triple-mutation. Single mutation models usually involve various *APP* transgenes only. Hence, in the *APP:V642I* mouse, there was an increase in $A\beta_{42}$ deposition, but no mature SP or NFT were formed [71], this result being fairly typical of such experiments. In the 'double Swedish model' (*APP: K670N, M671L*), however, Aβ deposits similar to those found in AD were formed, the deposits being immunoreactive for Apo E, but no NFT were observed [120]. In the 'Indian/Swedish mutation model', both diffuse and compact-type Aβ deposits were observed

at 9-10 months of age, amyloid deposition increasing with age, and neocortex and amygdala being affected first followed by hippocampus and thalamus [38]. In addition, using the *APP:Tg2576* mouse, increased Aβ-induced oxidative stress was observed which encouraged increased activity of stress-related kinases and subsequently, tau phosphorylation in neurites surrounding SP [107].

Double mutation models usually include mutations of both *APP* and *PS1* transgenes. In one study (*APP: K670N, M671L; PS1: M146L*), long-term potentiation (LTP) of neurons was observed as early as three months, reduced LTP paralleling the appearance of SP [135]. In a similar model, which also incorporated an *APP V717I* mutation, there was age-related loss of pyramidal neurons in the hippocampus CA sectors including at sites devoid of Aβ deposition [119]. In a further *APP/PS* model, Aβ deposits were observed at eight weeks and hyperphosphorylated tau as punctate deposits at 24 weeks, consistent with the ACH, but DN were not as heavily labelled as those in AD [74].

A few transgenic experiments have involved triple mutation models (*APP*, *PS1* and *tau*). In one experiment (*APP:* Swedish mutation*, PS1: M146V, tau: P301L*), Aβ and tau pathology was present in temporal lobe with regional specificity similar to AD, Aβ deposition occurring before tau formation as predicted by the ACH [98]. In further experiments involving this model, AD immunotherapy was found to reduce Aβ and early tau epitopes also suggesting a direct pathogenic relationship between the two pathologies [99].

Hence, the presence of an *APP* mutation alone or in combination with *PSEN1* can result in Aβ deposition, but apart from evidence of hyperphosphorylated tau in neurites associated with SP, do not appear to induce NFT or a significant inflammatory response. The presence of tau transgenes in the form of a triple model appears to be necessary to more fully replicate AD pathology consistent with independent formation of Aβ and tau. However, in an APP-transgenic model, a reduction in endogenous tau ameliorated some of the effects mediated by Aβ which suggests a link between the two pathologies [110,111].

In conclusion, it is difficult to decide whether the presence of a specific mutation directly causes cell death as a result of Aβ-mediated toxicity or determines whether Aβ is secreted by neurons already damaged by a different process or from aging. A further problem is formation of Aβ may initiate a secondary phase of neurodegeneration that is difficult to distinguish from primary neuronal damage due to other causes. Nevertheless, a recent model, viz., *TgF344-AD* which incorporates mutant *APP* and *PS1* genes, exhibited age-dependent amyloidosis, tauopathy, gliosis, apoptotic loss of neurons in cortex and hippocampus, in addition to cognitive disturbance, and may offer a more complete model of AD [29].

Therapies for Alzheimer's disease based on the amyloid cascade hypothesis

There are many potential targets for AD therapy including APP cleavage, cytoskeletal destruction, neurotubule and ion homeostasis, metal ion accumulation, protein misfolding, oxidative stress, neuronal death, and gene mutation [24]. Therapies based on the ACH, however, have received considerable attention. Possible treatment strategies based on the ACH include inhibition of APP, inhibition of the proteases that liberate Aβ, and retarding maturation of Aβ into SP [121].

Some therapies have been based on targeting βACE1 [41]. In mice lacking this gene, there was a little apparent effect on behaviour and promising results were obtained in reducing the levels of SP. In humans, however, βACE1 also cleaves substrates involved in myelination, retinal homoeostasis, brain circuitry, and synaptic function, all of which could be affected if the enzyme was targeted [41]. In addition, treatment with γ-secretase inhibitors has been tested in rodent models and in humans. In rodents, early treatment with γ-secretase inhibitor can prevent or ameliorate Aβ deposition but established SP [1] and hyperphosphorylated tau aggregates [99] appear more resistant. In this regard, the failure of semagacestat in clinical trials, a well-characterised γ-secretase inhibitor, was particularly notable as Aβ deposition was reduced by this compound in both transgenic mice and humans [95].

There have also been clinical trials designed to remove or prevent Aβ formation using specific antibodies. Such antibodies can capture peripheral Aβ and prevent its re-entry from the periphery to the brain [32,33]. In addition, binding of specific antibodies to Aβ in deposited SP could activate microglia, thereby potentially clearing plaques by phagocytosis

[118]. Hence, a vaccine against Aβ was developed by activating microglia to remove SP [92]. Nevertheless, in clinical trials, some patients exhibited brain inflammation as a result of lymphocyte infiltration and elevated protein levels suggesting a breakdown of the blood brain barrier and entry of T-cells into the brain. Hence, Aβ-specific activated T-helper cells may amplify existing pro-inflammatory conditions present in AD. In addition, cytotoxic T-cells could attack APP present on the surface of many cells including neurons and release Aβ.

Treatment with bapineuzumab resulted in an overall Aβ deposit load and degree of CAA similar to controls [113]. Treatment, however, also altered the Aβ peptide profile of the patient, decreasing the proportion of $A\beta_{42}$ and increasing that of $A\beta_{40}$, but none of the treated patients exhibited improved cognition [113]. Subsequently, there has been a cessation of phase III clinical trials involving bapineuzumab in patients with mild to moderate levels of disease [26]. No treatment benefits have been established and several side effects reported. One possible explanation is that Aβ oligomers are pro-oxidants which combine with redox-active metals to form reactive species [130]. Hence, reducing Aβ may fail to halt cognitive decline because it is the effect of oxidative stress rather than Aβ directly which results in AD, Aβ and tau being upregulated to address the redox imbalance, possibly further accelerating the disease process [130].

As a result, after nearly 25 years of the theory, no new therapeutic agents for AD have reached the clinic based on the ACH [93]. Recent remarks by Castellani and Perry [26] that studies of Aβ metabolism have essentially been 'exhausted to no avail' reinforce this conclusion. Nevertheless, there are two questions raised by these trials. First, by how much should Aβ be reduced in brain to obtain a therapeutic effect [69]? Estimates of the total amount of Aβ deposited in an AD brain vary from approx. 4 mg [94] to 10 mg per brain [53]. In addition, it is difficult to quantify the rate of production of new Aβ in humans, which is often extrapolated from rodent cell culture models [18], thus making it difficult to establish treatment dosage. Second, are treatments applied to patients 'too late' in the disease process, i.e., after significant neuronal degeneration has already occurred, for trials to be effective? Recent criteria for the identification of pre-symptomatic AD using biomarkers and brain scan [89] may enable treatments to be tested at a much earlier stage of the disease and therefore, a more rigorous trial of the various treatments based on the ACH are possible in future.

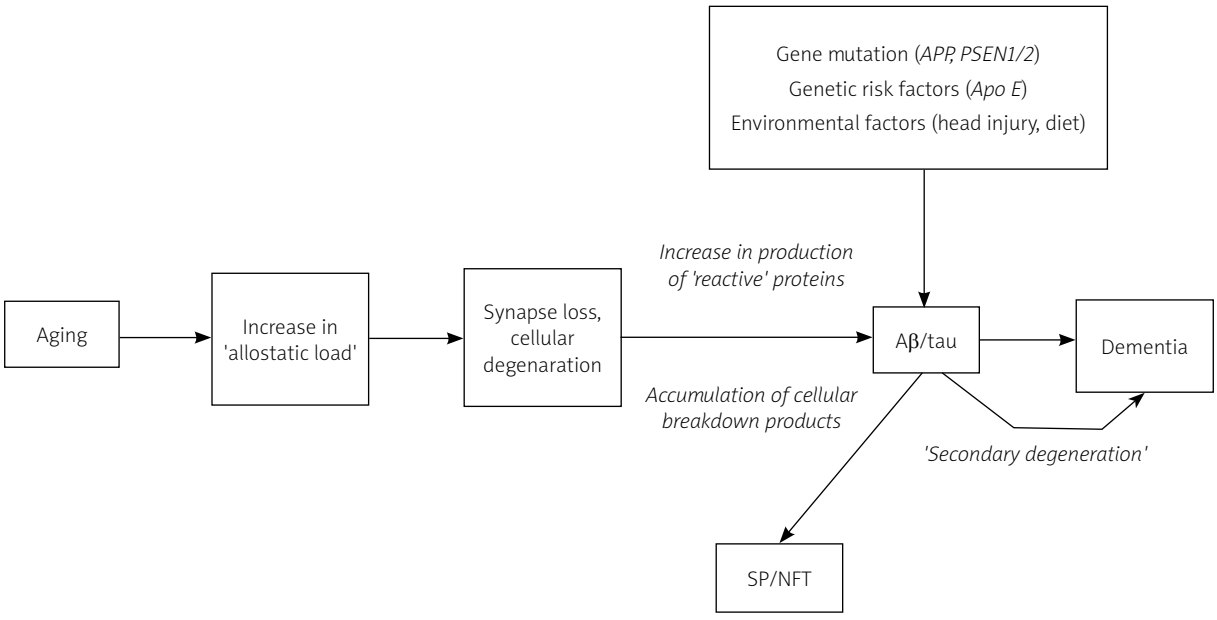

Aβ – β-amyloid, Apo E – apolipoprotein E, APP – amyloid precursor protein, PSEN1/2 – presenilin genes 1 and 2, NFT – neurofibrillary tangles, SP – senile plaques

Fig. 3. A modified scheme based on the amyloid cascade hypothesis (ACH).

A modified scheme for Alzheimer's disease pathogenesis

These observations taken together suggest that the ACH may not provide a complete explanation of AD pathogenesis. There is doubt regarding the primary role of Aβ, whether Aβ leads to tau formation, and whether SP and NFT are directly related to clinical dementia. There are two possible directions of future research. First, to attempt a further understanding of the mechanisms of Aβ-mediated neuronal loss within the context of the ACH [69] or second, to modify the ACH itself.

This review advocates the second approach and proposes a modified scheme based on the ACH, which incorporates the various concerns and questions raised (Fig. 3). First, the primary factor in this scheme is age-dependent breakdown of anatomical systems and pathways within the brain and consequent loss of synapses [25]. The extent of this aging effect, which begins early in life, is mediated by the degree of lifetime stress (the 'allostatic load'). The brain is the ultimate mediator of stress-related mortality through hormonal changes resulting in hypertension, glucose intolerance, cardiovascular disease, and immunological problems [25]. Second, the consequence of increasing allostatic load is gradual synaptic disconnection, neuronal degeneration, and the upregulation of genes determining various reactive and breakdown products resulting in the formation of Aβ and tau [14,96,108,138]. Third, in small numbers of families, specific *APP* or *PSEN* mutations influence the outcome of this age-related degeneration by determining the quantity, solubility, and/or toxicity of the molecular product. Cells have mechanisms to protect against the accumulation of misfolded and aggregated proteins including the ubiquitin system and the phagosome-lysosome system. Neuronal degeneration in individuals with specific mutations results in the accelerated formation of Aβ and tau, and then a further phase of 'secondary' neurodegeneration, which overwhelms the protection systems. Early-onset FAD is the consequence of this process. Fourth, in individuals without a specific genetic mutation, and where more complex genetic and environmental risk factors are present, the outcome of age-related loss of synapses is mainly soluble and smaller quantities of insoluble proteins which are degraded by the cellular protection systems and do not significantly accumulate to form SP and NFT. With advancing age, however, the protective systems become less effective resulting in slowly accumulating quantities of Aβ and tau. The result of these insidious processes is that the cellular protection systems do not become overwhelmed until much later in life, the consequence being late-onset SAD.

This modified scheme may explain the similarities in the phenotypes of FAD and SAD, why SP and NFT often appear to be distributed independently, and reflects data suggesting that Aβ and tau may be formed as a response to cellular degeneration.

Predictions of the modified hypothesis

The modified hypothesis makes a number of predictions that could be usefully investigated to test its validity. First, significant signs of neuronal degeneration should precede Aβ deposition especially in late-onset SAD. Second, any toxic effects of Aβ will be secondary rather than primary. Third, SP and NFT are both the consequences of neuronal degeneration essentially arising independently as a result of age-specific synapse loss. Fourth, in transgenic experiments, the effect of the transgene will be age-dependent. Hence, in a model which incorporates an *APP*: *V717I* mutation, for example, there was an age-related loss of pyramidal neurons in the hippocampus CA sectors including at sites devoid of plaque deposition [119], consistent with this prediction.

Implications of the modified hypothesis

The modified scheme has a number of implications. First, that SAD is not a disease linked primarily to defective genes but a complex syndrome dependant on the rate of aging and indirectly influenced by numerous genetic and environmental risk factors acting over a lifetime. Second, the hypothesis questions whether the presence, distribution, and molecular determinants of SP and/or NFT should continue to play a primary role in the pathological diagnosis of AD. If SP and NFT are ultimately the products of brain degeneration and not its initial cause [14], they may represent relatively late stages of the disease. Hence, there could be cases of AD that are difficult to classify pathologically because they may have insufficient numbers of SP and NFT or exhibit early developmental stages of these pathologies. In addition, if SP and NFT represent the consequence of neurodegeneration affecting different parts of neurons rather than being characteristic of a particular disease, there are likely to

be many cases that show combinations of pathological features, i.e., there will be some overlap between different disorders. Numerous examples of such cases have been reported in the literature, e.g., dementia with Lewy bodies (DLB) with associated AD pathology, Creutzfeldt-Jakob disease (CJD) with AD, Pick's disease (PkD) with AD, and these cases are often difficult to classify within the existing system [15]. Finally, should significant efforts continue to be devoted to immunotherapy and other treatments designed to remove Aβ from the brain? Such treatments could be beneficial in limiting the degree of secondary degeneration caused by Aβ. Nevertheless, Aβ might also be beneficial to the nervous system by promoting neurogenesis [80] and having a range of other protective functions [77]. In addition, excessive removal of Aβ could potentially reduce chelation within the brain resulting in enhanced oxidative stress [16].

Conclusions

Since 1992, the ACH has played the most influential role in explaining the pathogenesis of AD. It proposes that the deposition of Aβ is the initial pathological event leading to the formation of SP and NFT, death of neurons, and ultimately dementia. A number of major limitations of the ACH have been identified: (1) SP and NFT may develop independently, (2) SP and NFT may be the products rather than the cause of neurodegeneration in AD, (3) SP and NFT may not be closely correlated with the onset, severity and development of clinical dementia, (4) transgenic rodent models do not generally replicate all aspects of AD pathology, and (5) treatments based on the ACH have not been successful. A modification to the ACH is proposed which may better explain the pathogenesis of AD, especially in late-onset cases of the disease. The modified scheme makes a number of predictions which could be usefully investigated.

Disclosure

Author reports no conflict of interest.

References

1. Abramowski D, Wiederhold KH, Furrer U, Jaton AL, Neuenschwander A, Runser MJ, Danner S, Reichwald D, Ammaturo D, Staab D, Stoeckli M, Rueeger H, Neumann U, Staufenbiel M. Dynamics of Aβ turnover and deposition in different β-amyloid precursor protein transgenic mouse models following γ-secretase inhibition. J Pharmacol Exp Ther 2008; 327: 411-424.
2. Alzheimer A. On a peculiar disease of the cerebral cortex. Allgemeine Zeitschrift fur Psychiatrie und Psychish-Gerichtlich Medicin 1907; 64: 146-148.
3. Armstrong RA. Alzheimer's disease: Are cellular neurofibrillary tangles linked to β/A4 formation at the projection sites? Neurosci Res Commun 1992; 11: 171-178.
4. Armstrong RA. Is the clustering of neurofibrillary tangles in Alzheimer's patients related to the cells of origin of specific cortico-cortical projections? Neurosci Lett 1993; 160: 57-60.
5. Armstrong RA. Differences in β-amyloid (Aβ) deposition in human patients with Down's syndrome and sporadic Alzheimer's disease. Neurosci Lett 1994; 169: 133-136.
6. Armstrong RA. Plaques and tangles and the pathogenesis of Alzheimer's disease. Folia Neuropathol 2006; 44: 1-11.
7. Armstrong RA. The molecular biology of senile plaques and neurofibrillary tangles in Alzheimer's disease. Folia Neuropathol 2009; 47: 289-299.
8. Armstrong RA. What causes Alzheimer's disease? Folia Neuropathol 2013; 51: 169-188.
9. Armstrong RA, Smith CUM. β-amyloid (Aβ) deposition in the medial temporal lobe in Down's syndrome: effects of brain region and patient age. Neurobiol Dis 1995; 1: 139-144.
10. Armstrong RA, Nochlin D, Sumi M, Alvord EC. Neuropathological changes in the visual cortex in Alzheimer's disease. Neurosci Res Comm 1990; 6: 163-171.
11. Armstrong RA, Myers D, Smith CUM. The spatial patterns of plaques and tangles in Alzheimer's disease do not support the 'Cascade hypothesis'. Dementia 1993a; 4: 16-20.
12. Armstrong RA, Myers D, Smith CUM. The spatial patterns of β/A4 deposit subtypes in Alzheimer's disease. Acta Neuropathol 1993b; 86: 36-41.
13. Armstrong RA, Nochlin D, Bird TD. Neuropathological heterogeneity in Alzheimer's disease: A study of 80 cases using principal components analysis. Neuropathology 2000; 1: 31-37.
14. Armstrong RA, Cairns NJ, Lantos PL. Are pathological lesions in neurodegenerative disorders the cause or the effect of the degeneration? Neuropathology 2002; 22: 114-127.
15. Armstrong RA, Cairns NJ, Lantos PL. Overlap between neurodegenerative disorders. Neuropathology 2005; 25: 111-124.
16. Atwood CS, Obrenovich ME, Liu T, Chan H, Perry G, Smith MA, Martins RN. Amyloid-beta: a chameleon walking in two worlds: a review of the trophic and toxic properties of amyloid-β. Brain Res Rev 2003; 43: 1-16.
17. Bancher C, Lassman H, Breitschopf H, Jellinger KA. Mechanisms of cell death in Alzheimer's disease. J Neural Transm (Suppl.) 1997; 50: 141-152.
18. Bateman RJ, Siemers ER, Mawuenyega KG, Wen GL, Browning KR, Sigurdson WC, Yaresheski KE, Friedrich SW, DeMattos RB, May PC, Paul SM, Holzman DM. A γ-secretase inhibitor decreases amyloid-β production in the central nervous system. Ann Neurol 2009; 66: 48-54.
19. Beer RE, Ulrich J. Alzheimer plaque density and duration of dementia. Arch Gerontol Geriatr 1993; 16: 1-7.
20. Behl C, Davis JB, Klier FG, Schubert D. Amyloid-beta peptide induces necrosis rather that apoptosis. Brain Res 1994; 645: 253-264.

21. Bennett DA, Cochran EJ, Saper CB, Leverenz JB, Gilley DW, Wilson RS. Pathological changes in frontal cortex from biopsy to autopsy in Alzheimer's disease. Neurobiol Aging 1993; 14: 589-596.
22. Braak H, Braak E. Neuropathological staging of Alzheimer-related changes. Acta Neuropathol 1991; 82: 239-259.
23. Busciglio J, Lorenzo A, Yeh J, Yankner BA. β-amyloid fibrils induce tau phosphorylation and loss of microtubule binding. Neuron 1995; 14: 879-888.
24. Carreiras MC, Mendes E, Perry MJ, Francisco AP, Marco-Contelles J. The multifactorial nature of Alzheimer's disease for developing potential therapeutics. Curr Topics Med Chem 2013; 13: 1745-1770.
25. Carroll BJ. Ageing, stress and the brain. Endocrine Facets of Ageing. Novartis Foundation Symposium 2002; 242: 26-36.
26. Castellani RJ, Perry G. Pathogenesis and disease-modifying therapies in Alzheimer's disease: The flat line of progress. Arch Med Res 2012; 43: 694-698.
27. Chartier-Harlin M, Crawford F, Houlden H, Warren A, Hughes D, Fidani L, Goate A, Rossor M, Rocques P, Hardy J, Mullan M. Early onset Alzheimer's disease caused by mutations at codon 717 of the β-amyloid precursor protein gene. Nature 1991; 353: 844-846.
28. Chetelat G. Alzheimer's disease: A beta-independent processes- rethinking preclinical AD. Nature Rev Neurol 2013; 9: 123-124.
29. Cohen RM, Rezai-Zadeh K, Weitz TM, Rentsendorj A, Gate D, Spivak I, Bholat Y, Vasilevko V, Glabe CG, Breunig JJ, Rakic P, Davtyan H, Agadjanyan MG, Kepe V, Barrio JR, Bannykh S, Szekely CA, Pechnick RN, Town T. A transgenic Alzheimer rat with plaques, tau pathology, behavioural impairment, oligomeric A beta, and frank neuronal loss. J Neurosci 2013; 33: 6245-6256.
30. Cummings BJ, Cotman CW. Image analyses of β-amyloid load in Alzheimer's disease and relation to dementia severity. Lancet 1995; 346: 1524-1528.
31. De Lacoste M, White CL III. The role of cortical connectivity in Alzheimer's disease pathogenesis: a review and model system. Neurobiol Aging 1993; 14: 1-16.
32. DeMattos RB, Bales KR, Cummins DJ, Dodart JC, Paul SM, Holzman DM. Peripheral anti-Aβ antibody alters CNS and plasma Aβ clearance and decreases brain Aβ burden in a mouse model of Alzheimer's disease. Proc Natl Acad Sci U S A 2001; 98: 8850-8855.
33. DeMattos RB, Bales KR, Cummins DJ, Paul SM, Holzman DM. Brain to plasma amyloid-β efflux: a measure of brain amyloid burden in a mouse model of Alzheimer's disease. Science 2002; 295: 2264-2267.
34. De Strooper B, Saftig P, Craessaerts K, Vanderstichele H, Gulde G, Annaert W, Von Figura K, Van Leuven F. Deficiency of presenilin-1 inhibits the normal cleavage of amyloid precursor protein. Nature 1998; 391: 387-390.
35. Delacourte A, Sergeant N, Champain D. Wattez A, Maurage CA, Lebert F, Pasquier F, David JP. Nonoverlapping but synergetic tau and amyloid precursor protein pathologies in sporadic Alzheimer's disease. Neurology 2002; 59: 398-407.
36. Desai PP, Ikonomovic MD, Abrahamson EE, Hamilton RL, Isanski BA, Hope CE, Klunk WE, DeKosky ST, Kamboh MI. Apolipoprotein D is a component of compact but not diffuse amyloid-beta plaques in Alzheimer's disease temporal cortex. Neurobiol Dis 2005; 20: 574-582.
37. Drouet B, Pincon-Raymond M, Chambaz J, Pillot T. Molecular basis of Alzheimer's disease. Cell and Mole Life Sci 2000; 57: 705-715.
38. Dudal S, Krzywkowski P, Paquette J, Morissette C, Lacombe D, Tremblay P, Gervais F. Inflammation occurs early during Aβ deposition process in TgCRND8 mice. Neurobiol Aging 2004; 25: 861-871.
39. Duyckaerts C. Looking for the link between plaques and tangles. Neurobiol Aging 2004; 25: 735-739.
40. Eikelenboom P, Zhan SS, van Gool WA, Allsop D. Inflammatory mechanisms in Alzheimer's disease. Trends in Pharmacol Sci 1994; 15: 447-450.
41. Evin G, Hince C. BACE1 as a therapeutic target in Alzheimer's disease: rationale and current status. Drugs Aging 2013; 30: 755-764.
42. Frolich L, Hoyer S. The etiological and pathological heterogeneity of Alzheimer's disease. Nervenarzt 2002; 73: 422-427.
43. Funato H, Enya M, Yoshimura M, Morishima-Kawashima M, Ihara Y. Presence of sodium dodecyl sulphate-stable amyloid beta protein dimers in hippocampus CA1 not exhibiting neurofibrillary tangle formation. Am J Pathol 1999; 155: 23-28.
44. Games D, Adams D, Alessandrini R, Barbour R, Berthelette P, Blackwell C, Carr T, Clemens J, Donaldson T, Gillespie F, Hagopian S, Johnsonwood K, Khan K, Lee M, Lechowitz P, Lieberberg I, Little S, Masliah E, McConlogue L, Montoya-Zavala M, Mucke L, Paganini L, Pennimon E, Power M, Schenk D, Seubert P, Snyder B, Soriano F, Tan H, Vitale J, Wadsworth S, Wolozin B, Zhao J. Alzheimer-type neuropathology in transgenic mice overexpressing V717F β-amyloid precursor protein. Nature 1995; 373: 523-527.
45. Gentleman SM, Nash MJ, Sweeting CJ, Graham DI, Roberts GW. β-amyloid precusor protein (βAPP) as a marker for axonal injury after head injury. Neurosci Lett 1993; 160: 139-144.
46. Gessel MM, Bernstein S, Kemper M, Teplow DB, Bowers MT. Familial Alzheimer's disease mutations differentially alter amyloid beta protein oligomerization. ACS Chem Neurosci 2012; 3: 909-918.
47. Giasson BI, Lee VM, Trojanowski JQ. Interactions of amyloidogenic proteins. Neuromole Med 2003; 4: 49-58.
48. Glabe CG. Common mechanisms of amyloid oligomer pathogenesis in degenerative disease. Neurobiol Aging 2006; 27: 570-575.
49. Glenner GG, Wong CW. Alzheimer's disease and Down's syndrome: sharing of a unique cerebrovascular amyloid fibril protein. Biochem Biophys Res Commun 1984; 122: 1131-1135.
50. Goate R, Chartier-Harlin M, Mullan M, Brown J, Crawford F, Fidani L, Giuffra L, Haynes A, Irving N, James L, Mant R, Newton P, Rooke K, Roques P, Talbot C, Pericak-Vance M, Roses A, Williamson R, Rossor M, Owen M, Hardy J. Segregation of a missense mutation in the amyloid precursor protein gene with familial Alzheimer's disease. Nature 1991; 349: 704-706.
51. Gomez-Isla T, Hollister R, West H, Mui S, Growdon JH, Petersen RC, Parisi JE, Hyman BT. Neuronal loss correlates with but exceeds neurofibrillary tangles in Alzheimer's disease. Ann Neurol 1997; 41: 17-24.

52. Graeber MB, Kosel S, Egensperger R, Banati RB, Muller U, Bise K, Hoff P, Moller HJ, Fujisawa K, Mehraein P. Rediscovery of the case described by Alois Alzheimer in 1911: historical, histological and molecular genetic analysis. Neurogenetics 1997; 1: 73-80.
53. Gravina SA, Ho LB, Eckman LB, Long KE, Otvos L, Younkin LH, Suzuki N, Younkin SG. Amyloid β protein (Aβ) in Alzheimer's disease brain. Biochemical and immunocytochemical analysis with antibodies for forms ending at Aβ40 or Aβ42(43). J Biol Chem 1995; 270: 7013-7016.
54. Greenberg BD. The COOH-terminus of the Alzheimer amyloid Aβ peptide: Differences in length influence the process of amyloid deposition in Alzheimer brain, and tell us something about relationships among parenchymal and vessel-asssociated amyloid deposits. Amyloid 1995; 21: 195-203.
55. Gschwind M, Huber G. Apoptotic cell death induced by beta-amyloid 1-42 peptide is cell type dependent. J Neurochem 1995; 65: 292-300.
56. Hanger DP, Mann DMA, Neary D, Anderton BH. Tau pathology in a case of familial Alzheimer's disease with a valine to glycine mutation at position 717 in the amyloid precursor protein. Neurosci Lett 1992; 145: 178-180.
57. Hardy JA, Higgins GA. Alzheimer's disease: The amyloid cascade hypothesis. Science 1992; 256: 184-185.
58. Hardy J, Duff K, Hardy KG, Perez-Tur J, Hutton M. Genetic dissection of Alzheimer's disease and related dementias: Amyloid and relationship to tau. Nat Neurosci 1998; 1: 743-743.
59. Haupt M, Kurz A, Pollman S, Romero B. Alzheimer's disease: identical phenotypes of familial and non-familial cases. J Neurol 1992; 239: 248-250.
60. Hellstrom-Lindahl E, Viitanen M, Marutle A. Comparison of Aβ levels in the brain of familial and sporadic Alzheimer's disease. Neurochem Int 2009; 55: 243-252.
61. Honarnejad K, Herms J. Presenilins: Role in calcium homeostasis. Int J Biochem Cell Biol 2012; 44: 1983-1986.
62. Huber G, Bailly Y, Martin JR, Mariani J, Brugg B. Synaptic beta-amyloid precursor proteins increase with learning capacity in rats. Neuroscience 1997; 80: 313-320.
63. Huse JT, Doms RW. Closing in on the amyloid cascade: recent insights into the cell biology of Alzheimer's disease. Mol Neurobiol 2000; 22: 81-98.
64. Hyman BT, Tanzi RE. Amyloid, dementia and Alzheimer's disease. Curr Opin Neurol Neurosurg 1992; 5: 88-93.
65. Hyman BT, Marzloff K, Arriagada PV. The lack of accumulation of senile plaques or amyloid burden in Alzheimer's disease suggests a dynamic balance between amyloid deposition and resolution. J Neuropath Exp Neurol 1993; 52: 594-600.
66. Ihara Y. What mediates between β-amyloid and paired helical filaments. Neurobiol Aging 1989; 10: 573-574.
67. Kalaria RN, Perry G. Amyloid P component and other acute-phase proteins associated with cerebellar Aβ deposits in Alzheimer's disease. Brain Res 1993; 631: 151-155.
68. Kalaria RN, Bhatti SU, Perry G, Lust WD. The amyloid precursor protein in ischaemic brain injury and chronic hypoperfusion. Proc 7th Inter Study Group on Pharm Mem Dis Assoc with Aging 1993; pp. 291-294.
69. Karran E, Mercken M, de Strooper B. The amyloid cascade hypothesis for Alzheimer's disease: an appraisal for the development of therapeutics. Nature Rev Drug Disc 2011; 10: 698-712.
70. Kawarabayashi T, Shoji M, Harigaya Y, Yamaguchi H, Hirai S. Expression of amyloid precursor protein in early stage of brain damage. Brain Res 1991; 563: 334-338.
71. Kawasumi M, Chiba T, Yamada M, Miyamae-Kaneko M, Matsuoka M, Nakahara J, Tomita T, Iwatsubo T, Kato S, Aiso S, Nishimoto I, Kouyama K. Targeted introduction of *V642I* mutation in *APP* gene cause functional abnormality resembling early stage of Alzheimer's disease in aged mice. Eur J Neurosci 2004; 19: 2826-2838.
72. Khatchaturian ZS. Diagnosis of Alzheimer's disease. Arch Neurol 1985; 42: 1097-1005.
73. Kisilevsky R, Lyon AW, Young ID. A critical analysis of postulated pathogenic mechanisms in amyloidogenesis. Crit Rev Clin Lab Sci 1992; 29: 59-82.
74. Kurt MA, Davies DC, Kidd M, Duff K, Howlett DR. Hyperphosphorylated tau and PHF like structures in the brains of mice carrying mutant APP and mutant presenilin-1 transgenes. Neurobiol Dis 2003; 14: 89-97.
75. Lantos PL, Luthert PJ, Hanger D, Anderton BH, Mullan M, Rossor M. Familial Alzheimer's disease with the amyloid precursor protein position 717 mutation and sporadic Alzheimer's disease have the same cytoskeletal pathology. Neurosci Lett 1992; 137: 221-224.
76. Lasmann H. Patterns of synaptic and nerve cell pathology in Alzheimer's disease. Beh Brain Res 1996; 78: 9-14.
77. Lee HG, Casadesus G, Zhu X, Takeda A, Perry G, Smith MA. Challenging the Amyloid Cascade Hypothesis: Senile plaques and amyloid-β as protective adaptations to Alzheimer's disease. Ann NY Acad Sci 2004; 1019: 1-4.
78. Levy-Lahad E, Wasco W, Poorkaj P, Romano D, Oshima J, Pettingell W, Yu C, Jondro P, Schmidt S, Wang K, Crowley A, Fu Y, Guenette S, Galas D, Nemens E, Wijsman E, Bird T, Schellenberg G, Tanzi R. Candidate gene for chromosome 1 familial Alzheimer's disease locus. Science 1995; 269: 973-977.
79. Liepnieks JJ, Ghetti B, Farlow M, Roses AD, Benson MD. Characterization of amyloid fibril β-peptide in familial Alzheimer's disease with *APP717* mutations. Biochem Bioph Res Comms 1993; 197: 386-392.
80. Lopez-Toledano MA, Shelanski ML. Neurogenic effect of beta-amyloid peptide in the development of neural stem cells. J Neurosci 2004; 24: 5439-5444.
81. Ma JY, Yee A, Brewer HB, Das S, Potter H. Amyloid-associated proteins α_1-antichymotrypsin and apolipoprotein E promote assembly of Alzheimer β-protein into filaments. Nature 1994; 372: 92-94.
82. Mann DMA, Younis N, Jones D, Stoddart RW. The time course of pathological events in Down's syndrome with particular reference to the involvement of microglial cells and deposits of β/A4. Neurodegen 1992; 1: 201-215.
83. Maruyama K, Kawamura Y, Asada H, Ishiura S, Obata K. Cleavage at the N-terminal site of Alzheimer amyloid β/A4 protein is essential for its secretion. Biochem Biophys Res Comms 1994; 202: 1517-1523.

84. McGeer PL, McGeer EG. The amyloid cascade-inflammatory hypothesis of Alzheimer disease: implications for therapy. Acta Neuropathol 2013; 126: 479-497.
85. McKenzie JE, Gentleman SM, Roberts GW, Graham DI, Royston MC. Increased numbers of βAPP-immunoreactive neurons in the entorhinal cortex after head injury. Neuroreport 1994; 6: 161-164.
86. Miller DL, Papayannopoulos IA, Styles J, Bobin SA, Lin YY, Biemann K, Iqbal K. Peptide compositions of the cerebrovascular and senile plaque core amyloid deposits of Alzheimer's disease. Arch Biochem Biophys 1993; 301: 41-52.
87. Mirra S, Heyman A, McKeel D, Sumi S, Crain B, Brownlee L, Vogel F, Hughes J, van Belle G, Berg L. The consortium to establish a registry for Alzheimer's disease (CERAD). II. Standardisation of the neuropathological assessment of Alzheimer's disease. Neurology 1991; 41: 479-486.
88. Moro ML, Giaccone G, Lombardi R, Indaco A, Uggetti A, Morbin M, Saccucci S, Di Fede G, Catania M, Walsh DM, Demarchi A, Rozemuller A, Bogdanovic N, Bugiani F, Ghetti B, Tagliavini F. APP mutations in the A beta coding region are associated with abundant cerebral deposition of A beta 38. Acta Neuropathol 2012; 124: 809-821.
89. Morris JC, Blennow K, Froelich L, Nordberg A, Soininen H, Waldenar G, Wahlund L-O, Dubois B. Harmonized diagnostic criteria for Alzheimer's disease: recommendations. J Int Med 2014; 275: 204-213.
90. Mudher A, Lovestone S. Alzheimer's disease: do tauists and Baptists finally shake hands. TINS 2002; 25: 22-26.
91. Mullan M, Crawford F. Genetic and molecular advances in Alzheimer's disease. TINS 1993; 16: 398-403.
92. Munch G, Robinson SR. Potential neurotoxic inflammatory responses to A beta vaccination in humans. J Neural Transm 2002; 109: 1081-1087.
93. Nalivaeva NN, Turner AJ. The amyloid precursor protein: A biochemical enigma in brain development, function and disease. Febs Lett 2013; 587: 2046-2054.
94. Naslund J, Haroutunian V, Mohs R, Davies KL, Greengard P, Bauxbaum JD. Correlation between elevated levels of amyloid-β peptide in the brain and cognitive decline. JAMA 2000; 283: 1571-1577.
95. Ness DK, Boggs LN, Hepburn DL, Gitter B, Long GG, May PC, Piroozi KS, Schafer KA, Yang ZX. Reduced β-amyloid burden, increased C-99 concentrations and evaluation of neuropathology in the brains of PDAPP mice given LY450139 dihydrate daily by gavage for 5 months. Neurobiol Aging 2004; 25: S238-S239.
96. Newell KL, Boyer P, Gomez-Tortosa E, Hobbs W, Hedley-Whyte ET, Vonsattel JP, Hyman BT. Alpha-synuclein immunoreactivity is present in axonal swellings in neuroaxonal dystrophy and acute traumatic brain injury. J Neuropath Exp Neurol 1999; 58: 1263-1268.
97. Nochlin D, Van Belle G, Bird TD, Sumi SM. Comparison of the severity of neuropathological changes in familial and sporadic Alzheimer's disease. Alz Dis Assoc Dis 1993; 7: 212-222.
98. Oddo S, Caccamo A, Kitazawa M, Tseng BP, LaFerla FM. Amyloid deposition precedes tangle formation in a triple transgenic model of Alzheimer's disease. Neurobiol Aging 2003; 24: 1063-1070.
99. Oddo S, Billings L, Kesslak JP, Cribbs DH, LaFerla FM. Aβ immunotherapy leads to clearance of early, but not late, hyperphosphorylated tau aggregates via the proteosome. Neuron 2004; 43: 321-332.
100. Oyama F, Shimada H, Oyama R, Titani K, Ihara Y β-amyloid protein precursor and tau mRNA levels versus β-amyloid plaque and NFT in the aged human brain. J Neurochem 1993; 60: 1658-1664.
101. Oyama F, Shimada H, Oyama R, Ihara Y. Apolipoprotein E genotype, Alzheimer pathologies and related gene expression in the age population. Mol Brain Res 1995; 29: 92-98.
102. Pearson RCA, Esiri MM, Hiorns RW, Wilcock GK, Powell TPS. Anatomical correlates of the distribution of the pathological changes in the neocortex in Alzheimer's disease. Proc Natl Acad Sci USA 1985; 82: 4531-4534.
103. Perez M, Cuadros R, Benitez MJ, Jimeniz JS. Interaction of Alzheimer's disease Aβ peptide 25-35 with tau protein and with a tau peptide containing the microtubule binding domain. J Alz Dis 2004; 6: 461-470.
104. Perry G. Neuritic plaques in Alzheimer's disease originate from neurofibrillary tangles. Med Hypoth 1993; 40: 257-258.
105. Podlisny MB, Tolan DR, Selkoe DJ. Homology of amyloid beta protein precursor in monkey and human supports a primate model for Beta amyloidosis in Alzheimer's disease. Am J Pathol 1991; 138: 1423-1433.
106. Price JL, McKeel DW, Buckles VD, Roe CM, Xiong CJ, Grundman M, Hansen LA, Peterson RC, Parisi JE, Dickson DW, Smith CD, Davis DG, Schmitt FA, Markesbury WR, Kaye JF, Kurten R, Hulette C, Kurland BF, Higdon BF, Kukull W, Morris JC. Neuropathology of non-demented aging: presumptive evidence for preclinical Alzheimer's disease. Neurobiol Aging 2009; 30: 1026-1036.
107. Puig B, Gomez-Isla T, Ribe E, Cuadrado M, Torrejon-Escribano B, Dalfo E, Ferrer I. Expression of stress-activated kinases c-Jun N-terminal kinase (SAPK/JNK-P) and p38 kinase (p38-P) and tau phosphorylation in neurites surrounding beta A plaques in APP Tg2576 mice. Neuropathol Appl Neurobiol 2004; 30: 491-502.
108. Regland B, Gottfries CG. The role of amyloid β-protein in Alzheimer's disease. Lancet 1992; 340: 467-469.
109. Renkawek K, Dejong WW, Merck KB, Frenken CWGM, van Workum FPA, Bosman GJCGM. Alpha-B-crystallin is present in reactive glia in Creutzfeldt-Jakob disease. Acta Neuropathol 1992; 83: 324-327.
110. Roberson ED, Scearce-Levie K, Palop JJ, Yan FR, Cheng IH, Wu T, Gerstein H, Yu GQ, Mucke L. Reducing endogenous tau ameliorates amyloid β-induced deficits in an Alzheimer's disease mouse model. Science 2007; 316: 750-754.
111. Roberson ED, Halabisky B, Yoo JW, Yao JH, Chin JA, Yan FR, Wu TF, Hamto P, Devidze N, Yu GQ, Palop JJ, Noebels JL, Mucke L. Amyloid-β/Fyn-induced synaptic, network, and cognitive impairments depend on tau levels in multiple mouse models of Alzheimer's disease. J Neurosci 2011; 31: 700-711.
112. Roberts GW, Gentleman SM, Lynch A, Murray L, Landon M, Graham DI. β-amyloid protein deposition in the brain after severe head injury: implications for the pathogenesis of Alzheimer's disease. J Neurol Neurosurg Psychiatr 1994; 57: 419-425.

113. Roher AE, Cribbs DH, Kim RC, Maarouf CL, Whiteside CM, Kokjohn TA, Daugs ID, Head E, Liebsack C, Serrano G, Belden C, Sabbagh MN, Beach TG. Bapineuzumab alters A beta composition: implications for the amyloid cascade hypothesis and anti-amyloid immunotherapy. Plos One 2013; 8: e59735.
114. Russo C, Saido TC, DeBusk LM, Tabaton M, Gambetti P, Teller JK. Heterogeneity of water soluble amyloid beta peptide in Alzheimer's disease and Down's syndrome brains. Febs Lett 1997; 409: 411-416.
115. Saito T, Suemoto T, Brouwers N, Sleegers K, Funamoto S, Mihira N, Matsuba Y, Yamada K, Nilsson P, Takao J, Nishimura M, Iwata N, Van Broeckhoven C, Ihara Y, Saido TC. Potent amyloidogenicity and pathogenicity of $A\beta_{43}$. Nature Neurosci 2011; 14: 1023-1032.
116. Sambamurti K, Greig NH, Lahiri DK. Advances in the cellular and molecular biology of the beta-amyloid protein in Alzheimer's disease. Neuromol Med 2002; 1: 1-31.
117. Samuel W, Masliah E, Hill LR, Butters N, Terry R. Hippocampal connectivity and Alzheimer's dementia: Effects of synapse loss and tangle frequency in a two-component model. Neurology 1994; 44: 2081-2088.
118. Schenk D, Barbour R, Dunn W, Gordon G, Grajeda H, Guido T, Hu K, Huang JP, Johnson-Wood K, Khan K, Kholodenko D, Lee M, Liao ZM, Lieberburg I, Motter R, Mutter L, Soriano F, Shopp G, Vasquez N, Vandevert C, Walker S, Wogulis M, Yednock T, Games DL, Suebert P. Immunization with amyloid-β attenuates Alzheimer-disease-like pathology in the PDAPP mouse. Nature 1999; 400: 173-177.
119. Schmitz C, Rutten BP, Pielen A, Schafer S, Wirths O, Tremp G, Czech C, Blanchard V, Multhaup G, Rezaie P, Korr H, Steinbusch HW, Pradier L, Bayer TA. Hippocampal neuron loss exceeds amyloid plaque load in a transgenic mouse model of Alzheimer's disease. Am J Pathol 2004; 164: 1495-1502.
120. Schwab C, Hosokawa M, McGeer PL. Transgenic mice overexpressing amyloid beta protein are an incomplete model of Alzheimer's disease. Exp Neurol 2004; 188: 52-64.
121. Selkoe DJ. Amyloid protein and Alzheimer's disease. Sci Am 1991; 265: 68-71, 74-76, 78.
122. Shalit F, Sredni B, Stern L, Kott E, Huberman M. Elevated interleukin-6 secretion levels by mononuclear cells of Alzheimer's patients. Neurosci Lett 1994; 174: 130-132.
123. Sherrington R, Rogaev E, Liang Y, Rogaeva E, Levesque G, Ikeda M, Chi H, Lin C, Li G, Holman K, Tsuda T, Mar L, Foncin J, Bruni A, Moulese M, Sorbi S, Rainero I, Pinessi L, Nee L, Chumakov I, Pollen D, Brookes A, Sauseau P, Polinski R, Wasco R, Dasilva H, Haines J, Pericak-Vance M, Tanzi R, Roses A, Fraser P, Rommens J, St George-Hyslop P. Cloning of a gene bearing missense mutations in early onset familial Alzheimer's disease. Nature 1993; 375: 754-760.
124. Smith MA, Kalaria RN, Perry G. α_1-trypsin immunoreactivity in Alzheimer's disease. Biochem Biophys Res Communs 1993; 193: 579-584.
125. Smith MA, Siedlak SL, Richey PL, Mulvihill P, Ghiso J, Frangione B, Tagliavini F, Giaccone G, Bugiani O, Praprotnik D, Kalaria RN, Perry G. Tau protein directly interacts with the amyloid β-protein precursor: implications for Alzheimer's disease. Nat Med 1995; 1: 365-369.
126. Smith MA, Casadesus G, Joseph JA, Perry G. Amyloid-beta and tau serve antioxidant functions in the aging and Alzheimer brain. Free Rad Biol Med 2002; 33: 1194-1199.
127. Sommer B. Alzheimer's disease and the amyloid cascade hypothesis: Ten years on. Curr Opin Pharmacol 2002; 2: 87-92.
128. Styczyńska M, Strosznajder JB, Religa D, Chodakowska-Żebrowska M, Pfeffer A, Gabrylewicz T, Czapski GA, Kobryś M, Karciauskas G, Barcikowska M. Association between genetic and environmental factors and the risk of Alzheimer's disease. Folia Neuropathol 2008; 46: 249-254.
129. Sudoh S, Kawamura Y, Sato K. Wang R, Saido TC, Oyama F, Sakaki Y, Komano H, Yanagisawa K. Presenilin-1 mutations linked to FAD increase the intracellular levels of amyloid beta protein 1-42 and its n-terminally truncated variant(s) which are generated at distinct sites. J Neurochem 1998; 71: 1535-1543.
130. Sutherland GT, Chami B, Youssef P, Witting PK. Oxidative stress in Alzheimer's disease: primary villain or physiological by-product? Redox Rep 2013; 18: 134-141.
131. Suzuki N, Cheung TT, Cai XD, Odaka A, Otvos L, Eckman C, Golde TE, Younkin SG. An increased percentage of long amyloid β protein secreted by familial amyloid β protein precursor (βAPP717) mutation. Science 1994; 264: 1336-1340.
132. Takashima A, Noguchi K, Sato K, Hoshino T, Imahori K. Tau protein kinase I is essential for amyloid-β-protein-induced neurotoxicity. Proc Natl Acad Sci 1993; 90: 7789-7793.
133. Teplow DB. On the subject of rigor in the study of amyloid beta-protein assembly. Alzheimers Res Ther 2013; 5: 39.
134. Torack RM, Miller JW. Immunoreactive changes resulting from dopaminergic denervation of the dentate gyrus of the rat hippocampal formation. Neurosci Lett 1994; 169: 9-12.
135. Trinchese F, Liu SM, Battaglia F, Walter S, Mathews PM, Arancio O. Progressive age-related development of Alzheimer-like pathology in APP/PS1 mice. Ann Neurol 2004; 55: 801-814.
136. Van Gool D, Destrooper B de, Van Leuven F, Triau E, Dom R. α_2-Macroglobulin expression in neuritic-type plaques in patients with Alzheimer's disease. Neurobiol Aging 1993; 14: 233-237.
137. Verga L, Frangione B, Tagliavini F, Giaccone G, Migheli A, Bugiani O. Alzheimer's and Down's patients: cerebral preamyloid deposits differ ultrastructurally and histochemically from the amyloid of senile plaques. Neurosci Lett 1989; 105: 294-299.
138. Wallace WC, Ahlers ST, Gotlib J, Bragin V, Sugar J, Gluck R, Shea PA, Davis KL, Haroutunian V. Amyloid precursor protein in the cerebral cortex is rapidly and persistently induced by loss of subcortical innervation. Proc Natl Acad Sci U S A 1993; 90: 8712-8716.
139. Welander H, Franberg J, Graff C, Sundstrom E, Winblad B, Tjernberg LO. $A\beta_{43}$ is more frequent than $A\beta_{40}$ in amyloid plaque cores from Alzheimer's disease brains. J Neurochem 2009; 110: 697-706.
140. Wisniewski T, Ghiso J, Frangione B. Alzheimer's disease and soluble Aβ. Neurobiol Aging 1994; 15: 143-152.
141. Wolfe MS, Xia WM, Ostaszewski B, Diehl TS, Kimberly WT, Selkoe DJ. Two transmembrane aspartates in presenilin-1 required for presenilin endoproteolysis and γ-secretase activity. Nature 1999; 398: 513-517.

142. Wujek JR, Dority MD, Frederickson RCA, Brunden KR. Deposits of Aβ fibrils are not toxic to cortical and hippocampal neurons in vitro. Neurobiol Aging 1996; 17: 107-113.
143. Yamada M. Senile dementia of the neurofibrillary tangle type (tangle-only dementia): Neuropathological criteria and clinical guidelines for diagnosis. Neuropathology 2003; 23: 311-317.
144. Yamaguchi H, Nakazato Y, Shoji M, Okamoto K, Ihara Y, Morimatsu M, Hirai S. Secondary deposition of beta amyloid within extracellular tangles in Alzheimer-type dementia. Am J Pathol 1991; 138: 699-705.
145. Yamaguchi H, Ishiguro K, Sugihara S, Nakazato Y, Kawarabayashi T, Sun XY, Hirai S. Presence of apolipoprotein E on extracellular neurofibrillary tangles and on meningeal blood vessels precedes the Alzheimer β-amyloid deposition. Acta Neuropathol 1994; 88: 413-419.

Original article

Folia Neuropathologica

Abnormalities in the normal appearing white matter of the cerebral hemisphere contralateral to a malignant brain tumor detected by diffusion tensor imaging

Kai Kallenberg[1], Torben Goldmann[1,2], Jan Menke[3], Herwig Strik[4], Hans C. Bock[5], Alexander Mohr[1], Jan H. Buhk[6], Jens Frahm[7], Peter Dechent[8], Michael Knauth[1]

[1]Institute for Diagnostic and Interventional Neuroradiology, Georg-August University, Göttingen, [2]MR-Research in Neurology and Psychiatry, Georg-August University, Göttingen, [3]Institute for Diagnostic and Interventional Radiology, Georg-August University, Göttingen, [4]Department of Neurology, University Medical Center, Philipps University, Marburg, [5]Department of Neurosurgery, Georg-August University, Göttingen, [6]Department of Neuroradiology, University Medical Center Hamburg-Eppendorf, Hamburg, [7]Biomedizinische NMR Forschungs GmbH, Göttingen, [8]MR-Research in Neurology and Psychiatry, Department of Cognitive Neurology, Georg-August University, Göttingen, Germany

Folia Neuropathol 2014; 52 (3): 226-233 DOI: 10.5114/fn.2014.45563

Abstract

Introduction: *Malignant brain tumors tend to migration and invasion of surrounding brain tissue. Histopathological studies reported malignant cells in macroscopically unsuspicious parenchyma (normal appearing white matter – NAWM) remote from the tumor localization. In early stages, diffuse interneural infiltration with changes of the apparent diffusion coefficient (ADC) and fractional anisotropy (FA) is hypothesized.*

Material and methods: *Patients' ADC and FA values from NAWM of the hemisphere contralateral to a malignant glioma were compared to age- and sex-matched normal controls.*

Results: *Apparent diffusion coefficient levels of the entire contralateral hemisphere revealed a significant increase and a decrease of FA levels. An even more pronounced ADC increase was found in a region mirroring the glioma location.*

Conclusions: *In patients with previously untreated anaplastic astrocytoma or glioblastoma, an increase of the ADC and a reduction of FA were found in the brain parenchyma of the hemisphere contralateral to the tumor localization. In the absence of visible MRI abnormalities, this may be an early indicator of microstructural changes of the NAWM attributed to malignant brain tumor.*

Key words: *glioma, normal appearing white matter, diffusion tensor imaging.*

Introduction

Magnetic resonance imaging (MRI) plays a central role in the treatment algorithms of patients with brain tumors. While conventional MRI with T2, FLAIR, and contrast-enhanced T1-weighted sequences unravel the size, shape, and structure of lesions, the use of perfusion- and diffusion-weighted MRI adds information about the regional blood volume and microstructural architecture. Additionally, pro-

Communicating author:

Dr. Kai Kallenberg, Institut für Diagnostische und Interventionelle Neuroradiologie, Universitätsmedizin Göttingen, Postfach, 37099 Göttingen, Germany, e-mail: kai.kallenberg@med.uni-goettingen.de

ton MR spectroscopy (MRS) gives insights into tissue composition and intracellular metabolism [15]. However, the technical progress in glioma imaging techniques seems to be ahead of the therapeutic achievements – initial promising results of local chemotherapy were overshadowed by reports of wound healing disorders and even deaths [9] and the lack of long-term effects. Probably, microinvasive expansion is the main reason why malignant brain tumors still cannot be cured with local treatment such as surgery, focal irradiation or local chemotherapy [10]. Several studies have reported the infiltrative growth of glioblastoma multiforme (GBM) cells in apparently unaffected brain regions remote from the confirmed primary lesion [5,17,24,32] without correlating changes on computed tomographic or MR images [20,38]. Diffusion tensor imaging (DTI) [2,14,34] and localized proton MRS provided subtle hints towards remote infiltration of GBM cells [4,14,18]. This work investigated the use of DTI and corresponding metrics as putative indicators of the invasiveness of malignant brain tumors.

Material and methods

The local ethics committee approved this work according to the Declaration of Helsinki. Written informed consent was obtained from all patients and control subjects. Prospectively, over a time period of 2 years pre-operative DTI was performed in all cases of suspected brain tumor. Only patients with newly diagnosed and post-operative definite histopathological confirmation of malignant brain tumor (astrocytoma WHO grade III or glioblastoma WHO grade IV) were included if there was no history of previous malignancies. Healthy age- and sex-matched volunteers without any relevant medical history, especially tumor or systemic chemotherapy, served as normal controls – patients and volunteers were matched on an individual basis. Data analyses were performed retrospectively.

Two neuroradiologists blinded to the study (J.H.B., A.M.) reviewed the clinical MR images and ruled out MRI evidence of tumor infiltration of the hemisphere contralateral to the tumor or other pathologies (e.g. malformations, enlarged perivascular spaces, calcifications or blood remnants). The standard clinical MRI protocol comprised T2, FLAIR, DWI, and T1 sequences without and with contrast agent. An extra set of T2w and PDw images was acquired from the volunteers to rule out relevant abnormalities. Minor unspecific or microvascular signal alterations of the white matter usually referred to as "age related" (Fazekas scale grade 1 [8]) were present in some patients and controls as well and were not excluded if there was no history of related symptoms and if the lesions did not exceed an estimated 10% of the complete ROI.

Magnetic resonance imaging

All examinations were performed on the same 3 Tesla-MR system (Magnetom Trio, Siemens, Erlangen/Germany). Anatomical imaging included T1-weighted three-dimensional fast low-angle shot (FLASH) sequence (time-to-repetition TR 11 ms; time-to-echo TE 4.9 ms; flip angle 15°; isotropic image resolution $1 \times 1 \times 1$ mm^3). Diffusion tensor imaging employed single-shot stimulated echo acquisition mode (STEAM) MRI without diffusion gradients and with 24 different diffusion gradient directions (b-value 1000 s/mm^2, 38 axial sections, 3 acquisitions) at $2.2 \times 2.2 \times 2.2$ mm^3 image resolution. For further details see [28].

STEAM MRI acquisition is negligibly sensitive to magnetic field inhomogeneity, so the undistorted STEAM images as well as the resulting fractional anisotropy (FA) maps and apparent diffusion coefficient (ADC) maps are spatially congruent to the anatomical images. Without the need for a co-registration or alignment technique, which is usually accompanied by a certain degree of blurring, the present work allowed for a direct digital superposition of corresponding data matrices [13]. After preprocessing applying a Neeman correction [25] region-of-interest (ROI) measurements were performed on FA and ADC maps applying the dedicated software package *effective Diffusion Coefficient Navigator* (DeffCoN, for details see [23]) [3,6,12,13]. Each ROI was manually defined first on the anatomic images (Fig. 1) and subsequently confirmed on FA and ADC maps: The ROI "Hemisphere$_C$" refers to the normal appearing white matter (NAWM) of the cerebral hemisphere contralateral to the tumor 2 mm cranial to the lateral ventricle preventing partial volume artifacts. The ROI "ROI$_C$" denotes only the white matter in the contralateral hemisphere in an area mirroring the tumor site on the section with the largest tumor extends. ROI$_C$ was manually drawn to ensure confinement to white matter, since a simple mirror of the tumor would have included grey matter and/or CSF. In addition, the data from the tumor

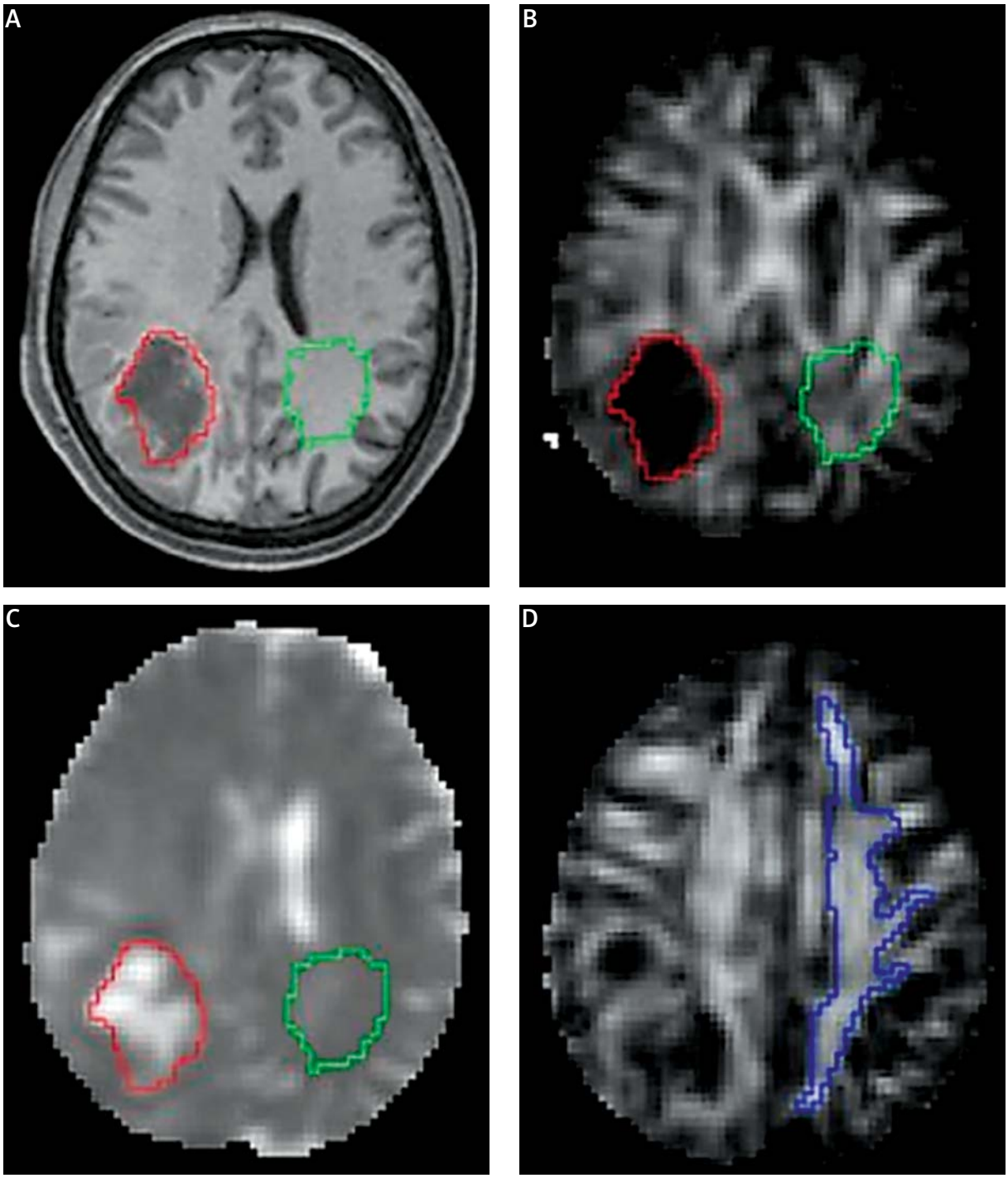

Fig. 1. A) Axial section of the 3D T1-weighted data set, **B)** FA map, **C)** ADC map, **D)** FA map 2 mm cranial of the left ventricle. The tumor is surrounded by a red line. A green line defines the ROI_C in the contralateral hemisphere mirroring the tumor; the blue line defines the $Hemisphere_C$ in the white matter of the contralateral hemisphere (**D**).

location (ROI of "tumor") were acquired in a similar manner. The control ROIs were placed in both hemispheres of the age- and sex-matched controls in the same anatomical location as the patients' ROIs. Then the mean of both control ROIs was compared to the patients' data. Distinct emphasis was put on

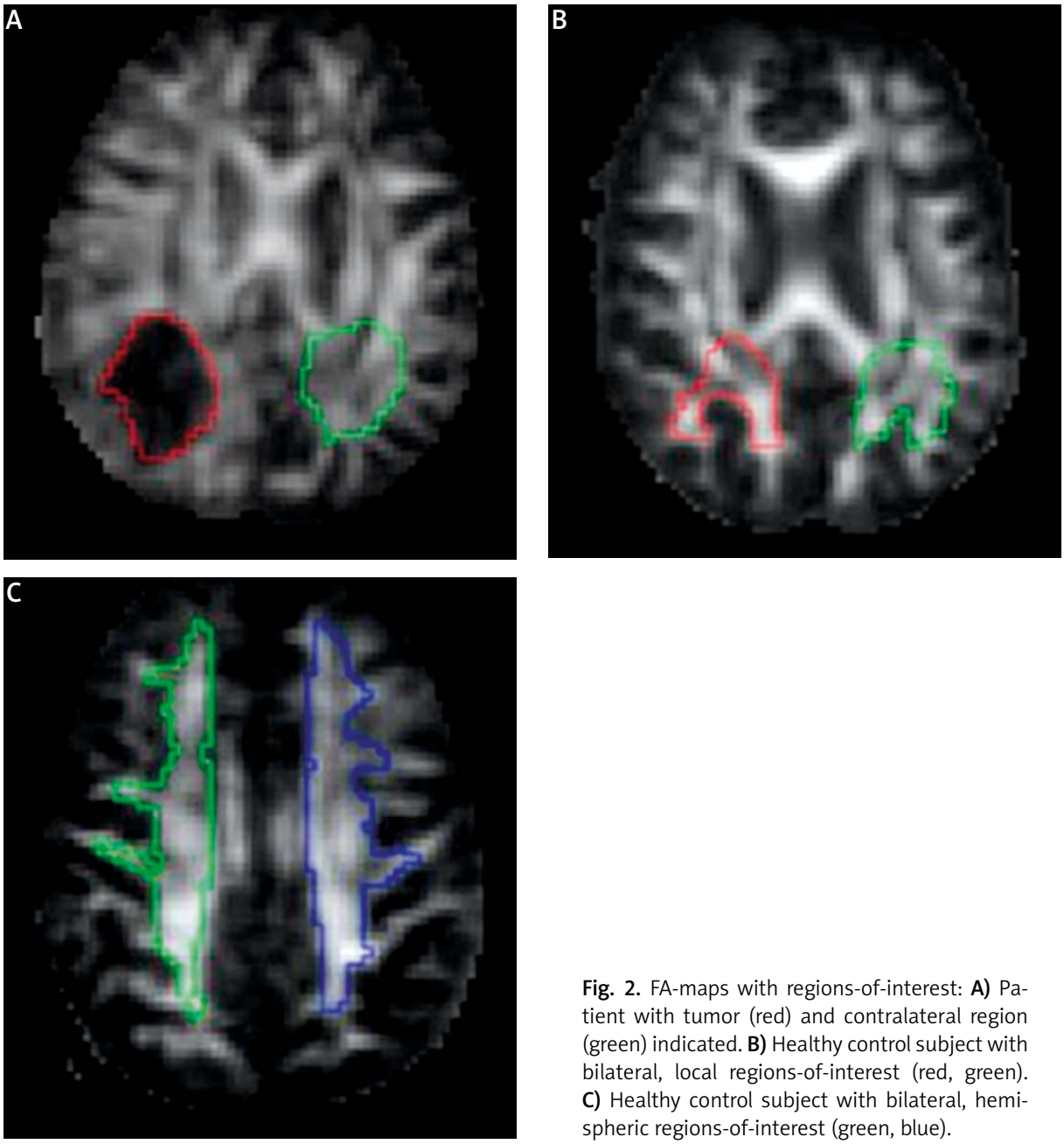

Fig. 2. FA-maps with regions-of-interest: **A)** Patient with tumor (red) and contralateral region (green) indicated. **B)** Healthy control subject with bilateral, local regions-of-interest (red, green). **C)** Healthy control subject with bilateral, hemispheric regions-of-interest (green, blue).

preventing partial volume effects, so that in cases of uncertainty the ROI was diminished and safety margins were considered. Differences in brain size or white matter volume resulted in minor ROI volume differences. The positioning was performed (T.G.) after adequate training and under supervision of an experienced neuroradiologist (K.K.). The person positioning the ROI and the supervising neuroradiologist were aware of the purpose of the study.

Statistical analyses

ADC and FA values of the patient group and the matched control group were compared using unpaired Student's *t*-tests. Additionally, intra-individual differences between the study parameters ROI_C vs. $Hemisphere_C$ were analyzed by paired *t*-tests, both for the patient group and the control group. The significance level was generally set to $p < 0.05$.

Results

Fifty-two patients were scanned according to the MRI protocol. Sixteen did not match the inclusion criteria and had to be excluded (3 patients with lymphoma, 6 with metastasis and 7 with low-grade tumors: 5 WHO II, 2 WHO I). One patient with tumor spread into the contralateral hemisphere was also excluded. One patient terminated the examination intentionally and 3 had to be excluded because of motion artifacts.

The analysis comprised 31 patients who completed the MRI scan and fulfilled the inclusion criteria: 13 females, 18 males; mean age 56.9 years (22-77 years). The post-operative neuropathological diagnosis was astrocytoma WHO grade III in 8 cases and glioblastoma multiforme WHO grade IV in 23 cases. DTI datasets of 31 healthy age- and sex-matched volunteers served as the control (mean age 57.3 years [23-81 years]).

The FA values were significantly lower in the NAWM ($Hemisphere_C$) of the tumor patients compared to controls ($p < 0.01$). Accordingly, the ADC values for NAWM in the contralateral hemisphere were elevated ($p < 0.01$). This finding was particularly pronounced in the area ROI_C mirroring the obvious tumor localization (Table I).

In the healthy controls the study parameters $Hemisphere_C$ and ROI_C showed no significant intra-individual differences (Table II), and the same applied for the FA values in the tumor patients ($p = 0.55$). However, in the tumor patients the ADC values of ROI_C were significantly higher compared to the ADC values of $Hemisphere_C$ ($p < 0.01$).

Discussion

Glioma cells initially infiltrate or spread microinvasively between and around neurons and pene-

Table I. Comparison of patients versus controls

Study parameter	Patients	Controls	Difference$	*p*-value*
	Mean (SD)	Mean (SD)	Mean (SD)	
Age (years)	56.9 (14.2)	57.3 (13.9)	–0.3 (7.1)	0.91
FA of ipsilateral tumor location#	0.077 (0.034)	0.285 (0.033)	–0.208 (0.017)	**< 0.01**
FA of contralateral ROI_C§	0.253 (0.040)	0.285 (0.033)	–0.033 (0.019)	**< 0.01**
FA of contralateral $Hemisphere_C$&	0.258 (0.028)	0.283 (0.018)	–0.025 (0.012)	**< 0.01**
ADC of ipsilateral tumor location#	1.357 (0.365)	0.724 (0.053)	0.632 (0.132)	**< 0.01**
ADC of contralateral ROI_C§	0.793 (0.093)	0.724 (0.053)	0.068 (0.038)	**< 0.01**
ADC of contralateral $Hemisphere_C$&	0.735 (0.045)	0.706 (0.035)	0.029 (0.020)	**< 0.01**

ADC – apparent diffusion coefficient (in units of 10^{-3} mm^2/s), FA – fractional anisotropy
*$ – mean difference of the patient group minus the control group, * – the patient and control groups were compared by unpaired t-tests, with significant differences (p < 0.05) printed in bold, & – $Hemisphere_C$ refers to the normal appearing white matter (NAWM) of the cerebral hemisphere contralateral to the tumor, 2 mm cranial to the lateral ventricle, § – ROI_C denotes only the white matter in the contralateral hemisphere in an area mirroring the tumor site on the slide with the largest tumor extent, # – in each patient the "tumor location" was mirrored to a similar anatomical region in the corresponding matched control*

Table II. Intra-individual comparison of $Hemisphere_C$ versus ROI_C

Study parameter	$Hemisphere_C$&	ROI_C§	Difference$	*p*-value*
	Mean (SD)	Mean (SD)	Mean (SD)	
FA in patients#	0.258 (0.028)	0.253 (0.040)	0.005 (0.016)	0.55
ADC in patients#	0.735 (0.045)	0.793 (0.093)	–0.058 (0.034)	**< 0.01**
FA in controls§	0.283 (0.018)	0.285 (0.033)	–0.003 (0.014)	0.70
ADC in controls§	0.706 (0.035)	0.724 (0.053)	–0.018 (0.019)	0.07

ADC – apparent diffusion coefficient (in units of 10^{-3} mm^2/s), FA – fractional anisotropy
*& – $Hemisphere_C$ refers to the normal appearing white matter (NAWM) of the cerebral hemisphere contralateral to the tumor, 2 mm cranial to the lateral ventricle, § – ROI_C denotes only the white matter in the contralateral hemisphere in an area mirroring the tumor site on the slide with the largest tumor extent, $ – mean difference of both study parameters ($Hemisphere_C$ minus ROI_C), * – the study parameters $Hemisphere_C$ versus ROI_C were compared by paired t-tests, with significant values (p < 0.05) printed in bold*

trate into the fiber tracts of the white matter. In early stages, tumor infiltration leads to increased cellularity without destruction of neurons, and to neovascularization [29]. Diffusion tensor imaging metrics are sensitive to changes of fiber tract architecture on a microscopic level [26,34]. Glioma cells in the early invasion stages cause local displacement of parenchyma without neuronal damage [26], resulting in increased ADC values analogous to the characteristics of low-grade gliomas [7]. In an animal model lower FA and higher perpendicular diffusivity were demonstrated in the infiltration zone of a glioblastoma xenograft compared to normal white matter of the same animal [37]. Inglese *et al.* found an increase of the ADC in the contralateral cerebral hemisphere of glioma patients [14]. A negative correlation of cell number and percentage of tumor infiltration with FA was reported by other groups [30,33]. Accordingly, a low FA value in the hemisphere contralateral to the tumor, as found in the present work, is compatible with early stages of tumor infiltration. In the further course of disease, nerve cells may be destroyed and replaced by tumor cells [29], resulting in an ADC decrease [11] and an FA increase [1]. The latter finding might not be expected to be a specific sign of early tumor formation, because the FA is regarded as an unspecific parameter for fiber tract integrity. However, there is a certain order in tumor cell architecture of vital glioblastoma tissue that causes an increase of FA and kurtosis [27,37].

Glioma cell invasion depends on destruction of extracellular matrix components as well as on penetration between adjacent normal brain structures [35]. This causes an increase in diffusivity and thus facilitates an increase of the ADC value. Furthermore, the growth of a tumor in the CNS is associated with a disturbance of the blood-brain barrier, which leads to a vasogenic edema and an increase in parenchymal water content, which in turn increases the extracellular space and the tissue ADC value [21].

In the present study, in the tumor patients increased ADC values were more pronounced in the parenchyma mirroring the tumor area (ROI_C) than in the entire contralateral hemisphere ($Hemisphere_C$). The corresponding FA differences were not significant. The ADC diffusion values underscore a mainly local effect and so make a uniform global brain edema improbable. The observed constellation may therefore be interpreted as infiltrating malignant cells at the time of MRI, in concordance with the previously described invasion pattern of malignant glioma cells along the fiber tracts of white matter [16]. The more pronounced ADC changes in ROI_C suggest a preference of tumor spread to the corresponding mirrored contralateral brain parenchyma before expanding into the entire contralateral hemisphere ($Hemisphere_C$). A possible explanation would be spreading along the commissural tracts. This is in line with previous DTI studies [19,22] and the observation that remote tumor cells histopathologically match the primary glioma [32].

Abnormal FA or ADC values are not a proof of malignant transformation as they cannot differentiate between tumor and edema [31]. Apparent diffusion coefficient may be influenced by several parameters such as cellular density, existence and distribution of vasogenic edema, and tissue hypoxia [11]. The results in this study may, to some extent, also be attributed to diaschisis, which refers to metabolic and functional changes remote from the origin but communicating with the damaged focus via anatomical structures [36]. However, previous MRS findings in normal appearing white matter in tumor patients indicate the presence of proliferative processes [18].

The present results add further evidence of alterations of normal appearing brain parenchyma in the cerebral hemisphere contralateral to a malignant brain tumor. In the context of previous histopathological studies this effect may be interpreted as an indication of malignant cells. In the present study, however, no neuropathological data were collected to prove this hypothesis.

Conclusion

In patients with previously untreated anaplastic astrocytoma or glioblastoma, an increase of the apparent diffusion coefficient (ADC) and a reduction of fractional anisotropy (FA) were found in the brain parenchyma of the hemisphere contralateral to the tumor localization. In the absence of visible MRI abnormalities, this may be an early indicator of microstructural changes of the NAWM attributed to malignant brain tumor.

Disclosure

The authors (K.K., J.H.B. and P.D.) were supported by the Volkswagen Stiftung (Grants ZN1635 and ZN 2193).

Authors report no conflict of interest.

References

1. Beppu T, Inoue T, Shibata Y, Yamada N, Kurose A, Ogasawara K, Ogawa A, Kabasawa H. Fractional anisotropy value by diffusion tensor magnetic resonance imaging as a predictor of cell density and proliferation activity of glioblastomas. Surg Neurol 2005; 63: 56-61.
2. Bobek-Billewicz B, Stasik-Pres G, Majchrzak K, Senczenko W, Majchrzak H, Jurkowski M, Poletek J. Fibre integrity and diffusivity of the pyramidal tract and motor cortex within and adjacent to brain tumour in patients with or without neurological deficits. Folia Neuropathol 2011; 49: 262-270.
3. Boretius S, Michaelis T, Tammer R, Ashery-Padan R, Frahm J, Stoykova A. In vivo MRI of altered brain anatomy and fiber connectivity in adult pax6 deficient mice. Cereb Cortex 2009; 19: 2838-2847.
4. Busch M, Liebenrodt K, Gottfried S, Weiland E, Vollmann W, Mateiescu S, Winter S, Lange S, Sahinbas H, Baier J, van Leeuwen P, Gronemeyer D. Influence of brain tumors on the MR spectra of healthy brain tissue. Magn Reson Med 2011; 65: 18-27.
5. de Bouard S, Christov C, Guillamo JS, Kassar-Duchossoy L, Palfi S, Leguerinel C, Masset M, Cohen-Hagenauer O, Peschanski M, Lefrancois T. Invasion of human glioma biopsy specimens in cultures of rodent brain slices: a quantitative analysis. J Neurosurg 2002; 97: 169-176.
6. Dreha-Kulaczewski SF, Helms G, Dechent P, Hofer S, Gartner J, Frahm J. Serial proton MR spectroscopy and diffusion tensor imaging in infantile Balo's concentric sclerosis. Neuroradiology 2009; 51: 113-121.
7. Essig M, Giesel F, Stieltjes B, Weber MA. Functional imaging for brain tumors (perfusion, DTI and MR spectroscopy). Radiologe 2007; 47: 513-519 [in German].
8. Fazekas F, Chawluk JB, Alavi A, Hurtig HI, Zimmerman RA. MR signal abnormalities at 1.5 T in Alzheimer's dementia and normal aging. AJR Am J Roentgenol 1987; 149: 351-356.
9. Gallego JM, Barcia JA, Barcia-Marino C. Fatal outcome related to carmustine implants in glioblastoma multiforme. Acta Neurochir (Wien) 2007; 149: 261-265.
10. Giese A, Bjerkvig R, Berens ME, Westphal M. Cost of migration: invasion of malignant gliomas and implications for treatment. J Clin Oncol 2003; 21: 1624-1636.
11. Hartmann M, Junkers R, Herold-Mende C, Ahmadi R, Heiland S. Pseudonormalization of diffusion weighted images: magnetic resonance imaging in an animal model (C6-glioma). Rofo 2005; 177: 114-118 [in German].
12. Hofer S, Frahm J. Topography of the human corpus callosum revisited – comprehensive fiber tractography using diffusion tensor magnetic resonance imaging. Neuroimage 2006; 32: 989-994.
13. Hofer S, Karaus A, Frahm J. Reconstruction and dissection of the entire human visual pathway using diffusion tensor MRI. Front Neuroanat 2010; 4: 15.
14. Inglese M, Brown S, Johnson G, Law M, Knopp E, Gonen O. Whole-brain N-acetylaspartate spectroscopy and diffusion tensor imaging in patients with newly diagnosed gliomas: a preliminary study. AJNR Am J Neuroradiol 2006; 27: 2137-2140.
15. Jaskolski DJ, Fortuniak J, Majos A, Gajewicz W, Papierz W, Liberski PP, Sikorska B, Stefanczyk L. Magnetic resonance spectroscopy in intracranial tumours of glial origin. Neurol Neurochir Pol 2013; 47: 438-449.
16. Johnson PC, Hunt SJ, Drayer BP. Human cerebral gliomas: correlation of postmortem MR imaging and neuropathologic findings. Radiology 1989; 170: 211-217.
17. Kageji T, Nagahiro S, Uyama S, Mizobuchi Y, Toi H, Nakamura M, Nakagawa Y. Histopathological findings in autopsied glioblastoma patients treated by mixed neutron beam BNCT. J Neurooncol 2004; 68: 25-32.
18. Kallenberg K, Bock HC, Helms G, Jung K, Wrede A, Buhk JH, Giese A, Frahm J, Strik H, Dechent P, Knauth M. Untreated glioblastoma multiforme: increased myo-inositol and glutamine levels in the contralateral cerebral hemisphere at proton MR spectroscopy. Radiology 2009; 253: 805-812.
19. Kallenberg K, Goldmann T, Menke J, Strik H, Bock HC, Stockhammer F, Buhk JH, Frahm J, Dechent P, Knauth M. Glioma infiltration of the corpus callosum: early signs detected by DTI. J Neurooncol 2013; 112: 217-222.
20. Kelly PJ, Daumas-Duport C, Kispert DB, Kall BA, Scheithauer BW, Illig JJ. Imaging-based stereotaxic serial biopsies in untreated intracranial glial neoplasms. J Neurosurg 1987; 66: 865-874.
21. Kono K, Inoue Y, Nakayama K, Shakudo M, Morino M, Ohata K, Wakasa K, Yamada R. The role of diffusion-weighted imaging in patients with brain tumors. AJNR Am J Neuroradiol 2001; 22: 1081-1088.
22. Krishnan AP, Asher IM, Davis D, Okunieff P, O'Dell WG. Evidence that MR diffusion tensor imaging (tractography) predicts the natural history of regional progression in patients irradiated conformally for primary brain tumors. Int J Radiat Oncol Biol Phys 2008; 71: 1553-1562.
23. Küntzel M. Parallele Datenakquisition zur Beschleunigung diffusions-gewichteter Kernspintomographie mit stimulierten Echos. Göttingen Georg-August-Universität, 2007.
24. Matsukado Y, Maccarty CS, Kernohan JW. The growth of glioblastoma multiforme (astrocytomas, grades 3 and 4) in neurosurgical practice. J Neurosurg 1961; 18: 636-644.
25. Neeman M, Freyer JP, Sillerud LO. A simple method for obtaining cross-term-free images for diffusion anisotropy studies in NMR microimaging. Magn Reson Med 1991; 21: 138-143.
26. Price SJ, Burnet NG, Donovan T, Green HA, Pena A, Antoun NM, Pickard JD, Carpenter TA, Gillard JH. Diffusion tensor imaging of brain tumours at 3T: a potential tool for assessing white matter tract invasion? Clin Radiol 2003; 58: 455-462.
27. Raab P, Hattingen E, Franz K, Zanella FE, Lanfermann H. Cerebral gliomas: diffusional kurtosis imaging analysis of microstructural differences. Radiology 2010; 254: 876-881.
28. Rieseberg S, Merboldt KD, Kuntzel M, Frahm J. Diffusion tensor imaging using partial Fourier STEAM MRI with projection onto convex subsets reconstruction. Magn Reson Med 2005; 54: 486-490.
29. Scherer HJ. Structural development in gliomas. Am J Cancer 1938; 34: 333-351.
30. Schluter M, Stieltjes B, Hahn HK, Rexilius J, Konrad-Verse O, Peitgen HO. Detection of tumour infiltration in axonal fibre

bundles using diffusion tensor imaging. Int J Med Robot 2005; 1: 80-86.
31. Server A, Kulle B, Maehlen J, Josefsen R, Schellhorn T, Kumar T, Langberg CW, Nakstad PH. Quantitative apparent diffusion coefficients in the characterization of brain tumors and associated peritumoral edema. Acta Radiol 2009; 50: 682-689.
32. Silbergeld DL, Chicoine MR. Isolation and characterization of human malignant glioma cells from histologically normal brain. J Neurosurg 1997; 86: 525-531.
33. Stadlbauer A, Ganslandt O, Buslei R, Hammen T, Gruber S, Moser E, Buchfelder M, Salomonowitz E, Nimsky C. Gliomas: histopathologic evaluation of changes in directionality and magnitude of water diffusion at diffusion-tensor MR imaging. Radiology 2006; 240: 803-810.
34. Stieltjes B, Schluter M, Didinger B, Weber MA, Hahn HK, Parzer P, Rexilius J, Konrad-Verse O, Peitgen HO, Essig M. Diffusion tensor imaging in primary brain tumors: reproducible quantitative analysis of corpus callosum infiltration and contralateral involvement using a probabilistic mixture model. Neuroimage 2006; 31: 531-542.
35. Tysnes BB, Mahesparan R. Biological mechanisms of glioma invasion and potential therapeutic targets. J Neurooncol 2001; 53: 129-147.
36. von Monakow C. Die Lokalisation im Grosshirn und der Abbau der Funktion durch kortikale Herde. J.F. Bergmann, Wiesbaden 1914, p. 1033.
37. Wang S, Zhou J. Diffusion tensor magnetic resonance imaging of rat glioma models: a correlation study of MR imaging and histology. J Comput Assist Tomogr 2012; 36: 739-744.
38. Watanabe M, Tanaka R, Takeda N. Magnetic-resonance-imaging and histopathology of cerebral gliomas. Neuroradiology 1992; 34: 463-469.

Original paper

Folia Neuropathologica

Expression of HIF-1 regulated proteins vascular endothelial growth factor, carbonic anhydrase IX and hypoxia inducible gene 2 in hemangioblastomas

Mei Li, Jie Song, Peter Pytel

Department of Pathology, University of Chicago, Chicago, USA

Folia Neuropathol 2014; 52 (3): 234-242 DOI: 10.5114/fn.2014.45564

Abstract

Introduction: *Hemangioblastomas occur as sporadic or as von Hippel-Lindau syndrome (VHL) associated tumors. In both settings, activation of the VHL-HIF-1 (hypoxia induced factor) pathway is thought to be important in tumor biology.*

Material and methods: *We performed immunohistochemical studies on 23 hemangioblastomas, 13 meningiomas and 4 hemangiopericytomas to evaluate expression of the VHL-HIF-1 regulated proteins vascular endothelial growth factor (VEGF), carbonic anhydrase IX (CAIX) and hypoxia inducible gene 2 (HIG-2).*

Results: *Hemangioblastomas showed significantly higher expression of CAIX and VEGF than the other tested tumors. They showed strong membranous expression of CAIX in a pattern identical to that observed in clear cell renal cell carcinomas (CCRCC). Interestingly, hemangioblastomas lacked significant reactivity for HIG-2.*

Conclusions: *The VHL-HIF-1 regulated genes VEGF and CAIX are expressed in hemangioblastomas but significant HIG-2 expression is not observed. Carbonic anhydrase IX staining in particular may be a helpful marker of hemangioblastomas but does not aid in the distinction from CCRCC.*

Key words: *hemangioblastoma, von Hippel-Lindau, carbonic anhydrase IX.*

Introduction

Hemangioblastomas are highly vascular tumors. Their two main components are prominent vascular channels and the so-called stromal cells. The latter are regarded as the true lesional cells but are of unclear histogenesis [11,29]. Common anatomic sites include the cerebellum (over 60% to 75%), spinal cord and brainstem [3,7,21].

Hemangioblastomas can be associated with the autosomal dominant familial tumor syndrome von Hippel-Lindau syndrome (VHL) or they can be sporadic [3,29].

Von Hippel-Lindau syndrome is a hereditary cancer syndrome. Affected patients have deactivating mutations of the VHL gene. This leads to an increased risk of developing a number of tumors including hemangioblastoma, clear cell renal cell carcinoma (CCRCC) and endolymphatic sac tumors [10,21]. Clear cell renal cell carcinomas are the leading cause of death in VHL patients [29]. Overall, some 20% to 30% of hemangioblastoma cases

Communicating author:

Peter Pytel, MD, Department of Pathology, MC6101, Room E609, 5841 S. Maryland Ave, Chicago, IL 60637, USA, phone: (773) 795-6751, fax: (773) 702-1243, e-mail: peter.pytel@uchospitals.edu

may be VHL syndrome associated [7]. Sporadic hemangioblastomas and sporadic CCRCC also commonly show bi-allelic VHL gene inactivation [15,16,23,29].

The VHL gene product pVHL is a master regulator of HIF-1α (hypoxia inducible factor-1 alpha). HIF-1 is a ubiquitously expressed heterodimeric basic-helix-loop-helix transcription factor composed of the highly unstable HIF-1α and the stable HIF-1β subunit [16]. HIF-1α is the main regulatory subunit. It helps to orchestrate the cellular response to hypoxic conditions. pVHL, elongin B and elongin C form the VBC complex that is a key regulator of the HIF-1α pathway [23]. Under normoxic conditions pVHL and the VBC complex direct HIF-1α for polyubiquitination and degradation. The oxygen dependent nature of this reaction results from the fact that pVHL only recognizes HIF-1α after oxygen-level sensitive hydroxylation of HIF-1α. Deactivating VHL mutations result in the abnormal accumulation of HIF-1α and the subsequent over-expression of its downstream targets [15]. These target genes include carbonic anhydrase IX (CAIX), vascular endothelial growth factor (VEGF), erythropoietin, glucose transporters and glycolytic enzymes [26,29].

Carbonic anhydrase IX (CAIX) is an isoenzyme of the α-carbonic anhydrase family, which regulates intra- and extracellular pH by the reversible hydration of CO_2 to form HCO^{3-} and protons [4]. Hypoxia is the main mechanism to induce expression of CAIX. Transcriptional activation of CAIX by hypoxia is mediated by HIF-1 via binding to the hypoxia-responsive element (HRE). In physiological conditions various normal tissues express CAIX at very low levels. It is overexpressed in CCRCC and under hypoxic conditions such as tissues around areas of necrosis. VHL-HIF-CAIX and VHL-HIF-VEGF pathways are thought to be important in the tumorigenesis of CCRCC in patients with or without VHL syndrome [5,12,13]. In CCRCC pVHL inactivation is found in preneoplastic renal tissue, suggesting that it represents an early step in carcinogenesis [15]. Induction of CAIX in tumor cells might contribute to an aggressive phenotype by promoting cell proliferation, invasion and acid tolerance [12]. Vortmeyer *et al.* looked at "tumorlet"-like microscopic spinal cord lesions in autopsy samples of VHL patients and were able to show activation of the VHL-HIF-CAIX pathway in this setting by immunohistochemical studies [27].

Strong uniform membranous expression of CAIX is characteristic of CCRCC and often used as a diagnostic marker. Hypoxia inducible gene-2 (HIG-2) is another downstream target upregulated by the VHL-HIF-1 pathway and has recently been described as another marker of CCRCC [1,6,25]. One study suggested that HIG-2 is a novel lipid droplet protein that can stimulate intracellular lipid accumulation [6].

In most cases hemangioblastoma is a diagnosis that can be made based solely on the H&E stain. In some instances and especially with fixation or thermal artifacts, the morphologic appearance of hemangioblastomas may mimic that of metastatic CCRCC and some primary intracranial tumors such as certain meningioma variants [22,24]. The differential diagnosis between metastatic CCRCC and hemangioblastoma is particularly critical in VHL syndrome patients since they are at increased risk of developing both of these tumors. This is illustrated by reports of VHL patients who were found to have metastatic carcinoma within CNS hemangioblastomas [8,14,19]. A few markers have been suggested as helpful in the diagnosis of hemangioblastoma and in distinguishing hemangioblastoma from CCRCC. Inhibin-A is expressed in 87% to 100% of hemangioblastomas [2,9,22,28]. Pax2 and Pax8 were shown to be negative in hemangioblastomas but positive in the vast majority of CCRCC [2,22]. Aquaporin 1 was found in nearly 100% of hemangioblastomas but only 18% of CCRCC [24,28]. Additionally the stromal cells are also reported to express vimentin (100%), CD56/NCAM (100%), VEGF (100%), S-100 (82%), Ezrin (59%), and CD99 (88%). Up to 36% of hemangioblastomas may be positive for EMA and some are positive for GFAP [11,28]. CD10 has been reported to be expressed in 12% of hemangioblastomas [22].

In the present study we conducted immunohistochemical staining of hemangioblastomas, hemangiopericytomas, and meningiomas including clear cell meningioma, microcystic meningioma as well as angiomatous meningioma. The aim was to address the following hypotheses: (A) Hemangioblastomas may express HIF-1 regulated proteins such as CAIX, VEGF and HIG-2 in a pattern similar to other VHL syndrome associated tumors, particularly CCRCC. (B) These HIF-1 regulated proteins may be useful diagnostic markers for distinguishing hemangioblastomas from possible mimics.

Material and methods

This study was approved by the Institutional Review Board of the University of Chicago Medical Center. A total of 41 intracranial tumors were collected from the archive of the Pathology Department at the University of Chicago Medical Center. These included 23 hemangioblastomas (3 with documented association with VHL syndrome), 14 meningiomas, and 4 hemangiopericytomas (Table I). Microcystic (3), angiomatous (3) and clear cell (2) variants of meningioma were included. All the tissues were fixed in 10% neutrally buffered formalin and paraffin embedded. Sections were cut at 4 µm and processed in batches for immunohistochemical staining using monoclonal anti-CAIX (obtained from Novus Biologicals, Littleton, Colorado, USA), monoclonal anti-VEGF (Santa Cruz Biotechnology, Santa Cruz, California, USA) and anti-HIG 2 (Novocastra/Leica Microsystems, Leica Microsystems, Buffalo Grove, Illinois, USA) antibodies.

Immunohistochemical staining was performed according to standard protocols. Briefly, sections were first deparaffinized and rehydrated, followed by antigen retrieval by heating the sections in EDTA buffer at pH 9 for 15 minutes. Endogenous peroxidase activity was removed by incubating the sections with 3% H_2O_2 in methanol for 5 minutes. Non-specific binding was minimized by incubation with Protein Block (DAKO, Carpinteria, CA) for 20 minutes. After that, the sections were incubated with the primary antibody for 1 hour, followed by the secondary antibody conjugated to a horseradish peroxidase-labeled polymer for 30 minutes. Slides were then developed with 3-30-diaminobenzidine chromogen and counterstained with hematoxylin.

The slides were reviewed and scored independently by two pathologists. Staining extent, staining intensity and subcellular localization were evaluated. The percentage of the tumor areas showing strong (3+), moderate (2+), weak (1+) or negative (0) staining respectively were recorded. The extent of staining was classified as diffuse (≥ 80% area with positive staining) or focal (1-79%) unless further specified.

The staining index was calculated as a single numerical value to summarize and compare the level of staining: the percentage of area with 3+ staining was multiplied by 3, the percentage of area showing 2+ staining was multiplied by 2, and the percentage of area with 1+ staining was multiplied by 1. The sum of these values is the staining index of an individual case [17,18].

Statistical analysis was performed using GraphPad Prism version 6.0 for MacOS X, GraphPad Software, La Jolla California USA. The Kruskal-Wallis test was used to determine whether the observed differences between meningiomas, hemangiopericytomas and hemangioblastomas were statistically significant. Post-test analysis was performed by Dunn's multiple comparison test. This statistical analysis was performed on two parts of the results: (1) the percentage of tumor area showing positive staining of any intensity and (2) the calculated staining index.

Results

The results of the performed immunohistochemical staining are summarized in Table I.

Carbonic anhydrase IX staining

Carbonic anhydrase IX expression was detected in all the examined hemangioblastomas (23/23) with a strong diffuse membranous staining pattern (Figs. 1A-B). This pattern is identical to that described in CCRCC. Carbonic anhydrase IX staining in hemangioblastomas was significantly stronger than in meningiomas and hemangiopericytomas (Kruskal-Wallis: $p < 0.0001$), none of which exhibited any strong membranous staining (Figs. 2A-B). In addition to strong membranous staining all the hemangioblastomas also showed at least focal weak cytoplasmic staining.

In meningiomas of various subtypes, only weak cytoplasmic staining, either focal or diffuse, was observed. The tumor cells of microcystic meningiomas showed focal or diffuse weak cytoplasmic staining, particularly surrounding the microcystic spaces. Angiomatous meningiomas and meningiomas with clear cell features also showed diffuse weak cytoplasmic staining. None of the meningiomas exhibited any significant membranous labeling.

All the hemangiopericytomas showed weak to moderate cytoplasmic staining of CAIX. In one hemangiopericytoma, tumor cells surrounding an area of necrosis exhibited strong membranous staining in a pattern interpreted as being the result of regional hypoxia.

Table I. Summary of immunohistochemical staining. This table summarizes the results for CAIX, VEGF and HIG-2 staining in the analyzed tumors. Six columns are shown for each marker: (1) percentage of tumor area with positive staining, (2) percentage of tumor with negative staining, (3) percentage of tumor with 1+ staining, (4) percentage of tumors with 2+ staining, (5) percentage of tumors with 3+ staining, (6) the calculated staining index. The thirteen meningiomas (M) include two clear cell meningiomas (clear), three microcystic meningiomas (micro) and three angiomatous meningiomas (angio). Four hemangiopericytomas (HPC) and 23 hemangioblastomas were included

	CAIX					VEGF					HIG-2				
	Pos. area (%)	1+ (%)	2+ (%)	3+ (%)	Staining index	Pos. area (%)	1+ (%)	2+ (%)	3+ (%)	Staining index	Pos. area (%)	1+ (%)	2+ (%)	3+ (%)	Staining index
M1	80	60	20	0	100	40	40	0	0	40	0	0	0	0	0
M2	80	60	20	0	100	30	30	0	0	30	0	0	0	0	0
M3	60	60	0	0	60	10	10	0	0	10	0	0	0	0	0
M4	80	40	40	0	120	90	80	10	0	100	0	0	0	0	0
M5	80	20	60	0	140	50	50	0	0	50	0	0	0	0	0
MC6	50	50	0	0	50	40	30	10	0	50					
MC7	80	80	0	0	80	10	10	0	0	10					
MM8	80	80	0	0	80	20	20	0	0	20					
MM9	80	80	0	0	80	20	20	0	0	20					
MM10	80	80	0	0	80	10	10	0	0	10					
MA11	100	20	80	0	180	20	20	0	0	20					
MA12	80	40	40	0	120	10	10	0	0	10					
MA13	80	0	80	0	160	30	30	0	0	30					
HPC1	80	80	0	0	80	40	40	0	0	40	10	10	0	0	10
HPC2	20	20	0	0	20	20	20	0	0	20	80	40	40	0	120
HPC3	20	0	0	20	60	50	30	20	0	70	10	0	0	0	0
HPC4	30	30	0	0	30	70	60	10	0	80	0	0	0	0	0
HBM1	100	20	60	20	200	80	40	40	0	120	0	0	0	0	0
HBM2	100	0	40	60	260	100	20	80	0	180	0	0	0	0	0
HBM3	100	0	30	70	270	80	80	0	0	80	0	0	0	0	0

Table I. Cont.

	CAIX					VEGF					HIG-2				
	Pos. area (%)	1+ (%)	2+ (%)	3+ (%)	Staining index	Pos. area (%)	1+ (%)	2+ (%)	3+ (%)	Staining index	Pos. area (%)	1+ (%)	2+ (%)	3+ (%)	Staining index
HBM4	100	0	20	80	280	100	30	70	0	170	0	0	0	0	0
HBM5	100	10	30	60	250	90	40	50	0	140	20	0	20	0	40
HBM6	100	0	40	60	260	80	40	40	0	120	0	0	0	0	0
HBM7	100	0	0	100	300	80	40	40	0	120	0	0	0	0	0
HBM8	100	10	10	80	270	90	30	60	0	150	0	0	0	0	0
HBM9	100	20	40	40	220	10	0	10	0	20	0	0	0	0	0
HBM10	100	0	0	100	300	90	40	50	0	140	10	0	10	0	20
HBM11	100	0	50	50	250	100	20	80	0	180	0	0	0	0	0
HBM12	100	0	20	80	280	100	20	80	0	180	0	0	0	0	0
HBM13	100	20	20	60	240	100	20	80	0	180	20	0	0	0	0
HBM14	100	20	20	60	240	100	20	80	0	180	0	0	0	0	0
HBM15	100	0	0	100	300	100	50	50	0	150	0	0	0	0	0
HBM16	100	0	0	100	300	100	0	100	0	200	0	0	0	0	0
HBM17	100	0	0	100	300	100	20	80	0	180	0	0	0	0	0
HBM18	100	0	0	100	300	80	20	60	0	140	0	0	0	0	0
HBM19	100	0	100	0	200	100	20	80	0	180	0	0	0	0	0
HBM20	100	0	0	100	300	100	0	80	0	160	0	0	0	0	0
HBM21	100	0	0	100	300	100	20	80	0	180	10	10	0	0	10
HBM22	100	0	0	100	300	100	20	80	0	180	0	0	0	0	0
HBM23	100	0	0	100	300	100	20	80	0	180	0	0	0	0	0

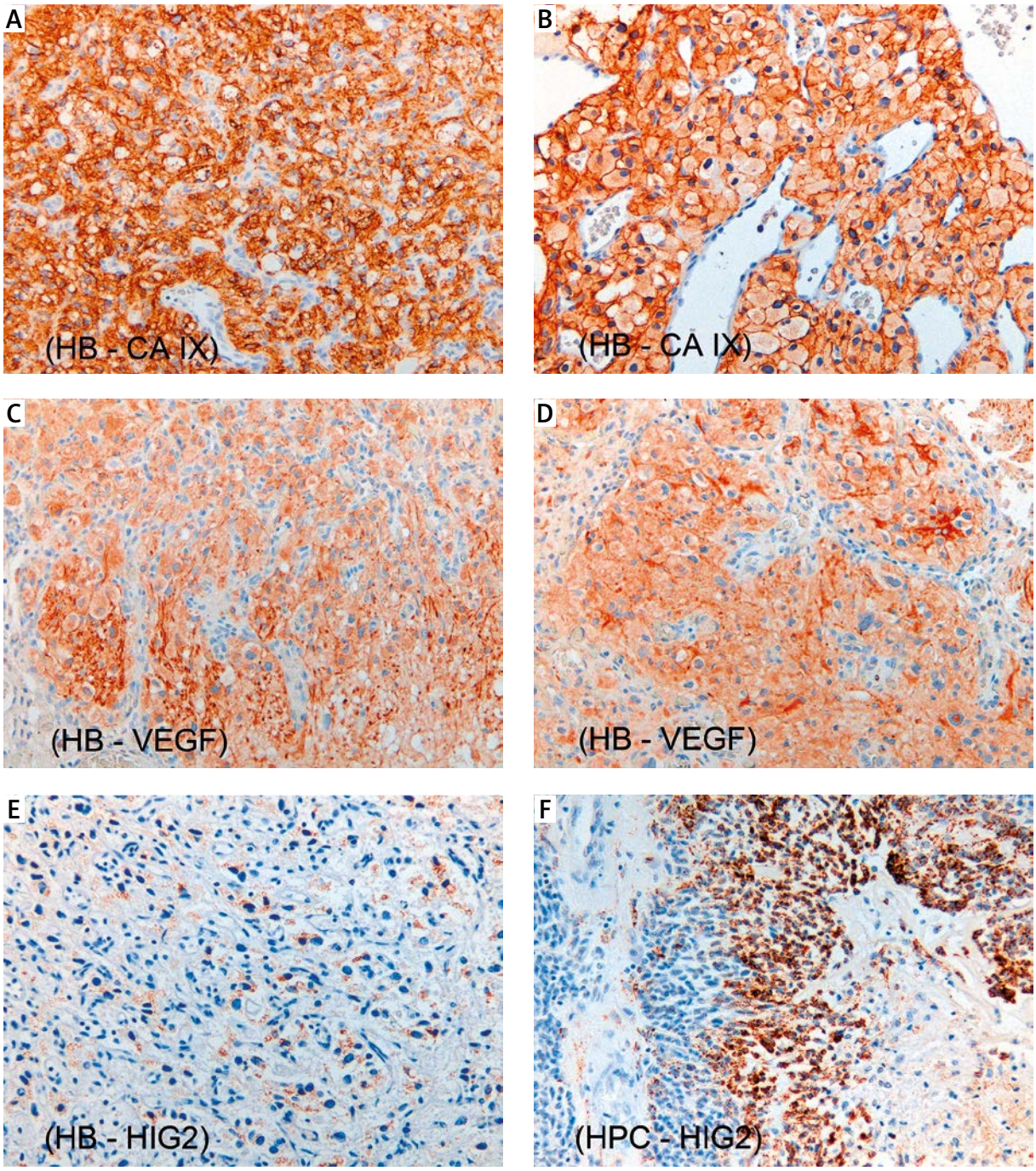

Fig. 1. Representative images of immunohistochemical staining. **A)** and **B)** illustrate staining in hemangioblastomas (HB). In general, these exhibited cytoplasmic staining of variable intensity and strong uniform cell membrane staining. **C)** and **D)** show two examples of VEGF staining in hemangioblastomas (HB). **E)** and **F)** illustrate the lack of significant HIG-2 staining in hemangioblastomas (**E**) and the focal distinct immunoreactivity in a hemangiopericytoma (**F**) around an area of necrosis.

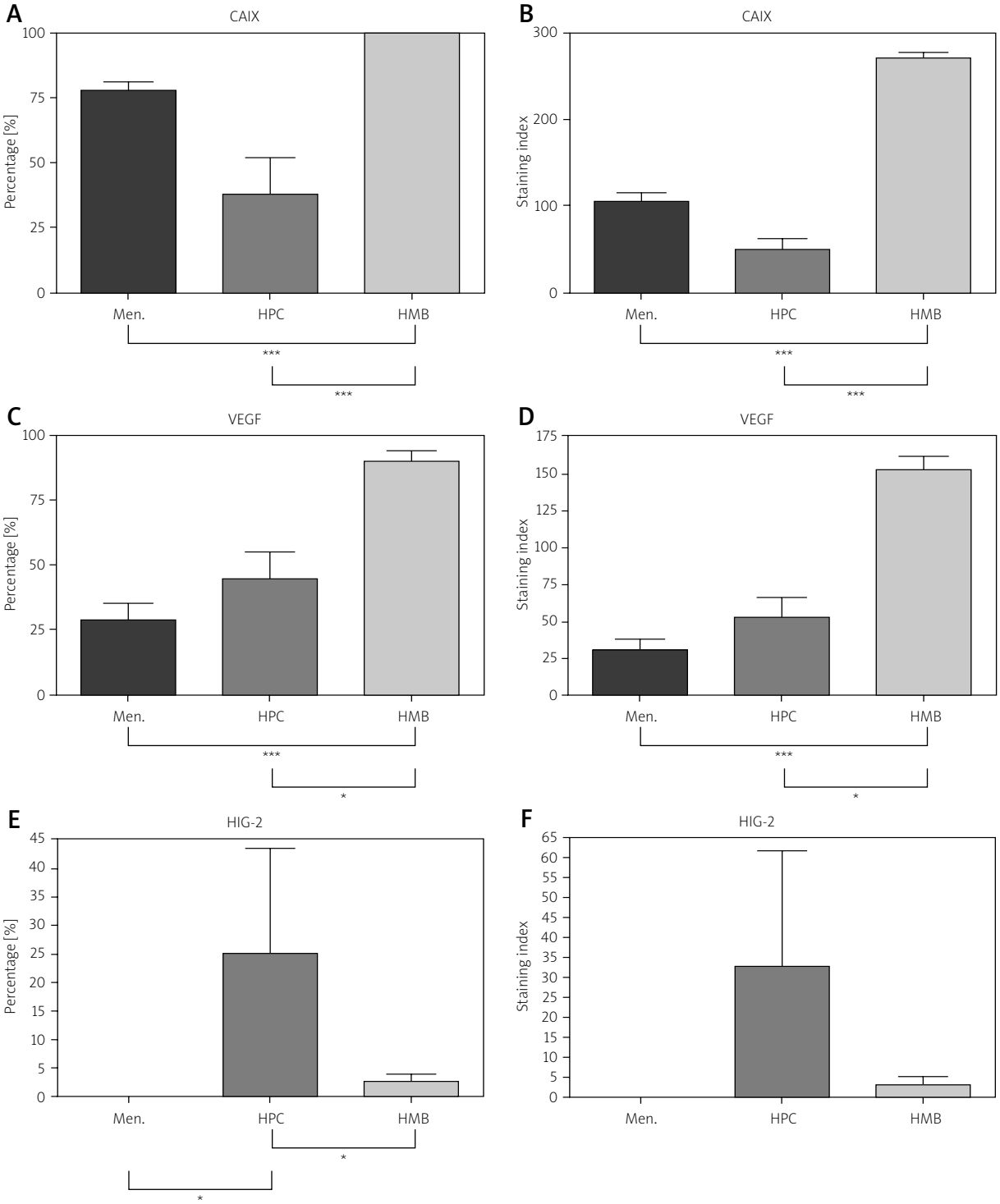

Fig. 2. The graphic representation of the results for CAIX (**A** and **B**), VEGF (**C** and **D**) and HIG-2 (**E** and **F**) include the comparison of two separate features: (1) the percentage of tumor labeled positive for a given marker irrespective of the intensity of staining (**A**, **C** and **E**) and the calculated staining index (**B**, **D** and **F**). The differences illustrated in figures **A**, **B**, **C** and **D** were all statistically significant with a p value of < 0.0001 in the Kruskal-Wallis test. Brackets at the bottom of individual graphs are used to indicate statistical significance in the pairwise comparison (*indicates a p value of 0.05, ***indicates a p value of < 0.001).

Vascular endothelial growth factor staining

All the hemangioblastomas (23/23) showed cytoplasmic staining (Figs. 1C-D). Most hemangioblastomas (17/23) demonstrated diffuse moderate cytoplasmic staining. Overall, hemangioblastomas exhibited significantly stronger VEGF immunoreactivity than the other two types of tumor (Kruskal-Wallis: $p < 0.0001$; see Figs. 2C-D). Most meningiomas (12/14) showed scattered, very focal (< 30% area) weak cytoplasmic staining.

Hypoxia inducible gene 2 staining

Hypoxia inducible gene 2 staining was low in all three types of tumor. Overall, hemangiopericytomas showed slightly higher expression of HIG-2 than hemangioblastomas or meningiomas (Figs. 1E-F). Some hemangiopericytomas showed strong expression of HIG-2 in perinecrotic areas (Fig. 1F). This was interpreted as an internal positive control that supports the adequacy of the stain.

Discussion

It has long been recognized that hemangioblastomas can be associated with polycythemia and with intratumoral extramedullary hematopoiesis [23]. These features have been attributed to erythropoietin overproduction – a sign of VHL-HIF-1 signaling pathway activation. Our study looked at the expression of other hypoxia induced markers. We hypothesized that these would be expressed in hemangioblastomas in analogy to findings in CCRCC and as a result of VHL-HIF-1 signaling pathway activation. Vascular endothelial growth factor expression in hemangioblastomas has been reported by Ishizawa [11]. We have seen similar results and found stronger VEGF expression in hemangioblastomas compared to meningiomas and hemangiopericytomas.

Proescholdt *et al*. conducted a study of CAIX expression in brain tumors of various type. They report strong CAIX staining in the few included cases of hemangioblastomas [20]. However, the staining pattern was not described and the potential diagnostic value was not discussed. We compared the expression of CAIX in hemangioblastomas with some of its potential mimickers. Similar to CCRCC, hemangioblastomas showed strong diffuse membranous expression of CAIX. Based on these results, CAIX cannot be relied on as a marker for establishing a diagnosis of CCRCC when hemangioblastoma is part of the differential diagnosis. Strong staining for CAIX with membranous accentuation is, however, a helpful diagnostic marker in distinguishing hemangioblastoma from other intracranial tumors. In the authors' opinion, CAIX provides more robust labeling of hemangioblastomas than other reported markers, including D2-40 and inhibin A.

Several HIF-1 inducible proteins such as erythropoietin, VEGF and CAIX are expressed in hemangioblastomas. In this context it is interesting to note that HIG-2 [1,6,25], as another hypoxia inducible and HIF-1 regulated protein, did not appear to be expressed in hemangioblastomas even though it has been shown to be a marker of CCRCC. This difference could point to differences in the detailed expression profile of hypoxia inducible genes between CCRCC and hemangioblastomas.

In summary, hemangioblastomas uniformly express VHL-HIF-1 regulated proteins including VEGF and CAIX. A strong membranous staining pattern for CAIX can be a helpful marker of hemangioblastoma in the distinction from other intracranial tumors but cannot be used to exclude the possibility of metastatic CCRCC.

Disclosure

Authors report no conflict of interest.

References

1. Argani P, Hicks J, De Marzo AM, Albadine R, Illei PB, Ladanyi M, Reuter VE, Netto GJ. Xp11 translocation renal cell carcinoma (RCC): extended immunohistochemical profile emphasizing novel RCC markers. Am J Surg Pathol 2010; 34: 1295-1303.
2. Carney EM, Banerjee P, Ellis CL, Albadine R, Sharma R, Chaux AM, Burger PC, Netto GJ. PAX2(–)/PAX8(–)/inhibin A(+) immunoprofile in hemangioblastoma: A helpful combination in the differential diagnosis with metastatic clear cell renal cell carcinoma to the central nervous system. Am J Surg Pathol 2011; 35: 262-267.
3. Catapano D, Muscarella LA, Guarnieri V, Zelante L, D'Angelo VA, D'Agruma L. Hemangioblastomas of central nervous system: molecular genetic analysis and clinical management. Neurosurgery 2005; 56: 1215-1221.
4. Chegwidden WR, Dodgson SJ, Spencer IM. The roles of carbonic anhydrase in metabolism, cell growth and cancer in animals. EXS 2000; 90: 343-363.
5. Clark PE. The role of VHL in clear-cell renal cell carcinoma and its relation to targeted therapy. Kidney Int 2009; 76: 939-945.
6. Gimm T, Wiese M, Teschemacher B, Deggerich A, Schodel J, Knaup KX, Hackenbeck T, Hellerbrand C, Amann K, Wiesener MS, Honing S, Eckardt KU, Warnecke C. Hypoxia-inducible protein 2

is a novel lipid droplet protein and a specific target gene of hypoxia-inducible factor-1. FASEB J 2010; 24: 4443-4458.
7. Glasker S. Central nervous system manifestations in VHL: genetics, pathology and clinical phenotypic features. Fam Cancer 2005; 4: 37-42.
8. Hamazaki S, Nakashima H, Matsumoto K, Taguchi K, Okada S. Metastasis of renal cell carcinoma to central nervous system hemangioblastoma in two patients with von Hippel-Lindau disease. Pathol Int 2001; 51: 948-953.
9. Hoang MP, Amirkhan RH. Inhibin alpha distinguishes hemangioblastoma from clear cell renal cell carcinoma. Am J Surg Pathol 2003; 27: 1152-1156.
10. Horiguchi H, Sano T, Toi H, Kageji T, Hirokawa M, Nagahiro S. Endolymphatic sac tumor associated with a von Hippel-Lindau disease patient: an immunohistochemical study. Mod Pathol 2001; 14: 727-732.
11. Ishizawa K, Komori T, Hirose T. Stromal cells in hemangioblastoma: neuroectodermal differentiation and morphological similarities to ependymoma. Pathol Int 2005; 55: 377-385.
12. Ivanov S, Liao SY, Ivanova A, Danilkovitch-Miagkova A, Tarasova N, Weirich G, Merrill MJ, Proescholdt MA, Oldfield EH, Lee J, Zavada J, Waheed A, Sly W, Lerman MI, Stanbridge EJ. Expression of hypoxia-inducible cell-surface transmembrane carbonic anhydrases in human cancer. Am J Pathol 2001; 158: 905-919.
13. Ivanov SV, Kuzmin I, Wei MH, Pack S, Geil L, Johnson BE, Stanbridge EJ, Lerman MI. Down-regulation of transmembrane carbonic anhydrases in renal cell carcinoma cell lines by wild-type von Hippel-Lindau transgenes. Proc Natl Acad Sci U S A 1998; 95: 12596-12601.
14. Jarrell ST, Vortmeyer AO, Linehan WM, Oldfield EH, Lonser RR. Metastases to hemangioblastomas in von Hippel-Lindau disease. J Neurosurg 2006; 105: 256-263.
15. Kaelin WG. The von Hippel-Lindau tumor suppressor protein: roles in cancer and oxygen sensing. Cold Spring Harb Symp Quant Biol 2005; 70: 159-166.
16. Kim WY, Kaelin WG. Role of VHL gene mutation in human cancer. J Clin Oncol 2004; 22: 4991-5004.
17. Luukkaa H, Klemi P, Hirsimaki P, Vahlberg T, Kivisaari A, Kahari VM, Grenman R. Matrix metalloproteinase (MMP)-1, -9 and -13 as prognostic factors in salivary gland cancer. Acta Otolaryngol 2008; 128: 482-490.
18. Menczer J, Schreiber L, Sukmanov O, Kravtsov V, Berger E, Golan A, Levy T. COX-2 expression in uterine carcinosarcoma. Acta Obstet Gynecol Scand 2010; 89: 120-125.
19. Polydorides AD, Rosenblum MK, Edgar MA. Metastatic renal cell carcinoma to hemangioblastoma in von Hippel-Lindau disease. Arch Pathol Lab Med 2007; 131: 641-645.
20. Proescholdt MA, Mayer C, Kubitza M, Schubert T, Liao SY, Stanbridge EJ, Ivanov S, Oldfield EH, Brawanski A, Merrill MJ. Expression of hypoxia-inducible carbonic anhydrases in brain tumors. Neuro Oncol 2005; 7: 465-475.
21. Richard S, David P, Marsot-Dupuch K, Giraud S, Beroud C, Resche F. Central nervous system hemangioblastomas, endolymphatic sac tumors, and von Hippel-Lindau disease. Neurosurg Rev 2000; 23: 1-22.
22. Rivera AL, Takei H, Zhai J, Shen SS, Ro JY, Powell SZ. Useful immunohistochemical markers in differentiating hemangioblastoma versus metastatic renal cell carcinoma. Neuropathology 2010; 30: 580-585.
23. Shuin T, Yamasaki I, Tamura K, Okuda H, Furihata M, Ashida S. Von Hippel-Lindau disease: molecular pathological basis, clinical criteria, genetic testing, clinical features of tumors and treatment. Jpn J Clin Oncol 2006; 36: 337-343.
24. Takei H, Powell SZ. Novel immunohistochemical markers in the diagnosis of nonglial tumors of nervous system. Adv Anat Pathol 2010; 17: 150-153.
25. Togashi A, Katagiri T, Ashida S, Fujioka T, Maruyama O, Wakumoto Y, Sakamoto Y, Fujime M, Kawachi Y, Shuin T, Nakamura Y. Hypoxia-inducible protein 2 (HIG2), a novel diagnostic marker for renal cell carcinoma and potential target for molecular therapy. Cancer Res 2005; 65: 4817-4826.
26. Tostain J, Li G, Gentil-Perret A, Gigante M. Carbonic anhydrase 9 in clear cell renal cell carcinoma: a marker for diagnosis, prognosis and treatment. Eur J Cancer 2010; 46: 3141-3148.
27. Vortmeyer AO, Tran MG, Zeng W, Glasker S, Riley C, Tsokos M, Ikejiri B, Merrill MJ, Raffeld M, Zhuang Z, Lonser RR, Maxwell PH, Oldfield EH. Evolution of VHL tumourigenesis in nerve root tissue. J Pathol 2006; 210: 374-382.
28. Weinbreck N, Marie B, Bressenot A, Montagne K, Joud A, Baumann C, Klein O, Vignaud JM. Immunohistochemical markers to distinguish between hemangioblastoma and metastatic clear-cell renal cell carcinoma in the brain: utility of aquaporin1 combined with cytokeratin AE1/AE3 immunostaining. Am J Surg Pathol 2008; 32: 1051-1059.
29. Zagzag D, Krishnamachary B, Yee H, Okuyama H, Chiriboga L, Ali MA, Melamed J, Semenza GL. Stromal cell-derived factor-1-alpha and CXCR4 expression in hemangioblastoma and clear cell-renal cell carcinoma: von Hippel-Lindau loss-of-function induces expression of a ligand and its receptor. Cancer Res 2005; 65: 6178-6188.

Original article

Folia Neuropathologica

Proliferation index revisited in neuroblastic tumors

Ewa Iżycka-Świeszewska[1*], Beata Stefania Lipska-Ziętkiewicz[2*], Elżbieta Adamkiewicz-Drożyńska[3], Wiesława Grajkowska[4,5], Blanka Hermann[1], Ewa Bień[3], Janusz Limon[2]

**Both authors contributed equally*

[1]Department of Pathology and Neuropathology, Medical University of Gdansk, Gdansk, [2]Department of Biology and Genetics, Medical University of Gdansk, Gdansk, [3]Department of Pediatrics, Hematology and Oncology, Medical University of Gdansk, Gdansk, [4]Department of Pathology, Children's Memorial Health Institute, Warsaw, [5]Department of Experimental and Clinical Neuropathology, Mossakowski Medical Research Centre, Polish Academy of Sciences, Warsaw, Poland

Folia Neuropathol 2014; 52 (3): 243-252 DOI: 10.5114/fn.2014.45565

Abstract

Neuroblastic tumors (NB) are the most common extracranial pediatric neural crest-derived tumors, with a dismal outcome in a substantial group of patients. The study objective was to evaluate the patho-clinical correlations and prognostic impact of the proliferation index (PI) measured with two markers, Ki67 and topoisomerase II alpha (Topo2A), in a NB series. A retrospective analysis of 118 NB from 103 consecutive patients was performed. Analyzed data included tumor stage, histology, mitosis/karyorrhexis index (MKI), MYCN status, and overall survival. Patients' median follow-up period was 50 months. Ki67 and Topo2A PI were assessed immunohistochemically on representative tissue slides in hot spots. PI for Ki67 was in the range 0-72% (median 18%) and for Topo2A was in the range 0-58% (median 20%), being strongly interrelated (r = 0.83). Median PIs with both markers were lower in children older than 18 months (> 18 m) than in the younger patients, with p = 0.0002 and p = 0.005 respectively. Higher Ki67 and Topo2A correlated with metastatic stage, higher MKI, and inversely with increasing tumor differentiation. The cut-off values of PI Ki67 > 30% and Topo2A > 20% were associated with fatal outcome of the disease. In the subgroup of patients > 18 m already at cut-offs Ki67 > 10% and Topo2A > 15% a fatal outcome was predicted by Kaplan-Meyer analysis. Cox regression analysis identified cumulative PI (joint Ki67 and Topo2A index) as an independent prognostic factor. The conclusion is that the proliferation index measured with the examined markers provides substantial prognostic information in NB, especially in infants. PI assessment should become an element of the standard pathological checkup list of NB tumors.

Key words: *neuroblastoma, proliferation index, Ki-67, topoisomerase II alpha, prognostic factors.*

Introduction

The evaluation of the proliferation index in tumor tissue has become an important element of diagnosis and risk assessment in many types of cancer. In adult cancers, such as neuroendocrine tumors, breast carcinoma, lymphomas, prostate cancer and gliomas, the Ki-67 labeling index is included in the routine diagnostics, having therapeutic implications [1,2,27]. Likewise, the assessment of topoisomerase II alpha (Topo2A) expression emerges as a prolifera-

Communicating author:
Ewa Iżycka-Świeszewska, MD, PhD, Department of Pathology and Neuropathology, Medical University of Gdansk, Nowe Ogrody 1-6 St., 80-803 Gdansk, e-mail: eczis@wp.pl

tion marker in several cancer types, including brain tumors [12,26,29]. Ki-67 nuclear protein is required for maintaining cell proliferation, as it is detectable in all active phases of the cell cycle (G1, S, G2 and M) but absent in the resting phase G0 [21,28]. Accordingly, it serves for the determination of the growth fraction of a given cell population. Topo2A is one of the key enzymes responsible for maintenance and replication of genomic DNA. The expression of Topo2A increases dramatically in late S phase of the cell cycle, and then decreases at the end of M phase [11]. Consistent with the above, high expression of Topo2A corresponds to high proliferation activity [5,11,12]. The other proliferation markers, with different prognostic and predictive value, are: proliferating cell nuclear antigen (PCNA), repp86, minichromosome maintenance protein 2 (MCM2), thymidine labeling index, thymidine kinase, cyclin E, cyclin D, and cyclin inhibitors p27 and p21 [5,14,15,17,18,24].

Neuroblastoma (NB) is the most common extracranial solid tumor of early childhood, deriving from the sympatheto-adrenal lineage. It presents considerable heterogeneity in clinical behavior, ranging from spontaneous regression or maturation to metastatic spread despite aggressive therapy [4,19,23]. The long-term survival rates remain unsatisfactory in the high-risk group accounting for almost half of all NB cases. Several biological features and molecular abnormalities have been identified as powerful predictors of the patients' prognosis and therapeutic response. The International Neuroblastoma Risk Group (INRG) classification [4,19] is based on stage of disease, patient's age, histological subtype and grade of differentiation, *MYCN* gene status, presence of chromosome 11q deletion and tumor ploidy. In fact, the mitosis-karyorrhexis index (MKI) remains the only marker relating to cellular proliferation in the modern diagnostic directives [4,13].

Several immunohistochemical markers of proliferation in NB have been examined by a few groups [2,3,5,8,15]. It was suggested that their assessment might merit inclusion in the panel of diagnostic and prognostic criteria [6,14]. Conversely, a few reports showed no significant correlations of proliferation markers with clinico-biological features in an NB series [25]. Hence, there is still no consensus regarding significance of the proliferation index (PI) in NB. Moreover, Topo2A expression has not yet been evaluated in NB.

In NB, despite advantages in understanding of the tumor biology, there is still a need for new reliable prognostic and predictive factors. The purpose of the current study is to evaluate the utility and patho-clinical associations of the proliferation index measured with two markers.

Material and methods

Patients

One hundred and three NB patients aged 1-169 months (mean: 40; median: 30) at diagnosis were enrolled in the study. In six patients tumor tissue samples from consecutive surgical procedures were available. These samples were subject to all analyses except for survival probability estimation, which was limited to primary tumors. Twenty-four patients were treated with chemotherapy before biopsy. Written informed consent was obtained from the relevant guardians of the children. The International Neuroblastoma Pathology Classification (INPC) was employed for histological typing and prognostic evaluation [23]. The archival tissue slides representative for each tumor were examined by two independent observers (EIS, WG). The MKI was determined in each untreated tumor according to the Shimada criteria [23]. Clinico-pathological characteristics of the patients are shown in Table I. The mean follow-up period was 54.5 months (median: 50; range: 3-162 months). During the observation period 34 patients died of the disease.

Immunohistochemistry

The following mouse monoclonal antibodies were used for the immunohistochemical evaluation: Ki-67 (1 : 100, DAKO, F0788) and Topo2A (1 : 50, DAKO, M7186) with appropriate positive and negative controls. The standard protocol with heat-induced antigen retrieval in citrate buffer was followed. Subsequently the slides were incubated with the primary antibody for 30 minutes at room temperature. Thereafter the visualization system EnVision and DAB (DAKO) with hematoxylin staining were used. The quantitative study was carried out semi-automatically using an image analyzer system (microscope BX 51 and digital camera SP-350 with Quick Photo Camera 2.2. software, Olympus). Tumor fields with the highest number of Ki-67 and Topo2A positive nuclei were identified (hot spots) and the total number of nuclei and immunopositive nuclei were manually indicated and counted on computer images at 200× magnification. The proportion of positive tumor cells was measured for at least 100-1000

Table I. Clinico-pathological characteristics of patients and their corresponding 5-year overall survival rates

Feature	Dichotomous covariate	All patients in the study			Patients > 18 months of age		
		n	5-year OS	*p* value (log-rank test)	*n*	5-year OS	*p* value (log-rank test)
Age	≤ 18 months of age	40	87.5%	0.004	–	–	–
	> 18 months of age	63	54.1%		–	–	
Stage	1, 2, 3, 4S	64	93.5%	< 0.001	31	90.1%	< 0.001
	4	39	25.2%		32	20.0%	
Prognostic group (INPC)	FH	49	90.0%	0.004	23	83.0%	0.026
	UH	30	66.6%		19	57.9%	
Histological type/subtype	GN	9	87.5%	0.014	9	87.5%	0.008
	GNB	20	61.0%		18	56.0%	
	NB DIFF	28	76.8%		17	66.5%	
	NB POO	40	68.0%		15	38.1%	
	NB UN	6	0%		4	0%	
MKI	Low	33	91.1%	< 0.001	22	86.2%	< 0.001
	Intermediate	26	88.2%		10	80.0%	
	High	20	54.8%		10	30.0%	
MYCN	Non-amplified	79	81.8%	< 0.001	43	71.7%	< 0.001
	Amplified	24	18.4%		20	16.2%	

FH – favorable histology, UH – unfavorable histology, GN – ganglioneuroma, GNB – ganglioneuroblastoma, NB – neuroblastoma, DIFF – differentiating, POO – poorly differentiated, UN – undifferentiated

cells, depending on tumor histology. Proliferation index was reported as percentage of positive cells.

Statistics

Descriptive analysis was performed for each variable, and associations between variables were analyzed using the chi-square test with adequate corrections, Mann-Whitney and Kruskal-Wallis tests when appropriate. The effect of on long-term survival rates were analyzed using Kaplan-Meier survival probability estimates and log-rank tests. The parameters shown by univariate analysis to be significant were also compared by means of multivariate Cox regression analysis for multiple proportional hazards using a stepwise (backward and forward) conditional approach. All calculations were performed using Statistica 9.0 (StatSoft Inc.) software.

Results

Characteristics of the analyzed group

Age at diagnosis over 18 months (> 18 m), metastatic disease (INSS stage 4), unfavorable histology subtype and *MYCN* amplification were found to be of prognostic significance (Table I). The distribution of patients with respect to these parameters has proven good representation of all the subtypes of the disease in the analyzed cohort.

Correlation of PIs with clinical, pathological and molecular parameters

Ki-67 and Topo2A-positive nuclei were distributed unevenly within the tumors, forming areas with higher concentrations ("hot spots") (Figs. 1A-B). In the whole series of tumors the mean value of Ki-67 was 22.5% (median: 18; range: 0-72%); and 20.7% for Topo2A (median: 20; range: 0-58%). These two markers were strongly interrelated (Spearman's correlation coefficient $r = 0.83$, $p < 0.05$; Fig. 2). In the NB Schwannian stroma poor subgroup the mean Ki-67 value was 29.1% (median: 27; range: 4-72) and 25.6% for Topo2A (median: 25; range: 4-58%), being significantly higher than in Schwannian stroma rich tumors ($p < 0.0001$). 6/113 tumors were negative for Ki-67 and 4/113 were negative for Topo2A, including three cases negative for both markers.

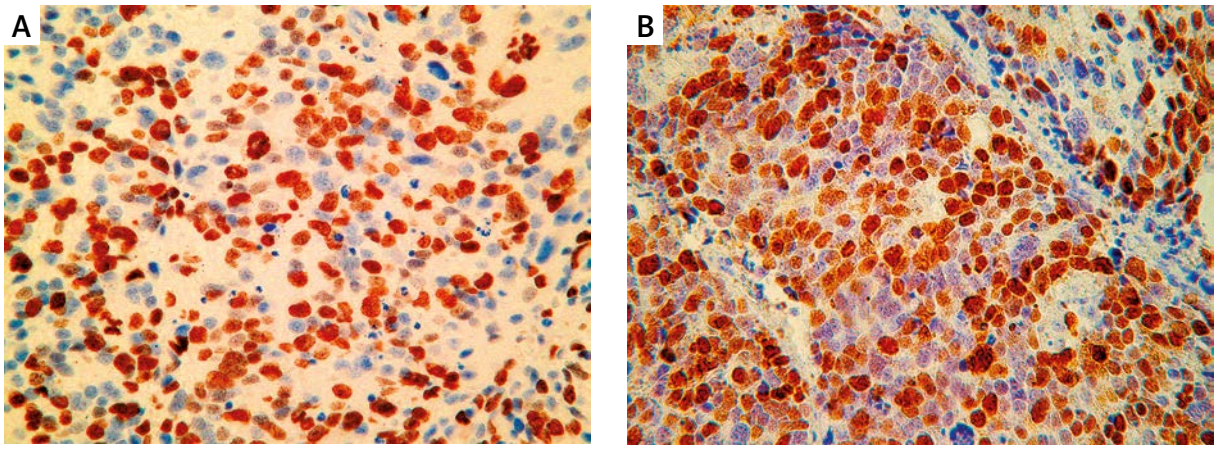

Fig. 1. Ki-67 **(A)** and Topo2A **(B)** labeling in Schwannian stroma-poor neuroblastoma in hot spot area (Ki-67, Topo2A immunostaining, 200×).

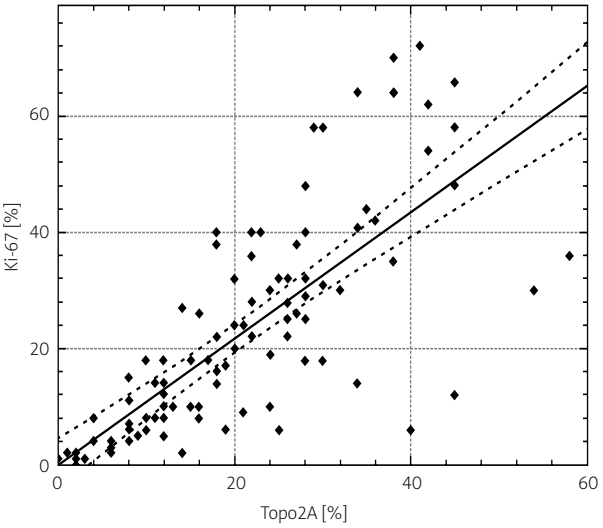

Fig. 2. Scatterplot diagram illustrating distribution of Ki-67 and Topo2A labeling indices in the whole series of NB tumors ($r = 0.83$; $p < 0.05$).

Both PIs were found significantly lower in the group of patients > 18 m (median: 27.5% vs. 10%, $p < 0.001$ for Ki-67 and median 23.5% vs. 14%, $p = 0.005$ for Topo2A). In view of this, we further analyzed PIs with respect to the age group.

In the whole series, higher Ki-67 and Topo2A correlated with higher INSS stage. PIs were low in stages 2 and 3, intermediate in stages 1 and 4s, and high in stage 4. Patients with metastatic disease had significantly higher PIs ($p = 0.008$, $p = 0.01$ for Ki-67 and Topo2A, respectively). PIs were inversely correlated with increasing tumor differentiation. The highest PI disclosed undifferentiated and poorly differentiated NB, while the lowest or even null index concerned ganglioneuroma. Analogously, cases with unfavorable histology according to INPC were found to have significantly higher PIs ($p < 0.001$ for both markers). PIs strongly correlated with MKI. There was no difference in mean PI values between the non-treated and pretreated cases. Conversely, the samples from consecutive operations of a single patient were characterized by a considerable drop in MKI, Ki67 and Topo2A values. Adrenal localization of the primary tumors was characterized by significantly higher PIs. *MYCN* amplification was found to be associated with higher PIs, but only for Topo2A did the observation reach the level of statistical significance ($p = 0.025$).

Survival analyses

PIs were predictive of poor prognosis at the cut-off values of 30% for Ki-67 and 20% for Topo2A (Table II, Fig. 3). The correlation remained significant in the subgroup of 79 chemonaive tumors. 27 patients (26%) had both indices – referred to subsequently as cumulative PI (cumPI) – exceeding the defined cut-off values, and these had the worst prognosis (Fig. 3C). Furthermore, cumPI had prognostic significance in the *MYCN* non-amplified group (5-OS rates 85.4% vs. 68.2%, $p = 0.048$). In the unfavorable histology (UH) group, the cumPI was related to survival (5-OS rates 82.4% vs. 45.6%, $p = 0.01$). In the stroma poor group the cumPI value was also highly predictive of survival (5-OS rates 79.2% vs. 45.2%; $p = 0.004$). In stage 4, a borderline tendency for worse survival in the group with intense proliferation established cumPI ($p = 0.06$).

Table II. Proliferation markers in the analyzed series of NB tumors and their corresponding 5-year overall survival rates

Feature	Dichotomous covariate	All patients in the study			Patients > 18 months of age		
		n	5-year OS	*p* value (log-rank test)	*n*	5-year OS	*p* value (log-rank test)
Ki-67	≤ 30%	73	73.6%	0.01	49	64.4%	0.001
	> 30%	30	50.1%		14	20.4%	
Topo2A	≤ 20%	54	74.1%	0.047	40	67.4%	0.003
	> 20%	49	59.1%		23	31.9%	
Ki-67 and Topo2A	other	76	74.5%	0.002	50	65.3%	< 0.001
	> 30% and > 20%	27	45.2%		13	13.8%	

Multivariate analyses

In the multivariate Cox regression analysis the initial testing was performed using two models. The first, comprising the whole series of tumors, used six covariates identified in univariate analyses (age < 18 months, stage 4, histology subtype, *MYCN* status, Ki-67 > 30% and Topo2A > 20%). Here, only stage 4 and age were identified as independent predictors of OS. In the second model, only the pre-treated cases were analyzed. Accordingly, two additional covariates (histological subtype and MKI) were added, and again, only stage 4 and age were significant. In the second step, individual PIs were replaced by the cumPI, yet still the analysis retrieved the same predictors. Finally, the stepwise conditional approach was used to identify the minimal set of markers predictive for OS. After backward elimination of the least significant covariates, the minimal models were built. For the whole series the independent prognostic factors were age, stage 4 and the cumPI (Table IIIA), while for the series of non-treated tumors the minimal model comprised age and INSS stage 4 only. Inclusion of information on *MYCN* status did not improve the model, probably due to a strong association between stage 4 and *MYCN* amplification (56% of patients with stage 4 harbored *MYCN* amplification; $p < 0.001$).

Significance of PIs in the group of children diagnosed over 18 months of age

The above correlations between PIs and stage 4, histological subtype, MKI and *MYCN* amplification were all also significant in the subgroup of > 18 m patients, with the statistical power higher than in the whole series. Conversely, no correlations were detected in the youngest children. In the patients > 18 m the cut-off values as identified for the whole series were also predictive for long-term survival (Table II). However, according to the significantly lower mean values of PIs in this group, the cut-off values lowered to 10% for Ki-67 and 15% for Topo2A achieved even higher statistical significance (Figs. 3D-E). The correlations remained significant in the non-treated subgroup and in Schwannian stroma poor patients. Twenty-six patients (41%) had both indices exceeding the cut-off values, with the worst 5-year overall survival (5-OS) (Fig. 3F). The multivariate Cox regression analyses were performed using the models as above. It identified INSS stage 4 and Ki-67 > 10% as the independent predictors of OS in the > 18 m group. The second, performed on non-treated > 18 m cases, identified INSS stage 4 as the only independent predictor. In the second step, individual PIs were replaced by the cumPI. The cumPI appeared as an independent prognostic factor in the whole series of > 18 m tumors but not in the pre-treatment subgroup. Eventually, the stepwise conditional approach through backward elimination of the least significant covariates allowed the minimal set of markers predictive for OS to be established. For the whole series of > 18 m tumors the independent prognostic factors were INSS stage 4 and the cumPI (Table IIIB), while for the series of non-treated > 18 m tumors the minimal model comprised INSS stage 4 only.

Discussion

The basic, direct method of cellular proliferation assessment in tumor tissue samples is the mitotic

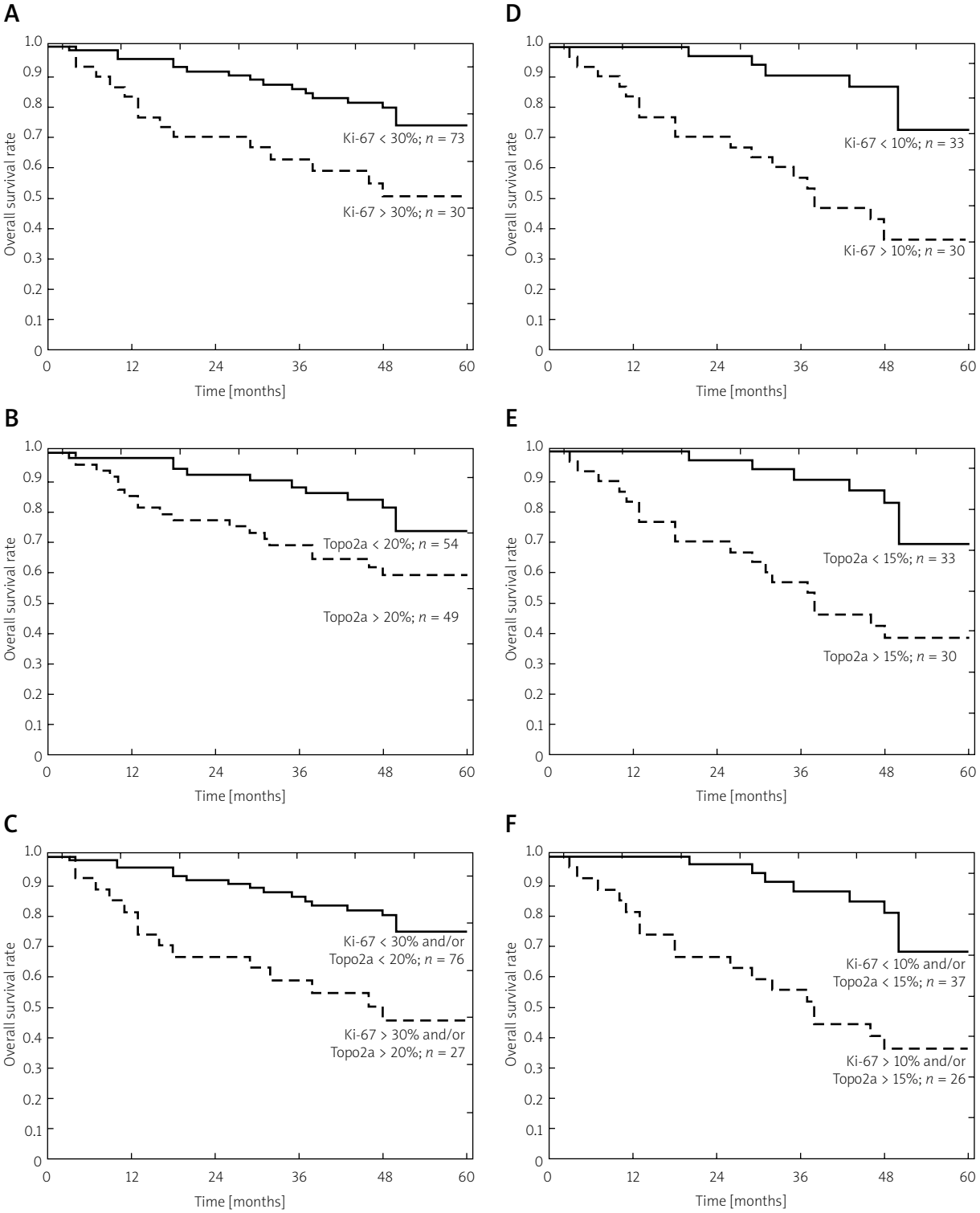

Fig. 3. Kaplan-Meier estimates of 5-year OS for neuroblastic tumors (NB) patients **(A, B, C)** and 5-year OS for NB patients over 18 months of age **(D, E, F)** with respect to PI measured with Ki-67 **(A, D)**, Topo2A **(B, E)** and the cumulative PI **(C, F)**.

Table III. Independent prognostic factors of the long-term OS rates identified by multivariate Cox hazard regression model A in the whole series of tumors and B in the group of patients diagnosed over the age of 18 months (overall significance of the models at $p < 0.001$)

A

Feature	HR	95% CI	*p* value (Wald statistics)
Age < 18 months	0.1	0.04-0.4	< 0.001
INSS stage 4	3.5	1.7-7.1	< 0.001
Ki-67 > 30% and Topo2A > 20%; cumulative PI	2.1	1.02-4.4	0.045

B

Feature	HR	95% CI	*p* value (Wald statistics)
INSS stage 4	7.2	2.6-20.0	< 0.001
Ki-67 > 10% and Topo2A > 15%; cumulative PI	2.4	1.1-5.2	0.03

HR – hazard ratio, CI – confidence interval

count or mitotic index. The mitotic count is used in many tumors as a diagnostic (smooth muscle tumors, meningiomas) or prognostic factor useful in the therapeutic approach (GISTs, neuroendocrine tumors, breast cancer) [16,18,27]. In pathological reports of many tumors, parallel data on the mitotic count and proliferative index are needed nowadays [1,7,18]. The mitotic count represents only a small fraction of cells at a cell cycle point, while markers of proliferation detectable by immunohistochemistry can identify the entire active cell population. Among several markers of proliferation, Ki67 is the most popular and reliable one. Topoisomerase 2A was accepted as a proliferative marker in gliomas and a few other cancers [17,29]. PI may be evaluated in the highest staining region (hot spot PI), or as an average count from randomly chosen fields (random PI). Most often Ki67 is evaluated based on the hot spot approach, which is a more reliable procedure [14,15,25,27]. Depending on the type of the tumor, large discrepancies between the number of cells per field and hence random selection of fields for PI evaluation might bias its score and produce unrepeatable results. Several tumor-type criteria for PI establishment have been elaborated. Digital image analysis systems can further improve the reliability of PI assessment [1,13,26].

Neuroblastic tumors constitute a heterogeneous group of tumors, presenting up-regulated proliferation, prolonged cell survival, inhibited apoptosis and disturbed neuronal differentiation [19]. The significance of the proliferation index in NB has been elaborated in several studies, but the MKI is the only parameter related to proliferation to be generally accepted in the last 30 years [4,19,23]. The Shimada classification originally published in 1984, with a few subsequent modifications, is a widely accepted, histopathological age-based prognostic system for NB [10,23]. The MKI was introduced in this system, as the density sum of mitotic and karyorrhectic cells in 5000 neoplastic cells. The MKI was evaluated and critically discussed soon after it was introduced into practice [10]. The biological nature of karyorrhectic cells is debatable, but a high MKI in stroma-poor tumors is an indicator of poor prognosis [9,10]. The karyorrhectic cells were shown to be either proliferating or undergoing apoptosis [9,25]. Furthermore, a high cellular density of proliferating cells correlates with poor prognosis, whereas a high density of apoptosis indicates a favorable outcome [13]. Moreover, the assessment of mitotic rate in an NB tumor section is time-consuming and can be difficult to perform due to the specificity of tumor histology. In undifferentiated and poorly differentiated NB, application of the mitotic count is still controversial because of the high cellularity and mutual resemblance of mitotic and karyorrhectic cells [9,10,25].

In the current study, both of the analyzed PIs strongly correlated with the MKI (Fig. 1). Previously, a Spanish group also reported a significant association between the MKI and Ki-67 index [3]. Conversely, in their simplified dichotomous (low vs intermedi-

ate and high MKI) analysis performed on a smaller group of 60 NB tumors, Uccini *et al*. [25] observed such a correlation only in the subgroup of *MYCN* amplified tumors. Moreover, contrary to MKI, immunohistochemical markers can be assessed not only in the pre-treatment specimens but also in tumors that were resected after inductive chemotherapy [8]. No difference in mean PI values was found between pre-treated and non-treated cases – which is in line with a previous report by Krams *et al*. [14,15]. In our study, we also analyzed PIs in tissue samples from consecutive biopsies of single patients. Here we observed a considerable drop in PI values after chemotherapy parallel to tumor maturation. The two surviving patients were the only ones with non-metastatic disease. Recently, it has been proposed that examination of NB samples after the inductive chemotherapy gives prognostic information [8]. In general, a shift from an intermediate/high to low MKI was observed. Following induction therapy, persistence of intermediate/high tumor MKI and high proliferative activity portends a poor outcome [8].

Rudolph *et al*. [22] proposed Ki-67 as a reliable means for the assessment of the tumor growth fraction in NB. Ki-67 was significantly correlated with histopathological grade and predictive for long-term OS at a cut-off level of 25%. Also, the Ki-67 index was significantly higher in stage 4 cases, and the Ki-67 PI enabled risk stratification in tumors with and without *MYCN* amplification. Moreover, the 30% cut-off value was identified in Cox regression analysis as an independent prognostic factor along with stage [14,15,22]. Del Carmen *et al.* confirmed a significant correlation with histologic subtype, MKI and disease stage [6]. Later, analysis of a 182 Spanish NB registry revealed that the death rate increased markedly with the index exceeding 30% [3]. Our results are in line with the abovementioned reports.

Our study is the first to analyze Topo2A expression in NB. It has been suggested that due to selective expression during the cell cycle Topo2A might provide a better estimate of the number of actively cycling cells than Ki-67 [11]. The assessment of whether the prognostic impact of Topo2A is due to its value as a predictor of response to a treatment-based regimen or as a pure prognostic factor is still difficult to establish [5,12,29]. Similar to the studies on other cancers [1,5,18,21], we have shown that NB patients with high Topo2A PI experience significantly shorter OS. Also, Topo2A strongly correlated with Ki-67 (Fig. 1) and MKI. The addition of this parameter to the Ki67 proliferation index allowed for more precise prediction of patient risk in multivariate analyses (cumulative PI). Interestingly, Korija *et al*. [13] found that the anti-Ki-67 assessed proliferation activity was significantly higher in *MYCN*-amplified than in non-amplified hotspots. The proliferation indices of the hotspots also had a significant correlation with the prognosis and histological type. Hotspot focusing provides a means of analyzing proliferation-associated markers in neuroblastomas, and together with the FISH detection of the *MYCN* copy number enables an easy and reliable examination of *MYCN* status in neuroblastomas.

The novelty and the impact of our study is the consequence of two particularities. Firstly, the analysis of the percentages of Ki-67-positive and/or Topo2A-positive cells as a continuous value allowed us to avoid a potential bias inherent in the use of an arbitrary cutoff point, and supported the association of high Ki-67 and or Topo2A expression with a high risk of death due to disease. From the practical point of view, values above 30% for Ki67 and 20% for Topo2A were related to a dismal outcome in the whole group and also in the stroma poor NB subgroup.

Furthermore, for the first time the analysis of PIs with respect to the age of the patients as a stratifying parameter was performed. The age of NB patients is an important prognostic and risk factor with the cut-off eventually defined recently at 18 months of age [4,20]. Age can be thought of as a surrogate risk factor for genetic or biologic markers of risk that are yet undiscovered or unproven [19,20]. Of note, del Carmen Mejia *et al*. [6] also observed the peculiar correlation between age at diagnosis and Ki-67 expression, but the authors could not propose a consistent explanation for this. In the younger subgroup of our patients, moderate proliferation is not related to adverse prognosis. Probably it is just a manifestation of the ongoing processes of maturation of neoplastic cells [10,23]. Conversely, the older patients have, on average, lower proliferation. However, a fraction of them will have poorly differentiated histology and intense proliferation with unfavorable outcome of the disease. This double-faced nature of proliferation in NB converts into two cut-off values of PIs, age-dependent, identified in the current study.

The presented analysis of PIs provides further insight into the distinctive biological heterogeneity of NB, especially with respect to the age of the

patient. It seems that the immunohistochemically assessed PI should be introduced in parallel to the MKI to the routine diagnostics of NB tumors, especially the Schwannian stroma poor group. However, the significance of PI needs further validation on larger prospective groups of patients.

Acknowledgments

The study was supported by the Polish Ministry of Science and Higher Education grant N401 197339.

Disclosure

Authors report no conflict of interest.

References

1. Arnold CN, Nagasaka T, Goel A, Scharf I, Grabowski P, Sosnowski A, Schmitt-Gräff A, Boland CR, Arnold R, Blum HE. Molecular characteristics and predictors of survival in patients with malignant neuroendocrine tumors. Int J Cancer 2008; 123: 1556-1564.
2. Berney DM, Gopalan A, Kudahetti S, Fisher G, Ambroisine L, Foster CS, Reuter V, Eastham J, Moller H, Kattan MW, Gerald W, Cooper C, Scardino P, Cuzick J. Ki-67 and outcome in clinically localised prostate cancer: analysis of conservatively treated prostate cancer patients from the Trans-Atlantic Prostate Group study. Br J Cancer 2009; 100: 888-893.
3. Burgues O, Navarro S, Noguera R, Pellín A, Ruiz A, Castel V, Llombart-Bosch A. Prognostic value of the International Neuroblastoma Pathology Classification in neuroblastoma (Schwannian stroma-poor) and comparison with other prognostic factors: a study of 182 cases from the Spanish neuroblastoma registry. Virchows Arch 2006; 449: 410-420.
4. Cohn SL, Pearson AD, London WB, Monclair T, Ambros PF, Brodeur GM, Faldum A, Hero B, Iehara T, Machin D, Mosseri V, Simon T, Garaventa A, Castel V, Matthay KK. The International Neuroblastoma Risk Group (INRG) Classification System: An INRG Task Force Report. J Clin Oncol 2009; 27: 289-297.
5. Colozza M, Azambuja E, Cardoso F, Sotiriou C, Larsimont D, Piccart MJ. Proliferative markers as prognostic and predictive tools in early breast cancer: where are we now? Ann Oncol 2005; 16: 1723-1739.
6. Del Carmen Mejía M, Navarro S, Pellín A, Ruíz A, Castel V, Llombart-Bosch A. Study of proliferation and apoptosis in neuroblastoma. Their relation with other prognostic factors. Arch Med Res 2002; 33: 466-472.
7. Gauchotte G, Vigouroux C, Rech F, Battaglia-Hsu SF, Soudant M, Pinelli C, Civit T, Taillandier L, Vignaud JM, Bressenot A. Expression of minichromosome maintenance MCM6 protein in meningiomas is strongly correlated with histologic grade and clinical outcome. Am J Surg Pathol 2012; 36: 283-291.
8. George RE, Perez-Atayde AR, Yao X, London WB, Shamberger RC, Neuberg D, Diller L. Tumor histology during induction therapy in patients with high-risk neuroblastoma. J Clin Oncol 2011; 29: 4358-4364.
9. Gestblom C, Hoehner J, Pahlman S. Proliferation and apoptosis in NB: subdividing the mitosis karryorhexis index. Eur J Cancer 1995; 31A: 458-463.
10. Joshi VV1, Rao PV, Cantor AB, Altshuler G, Shuster JJ, Castleberry RP. Modified histologic grading of neuroblastomas by replacement of mitotic rate with mitosis karyorrhexis index. A clinicopathologic study of 223 cases from the Pediatric Oncology Group. Cancer 1996; 77: 1582-1588.
11. Kellner U, Sehested M, Jensen PB, Gieseler F, Rudolph P. Culprit and victim – DNA topoisomerase II. Lancet Oncol 2002; 4: 235-243.
12. Kim EJ, Lee YS, Kim YJ, Kim MJ, Ha YS, Jeong P, Lee OJ, Kim WJ. Clinical implications and prognostic values of topoisomerase-II alpha expression in primary non-muscle-invasive bladder cancer. Urology 2010; 75: 1516.e9-e13.
13. Korja M, Finne J, Salmi TT, Kalimo H, Karikoski R, Tanner M, Isola J, Haapasalo H. Chromogenic in situ hybridization-detected hotspot MYCN amplification associates with Ki-67 expression and inversely with nestin expression in neuroblastomas. Mod Pathol 2005; 18: 1599-1605.
14. Krams M, Heidebrecht HJ, Hero B, Berthold F, Harms D, Parwaresch R, Rudolph P. Repp86 expression and outcome in patients with Neuroblastoma. J Clin Oncol 2003; 21: 1810-1818.
15. Krams M, Hero B, Berthold F, Parwaresch R, Harms D, Rudolph P. Proliferation marker Ki-S5 discriminates between favorable and adverse prognosis in advanced stages of Neuroblastoma with and without MYCN amplification. Cancer 2002; 94: 854-861.
16. Larysz D, Blamek S, Rudnik A. Clinical aspects of molecular biology of pituitary adenomas. Folia Neuropathol 2012; 50: 110-117.
17. Lind-Landström T, Varughese RK, Sundstrøm S, Torp SH. Expression and clinical significance of the proliferation marker minichromosome maintenance protein 2 (Mcm2) in diffuse astrocytomas WHO grade II. Diagn Pathol 2013; 8: 67.
18. Lowe K, Khithani A, Liu E, Winston T, Christian D, Saad J, Jeyarajah DR. Ki-67 labeling: a more sensitive indicator of malignant phenotype than mitotic count or tumor size? J Surg Oncol 2012; 106: 724-727.
19. Maris JM. Recent advantages in neuroblastoma. N Engl J Med 2010; 362: 2202-2211.
20. Moroz V, Machin D, Faldum A, Hero B, Iehara T, Mosseri V, Ladenstein R, De Bernardi B, Rubie H, Berthold F, Matthay KK, Monclair T, Ambros PF, Pearson AD, Cohn SL, London WB. Changes over three decades in outcome and the prognostic influence of age-at-diagnosis in young patients with neuroblastoma: A report from the International Neuroblastoma Risk Group Project. Eur J Cancer 2011; 47: 561-571.
21. Preusser M, Hoeftberger R, Woehrer A, Gelpi E, Kouwenhoven M, Kros JM, Sanson M, Idbaih A, Brandes AA, Heinzl H, Gorlia T, Hainfellner JA, van den Bent M. Prognostic value of Ki67 index in anaplastic oligodendroglial tumours – a translational study of the European Organization for Research and Treatment of Cancer Brain Tumor Group. Histopathology 2012; 60: 885-894.
22. Rudolph P, Lappe T, Hero B, Berthold F, Parwaresch R, Harms D, Schmidt D. Prognostic significance of the proliferative activity in neuroblastoma. Am J Path 1997; 150: 133-145.
23. Shimada H, Ambros IM, Dehner LP, Hata J, Joshi VV, Roald B, Stram DO, Gerbing RB, Lukens JN, Matthay KK, Castleberry RP.

The International Neuroblastoma Pathology Classification (The Shimada system). Cancer 1999; 86: 364-372.
24. Taran K, Owecka A, Kobos J. Prognostic importance of cyclin-E1 expression in neuroblastoma tumors in children. Pol J Pathol 2013; 64: 149-52.
25. Uccini S, Colarossi C, Scarpino S, Boldrini R, Natali PG, Nicotra MR, Perla FM, Mannarino O, Altavista P, Boglino C, Cappelli CA, Cozzi D, Donfrancesco A, Kokai G, Losty PD, McDowell HP, Dominici C. Morphological and molecular assessment of apoptotic mechanisms in peripherial neuroblastic tumours. Br J Cancer 2006; 95: 49-55.
26. Yang QC, Zhu Y, Liou HB, Zhang XJ, Shen Y, Ji XH. A cocktail of MCM2 and TOP2A, p16INK4a and Ki-67 as biomarkers for the improved diagnosis of cervical intraepithelial lesion. Pol J Pathol 2013; 64: 21-27.
27. Yerushalmi R, Woods R, Ravdin PM, Hayes MM, Gelmon KA. Ki67 in breast cancer: prognostic and predictive potential. Lancet Oncol 2010; 11: 174-183.
28. Zawrocki A, Iżycka-Świeszewska E, Papierz W, Liberski PP, Zakrzewski K, Biernat W. Analysis of the prognostic significance of selected morphological and immunohistochemical markers in ependymomas, with literature review. Folia Neuropathol 2011; 49: 94-102.
29. Zhao H, Yu H, Liu Y, Wang Y, Cai W. DNA topoisomerase II-alpha as a proliferation marker in human gliomas: correlation with PCNA expression and patient survival. Clin Neuropathol 2008; 27: 83-90.

Original article

Folia Neuropathologica

Angiocentric glioma: a rare intractable epilepsy-related tumour in children

Wiesława Grajkowska[1], Ewa Matyja[2], Paweł Daszkiewicz[3], Marcin Roszkowski[3], Jarosław Peregud-Pogorzelski[4], Elżbieta Jurkiewicz[5]

[1]Department of Pathology, The Children's Memorial Health Institute, Warsaw, [2]Department of Clinical and Experimental Neuropathology, Mossakowski Medical Research Centre Polish Academy of Sciences, Warsaw, [3]Department of Neurosurgery, The Children's Memorial Health Institute, Warsaw, [4]Department of Pediatrics, Pediatric Hematology and Oncology, Pomeranian Medical University, Szczecin, [5]Department of Radiology, The Children's Memorial Health Institute, Warsaw, Poland

Folia Neuropathol 2014; 52 (3): 253-259 DOI: 10.5114/fn.2014.45566

Abstract

Angiocentric glioma is a low-grade tumour that occurs in children and young adults with a long-standing epilepsy. The typical histopathological features of this tumour is the presence of spindle-shaped cells, radially oriented around the cortical blood vessels.

We present two teenage cases of the angiocentric variant of glioma: 1) a 15-year-old girl with a chronic and intractable partial epilepsy with cystic tumour located in the right temporal lobe and 2) a 14-year-old boy with intractable seizures and an extensive cortical lesion in the left parieto-occipital area. In both cases, the total tumours excision was performed. The histopathological findings revealed a characteristic angiocentric pattern that was composed of elongated cells arranging in pseudorosette-like structures around blood vessels. Moreover, schwannoma-like areas and subpial neoplastic infiltration with palisading of tumour cells at the brain surface were seen. The neoplastic cells displayed immunoreactivity for GFAP, S-100 protein and vimentin. A slight "dot-like" EMA staining, suggesting ependymal differentiation, was detected. The clinical and pathological picture allowed to establish the diagnosis of angiocentric gliomas. The patients were discharged home in a good condition and without seizures. During the 4-year follow-up, the tumour recurrence and seizures were not observed. The appropriate diagnosis of this peculiar type of usually low-grade glial tumour is important for adequate and successful treatment. The differential diagnosis requires the exclusion of other tumours with an angiocentric pattern, i.e. ependymoma, astroblastoma, which are associated with more aggressive biology.

Key words: *angiocentric glioma, intractable epilepsy, paediatric brain tumour, schwannoma-like pattern.*

Introduction

Angiocentric glioma (AG) is a rare, low-grade brain tumour in children and young adults with a long-standing epilepsy [6,8]. It has been included into the group of "other neuroepithelial tumours" in the current WHO Classification of Tumours of the Central Nervous System 2007 [3,5]. It is a slowly growing,

Communicating author:

Prof. Ewa Matyja, Department of Clinical and Experimental Neuropathology, Mossakowski Medical Research Centre Polish Academy of Sciences, 5 Pawinskiego St., 02-106 Warsaw, Poland, e-mail: ematyja@imdik.pan.pl

indolent neoplasm, classified as WHO grade I. Angiocentric glioma occurs within a wide range of 2.3-70 years but it is mostly encountered in childhood and adolescence (mean age 17 years) [2].

Angiocentric gliomas usually develop in the cerebral hemispheres. Majority of them are located superficially in the frontal, temporal or parietal lobes, as well as in the hippocampal region. The case with features of angiocentric glioma in the posterior midbrain was also described [7]. Although AGs are typically localized within the cerebral cortex, they may extend into the adjacent white matter. On MR imaging, AGs are T2- and FLAIR hyperintense and hypointense on T1-weighted images, without contrast enhancement [10,19]. Calcifications are rarely encountered. More than 90% of patients with AG suffer from a long-standing epilepsy with intractable partial seizures. The diagnosis of AG is established by histopathological examination which should confirm the main angiocentric tumour pattern. Immunohistochemical study documented the glial origin of neoplastic cells with an expression of glial fibrillary acidic protein, S-100 protein and vimentin.

During the last years, the increasing histopathological and clinical data on angiocentric gliomas have been reported but the biology of this tumour is not enough understood [2,4,9,18,19]. We report two additional teenage cases of AGs with a well-documented long, 4-year follow-up.

Cases report

Case 1

A 15-year-old girl with a chronic and intractable partial epilepsy was admitted to the Neurosurgical Department of the Pomeranian Medical University in 2010. Psychomotor development was normal and familial history was insignificant. Physical examination did not reveal any focal deficits or signs of increased intracranial pressure. EEG showed the presence of fairy regular basic activity with series of slow waves (frequency 3.3-4 Hz and voltage 120 mkV) in the frontal-occipital-temporal lobes of the right hemisphere with tendency for generalization. Ophthalmological examination revealed a normal disc of the optic nerve with distinct borders within the fundus. MRI scan revealed a well-delineated, cystic lesion, measuring 12 × 20 × 20 mm, located within the middle areas of the temporal lobe of the right hemisphere (Fig. 1A). The lesion did not show any enhancement after contrast administration. Surgical treatment was performed with a total tumour excision. The histopathological diagnosis was angiocentric glioma. Control MRI head scan performed 8 months following the surgery did not detect any relapse. Axial FLAIR and postcontrast T1-weighted images showed the resection cavity with a small hyperintensive area, probably corresponding with gliosis, without contrast enhancement (Figs. 1B-C). The patient was discharged home

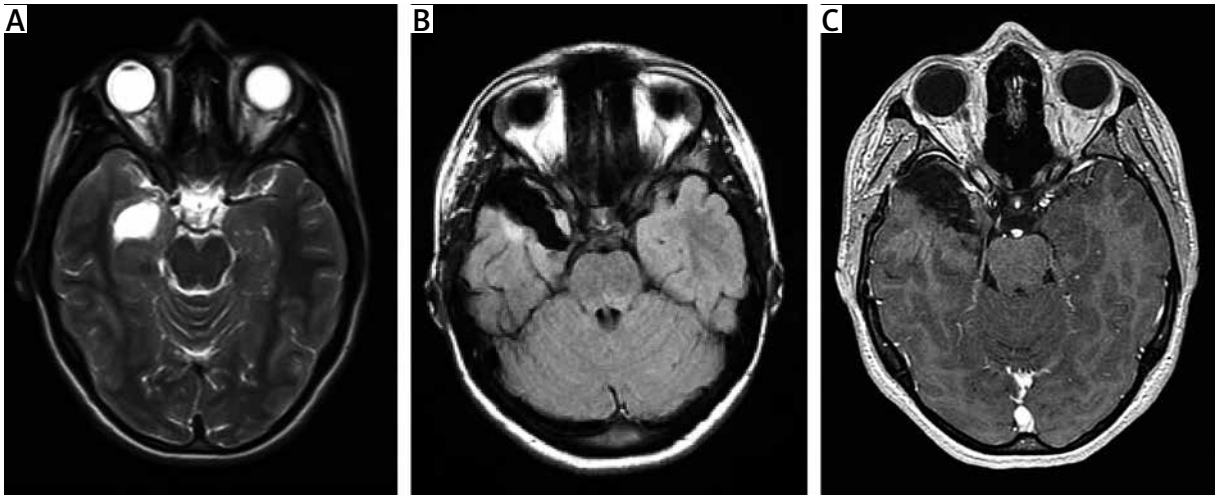

Fig. 1. MRI feature. Case 1. **A**) Preoperative MR brain examination. Axial T2-weighted image showing a well-delineated hyperintense lesion located in the right temporal lobe. **B, C**) Post-operative MR images. Axial FLAIR (**B**) and postcontrast T1-weighted (**C**) images showing a resection cavity with the small hyperintensive area – gliosis. No contrast enhancement.

in a good condition with no seizure recurrence. Due to abnormal EEG the patient was on long-term carbamazepine 2 × 200 mg/d treatment.

Case 2

A 14-year-old boy was admitted to the Department of Neurosurgery of the Children's Memorial Health Institute. He had a history of prematurity and developed his first generalized seizure at the age of 3. Thereafter, his psychosomatic development progressed normally, except for a mild horizontal nystagmus. Since the age of 11, he presented the simple focal seizures (paroxysmal right-sided hemianopsia, monoparesis of the left leg with auras in the form of scintillating scotomas) at the mean rate of 5 per day. The first imaging studies (CT) revealed an extensive lesion within the medial structures of left parieto-occipital lobes. The ventricular system was symmetrical and not enlarged. MRI revealed the irregular area of signal intensity on T2-weighted and FLAIR images (Fig. 2A) and T1-weighted with only a slight enhancement of a part of the tumour (Fig. 2B). HMRS spectrum revealed a slight elevation of the choline peak and slight depression of the N-acetyl-aspartate (NAA) peak. Overall, MR appearance was consistent with focal cortical dysplasia or benign tumour. EEG study revealed moderate focal discharges in the left tempo-ro-occipital and parietal areas, with a slight tendency to generalize over the entire ipsilateral and posterior aspects of contralateral hemispheres. Discharges were enhanced by hyperventilation and somnolence. Moderate clinical response was obtained upon application of anti-epileptic medication (valproic acid and levetiracetam). At admission to the Department of Neurosurgery, he was in a good overall condition with no neurological deficits. The left-sided parieto-occipital craniotomy was performed under neuronavigation guidance and the lesion within the parietal lobe, parieto-occipital fissure and crus of the hippocampus was totally excised. The histopathological diagnosis was angiocentric glioma. After surgery, the patient presented right-sided hemianopsia with no other neurological deficits. Post-operative MRI study revealed a well-delineated resection cavity with hyperintensity at its posterior margin, probably corresponding with gliosis, on axial FLAIR (Fig. 2C) and post contrast T1-weighted images. There was no contrast enhancement. Pre-discharge CT revealed a postoperative site with a moderate-sized pericerebral hematoma with no mass effect and no disturbances of cerebral circulation. He was discharged home in a good overall condition, fully mobile and fit. The patient has been without tumour recurrence and seizures for 4-year follow-up.

Material and methods

The surgical material was prepared by standard methodology. Biopsy tissue was fixed in 10% neu-

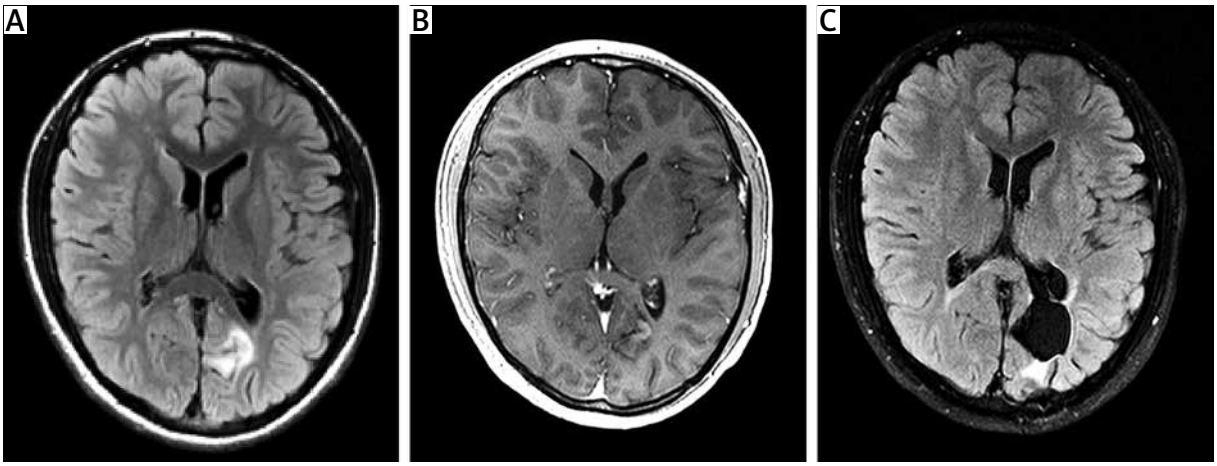

Fig. 2. MRI feature. Case 2. **A**) Preoperative MR brain examination. Axial FLAIR image showing a cortico-subcortical mass with high signal intensity, involving the left parieto-occipital lobes, without mass effect. **B**) Preoperative MR brain examination. Contrast-enhanced axial T1-weighted image at the same level showing a slight enhancement of a part of the tumour. **C**) Post-operative MR images. Axial FLAIR image showing a well-delineated resection cavity.

tral-buffered formalin, embedded in paraffin blocks, sectioned at 5 µm thick slices, and stained with hematoxylin-eosin (H&E). Immunohistochemistry was performed on paraffin-embedded specimens; labelling was carried out by the avidin-biotin complex (ABC) method with 3,3'-diaminobenzidine (DAB) as a chromogen. Primary antibodies were used against glial fibrillary acidic protein (GFAP; dilution 1 : 800), S-100 protein (dilution 1 : 500), epithelial membrane antigen (EMA; dilution 1 : 100), vimentin (dilution 1 : 100), synaptophysin (dilution 1 : 200), CD56 (dilution 1 : 100), cytokeratin-AE1/AE3 (dilution 1 : 400), and Ki67 (clone MIB-1, dilution 1 : 100). All antigens were obtained from Dako.

Histopathological findings

In both cases, histopathological studies of biopsy material revealed glial tumours composed predominately of elongated cells, aggregating around blood vessels and forming pseudorosette-like structures that closely resembled those of ependymoma (Figs. 3A-B). The neoplastic cells were mostly spindle-shaped, bipolar with eosinophilic cytoplasm and oval to elongate nuclei with irregular nuclear contours and granular chromatin. Moreover, the palisading pattern of tumour cells, mimicking schwannoma-like areas, was focally found (Figs. 3C-D). Compact, elongated cells were also seen in the superficial layers of cerebral cortex (Fig. 4E). Infiltration with palisade arrangement of the neoplastic cells was observed in the subpial areas at the brain surface (Fig. 3F). Mitotic figures were absent and necroses or vascular proliferation were not seen.

Immunohistochemical staining

The neoplastic cells displayed variable immunoreactivity for GFAP (Fig. 4A) and vimentin (Fig. 4B). The tumour cells were also immunopositive for S-100 protein (Fig. 4C). Moreover, the "dot-like" intracytoplasmic EMA positivity could be identified (Fig. 4D). The neoplastic cells were essentially negative for neuronal markers (synaptophysin, CD56) and cytokeratin AE1/AE3. The overall MIB-1 labelling index was low, less than 1%.

The prominent angiocentric pattern of tumours growth allowed to establish the diagnosis of angiocentric gliomas.

Discussion

Angiocentric glioma is a rare, clinico-pathological entity that presents particularly in a childhood, often in association with medically intractable epilepsy [5, 6,8,18]. The appropriate diagnosis of this entity is critical, as this tumour is usually slow-growing and treatable by surgical excision alone [1,18]. AGs are sometimes associated with adjacent foci of cortical dysplasia, thus careful pre-surgical evaluation of the lesion is necessary to plan the extent of resection and achieve a better seizure-free outcome [11,20]. Such association with coexistent malformation of cortical development/cortical dysplasia might suggest a developmental basis of their origin [14].

AG displays various histopathological features, which resemble ependymoma, astroblastoma, pilocytic/pilomyxoid astrocytoma and schwannoma. It is particularly difficult to distinguish AG from other gliomas that exhibit perivascular arrangement of neoplastic cells. Angiocentric glioma is focally composed of spindle cells with eosinophilic cytoplasm arranged around cortical and white matter blood vessels, mimicking ependymal or astroblastomatous pseudorosettes. The case with atypical histopathology including astroblastoma-like features and onion-like structures were described [16]. All sizes of vessels are involved, including large arteries of cortical surface as well as more deeply situated capillaries. The proper classification of angiocentric glioma and separation it from other similar entities might be particularly difficult in limited biopsy material.

The cases presented here displayed characteristic perivascular orientation of neoplastic cells, accompanied by a schwannoma-like component and subpial spreading. The glial origin of the tumours was confirmed by cytoplasmic GFAP immunoreactivity. In both cases, the neoplastic cells revealed EMA staining of a dot-like pattern. The presence of pseudorosette-like fashion around blood vessels and intracytoplasmic "dot-like" EMA immunostaining are characteristic of ependymoma and might be related with ependymal differentiation of neoplastic cells. It has been documented that the specific "dot-like" EMA staining corresponds to microlumens. The presence of microlumens and microvilli, typical of ependymal cells, has been described in some electron microscopic evaluations of AG cases [15,18]. These findings supported ependymal differentiation in angiocentric gliomas, thus the distinction of AG from classic ependymoma ought to be very carefully validated. Ependymoma is usually more monomorphic and sometimes exhibits true central-lumen rosettes, ependymal canals and dis-

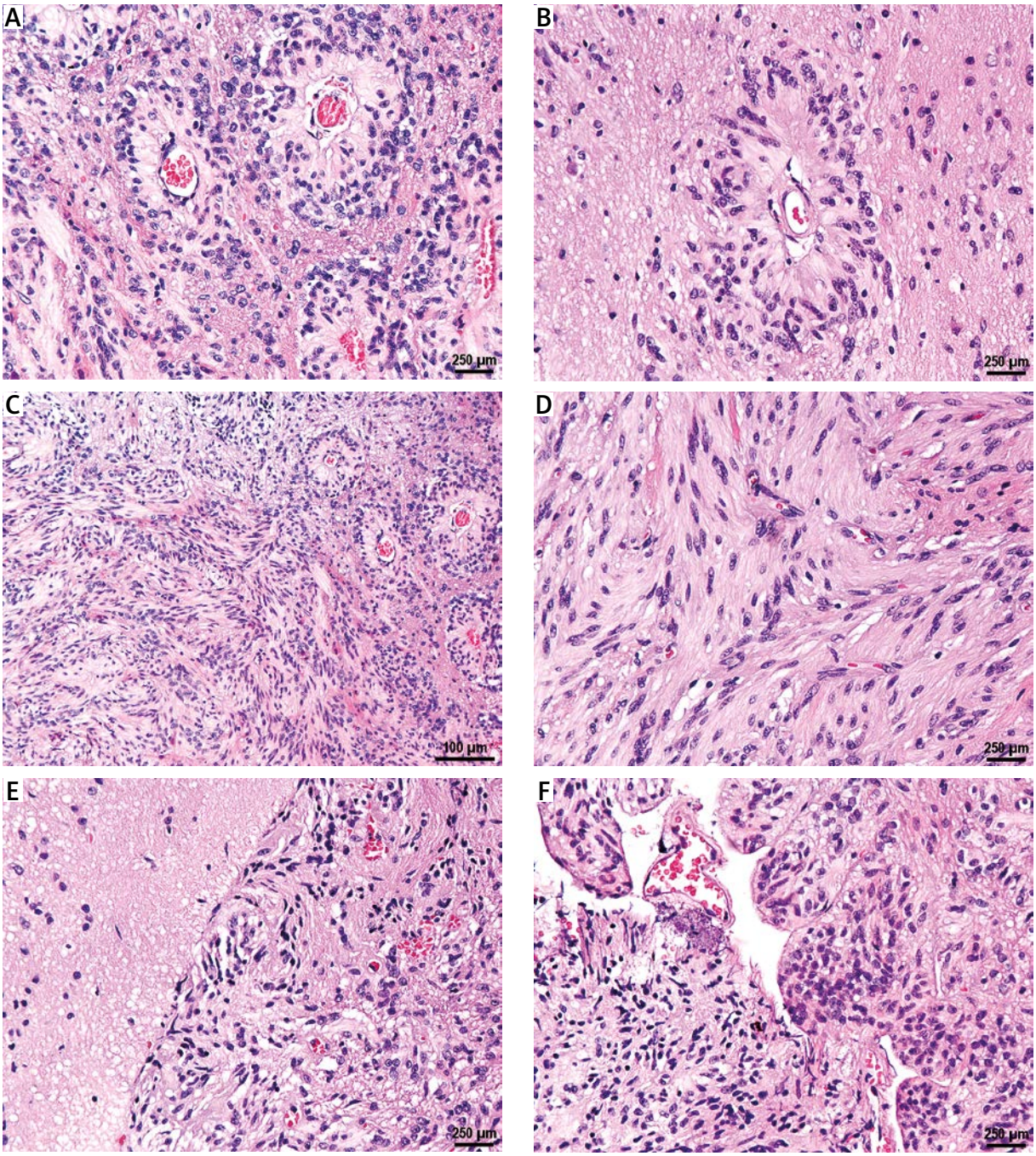

Fig. 3. Histopathological features of tumours. **A, B**) Angiocentric growth pattern with perivascular pseudorosettes, mimicking ependymoma. **C**) Compact masses of elongated neoplastic cells, mimicking schwannoma-like pattern. **D**) Palisade arrangement of the spindle-shaped tumour. **E**) Compact, elongated cells infiltrating the superficial layers of cerebral cortex. **F**) Subpial orthogonal aggregation of tumour cells in the subpial region of the cortex. H&E.

tinct fibrillary cytoplasmic processes. Its extraventricular, occasionally superficial location is unique and a long history of seizures is not typical. Moreover, the ependymoma is usually well-circumscribed, whereas angiocentric glioma presented more infiltrative growth. The correct identification of these

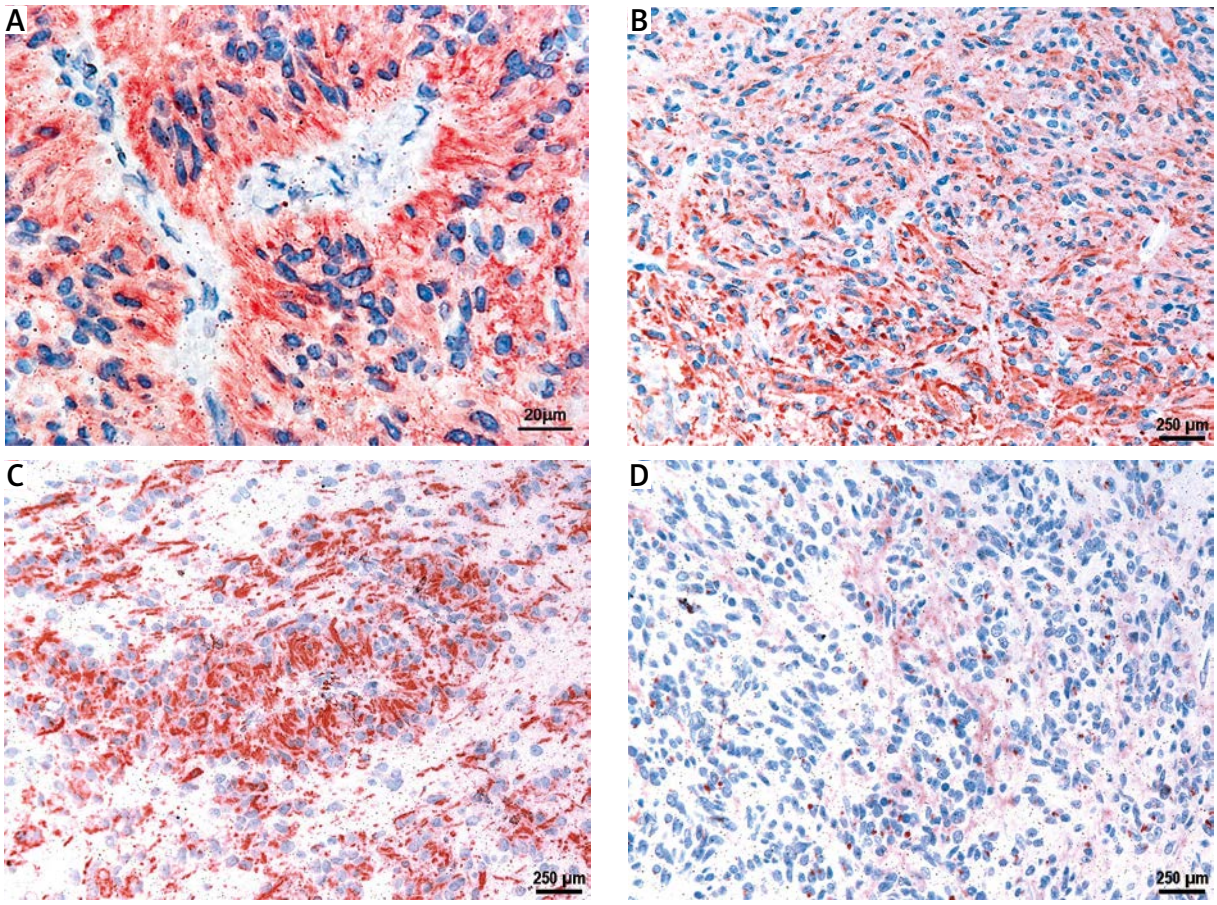

Fig. 4. Immunohistochemical staining. **A**) Strong cytoplasmic immunoreactivity for GFAP in bipolar tumour cells. **B**) Immunohistochemical stain for vimentin. **C**) S-100 protein immunoreactivity. **D**) Intracytoplasmic "dot-like" staining for EMA.

two brain tumours is crucial for their prognosis and treatment. However, the evidence of admixed features of these both entities might suggest their close relationship [13,21].

Angiocentric glioma may also resemble pilocytic astrocytoma, especially its pilomyxoid variant. However, pilocytic tumours are usually well-defined with myxoid background and their perivascular formations are not so distinct and compact as it is observed in angiocentric gliomas.

Other tumours of different histogenesis as astroblastoma and schwannoma ought to be also included in differential diagnosis. The distinction between AG and astroblastoma was a challenge as both tumours are characterized by a angiocentric growth pattern and strong GFAP expression. However, astroblastoma is a rare and controversial glia-derived neoplasm that is not universally accepted as a distinct entity. The so-called astroblastoma typically exhibits marked hyalinization of the blood vessels which is not characteristic of AG.

Another misleading feature of AG is palisading arrangement of neoplastic cells at the brain surface that resemble schwannoma-like structures. Less frequently, the neoplastic cells may be arranged in solid nests or nodules. Mitotic figures are usually not apparent but in some cases the increased mitotic activity accompanied by malignant features i.e. microvascular proliferation and necroses has been described [12,17]. In such high grade variant of AG with malignant features and tendency to recurrence, the postoperative radio- or chemo-therapy ought to be considered.

The histogenesis of AG is controversial. Angiocentric growth, "dot-like" EMA positivity and ultrastructural features suggest the ependymal differentiation of neoplastic cells. An origin from radial glial cells has been proposed. The molecular features connect-

ing with IDH1, IDH2 and BRAFV600E mutational status were described in three paediatric cases of this rare entity [4]. The loss of chromosomal bands 6q24 to q25 was evidenced in 1 of 8 analyzed cases [18].

Angiocentric glioma is an epileptogenic tumour and might be associated with adjacent cortical dysplasia. The outcome of majority of AG patients is very good with freedom from seizures following a gross total resection. Our two cases with a long follow-up illustrated that a complete excision leads to surgical cure and provides a seizure-free outcome.

Disclosure

Authors report no conflict of interest.

References

1. Alexandru D, Haghighi B, Muhonen MG. The treatment of angiocentric glioma: case report and literature review. Perm J 2013; 17: e100-102.
2. Arsene D, Ardeleanu C, Ogrezeanu I, Danaila L. Angiocentric glioma: presentation of two cases with dissimilar histology. Clin Neuropathol 2008; 27: 391-395.
3. Brat DJ, Scheithauer BW, Fuller GN, Tihan T. Newly codified glial neoplasms of the 2007 WHO Classification of Tumours of the Central Nervous System: angiocentric glioma, pilomyxoid astrocytoma and pituicytoma. Brain Pathol 2007; 17: 319-324.
4. Buccoliero AM, Castiglione F, Degl'innocenti DR, Moncini D, Spacca B, Giordano F, Genitori L, Taddei GL. Angiocentric glioma: clinical, morphological, immunohistochemical and molecular features in three pediatric cases. Clin Neuropathol 2013; 32: 107-113.
5. Burger PC, Jouvet A, Preusser M, Hans VH, Rosenblum MK, Lellouch-Tubiana A. Angiocentric glioma. In: Louis DN, Oghaki H, Wiesttler D, Cavenee WK (eds.). WHO Classification of Tumors of the Central Nervous System. 4th ed. IARC Press, Lyon 2007, pp. 92-93.
6. Chen G, Wang L, Wu J, Jin Y, Wang X, Jin Y. Intractable epilepsy due to angiocentric glioma: A case report and minireview. Exp Ther Med 2014; 7: 61-65.
7. Covington DB, Rosenblum MK, Brathwaite CD, Sandberg DI. Angiocentric glioma-like tumor of the midbrain. Pediatr Neurosurg 2009; 45: 429-433.
8. Fulton SP, Clarke DF, Wheless JW, Ellison DW, Ogg R, Boop FA. Angiocentric glioma-induced seizures in a 2-year-old child. J Child Neurol 2009; 24: 852-856.
9. Koral K. Angiocentric glioma. J Neurosurg Pediatr 2013; 12: 666.
10. Koral K, Koral KM, Sklar F. Angiocentric glioma in a 4-year-old boy: imaging characteristics and review of the literature. Clin Imaging 2012; 36: 61-64.
11. Liu CQ, Zhou J, Qi X, Luan GM. Refractory temporal lobe epilepsy caused by angiocentric glioma complicated with focal cortical dysplasia: a surgical case series. J Neurooncol 2012; 110: 375-380.
12. Lu JQ, Patel S, Wilson BA, Pugh J, Mehta V. Malignant glioma with angiocentric features. J Neurosurg Pediatr 2013; 11: 350-355.
13. Lum DJ, Halliday W, Watson M, Smith A, Law A. Cortical ependymoma or monomorphous angiocentric glioma? Neuropathology 2008; 28: 81-86.
14. Marburger T, Prayson R. Angiocentric glioma: a clinicopathologic review of 5 tumors with identification of associated cortical dysplasia. Arch Pathol Lab Med 2011; 135: 1037-1041.
15. Miyata H, Ryufuku M, Kubota Y, Ochiai T, Niimura K, Hori T. Adult-onset angiocentric glioma of epithelioid cell-predominant type of the mesial temporal lobe suggestive of a rare but distinct clinicopathological subset within a spectrum of angiocentric cortical ependymal tumors. Neuropathology 2012; 32: 479-491.
16. Ni HC, Chen SY, Chen L, Lu DH, Fu YJ, Piao YS. Angiocentric glioma: A report of nine new cases, including four with atypical histological features. Neuropathol Appl Neurobiol 2014; doi: 10.1111/nan.12158 [Epub ahead of print].
17. Pokharel S, Parker JR, Parker JC, Jr., Coventry S, Stevenson CB, Moeller KK. Angiocentric glioma with high proliferative index: case report and review of the literature. Ann Clin Lab Sci 2011; 41: 257-261.
18. Preusser M, Hoischen A, Novak K, Czech T, Prayer D, Hainfellner JA, Baumgartner C, Woermann FG, Tuxhorn IE, Pannek HW, Bergmann M, Radlwimmer B, Villagran R, Weber RG, Hans VH. Angiocentric glioma: report of clinico-pathologic and genetic findings in 8 cases. Am J Surg Pathol 2007; 31: 1709-1718.
19. Shakur SF, McGirt MJ, Johnson MW, Burger PC, Ahn E, Carson BS, Jallo GI. Angiocentric glioma: a case series. J Neurosurg Pediatr 2009; 3: 197-202.
20. Takada S, Iwasaki M, Suzuki H, Nakasato N, Kumabe T, Tominaga T. Angiocentric glioma and surrounding cortical dysplasia manifesting as intractable frontal lobe epilepsy – case report. Neurol Med Chir (Tokyo) 2011; 51: 522-526.
21. Wang M, Tihan T, Rojiani AM, Bodhireddy SR, Prayson RA, Iacuone JJ, Alles AJ, Donahue DJ, Hessler RB, Kim JH, Haas M, Rosenblum MK, Burger PC. Monomorphous angiocentric glioma: a distinctive epileptogenic neoplasm with features of infiltrating astrocytoma and ependymoma. J Neuropathol Exp Neurol 2005; 64: 875-881.

Original article

Folia Neuropathologica

The key role of sphingosine kinases in the molecular mechanism of neuronal cell survival and death in an experimental model of Parkinson's disease

Joanna A. Pyszko, Joanna B. Strosznajder

Department of Cellular Signalling, Mossakowski Medical Research Centre, Polish Academy of Sciences, Warsaw, Poland

Folia Neuropathol 2014; 52 (3): 260-269 DOI: 10.5114/fn.2014.45567

Abstract

Sphingosine kinases (Sphk1/2 EC 2.7.1.91) are responsible for synthesis of sphingosine-1-phosphate (S1P) and for regulation of the bioactive sphingolipids homeostasis. Sphingosine-1-phosphate can act as a potent messenger in an autocrine/paracrine manner through five specific G protein-coupled receptors (GPCR) S1P1-5. This sphingolipid is involved in the mechanism of transcription, mitochondrial function, neuronal viability and degeneration. Until now the involvement of Sphk1/2 and sphingolipid alterations in Parkinson's disease (PD) remains unknown. Recent studies have indicated the role of sphingolipids in the regulation of alpha-synuclein (ASN) in the PD brain. Our latest data demonstrated significant inhibition of Sphk1 gene expression and activity in an in vitro PD model, induced by 1-methyl-4-phenylpyridinium (MPP+). The aim of this study was to investigate the role of Sphks inhibition in ASN secretion and in the molecular mechanism of neuronal death in the PD model. Our study was carried out using neuronal dopaminergic SH-SY5Y control cells, transfected with the human gene for ASN or with an empty vector. These cells were treated with MPP+ (1-3 mM), which represents an experimental PD model, or with the Sphks inhibitor (1-5 μM SKI II) for 3-24 h. Our data indicated that MPP+ (3 mM) induced significant alterations of Sphks and S1P lyase (SPL) gene expression. Reduced activity of Sphk1 and Sphk2 in the cytosolic fraction and in the crude nuclear fraction, respectively, was observed. Sphks inhibition evoked enhancement of ASN secretion, suppression of PI3K/Akt phosphorylation and activation of gene expression for the pro-apoptotic Bcl-2 proteins Bax and BH3-only protein Harakiri. Moreover, a lower level of cytochrome c in the mitochondrial fraction and caspase-dependent degradation of DNA-bound enzyme poly(ADP-ribose) polymerase (PARP-1) were observed. The caspase inhibitor (20 μM Z-VAD-FMK) significantly enhanced neuronal cell viability in MPP+ oxidative stress. However, exogenous S1P (1 μM) exerted a more efficient neuroprotective effect as compared to Z-VAD-FMK. In summary, these data indicated that Sphk1 inhibition plays an important role in caspase-dependent apoptotic neuronal death in an experimental PD model.

Key words: *sphingosine kinases, dopaminergic neurons, apoptosis, PD model.*

Communicating author:

Prof. M.D., Ph.D. Joanna B. Strosznajder, Department of Cellular Signalling Mossakowski Medical Research Centre Polish Academy of Sciences, e-mail: jstrosznajder@imdik.pan.pl

Introduction

Sphingosine kinases (Sphk1 and Sphk2) catalyse ATP-dependent phosphorylation of sphingosine (Sph) to sphingosine 1-phosphate (S1P). Sphks are crucial enzymes in maintaining a balance between the lipid signalling molecules, such as ceramide/sphingosine, and S1P [36,37,50,53]. Sphk1 and Sphk2 share overall homology and synthesize S1P, which depending on intracellular localisations of Sphks isoforms plays different roles within the cell [36,50,55]. Sphk2 is located mainly in the nucleus, although it is also present in the other cell compartments (mitochondria, endoplasmic reticulum). The S1P pool synthesized by this isoform is demonstrated to exert an anti-proliferative and pro-apoptotic effect [22,29]. S1P synthesized by Sphk2 enhances histone H3 acetylation and is involved in regulation of genes encoding the cyclin-dependent kinase inhibitor p21 and c-fos [19]. The latest data reported by Takasugi *et al*. [52] indicated that the S1P pool synthesized by Sphk2 regulates β-amyloid (Aβ) precursor protein (APP) cleaving enzyme 1 (BACE1) activity and the Aβ level. Sphk1 resides predominantly in the cytosol and is translocated to the plasma membrane followed by ERK1/2-mediated phosphorylation [39,45,47]. Sphk1 is well known to synthesize the S1P pool, which exerts pro-survival effects within the cells. Sphk1 can be stimulated in response to neuronal growth factor and cytokines [13,32,46,58]. The S1P pool synthesized by Sphk1 can promote cell survival, proliferation and migration, and can also regulate differentiation, neurogenesis, angiogenesis, carcinogenesis and inflammation [16,33,50]. The level of intracellular S1P is regulated not only by Sphks but also by enzymes involved in its degradation, that means by S1P lyase (SPL) and by specific S1P phosphatase (SPP1) and also by less-specific SPP2 and other phosphatases (Fig. 1) [36,37]. S1P formed at the plasma membrane can be easily exported from the cell and can act in an autocrine or paracrine fashion through five specific G protein-coupled receptors (S1P1-S1P5), located in sphingolipid microdomains of cell membranes [49]. It is known that sphingolipids play a very important role in Alzheimer's disease (AD). However, there are only a few data about the involvement of sphingolipid metabolism in the pathogenesis/pathomechanism of Parkinson's disease (PD). Brugg *et al.* [28] reported that dopaminergic neurons in PD undergo apoptosis through a ceramide-dependent mechanism [5]. Recent observations indicated that heterozygous mutations in glucocerebrosidase (GBA), which catalyses the breakdown of glucosylceramide to ceramide and glucose, predispose to PD [28]. A recent study by Abbott *et al.* [1] showed an altered level of ceramide and ceramide synthase-1 gene expression in PD anterior cingulate cortex, containing Lewy body pathology. The main component of a Lewy body is α-synuclein (ASN), a small presynaptic protein that easily changes conformation under different types of stress [54,56]. Overexpression of ASN or its mutation plays a crucial role in PD pathogenesis/pathomechanism [40,56]. The ASN mutation is responsible for the familiar form of PD. ASN can be secreted from the cells and can act not only intra- but also extracellularly and can transmit protein pathology from cell to cell [56]. ASN is most toxic in the form of oligomers [20,56]. It was observed that ASN binds with high affinity to glycolipoprotein microdomains termed lipid rafts, which are enriched in sphingolipids [15]. The relationship between sphingolipids and ASN in neurodegeneration remains poorly understood. A study by Gómez-Santos *et al.* (2002) showed that MPP+ increases ASN expression in SH-SY5Y

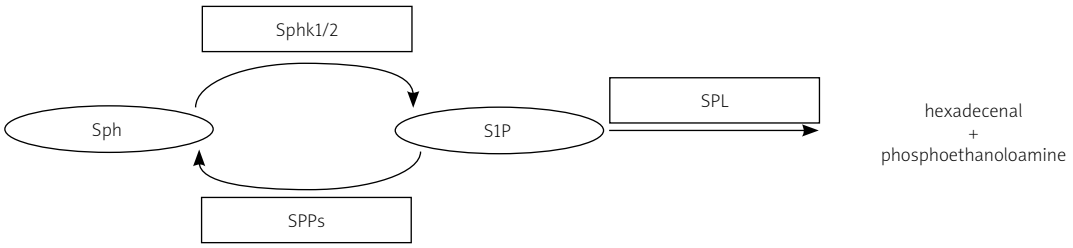

Sph – sphingosine, Sphk1/2 – sphingosine kinases 1/2, SPL – S1P lyase, SPPs – S1P phosphatases, S1P – sphingosine 1-phosphate

Fig. 1. Schematic representation of sphingosine-1-phosphate metabolic pathway.

cells and suggested that ASN could play an important role in this cellular model of PD [18]. Our latest data demonstrated that MPP+ and Sphks inhibition enhanced the free radical level and down-regulated Sphk1 expression and activity in the SH-SY5Y. Moreover, we observed that S1P protected against MPP+ evoked oxidative stress and alteration of gene expression for Sphk1 and for pro-apoptotic proteins (Bax, Hrk/DP5). S1P significantly enhanced cell viability mainly by activation of S1P1 receptor mediated signalling [41]. In our previous and in this study we used human dopaminergic SH-SY5Y cells, because they express tyrosine hydroxylase (HT), dopamine β-hydroxylase (DBH) [38] and the dopamine transporter (DAT) [24,51,59] and have been widely used to gain a better understanding of the molecular processes and pathomechanism of PD. In the present study we investigated gene expression for Sphk1/2 and for enzymes involved in S1P degradation (SPL and SPP). Moreover, we analyzed the role of Sphks activity inhibition in ASN secretion and in the molecular mechanism of neuronal cell death in oxidative stress induced by MPP+.

Material and methods

Cell culture

The studies were carried out using the human neuroblastoma cell line SH-SY5Y, control (non-transfected) and transfected with the human gene for alpha-synuclein (ASN), SH-SY5Y-T, or with an empty vector, SH-SY5Y-V (a kind gift from Prof. Nakamura, Kobe University Graduate School of Medicine, Japan; control SH-SY5Y cells were a kind gift from Prof. Anne Eckert, Neurobiology Laboratory for Brain Aging and Mental Health, Psychiatric University Clinics, University of Basel). The cells were cultured in MEM/F-12 Ham Nutrient Mixtures (1 : 1) supplemented with 15% heat-inactivated fetal bovine serum (FBS), 1% penicillin/streptomycin and 2 mM glutamine. The cells were maintained at 37°C in a humidified incubator containing 5% CO_2. For the experiments, SH-SY5Y control cells were sub-cultured into collagen-coated 100 mm^2 dishes. Prior to treatment, the medium was changed to low-serum medium (2% FBS). SH-SY5Y cells transfected with the gene for ASN and with the empty vector were sub-cultured into 6-well clusters at 4×10^4 cells/well and differentiated with 10 μM all-trans-retinoic acid (ATRA) for 5 days. Prior to treatment, the medium was changed to a serum-free medium with 10 μM ATRA.

Cell treatment protocols

SH-SY5Y control cells (non-transfected) were treated with 3 mM MPP+ (Sigma-Aldrich), with the Sphk1 inhibitor (SKI II 5 μM, Sigma-Aldrich) or with staurosporine (100 nM, Sigma-Aldrich) for 3-24 h. In some experiments the cells were pre-incubated with 1 μM S1P (Enzo Life Sciences) or with the caspase inhibitor (Z-VAD-FMK 20 μM, R&D Systems) added to the culture medium 1-2 h before MPP+, SKI II treatment or staurosporine treatment. SH-SY5Y-T or SH-SY5Y-V were treated with 1 mM MPP+ or with 1 μM SKI II for 24 h.

Assay of alpha-synuclein precipitation and immunochemical detection

The extracellular medium from SH-SY5Y treated cells and transfected with the ASN gene or with the empty vector was collected and rapidly frozen in liquid nitrogen for 0.5 h. After thawing at 95°C, 50 μg of BSA as a carrier protein was added. Protein precipitation was carried out by the addition of 100% TCA and incubating for 0.5 h at room temperature (RT). This mixture was then centrifuged at 13 000 × g for 4 min. Then the pellet was washed twice with 1.5 ml and 0.2 ml of cold acetone and centrifuged at 13 000 × g for 4 min. The pellet was dried at 95°C for 10 min to remove acetone, then resuspended in 25 μl of PBS and incubated at RT for 1 h. The pellet was denatured with 0.55 M Tris-based sample buffer (pH = 6.8) for 10 min. 40 μg of proteins were loaded into 15% polyacrylamide denaturing gels and subjected to electrophoresis (applied constant voltage, 100 V). After protein separation, each gel was placed on a nitrocellulose membrane (Amersham Biosciences) in a transfer buffer and the proteins were transferred to the membrane by applying 50 V for 2 h. After the transfer was completed the ASN level was detected by immunochemical reaction (Western blot) analysis. In order to block non-specific binding, the membrane was incubated at RT for 1 h in 5% dried skimmed milk and 0.3% Tween 20 in phosphate-buffered saline (PBS), pH 7.4. Incubation with primary antibody (anti-α synuclein 1 : 1000 dilution, Sigma-Aldrich) in PBS with 0.1% Tween 20 and 1% bovine serum albumin (BSA) was performed overnight at 4°C. Then the blots were washed three times for 15 min at RT in PBS with 0.1% Tween 20.

The membranes were then incubated with horseradish peroxidase (HRP)-conjugated anti-rabbit IgG secondary antibody diluted 1 : 800 (Sigma-Aldrich) at RT for 1 h. Then the blots were washed as described above and bound antibodies were visualised by enhanced chemiluminescence (Thermo Scientific). Incubation with the anti-β-actin antibody additionally confirmed equal protein loading.

Cell viability analysis

Mitochondrial function and cellular viability were evaluated by using 2-(4,5-dimethylthiazol-2-yl)-2,5-diphenyltetrazolium bromide (MTT). After 24 h incubation with appropriate compounds, MTT (2.5 mg/ml) was added to all of the wells. The cells were incubated at 37°C for 2 h. Then the cells were lysed in DMSO and spectrophotometric measurement at 595 nm was performed.

Preparation of the subcellular fraction

Preparation of the subcellular fraction was performed as described previously by Cieślik *et al*. (2013) [8]. Cells were washed and scraped into ice-cold PBS and were pelleted at 1000 rpm for 3 min at 4°C. The pellet was resuspended in hypotonic buffer (10 mM Tris, pH 7.4, 1 mM EDTA, 1 mM EGTA, 1 mM DTT, 1.5 mM $MgCl_2$, 10 mM KCl and protease inhibitor cocktail). The homogenate was prepared using a 26-gauge needle (10 passes). Then it was pelleted at 500 g for 10 min at 4°C. The pellet (P1, the crude nuclear fraction) was resuspended in 25 mM Tris, pH 7.4 with protease inhibitors and was used for Western blot analysis. The supernatant (S1) was centrifuged at 15 000 g for 15 min at 4°C to obtain a cytosolic (S2) and crude mitochondrial fraction (P2).

Measurement of Sphk1 and Sphk2 activity

Sphk activity assay was performed according to a previous report [52]. The pellet, P1 (the crude nuclear fraction), or supernatant, S1 (cytosolic together with the crude mitochondrial fraction), was resuspended in lysis buffer and used for enzymatic reaction. A total of 100 μg of protein of P1, S1 and NBD-Sphingosine (10 μM; Avanti Polar Lipids) was mixed in the reaction buffer (50 mM HEPES, pH 7.4, 15 mM $MgCl_2$, 0.5 mM KCl, 10% glycerol, and 2 mM ATP) and incubated in a final volume of 100 μl for 30 min at 30°C. The reactions were stopped by the addition of an equal amount of 1 M potassium phosphate, pH 8.5, followed by the addition of 500 μl of chloroform/methanol (2 : 1), and then centrifuged at 15 000 rpm for 1 min. The reactant NBD-S1P (but not the substrate NBD-Sphingosine) was collected into the alkaline aqueous phase. After the aqueous phase was combined with an equal amount of dimethylformamide, the fluorescence value was measured (λex = 485 nm, λem = 538 nm).

Determination of PARP-1 and cytochrome c protein level

After protein measurement according to Lowry, the homogenate of SH-SY5Y cells and the mitochondrial fraction were mixed with 5 × Laemmli sample buffer and denatured for 5 min at 95°C. A total of 40 μg of protein was loaded per lane on 10% acrylamide gels and examined by SDS-PAGE. The proteins were transferred onto PVDF membranes at 100 V. The membranes were incubated in 5% dry milk in TBS with Tween 20 (TBS-T) for 1 h and exposed overnight to specific antibodies: anti-cytochrome c (1 : 750, from Santa Cruz Biotechnology), anti-Actin (1 : 4000, from MP Biomedicals), anti-PARP-1 (1 : 500, from Sigma-Aldrich), anti-phospho-Akt (Ser473) and anti-Akt (1 : 750, Cell Signaling). After treatment for 1 h with horseradish-peroxidase-coupled secondary antibodies (anti-rabbit from Amersham Biosciences or anti-mouse from GE Healthcare), the protein bands were detected by ECL reagent (Thermo Scientific). Then the membranes were treated with stripping buffer (50 mM glycine, pH 2.5, 1% SDS) for further blots.

Analysis of the mRNA level using real-time PCR

RNA was isolated using a TRI reagent from Sigma-Aldrich. The isolated RNA was dissolved in RNase-free water (Ambion). The amount and purity of the RNA were determined using spectrophotometric measurement at 260 and 280 nm. The OD260/OD280 ratio of the RNA samples ranged from 1.8 to 2.0. Isolated RNA (5 μg) was treated with DNase and then used in RT-PCR. Reverse transcription was performed by using a High Capacity cDNA Reverse Transcription Kit according to the manufacturer's protocol (Applied Biosystems). Quantitative PCR was performed by using pre-developed TaqMan Gene Expression Assays (Applied Biosystems): actb Hs99999903_m1,

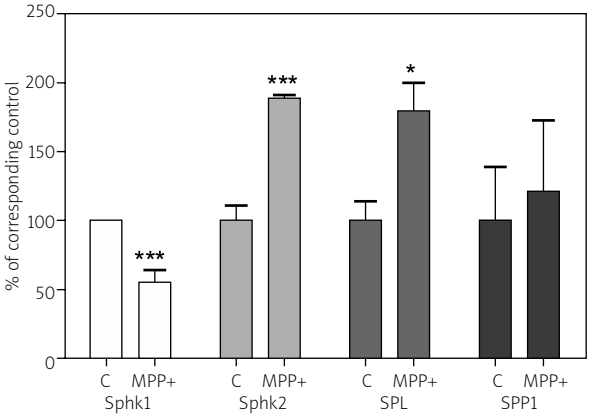

Fig. 2. Sphk1/2, SPL and SPP1 gene expression in MPP+-treated SH-SY5Y cells. SH-SY5Y cells were treated with MPP+ (3 mM) for 12 h. The mRNA level for Sphk1/2, SPL and SPP1 was normalized against β-actin (Actb). The relative level of mRNA was calculated by the ΔΔCt method. Data represent the mean value ± S.E.M from three independent experiments with three replications. Student's *t*-test was used. **p* < 0.05, ****p* < 0.001 – vs. control (non-treated) SH-SY5Y cells

bax Hs00180269_m1, hrk Hs02621354_s1, sphk1 Hs01116530_g1, sphk2 Hs01016543_g1, sgpl1 Hs00187407_m1, sgpp1 Hs00229266_m1 on an ABI PRISM 7500 apparatus according to the manufacturer's instructions. Actb was selected and used in all of the studies as a reference gene. The level of mRNA was calculated by the ΔΔCt method.

Statistical analysis

The results were expressed as mean values ± S.E.M. Differences between means were analysed using Student's *t*-test or one-way ANOVA followed by the Newman-Keuls *post hoc* test. Values of $p < 0.05$ were considered statistically significant.

Results

Human dopaminergic cells (SH-SY5Y) were exposed to 3 mM MPP+ for 24 h. Significant changes in the gene expression level for enzymes involved in the synthesis and degradation of S1P in MPP+-treated SH-SY5Y cells took place. It was observed that MPP+ reduced gene expression for Sphk1 and up-regulated Sphk2. These changes were accompanied by signif-

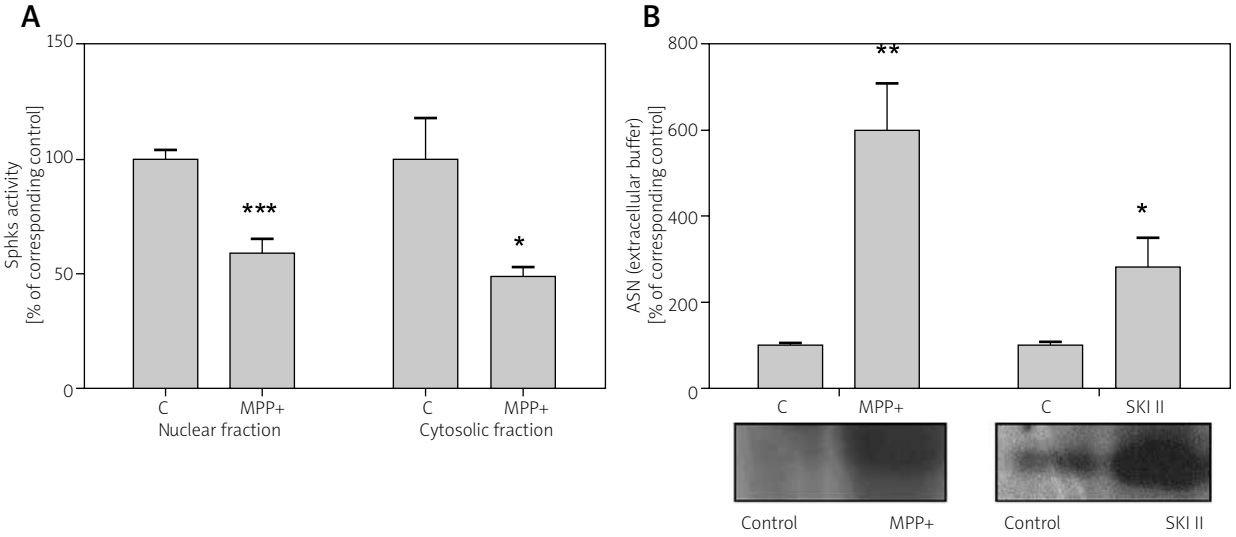

Fig. 3. Sphk1/2 activity in MPP+-treated SH-SY5Y cells and the role of Sphks inhibition and MPP+ in ASN release from the SH-SY5Y-T cells. **A)** SH-SY5Y cells were treated with MPP+ (3 mM) for 24 h. Sphks activity was measured in the cytosolic and crude nuclear fraction. Data represent the mean value ± S.E.M from three independent experiments with two replications. Student's *t*-test was used; **p* < 0.05, ****p* < 0.001 – vs. control (non-treated) SH-SY5Y cells. **B)** SH-SY5Y-T cells were treated with MPP+ (1 mM) and SKI II (1 μM) for 24 h. Control represents non-treated SH-SY5Y-T cells. The immunochemical level of ASN in the extracellular buffer was detected. Data represent the mean value ± S.E.M from three independent experiments. Student's *t*-test was used. **p* < 0.05, ***p* < 0.01 – vs. control (non-treated) SH-SY5Y-T cells.

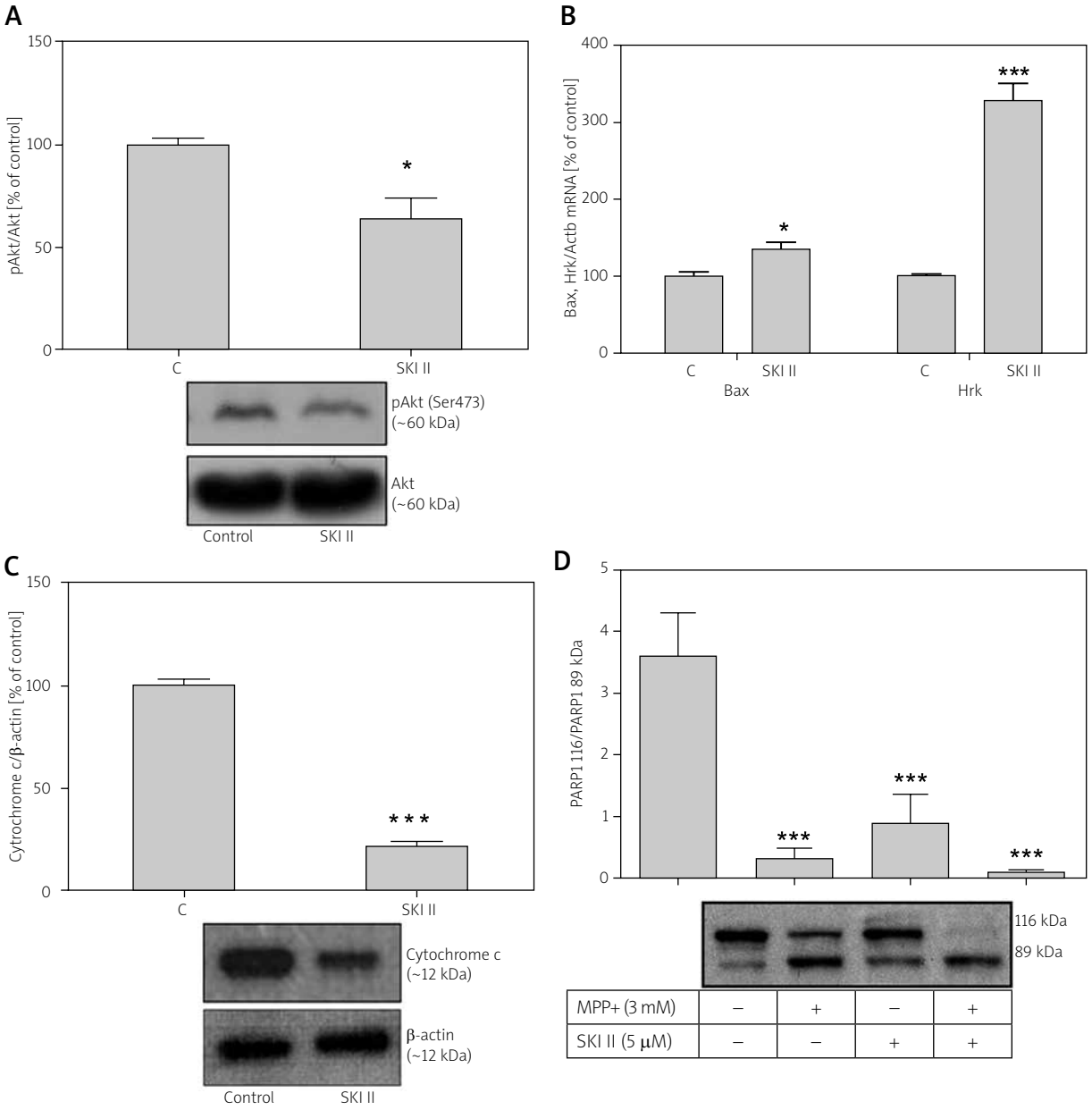

Fig. 4. Effect of Sphks inhibition (using SKI II) on Akt phosphorylation, Bax and Hrk gene expression, level of cytochrome c in the mitochondrial fraction and PARP1 degradation. **A)** SH-SY5Y cells were treated with SKI II (5 μM) for 24 h. Immunochemical detection of pAkt(Ser473)/Akt in cell homogenate was measured. Data represent the mean value ± S.E.M from four independent experiments. Student's *t*-test was used. **p* < 0.05 – vs. control (non-treated) SH-SY5Y cells. **B)** The mRNA level for Bax and Hrk was normalized against β-actin (Actb). The relative level of mRNA was calculated by the ΔΔCt method. Data represent the mean value ± S.E.M from three independent experiments with three replications. Student's *t*-test was used. **p* < 0.05, ****p* < 0.001 – vs. control (non-treated) SH-SY5Y cells. **C)** Immunochemical detection of cytochrome c/β-actin in the mitochondrial fraction was measured. Data represent the mean value ± S.E.M from four independent experiments. Student's *t*-test was used. ****p* < 0.001 – vs. control (non-treated) SH-SY5Y cells. **D)** SH-SY5Y cells were treated with 3 mM MPP+, 5 μM SKI II and with both compounds together for 24 h. The immunochemical detection of PARP1 116 kDa/PARP1 89 kDa in cell homogenate was measured. Data represent the mean value ± S.E.M from four independent experiments. One-way ANOVA followed by the Newman-Keuls *post-hoc* test was used. ****p* < 0.001 – vs. control (non-treated) SH-SY5Y cells.

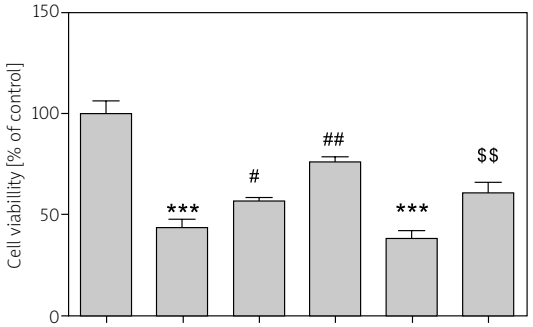

MPP + 3 mM	–	+	+	+	–	–
Z-VAD-FMK 20 μM	–	–	+	–	–	+
S1P 1 μM	–	–	–	+	–	–
Staurospo-rine 100 nM	–	–	–	–	+	+

Fig. 5. Effect of caspase inhibitor and S1P on MPP+-treated SH-SY5Y cell viability. SH-SY5Y cells were treated with caspase inhibitor (20 μM Z-VAD-FMK) for 2 h or with 1 μM S1P for 1 h and then exposed to 3 mM MPP+ or 100 nM staurosporine for 24 h. Cell viability was determined using MTT assay. Data represent the mean value ± S.E.M from four independent experiments with 4-6 replications. One-way ANOVA followed by the Newman-Keuls post-hoc test was used. $^{***}p < 0.001$ vs. control (non-treated) SH-SY5Y cells; $^{\#}p < 0.05$, $^{\#\#}p < 0.01$ vs. MPP+-treated cells; $^{\$\$} < 0.01$ – vs. staurosporine-treated cells.

icant enhancement of mRNA for SPL, but there was no alteration of S1P phosphatase (SPP1) gene expression (Fig. 2). In these stress conditions, Sphk1 activity in the cytosolic fraction and Sphk2 in the nuclear fraction were measured. Spectrofluorometric analysis indicated that the activity of both enzymes was reduced in MPP+-treated cells (Fig. 3A). Subsequently, we examined the effect of Sphks inhibitor (SKI II 1 μM) and MPP+ (1 mM) (at a concentration that did not change cell viability) on ASN secretion from ASN-transfected cells (SH-SY5Y-T and SH-SY5Y-V). Our data indicated that these compounds significantly enhanced ASN release into the extracellular space (Fig. 3B). Then the role of Sphks inhibition in other molecular events involved in neuronal death, evoked by MPP+, was analyzed. Here we found that the Sphks inhibitor (5 μM SKI II) caused significant suppression of PI3K/Akt phosphorylation/activity (Fig. 4A) and an increase in gene expression for the pro-apoptotic Bcl-2 proteins Bax and Hrk (Fig. 4B). Moreover, Sphks inhibition by 5 μM SKI II significantly reduced the level of cytochrome c in the mitochondrial fraction from the SH-SY5Y cells (Fig. 4C). It was also demonstrated that Sphks inhibition led to degradation of nuclear enzyme poly(ADP-ribose) polymerase PARP1, the preferential substrate for caspase 3 (Fig. 4D). A similar effect of PARP1 degradation was evoked by MPP+. Inhibitor of caspases (20 μM Z-VAD-FMK) enhanced cell viability in MPP+ evoked oxidative stress. However, 1 μM S1P exerts a more efficient neuroprotective effect (Fig. 5).

Discussion

In this study we analysed the role of Sphks inhibition on ASN secretion and in the molecular mechanism of dopaminergic neuronal death in oxidative stress evoked by MPP+. We found altered gene expression and activity of both Sphk1 and Sphk2. The activity of both kinases was significantly decreased in MPP+-evoked stress. We demonstrated that Sphks inhibition evoked death signalling by stimulation of ASN secretion and several molecular events, including inhibition of PI3K/Akt, activation of pro-apoptotic protein expression, release of cytochrome c from the mitochondria and caspase-dependent apoptosis. PI3K/Akt participates in Bax phosphorylation and in stabilization of Bad/14-3-3 complexes [12,42,48]. These events protect against translocation of the pro-apoptotic proteins from the cytosol to the mitochondria and reduce cell death. Several studies have found that S1P, synthesized by Sphk1, is responsible for promoting pro-survival processes through PI3K/Akt [27,31,35]. Here we demonstrated that inhibition of Sphks/S1P formation by SKI II reduced PI3K/Akt phosphorylation on Serine 473 and reduced its activity. Subsequently, these events may reduce BAD phosphorylation. In our experiments we observed lower BAD phosphorylation, but the results were statistically insignificant (data not shown). In this study we found that inhibition of Sphks induced significant up-regulation of Bax and Hrk. Both of these pro-apoptotic proteins are engaged in alteration of mitochondrial membrane potential/permeability and cytochrome c release. Lower content of cytochrome c in mitochondria was observed in our study. It was previously demonstrated that S1P regulates cell survival/death through Bcl-2 proteins [3,4,9,26,43]. Exogenous S1P (1 μM)

enhanced the expression of anti-apoptotic Bcl-2 protein and cell survival in oxidative stress evoked by ceramide [11]. Recently, we demonstrated that S1P (1 μM) reduced the Bax and Hrk mRNA level in MPP+-treated SH-SY5Y cells [41]. In this study we observed that S1P (1 μM) exerted a more efficient neuroprotective effect than the caspase inhibitor. There are no data showing Sphk1/S1P alteration in the PD human brain, as opposed to several post-mortem studies on AD brains demonstrating disturbances in sphingolipid metabolism, including changes in the expression of Sphk1/2, SPL and SPP [6,21,23]. It was shown that Sphk1 and Sphk2 activity declined concomitantly with progression of AD pathology in the hippocampus and in temporal grey matter. Subsequently, the S1P/sphingosine ratio decreased in parallel with an increase in neuropathological changes as described in Braak stages in AD [10]. Recent data demonstrated ceramide and lipid rafts alterations in PD [7,14,15]. It was found that reduced glucocerebrosidase and, in consequence, accumulation of glucosylceramide are associated with an increased ASN level in sporadic PD [34]. The data of Martinez *et al*. [30], Czubowicz and Strosznajder [11] demonstrated that ceramide dose-dependently reduced the viability of primary dopaminergic neurons and neuroblastoma cells respectively. Moreover, the data of Martinez *et al*. [30] showed that the inhibitors of sphingomyelinases protected dopaminergic neurons against ceramide formation, endoplasmic stress, caspase 3 activation and decrease in Akt phosphorylation. Our data suggest that inhibition of Sphks could be responsible for the transient enhancement of sphingosine and for the accumulation of ceramide. The latest study by Murphy *et al*. [34] indicated a significant relationship between lipids and ASN in PD. Our results demonstrated that inhibition of Sphks leads to ASN secretion from dopaminergic neuronal cells. Sphks inhibition and S1P have no effect on ASN gene expression and protein level (data not shown). It was found that MPP+ also evoked ASN release. A previous study suggested that ASN might be a key player in oxidative stress and in MPP+-induced mitochondrial dysfunction of SH-SY5Y cells [57]. Oxidative/nitrosative stress, evoked by different experimental conditions, leads to ASN release from the brain synaptosomal fraction [2]. It seems that in our experimental conditions, the enhanced free radical level and oxidative stress could also be involved in ASN release. Extracellular ASN may be responsible for propagation of pathology from cell to cell. ASN oligomerisation causes oxidative stress and leads to mitochondrial failure and cell death. A rapidly growing amount of evidence indicates that extracellular ASN in oligomeric form contributes to PD pathology [25,56]. In summary, our data indicate that Sphk1 inhibition plays an important role in ASN release and in caspase-dependent apoptotic dopaminergic neuronal death in the experimental PD model.

Acknowledgement

Supported by NCN Grant 5870/B/PO1/2011/40.

Disclosure

Authors report no conflict of interest.

References

1. Abbott SK, Li H, Muñoz SS, Knoch B, Batterham M, Murphy KE, Halliday GM, Garner B. Altered ceramide acyl chain length and ceramide synthase gene expression in Parkinson's disease. Mov Disord 2014; 29: 518-526.
2. Adamczyk A, Kacprzak M, Kazmierczak A. Alpha-synuclein decreases arachidonic acid incorporation into rat striatal synaptoneurosomes. Folia Neuropathol 2007; 45: 230-235.
3. Bektas M, Jolly PS, Müller C, Eberle J, Spiegel S, Geilen CC. Sphingosine kinase activity counteracts ceramide-mediated cell death in human melanoma cells: role of Bcl-2 expression. Oncogene 2005; 24: 178-187.
4. Betito S, Cuvillier O. Regulation by sphingosine 1-phosphate of Bax and Bad activities during apoptosis in a MEK-dependent manner. Biochem Biophys Res Commun 2006; 340: 1273-1277.
5. Brugg B, Michel PP, Agid Y, Ruberg M. Ceramide induces apoptosis in cultured mesencephalic neurons. Neurochem J 1996; 66: 733-739.
6. Ceccom J, Loukh N, Lauwers-Cances V, Touriol C, Nicaise Y, Gentil C, Uro-Coste E, Pitson S, Maurage CA, Duyckaerts C, Cuvillier O, Delisle MB. Reduced sphingosine kinase-1 and enhanced sphingosine 1-phosphate lyase expression demonstrate deregulated sphingosine 1-phosphate signaling in Alzheimer's disease. Acta Neuropathol Commun 2014; 2: 12.
7. Cheng D, Jenner AM, Shui G, Cheong WF, Mitchell TW, Nealon JR, Kim WS, McCann H, Wenk MR, Halliday GM, Garner B. Lipid pathway alterations in Parkinson's disease primary visual cortex. PLoS One 2011; 6: e17299.
8. Cieslik M, Pyszko J, Strosznajder JB. Docosahexaenoic acid and tetracyclines as promising neuroprotective compounds with poly(ADP-ribose) polymerase inhibitory activities for oxidative/genotoxic stress treatment. Neurochem Int 2013; 62: 626-636.
9. Colié S, Van Veldhoven PP, Kedjouar B, Bedia C, Albinet V, Sorli SC, Garcia V, Djavaheri-Mergny M, Bauvy C, Codogno P, Levade T, Andrieu-Abadie N. Disruption of sphingosine 1-phosphate lyase confers resistance to chemotherapy and promotes

oncogenesis through Bcl-2/Bcl-xL up-regulation. Cancer Res 2009; 69: 9346-9353.
10. Couttas TA, Kain N, Daniels B, Lim XY, Shepherd C, Kril J, Pickford R, Li H, Garner B, Don AS. Loss of the neuroprotective factor Sphingosine 1-phosphate early in Alzheimer's disease pathogenesis. Acta Neuropathol Commun 2014; 2: 9.
11. Czubowicz K, Strosznajder R. Ceramide in the Molecular Mechanisms of Neuronal Cell Death. The Role of Sphingosine-1-Phosphate. Mol Neurobiol 2014; doi: 10.1007/s12035-013-8606-4.
12. Datta SR, Dudek H, Tao X, Masters S, Fu H, Gotoh Y, Greenberg ME. Akt phosphorylation of BAD couples survival signals to the cell-intrinsic death machinery. Cell 1997; 91: 231-241.
13. Edsall LC, Pirianov GG, Spiegel S. Involvement of sphingosine 1-phosphate in nerve growth factor-mediated neuronal survival and differentiation. J Neurosci 1997; 17: 6952-6960.
14. Fabelo N, Martín V, Santpere G, Marín R, Torrent L, Ferrer I, Díaz M. Severe alterations in lipid composition of frontal cortex lipid rafts from Parkinson's disease and incidental Parkinson's disease. Mol Med 2011; 17: 1107-1118.
15. Fortin DL, Troyer MD, Nakamura K, Kubo S, Anthony MD, Edwards RH. Lipid rafts mediate the synaptic localization of alpha-synuclein. J Neurosci 2004; 24: 6715-6723.
16. Fyrst H, Saba JD. An update on sphingosine-1-phosphate and other sphingolipid mediators. Nat Chem Biol 2010; 6: 489-497.
17. Giasson B, Duda JE, Murray IV, Chen Q, Souza JM, Hurtig HI, Ischiropoulos H, Trojanowski JQ, Lee VM. Oxidative damage linked to neurodegeneration by selective alpha-synuclein nitration in synucleinopathy lesions. Science 2000; 290: 985-989.
18. Gómez-Santos C, Ferrer I, Reiriz J, Viñals F, Barrachina M, Ambrosio S. MPP+ increases alpha-synuclein expression and ERK/MAP-kinase phosphorylation in human neuroblastoma SH-SY5Y cells. Brain Res 2002; 935: 32-39.
19. Hait NC, Allegood J, Maceyka M, Strub GM, Harikumar KB, Singh SK, Luo C, Marmorstein R, Kordula T, Milstien S, Spiegel S. Regulation of histone acetylation in the nucleus by sphingosine-1-phosphate. Science 2009; 325: 1254-1257.
20. Hansen C, Angot E, Bergström AL, Steiner JA, Pieri L, Paul G, Outeiro TF, Melki R, Kallunki P, Fog K, Li JY, Brundin P. α-Synuclein propagates from mouse brain to grafted dopaminergic neurons and seeds aggregation in cultured human cells. J Clin Invest 2011; 121: 715-725.
21. He X, Huang Y, Li B, Gong CX, Schuchman EH. Deregulation of sphingolipid metabolism in Alzheimer's disease. Neurobiol Aging 2010; 31: 398-408.
22. Igarashi N, Okada T, Hayashi S, Fujita T, Jahangeer S, Nakamura S. Sphingosine kinase 2 is a nuclear protein and inhibits DNA synthesis. J Biol Chem 2003; 278: 46832-46839.
23. Katsel P, Li C, Haroutunian V. Gene expression alterations in the sphingolipid metabolism pathways during progression of dementia and Alzheimer's disease: a shift toward ceramide accumulation at the earliest recognizable stages of Alzheimer's disease? Neurochem Res 2007; 32: 845-856.
24. Korecka JA, van Kesteren RE, Blaas E, Spitzer SO, Kamstra JH, Smit AB, Swaab DF, Verhaagen J, Bossers K. Phenotypic characterization of retinoic acid differentiated SH-SY5Y cells by transcriptional profiling. PLoS One 2013; 8: e63862.
25. Lee HJ, Bae EJ, Lee SJ. Extracellular α-synuclein-a novel and crucial factor in Lewy body diseases. Nat Rev Neurol 2014; 10: 92-98.
26. Li QF, Wu CT, Guo Q, Wang H, Wang LS. Sphingosine 1-phosphate induces Mcl-1 upregulation and protects multiple myeloma cells against apoptosis. Biochem Biophys Res Commun 2008; 371: 159-162.
27. Limaye V, Li X, Hahn C, Xia P, Berndt MC, Vadas MA, Gamble JR. Sphingosine kinase-1 enhances endothelial cell survival through a PECAM-1-dependent activation of PI-3K/Akt and regulation of Bcl-2 family members. Blood 2005; 105: 3169-3177.
28. Lwin A, Orvisky E, Goker-Alpan O, LaMarca ME, Sidransky E. Glucocerebrosidase mutations in subjects with parkinsonism. Mol Genet Metab 2004; 81: 70-73.
29. Maceyka M, Sankala H, Hait NC, Le Stunff H, Liu H, Toman R, Collier C, Zhang M, Satin LS, Merrill AH Jr, Milstien S, Spiegel S. SphK1 and SphK2, sphingosine kinase isoenzymes with opposing functions in sphingolipid metabolism. J Biol Chem 2005; 280: 37118-37129.
30. Martinez TN, Chen X, Bandyopadhyay S, Merrill AH, Tansey MG. Ceramidesphingolipid signaling mediates Tumor Necrosis Factor (TNF)-dependent toxicity via caspase signaling in dopaminergic neurons. Mol Neurodegener 2012; 7: 45.
31. Means CK, Xiao CY, Li Z, Zhang T, Omens JH, Ishii I, Chun J, Brown JH. Sphingosine 1-phosphate S1P2 and S1P3 receptor-mediated Akt activation protects against in vivo myocardial ischemia-reperfusion injury. Am J Physiol Heart Circ Physiol 2007; 292: H2944-2951.
32. Meyer zu Heringdorf D, Lass H, Kuchar I, Lipinski M, Alemany R, Rumenapp U, Jakobs KH. Stimulation of intracellular sphingosine-1-phosphate production by G-protein-coupled sphingosine-1-phosphate receptors. Eur J Pharmacol 2001; 414: 145-154.
33. Mizugishi K, Yamashita T, Olivera A, Miller GF, Spiegel S, Proia RL. Essential role for sphingosine kinases in neural and vascular development. Mol Cell Biol 2005; 25: 11113-11121.
34. Murphy KE, Gysbers AM, Abbott SK, Tayebi N, Kim WS, Sidransky E, Cooper A, Garner B, Halliday GM. Reduced glucocerebrosidase is associated with increased α-synuclein in sporadic Parkinson's disease. Brain 2014; 137: 834-848.
35. Nakahara T, Iwase A, Nakamura T, Kondo M, Bayasula, Kobayashi H, Takikawa S, Manabe S, Goto M, Kotani T, Kikkawa F. Sphingosine-1-phosphate inhibits H2O2-induced granulosa cell apoptosis via the PI3K/Akt signaling pathway. Fertil Steril 2012; 98: 1001-1008.
36. Neubauer HA, Pitson SM. Roles, regulation and inhibitors of sphingosine kinase 2. FEBS J 2013; 280: 5317-5336.
37. Orr Gandy KA, Obeid LM. Targeting the sphingosine kinase/sphingosine 1-phosphate pathway in disease: review of sphingosine kinase inhibitors. Biochim Biophys Acta 2013; 1831: 157-166.
38. Oyarce AM, Fleming PJ. Multiple forms of human dopamine beta-hydroxylase in SH-SY5Y neuroblastoma cells. Arch Biochem Biophys 1991; 290: 503-510.
39. Pitson SM, Moretti PA, Zebol JR, Lynn HE, Xia P, Vadas MA, Wattenberg BW. Activation of sphingosine kinase 1 by ERK1/2-mediated phosphorylation. EMBO J 2003; 22: 5491-5500.
40. Polymeropoulos MH, Lavedan C, Leroy E, Ide SE, Dehejia A, Dutra A, Pike B, Root H, Rubenstein J, Boyer R, Stenroos ES, Chandrasekharappa S, Athanassiadou A, Papapetropoulos T, John-

son WG, Lazzarini AM, Duvoisin RC, Di Iorio G, Golbe LI, Nussbaum RL. Mutation in the alpha-synuclein gene identified in families with Parkinson's disease. Science 1997; 276: 2045-2047.
41. Pyszko J, Strosznajder JB. Sphingosine Kinase 1 and Sphingosine-1-Phosphate in Oxidative Stress Evoked by 1-Methyl-4-Phenylpyridinium (MPP+) in Human Dopaminergic Neuronal Cells. Mol Neurobiol 2014; doi: 10.1007/s12035-013-8622-4 [Epub ahead of print].
42. Rosenquist M. 14-3-3 proteins in apoptosis. Braz J Med Biol Res 2003; 36: 403-408.
43. Sauer B, Gonska H, Manggau M, Kim DS, Schraut C, Schäfer-Korting M, Kleuser B. Sphingosine 1-phosphate is involved in cytoprotective actions of calcitriol in human fibroblasts and enhances the intracellular Bcl-2/Bax rheostat. Pharmazie 2005; 60: 298-304.
44. Spiegel S, Milstien S. Sphingosine-1-phosphate: an enigmatic signalling lipid. Nat Rev Mol Cell Biol 2003; 4: 397-407.
45. Stahelin RV, Hwang JH, Kim JH, Park ZY, Johnson KR, Obeid LM, Cho W. The mechanism of membrane targeting of human sphingosine kinase 1. J Biol Chem 2005; 280: 43030-43038.
46. Sukocheva OA, Wadham C, Holmes A, Albanese N, Verrier E, Feng F, Bernal A, Derian CK, Ullrich A, Vadas MA, Xia P. Estrogen transactivates EGFR via the sphingosine 1-phosphate receptor Edg-3: the role of sphingosine kinase-1. J Cell Biol 2006; 173: 301-310.
47. Sutherland CM, Moretti PA, Hewitt NM, Bagley CJ, Vadas MA, Pitson SM. The calmodulin binding site of sphingosine kinase and its role in agonist-dependent translocation of sphingosine kinase 1 to the plasma membrane. J Biol Chem 2006; 281: 11693-11701.
48. Szanto A, Bognar Z, Szigeti A, Szabo A, Farkas L, Gallyas F Jr. Critical role of bad phosphorylation by Akt in cytostatic resistance of human bladder cancer cells. Anticancer Res 2009; 29: 159-164.
49. Taha TA, Argraves KM, Obeid LM. Sphingosine-1-phosphate receptors: receptor specificity versus functional redundancy. Biochim Biophys Acta 2004; 1682: 48-55.
50. Takabe K, Paugh SW, Milstien S, Spiegel S. "Inside-out" signaling of sphingosine-1-phosphate: therapeutic targets. Pharmacol Rev 2008; 60: 181-195.
51. Takahashi T, Deng Y, Maruyama W, Dostert P, Kawai M, Naoi M. Uptake of a neurotoxin-candidate, (R)-1,2-dimethyl-6,7-dihydroxy-1,2,3,4-tetrahydroisoquinoline into human dopaminergic neuroblastoma SH-SY5Y cells by dopamine transport system. J Neural Transm Gen Sect 1994; 98: 107-118.
52. Takasugi N, Sasaki T, Suzuki K, Osawa S, Isshiki H, Hori Y, Shimada N, Higo T, Yokoshima S, Fukuyama T, Lee VM, Trojanowski JQ, Tomita T, Iwatsubo T. BACE1 activity is modulated by cell-associated sphingosine-1-phosphate. J Neurosci 2011; 31: 6850-6857.
53. Takuwa Y, Okamoto Y, Yoshioka K, Takuwa N. Sphingosine-1 -phosphate signaling in physiology and diseases. Biofactors 2012; 38: 329-337.
54. Uversky VN, Eliezer D. Biophysics of Parkinson's disease: structure and aggregation of alpha-synuclein. Curr Protein Pept Sci 2009; 10: 483-499.
55. Van Brocklyn JR, Williams JB. The control of the balance between ceramide and sphingosine-1-phosphate by sphingosine kinase: oxidative stress and the seesaw of cell survival and death. Comp Biochem Physiol B Biochem Mol Biol 2012; 163: 26-36.
56. Wilkaniec A, Strosznajder JB, Adamczyk A. Toxicity of extracellular secreted alpha-synuclein: Its role in nitrosative stress and neurodegeneration. Neurochem Int 2013; 62: 776-783.
57. Wu F, Poon WS, Lu G, Wang A, Meng H, Feng L, Li Z, Liu S. Alpha-synuclein knockdown attenuates MPP+ induced mitochondrial dysfunction of SH-SY5Y cells. Brain Res 2009; 1292: 173-179.
58. Xia P, Wang L, Moretti PA, Albanese N, Chai F, Pitson SM, D'Andrea RJ, Gamble JR, Vadas MA. Sphingosine kinase interacts with TRAF2 and dissects tumor necrosis factor-alpha signaling. J Biol Chem 2002; 277: 7996-8003.
59. Xie HR, Hu LS, Li GY. SH-SY5Y human neuroblastoma cell line: in vitro cell model of dopaminergic neurons in Parkinson's disease. Chin Med J (Engl) 2010; 123: 1086-1092.

Original article

Folia Neuropathologica

Delayed preconditioning with NMDA receptor antagonists in a rat model of perinatal asphyxia

Dorota Makarewicz[1], Dorota Sulejczak[2], Małgorzata Duszczyk[1], Michał Małek[1], Marta Słomka[1], Jerzy W. Lazarewicz[1]

[1]Department of Neurochemistry, Mossakowski Medical Research Centre, Polish Academy of Sciences, Warsaw, [2]Department of Experimental Pharmacology, Mossakowski Medical Research Centre, Polish Academy of Sciences, Warsaw, Poland

Folia Neuropathol 2014; 52 (3): 270-284 DOI: 10.5114/fn.2014.45568

Abstract

Introduction: *In vitro experiments have demonstrated that preconditioning primary neuronal cultures by temporary application of NMDA receptor antagonists induces long-term tolerance against lethal insults. In the present study we tested whether similar effects also occur in brain submitted to ischemia in vivo and whether the potential benefit outweighs the danger of enhancing the constitutive apoptosis in the developing brain.*

Material and methods: *Memantine in pharmacologically relevant doses of 5 mg/kg or (+)MK-801 (3 mg/kg) was administered i.p. 24, 48, 72 and 96 h before 3-min global forebrain ischemia in adult Mongolian gerbils or prior to hypoxia/ischemia in 7-day-old rats. Neuronal loss in the hippocampal CA1 in gerbils or weight deficit of the ischemic hemispheres in the rat pups was evaluated after 14 days. Also, the number of apoptotic neurons in the immature rat brain was evaluated.*

Results**:** *In gerbils only the application of (+)MK-801 24 h before ischemia resulted in significant prevention of the loss of pyramidal neurons. In rat pups administration of (+)MK-801 at all studied times before hypoxia-ischemia, or pretreatment with memantine or with hypoxia taken as a positive control 48 to 92 h before the insult, significantly reduced brain damage. Both NMDA receptor antagonists equally reduced the number of apoptotic neurons after hypoxia-ischemia, while (+)MK-801-evoked potentiation of constitutive apoptosis greatly exceeded the effect of memantine.*

Conclusions**:** *We ascribe neuroprotection induced in the immature rats by the pretreatment with both NMDA receptor antagonists 48 to 92 h before hypoxia-ischemia to tolerance evoked by preconditioning, while the neuroprotective effect of (+)MK-801 applied 24 h before the insults may be attributed to direct consequences of the inhibition of NMDA receptors. This is the first report demonstrating the phenomenon of inducing tolerance against hypoxia-ischemia in vivo in developing rat brain by preconditioning with NMDA receptor antagonists.*

Key words**:** *apoptosis, gerbil, ischemia, neuroprotection, perinatal asphyxia, NMDA receptor.*

Introduction

Brain ischemia, which encompasses a variety of forms including stroke, global brain ischemia evoked by cardiac arrest and perinatal asphyxia [45,69], is one of the most frequent causes of death and permanent disability in developed countries [56]. The cellular and molecular mechanisms of ischemia-evoked brain damage have been well documented. They include NMDA receptor mediated excitotoxicity, cal-

Communicating author:
Dorota Makarewicz, PhD, Laboratory of Pharmaconeurochemistry, Department of Neurochemistry, Mossakowski Medical Research Centre, Polish Academy of Sciences, Pawińskiego 5, 02-106 Warsaw, phone/fax: +48 22 608 66 23, phone +48 22 608 65 78, e-mail: dorota.makarewicz@gmail.com

cium imbalance, oxidative stress and disturbed intracellular signaling [5,14,25,50,51]. These mechanisms appear to be promising targets for therapeutic interventions. For instance, preclinical studies demonstrated the neuroprotective potential of the NMDA receptor antagonists in *in vitro* and *in vivo* experimental models of brain ischemia [65], but these effects have been overshadowed by numerous side effects of (+)MK-801 and other high-affinity NMDA receptor antagonists in animals and humans [26,44,66]. Moreover, none of glutamate receptor antagonists or other potential neuroprotective drugs have positively passed the clinical tests in stroke [9]. In consequence, treatment of stroke is limited to thrombolytic therapy combined with improved care for stroke survivors [7,32], while hypothermia has been introduced in treating the victims of perinatal asphyxia and cardiac arrest [20,58].

One of the novel therapeutic strategies in brain ischemia that are alternative to classical pharmacological neuroprotection is inducing brain tolerance to ischemia by its preconditioning with different stressors that are sublethal to neurons [33,35,38] (for a recent review see [73]). These stressors may also be applied after the insult, and this promising therapeutic strategy is referred to as postconditioning [7,19,74]. Inducing brain tolerance to ischemia with pre- and postconditioning is still in the stage of preclinical tests or medical experiments. Several pathophysiological and mechanistic characteristics of this phenomenon have been revealed (for reviews see [13,46]). In particular the long list of preconditioning stressors includes hyperthermia, mild hypoxia and brief episodes of brain ischemia, as well as the application of different pharmacological compounds [13,73]. The role of activation of NMDA receptors in the mechanisms of inducing neuronal tolerance to hypoxia, ischemia and glutamatergic over-excitation has been repeatedly suggested [22,31,59,72]. These data seem to be consistent with the *in vivo* findings that (+)MK-801 inhibits ischemic preconditioning [6,33], although other data do not support these claims [15,71].

In addition to and independent of the possible role of NMDA receptor activation in the mechanisms of brain preconditioning, it has been demonstrated that even brief exposure of the primary cultures of hippocampal neurons to antagonists of NMDA receptors induces long lasting tolerance to excitotoxicity and to staurosporine-evoked apoptosis [64]. More recently we confirmed these data in cultured cerebellar granule cells (CGC) [36]. In addition, our recent unpublished data demonstrate that in CGC both (+)MK-801 and memantine induce tolerance to oxygen and glucose deprivation (OGD), which is an *in vitro* model of brain ischemia. This suggests that inducing brain tolerance to ischemia may be a new mechanism of neuroprotection extended by NMDA receptor antagonists. However, it is not clear whether the results of experiments on neuronal cultures *in vitro* apply to all forms of brain ischemia *in vivo*, in both adult and immature subjects. Also, one should keep in mind the side effects of NMDA antagonists, which may outweigh the putative benefits. In particular this concerns the well-known apoptosis-inducing effect of high-affinity NMDA receptor antagonists in the developing brain [28,47]. Memantine is an NMDA receptor antagonist with low affinity, which has been approved in human medicine, particularly in the treatment of dementia in moderate-to-severe Alzheimer's disease [12,39]. A recent study examining the effects of NMDA receptor antagonists on constitutive apoptosis in the brain of normal immature rats demonstrated relatively low neurotoxicity of memantine compared to (+)MK-801 [42]. However, it is not known how apoptosis would be affected in the developing brain by superposition of memantine or (+)MK-801 application, and brain ischemia, which also induces apoptosis.

The aim of the present study was to evaluate the ability of NMDA receptor antagonists to induce tolerance to ischemia *in vivo* in animal models, taking into account their side effects in the developing brain. We used two uncompetitive antagonists with different affinities to NMDA receptors – (+)MK-801 and memantine. Global forebrain ischemia was induced in adult Mongolian gerbils by bilateral carotid occlusion, whereas hypoxia-ischemia in 7-day-old rats was a model of perinatal asphyxia. The latter animals were used to assess the effects of the NMDA receptor antagonists on constitutive and ischemia-induced apoptosis.

Material and methods

Animals

Male Mongolian gerbils (*Meriones unguiculatus*) and Wistar rats at postnatal day 7 (PND7) with their dams were bred in the Animal Colony of the Mossakowski Medical Research Centre, Polish Academy of Sciences in Warsaw. The animals were fed and water-

ed *ad libitum* and kept on a 12 : 12 h dark-light cycle, at room temperature with constant humidity of approximately 60%. The experiments were conducted in conformity with the institutional guidelines, in compliance with the Polish governmental and the European Community regulations concerning experiments on animals. The Fourth Local Ethical Committee in Warsaw approved the procedures involving animals. All efforts were made to minimize animal suffering and the number of animals required.

Induction of global forebrain ischemia and evaluation of neuronal damage in gerbils

Mongolian gerbils aged 12-13 weeks, weighing about 60 g, were randomly assigned to experimental groups. Global ischemia was induced according to Duszczyk *et al*. [15]. The gerbils were anesthetized with 4% halothane in a gas mixture containing 30% O_2 and 70% N_2O. Two minutes before the operation, halothane concentration was reduced to 2% and then maintained at this level during ischemia. The carotid arteries were isolated through an anterior midline cervical incision made after the injection of local anesthetics. Cerebral ischemia was induced by the occlusion of both common carotid arteries with miniature aneurismal clips for 3 min (test ischemia). Sham-operated animals were exposed to the surgery without carotid occlusion. During the surgery animals were kept on a heating pad set at 38°C. After wound closure, animals were kept at an ambient temperature of 21-24°C for 3-4 hours. Then the gerbils were moved to the animal house for 14 days. In this study, the mortality that could be associated with the experimental protocol was not observed.

Fourteen days after ischemia the animals were anesthetized with halothane and subjected to intracardiac perfusion fixation with 4% neutralized formalin solution. The brains were removed, immersed in 4% formalin solution for 1 week, transferred to absolute ethanol and embedded in paraffin. The 10 μm thick cross sections from the dorsal part of the hippocampus at the level of between 2.2 and 3.5 mm posterior to Bregma were stained with cresyl violet. For each animal at least 5 sections of the central part of CA1 in both hippocampi were analyzed using a light microscope set at × 400 magnification. The density of viable CA1 pyramidal neurons was quantified in ten 0.1 mm portions per section, and the average number of neurons is presented in Figure 1.

Moreover, in sham-operated gerbils, submitted to 3 min forebrain ischemia and preconditioned with (+)MK-801 or memantine 24, 48, 72, or 96 hours before test ischemia the nest building behavior was evaluated as has been described previously [16]. Some of these animals were subsequently used for

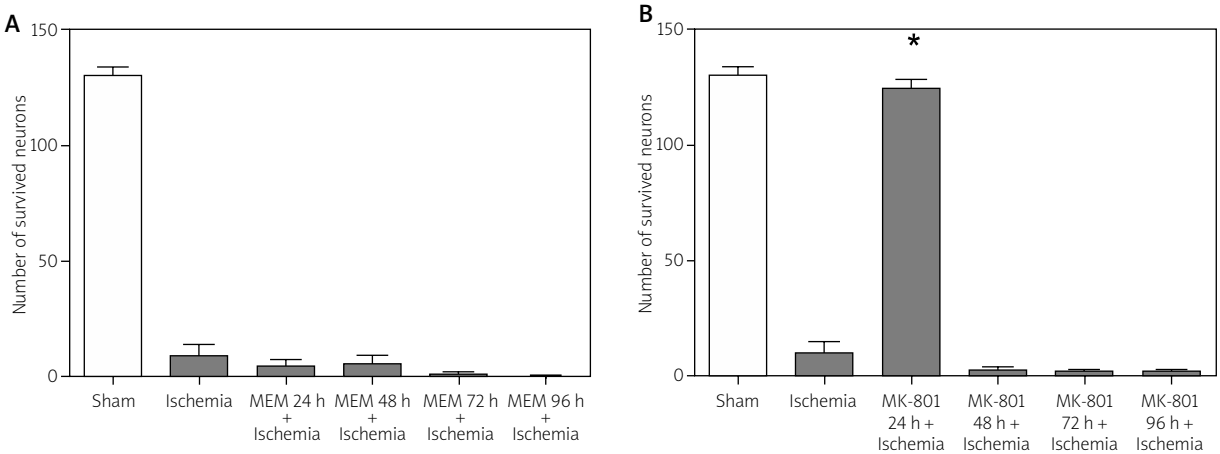

Fig. 1. The effect of preconditioning with NMDA receptor antagonists memantine (**A**) and (+)MK-801 (**B**) on CA1 lesion in a gerbil model of global cerebral ischemia. Memantine (MEM) in the dose of 5 mg/kg and (+)MK-801 in the dose of 3 mg/kg were applied *i.p*. 24, 48, 72 or 96 hours before brain ischemia evoked by 3-minute-long bilateral carotid occlusion. Histological damage in the CA1 area of the gerbil hippocampus was assessed 14 days after the insult. Bars represent means ± SEM. Significant differences from the untreated ischemia were tested by ANOVA followed by Tukey's multiple comparison test. *$p < 0.0001$ vs. 3 min ischemia. Group size: sham $n = 10$; ischemia $n = 9$; (+)MK-801 each time group $n = 10$.

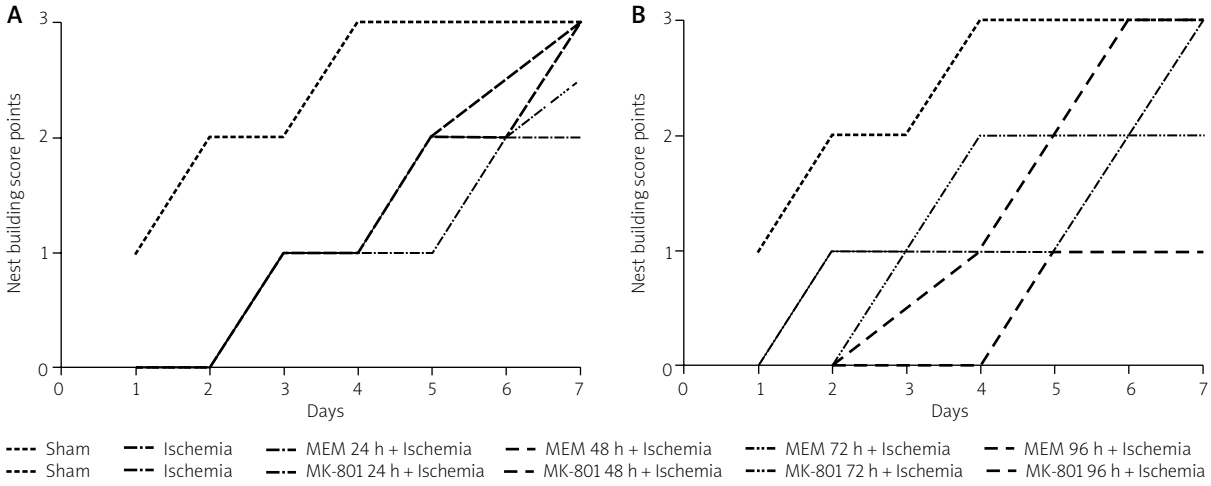

Fig. 2. Nest-building behavior in gerbils after preconditioning with NMDA receptor antagonists: memantine (MEM) (**A**) in the dose of 5 mg/kg and (+)MK-801 (**B**) in the dose of 3 mg/kg. Both substances were applied 24, 48, 72 or 96 hours prior to ischemia. Nest building was assessed each day for 7 days following the ischemic episode. Values are median nest-building score, IQR for each data point ≤ 1. Group size: sham *n* = 10; ischemia *n* = 9; (+)MK-801 each time group *n* = 10.

the evaluation of neuronal damage. One day after surgery, a paper towel was placed in each cage. Nest building was assessed each day for 7 days following the ischemic episode. Paper shredding was scored on a 4-point scale adapted from Baldwin *et al.* [1]: 0 = none; 1 = pieces > 4 cm^2; 2 = pieces between 2 and 4 cm^2; 3 = pieces < 2 cm^2 (Fig. 2).

Induction of hypoxia-ischemia in PND7 rats and evaluation of brain damage

Hypoxia-ischemia (HI) in neonatal rats was induced according to Rice *et al.* [55] as had been described previously [41]. Wistar rat pups were anesthetized using halothane (4% for induction, and 1.5-2.0% for maintenance) in a mixture of nitrous oxide and oxygen (0.6 : 1). The left common carotid artery was dissected. After surgery, the pups were left to recover for 1 h. Then the litters were challenged for 75 min with a hypoxic gas mixture containing 7.3% oxygen in nitrogen. The pups were then returned to their dams and housed at environmental temperature (20°C), with a 12 : 12 h light-dark cycle with ample food and water. Fourteen days after the insult (at PND21) the rats were anesthetized with halothane and decapitated. The cerebral hemispheres were weighed and brain damage was assessed by the deficit in weight of the ipsilateral (left) hemisphere and expressed as a percentage of the weight of the contralateral hemisphere [41] (Fig. 3).

Hypoxic and pharmacological preconditioning

In newborn rats, a hypoxic preconditioning procedure was used as a positive control to pharmacological preconditioning (see below). 24, 48, 72 or 96 hours before hypoxia-ischemia the animals were submitted to hypoxia for 75 min with a hypoxic gas mixture containing 10.0% oxygen in nitrogen, at 35°C. (+)MK-801 maleate (dizocilpine; [5R,10S]-[+]-5-methyl-10,11-dihydro-5*H*-dibenzo[*a*,*d*]cyclohepten-5,10-imine) and memantine (3,5-dimethyladamantan-1-amine) were obtained from Tocris Bioscience (Bristol, UK). All other chemicals used for the dissolution of drugs were of analytical grade. For preconditioning of the animals, (+)MK-801 in a dose of 3 mg/kg or memantine in a dose of 5 mg/kg was dissolved in saline and applied as a single *i.p.* injection 24, 48, 72 or 96 hours before hypoxia-ischemia. In selected experiments (Fig. 4) ebselen purchased from Santa Cruz Biotechnology Inc. (Dallas, TX, USA) and dissolved in 50% DMSO + 50% PEG30 was injected *i.p.* in the dose of 10 mg/kg, 30 min prior to the administration of NMDA receptor antagonists. In these experiments (+)MK-801 was applied 48 hours and memantine 72 hours before hypoxia-ischemia. In other groups only ebselen or its vehicle was injected 72 h before hypoxia-ischemia. The total volume of injected fluid was 50 µl. Moreover, in some experiments the rats at PND7 were injected

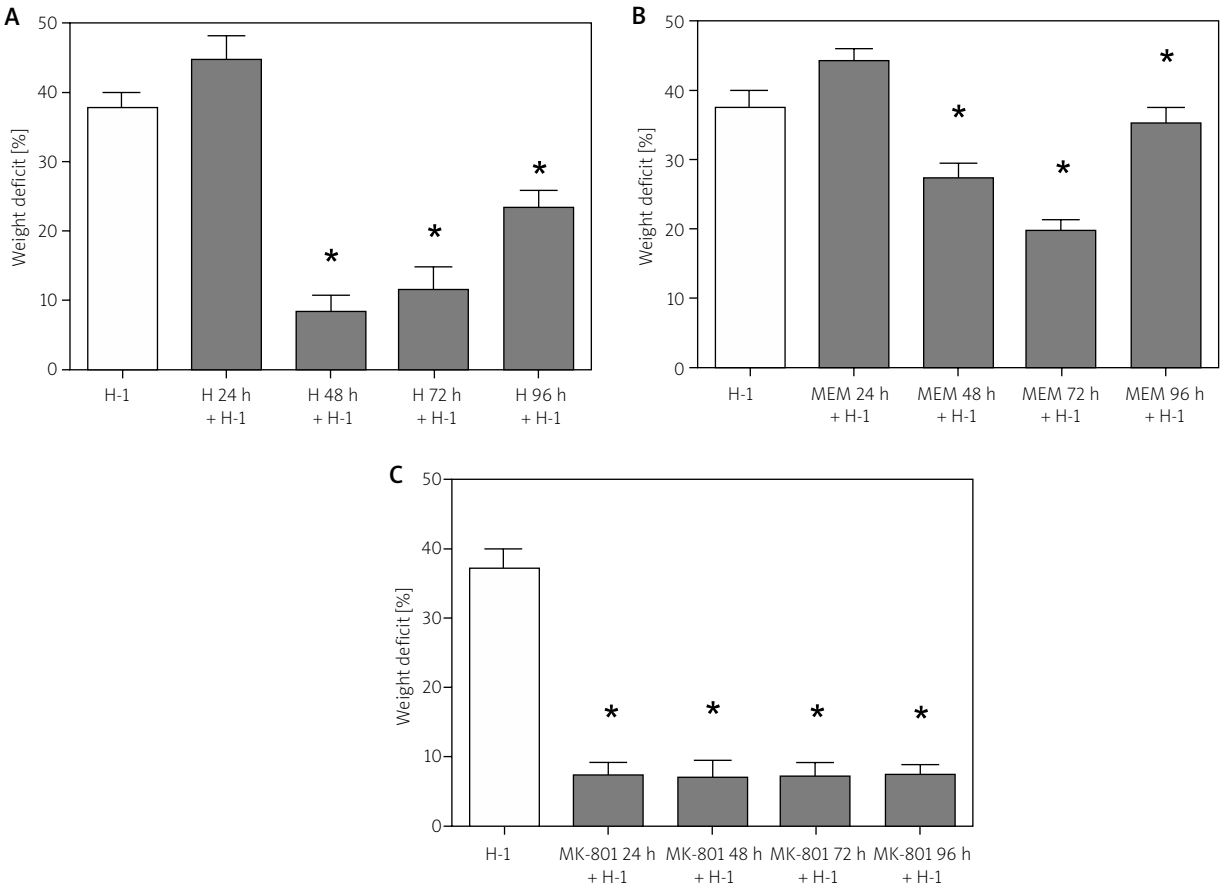

Fig. 3. The effects of preconditioning with hypoxia (**A**) or with NMDA receptor antagonists memantine (**B**) and (+)MK-801 (**C**) on brain damage induced by hypoxia-ischemia in 7-day-old rats. Preconditioning with 7.2% O_2 in N_2 hypoxia (H) for 75 minutes, and with (+)MK-801 or memantine (MEM) applied *i.p.* in the doses of 3 mg/kg or 5 mg/kg, respectively, was performed 24, 48, 72 or 96 hours before hypoxia-ischemia (H-I). Brain damage was evaluated by weighing the brain hemispheres 14 days after hypoxia-ischemia and expressed as the deficit in weight of the ipsilateral hemisphere in per cent of weight of the contralateral hemisphere. Bars represent means ± SEM (group size: $n \geq 14$ rats per time point in each group). Significant differences from the ischemic control (H-I) were tested by ANOVA followed by Tukey's multiple comparison test. *$p < 0.05$.

with NMDA receptor antagonists as described above, without following hypoxia-ischemia. After 14 days they were anesthetized with halothane and decapitated. The brains were removed, weighed and the results were compared to untreated control (Fig. 8).

Histochemical analysis of immature rat brains

In order to evaluate the effects of pharmacological preconditioning with memantine or (+)MK-801 72 or 48 hours before hypoxia-ischemia, respectively, on ischemia-induced apoptosis, the animals treated as described above were sacrificed 24 or 48 hours after hypoxia-ischemia. In turn, rats that were designed to study the effect of NMDA receptor antagonists on constitutive apoptosis, at PND7 received an intraperitoneal injection of memantine or (+)MK-801 as described above and were sacrificed 24 or 48 hours later. The animals were deeply anesthetized using Nembutal (80 mg/kg b.w., *i.p.*) and perfused through the ascending aorta with 0.9% NaCl in 0.01 M sodium-potassium phosphate buffer pH 7.4 (PBS), followed by *in situ* perfusion-fixation with ice-cold fixatives applied under gravity. For the light microscopy 4% formaldehyde in 0.1 M phosphate buffer pH 7.4 was used as described previously [18]. Following perfusion, the brains were removed from

the skulls and immersed for 2 h in the same fixing agent. Afterwards, the brains were saturated with sucrose through immersing in 10, 20 and 30% (w/v) sucrose solutions in PBS and cut into 40 μm-thick free-floating coronal sections using a cryostat (CM 1850 UV, Leica, Germany). Morphology of cell nuclei was examined on brain sections mounted on microscope slides. Sections were washed in PBS and incubated in a 1 μg/ml solution of Hoechst stain (bisbenzimide dye, No 33258, B-2883, Sigma; prepared in PBS) for 2 minutes, at room temperature. The stain was then drained off and cover slipped with PBS for visualization. Induction of apoptosis was evaluated using a model Optiphot-2 Nikon fluorescent microscope (Japan) equipped with appropriate filters, and recorded with a DS-L1 Nikon camera (Japan). The number of apoptotic cells at the last stage of apoptosis (apoptotic bodies formation) was measured. Three to four animals from each experimental group were investigated. For each animal we analyzed 6-8 sections. The dying cells were counted within 10 microscopic fields of observation located randomly within the somatosensory region of the cerebral cortex (Figs. 5-7).

Statistical methods

All studies apart from nest building scores were performed with at least 9 or 10 rats or gerbils per time point in each group. Data were expressed as mean ± SEM, and statistical analysis was performed by the ANOVA followed by post hoc Tukey's test. Nest building scores were presented as medians and tested by the Mann-Whitney *U* test. Significance refers to results for which $p < 0.05$ was obtained.

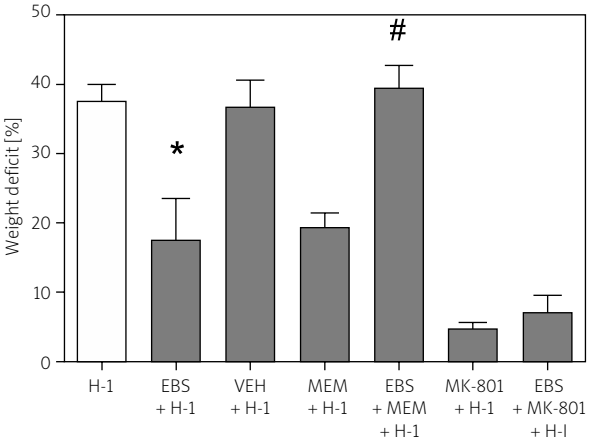

Fig. 4. Free radical scavenger ebselen reverses tolerance of 7-day-old rats to hypoxia-ischemia induced by preconditioning with memantine, but not that evoked by (+)MK-801. Rats were preconditioned with memantine (MEM) in the dose of 5 mg/kg or (+)MK-801 in the dose of 3 mg/kg applied *i.p.* 72 h or 48 h before hypoxia-ischemia (H-I), respectively. Ebselen (EBS) in the dose of 10 g/kg was applied *i.p.* 30 minutes before (+)MK-801 or memantine, otherwise EBS or vehicle (VEH) was applied alone 72 h before H-I. Brain damage was evaluated by weighing the brain hemispheres 14 days after hypoxia-ischemia and expressed as the deficit in weight of the ipsilateral hemisphere in per cent of weight of the contralateral hemisphere. Bars represent means ± SEM (group size: $n \geq 10$ rats per time point in each group). Significant differences from the appropriate ischemic control (H-I) were tested by ANOVA followed by Tukey's multiple comparison test. $^{*}p < 0.05$ vs. ischemic control (H-I), $^{\#}p < 0.05$ vs. MEM + H-I.

Results

Tolerance to global forebrain ischemia in adult Mongolian gerbils induced by preconditioning with NMDA receptor antagonists

In order to assess the ability of NMDA receptor antagonists to induce tolerance to brain ischemia in adult animals we used a gerbil model of global forebrain ischemia and evaluated the number of neurons in the hippocampal CA1 that survived 3-minute-long occlusion of the common carotid arteries. As presented in Figure 1A-B, 3-minute-long ischemia almost completely destroyed the pyramidal neurons. This effect remained unchanged after the injection of memantine 24, 48, 72 and 96 h before the insult (Fig. 1A). (+)MK-801 injected 24 h before ischemia almost completely prevented neuronal damage in CA1; however, this neuroprotective effect disappeared with the extension of the interval between the pretreatment with (+)MK-801 and the induction of ischemia (Fig. 1B).

Figure 2 presents the nest building behavior score. These results demonstrate normal development of the nest building behavior in sham-operated animals, i.e. its immediate beginning and completion of the task after 4 days, while the animals submitted to 3-minute-long global forebrain ischemia showed a delay of two or three days in starting to build a nest, and this delay was maintained throughout the test

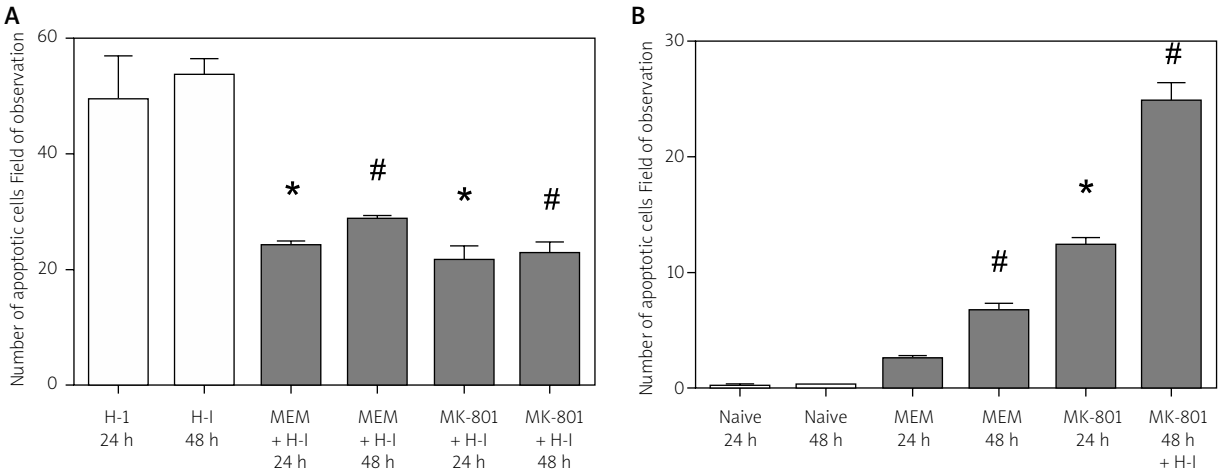

Fig. 5. The effect of NMDA receptor antagonists on hypoxia-ischemia evoked induction of brain apoptosis (**A**) and on constitutive apoptosis (**B**) in brain of immature rats. Memantine (MEM) in the dose of 5 mg/kg or (+)MK-801 in the dose of 3 mg/kg was applied *i.p.* to rats 72 h or 48 h before hypoxia-ischemia (H-I), respectively (**A**). Alternatively, the same doses of NMDA receptor antagonists were applied to untreated rats (**B**). The number of apoptotic cells was assessed 24 or 48 hours after H-I (**A**) or after the application of NMDA receptor antagonists (**B**). Bars represent means ± SEM (n = 3 or 4 animals for each experimental group were investigated. For each animal we analyzed 6-8 sections). Significant differences from the appropriate ischemic control (H-I) were tested by ANOVA followed by Tukey's multiple comparison test. *$p < 0.05$ vs. number of apoptotic cells assessed in the 24 h control group. #$p < 0.05$ vs. number of apoptotic cells assessed in the 48 h control group.

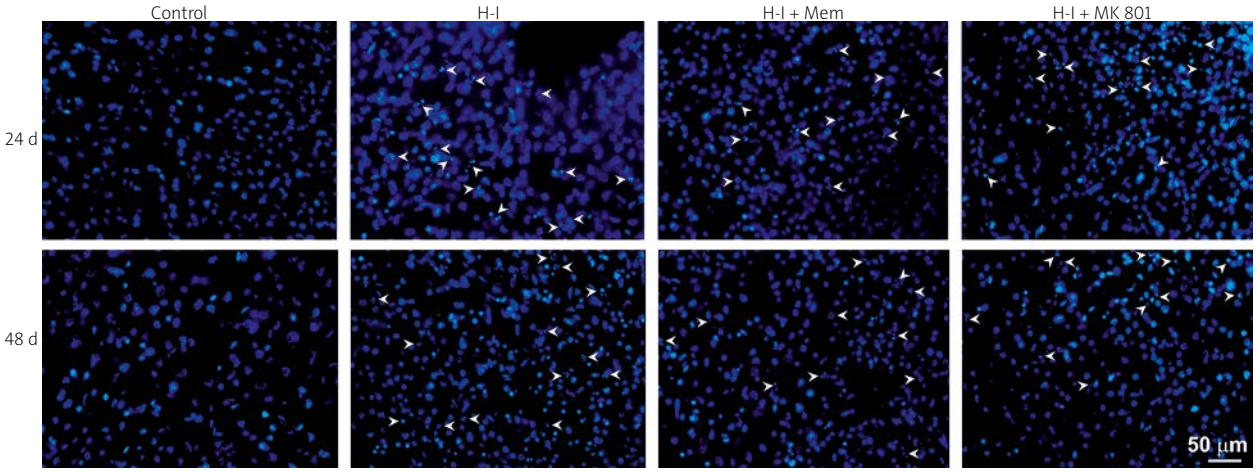

Fig. 6. Morphology of cortical cell nuclei visualized by Hoechst (bisbenzimide) staining. Note many apoptotic cells within the sections of rats subjected to HI. Note the reduction of apoptotic cell number within the material of animals pretreated with memantine or (+)MK 801. Arrowheads point to apoptotic bodies.

(Figs. 2A-B). Preconditioning with memantine had no effect on the nest building behavior after ischemia (Fig. 2A). Also, the application of (+)MK-801 did not improve the disturbances in the nest building behavior score evoked by cerebral ischemia, although a tendency for unspecific modifications of the behavior was observed in these groups (Fig. 2B).

Tolerance to hypoxia-ischemia in 7-day-old rats induced by preconditioning with NMDA receptor antagonists

In order to evaluate the effectiveness of brain tolerance against the ischemic insults that might be induced by the NMDA receptor antagonists in the

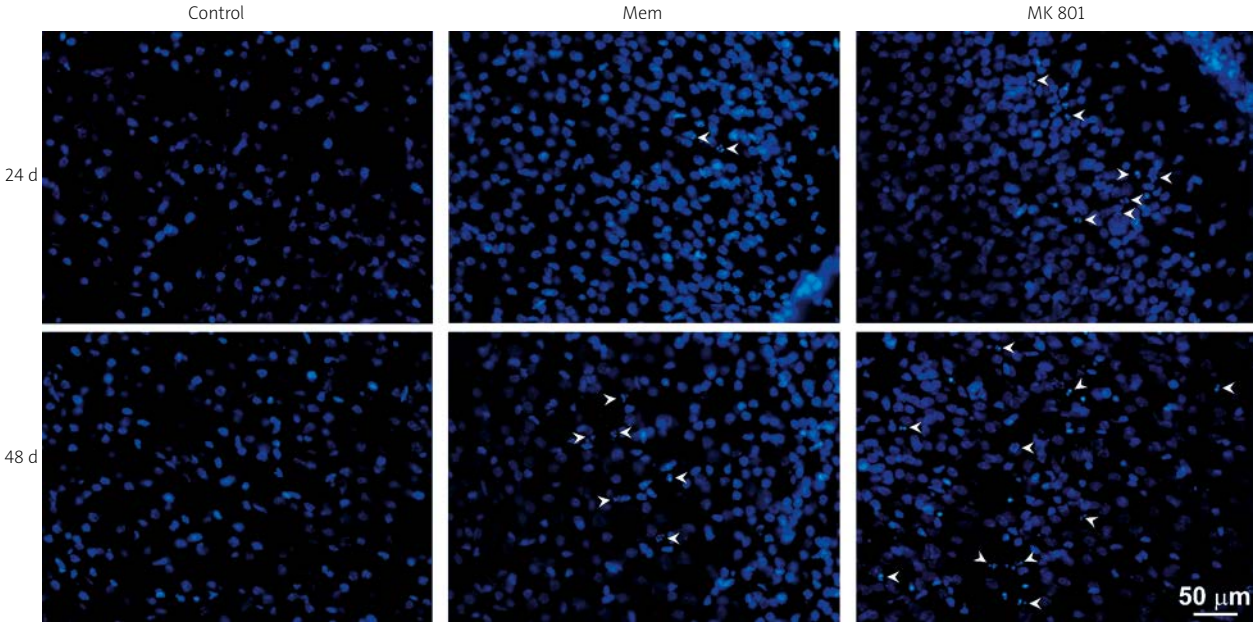

Fig. 7. Morphology of nuclei of cerebral cortex cells stained with Hoechst (bisbenzimide). Note the small number of apoptotic cells within the material from animals pretreated with memantine and higher number of apoptotic bodies in the sections of (+)MK 801 pretreated rats. Arrowheads point to apoptotic bodies.

immature animals we used hypoxia/ischemia in 7-day-old rats, which is an animal model of perinatal asphyxia. Like in the gerbil experiments, memantine or (+)MK-801 in single doses of 5 mg/kg and 3 mg/kg respectively, was injected into animals 24, 48, 72 or 96 hours prior to the insult. As a positive control hypoxic preconditioning was used. For this purpose 75-minute long episodes of normobaric hypoxia (10% O_2 in N_2) were applied at the same times as pharmacological preconditioning. The obtained results demonstrated that untreated hypoxia/ischemia induces a deficit in the weight of ipsilateral (ischemic) brain hemisphere of almost 40% compared to the contralateral (control) hemisphere (Fig. 3).

As presented in Figure 3A, preconditioning with one episode of hypoxia applied 24 h before the insult tended to exacerbate brain damage evoked by hypoxia-ischemia. However, treatment with hypoxia 48 h before hypoxia-ischemia resulted in a highly significant reduction of the weight deficit by 73.6%. Neuroprotection induced by hypoxic preconditioning and applied 72 h before hypoxia-ischemia remained at a similar level. Even 96 h after hypoxia, the neuroprotection was still significant as it remained at the level of 32.0% (Fig. 3A). As in the case of hypoxic preconditioning, pretreatment with memantine was also ineffective when applied 24 h before hypoxia-ischemia (Fig. 3B). Application of memantine 48 and 72 h before the insult significantly reduced the brain weight deficit by 23.9%, and 59.8%, respectively. A 96-hour-long delay in testing with hypoxia-ischemia significantly reduced neuroprotection; however, the reduction of the brain weight deficit remained statistically significant (Fig. 3B). In turn, preconditioning with (+)MK-801 as early as 24 h before the insult resulted in a highly significant reduction of brain damage by about 80%, and neuroprotection remained at the same level even when the antagonist was applied 96 h before hypoxia-ischemia (Fig. 3C).

To evaluate the role of oxidative stress in the induction by NMDA receptor antagonists of brain tolerance to hypoxia-ischemia, ebselen, a free radical scavenger, was injected 30 minutes before the application of memantine or (+)MK-801. After this treatment, hypoxia-ischemia was induced when the maximal neuroprotection by memantine or (+)MK-801 was observed, i.e. with a delay of 72 h or 48 h, respectively (see Figs. 3B-C). As presented in Figure 4, ebselen completely reversed the neuroprotection induced by preconditioning with memantine, while the neuroprotection evoked by preconditioning with (+)MK-801 was practically unaffected. The unexpected result of this study was that injection of ebselen 72 h before hypoxia-ischemia itself

induced significant neuroprotection as it reduced the level of brain damage to the range observed after preconditioning with memantine (Fig. 4).

Effects of preconditioning with NMDA receptor antagonists on hypoxia/ischemia-induced apoptosis in brain of immature rats

In order to investigate the influence of NMDA receptor antagonists on apoptosis in the rat brain, evoked by hypoxia-ischemia, the animals were preconditioned 48 or 72 hours prior to hypoxia-ischemia with (+)MK-801 (3 mg/kg) or memantine (5 mg/kg), respectively. Then, the number of apoptotic neurons was assessed 24 or 48 hours after the insult. The results presented in Figure 5A and Figure 6 demonstrate that in a group of rats decapitated 24 or 48 hours after hypoxia-ischemia, the mean number of apoptotic cells per field of observation was 43.62 and 51.07, respectively. Preconditioning with memantine significantly reduced the number of apoptotic cells by 43.7% in the group studied 24 h after the insult and by 43.3% in the group studied 48 h after the insult. A similar effect was observed in the groups preconditioned with (+)MK-801, where the mean number of apoptotic cells was reduced by 53.14% and 54.1% in the groups studied 24 or 48 hours after hypoxia-ischemia, respectively.

Effects of preconditioning with NMDA receptor antagonists on constitutive apoptosis and brain weight of immature rats

As presented in Figure 5B and Figure 7, a low level of constitutive apoptosis in a developing rat brain was observed. The mean number of apoptosis per field of observation was 0.20 in PND7 rats and 0.24 in PND8 rats. These numbers represent the corresponding controls to groups treated with memantine or (+)MK-801 48 h and 24 h earlier, respectively. A single injection of memantine increased the number of apoptotic cells up to 2.63 and 6.80 at 24 or 48 hours after the injection, respectively. Much more pronounced was the increase of the mean number of apoptotic cells per field of observation in brains of the rats that were preconditioned with (+)MK-801, which in the groups studied 24 or 48 hours after injection reached 12.18 and 25.32, respectively.

For a rough assessment of the impact of a single injection of memantine or (+)MK-801 into immature rats on brain development, we compared the brain weight of the animals in the control-, (+)MK-801- and memantine-treated groups. As presented in Figure 8, injection of memantine (5 mg/kg) into 7-day-old rats did not interfere with brain weight at postnatal day 21, whereas a single injection of (+)MK-801 (3 mg/kg) resulted in a statistically significant reduction in brain weight by 11.87%.

Discussion

The results of this study demonstrate for the first time that a single administration of the NMDA receptor antagonist memantine or (+)MK-801 into immature rats induces in their brain *in vivo* a tolerance to hypoxia-ischemia lasting 48 to at least 96 hours. The free radical scavenger ebselen prevented memantine-induced neuroprotection. Moreover, pretreatment with memantine and (+)MK-801 reduced ischemia-evoked apoptosis in the immature rat brain. We attribute these effects to the phenomenon of brain preconditioning-induced tolerance against ischemia. In contrast to these findings, in the adult gerbil model of global forebrain ischemia, induction by memantine or (+)MK-801 of brain tolerance lasting longer than 24 h was not detected, which may suggest that only the early stages of the ontogenetic development of the brain may determine its susceptibility to preconditioning with the NMDA receptor antagonists. Our results also confirmed that application of (+)MK-801 significantly increases constitutive neuronal apoptosis in the developing brain, and demonstrated that such an effect of memantine, although noticeable, is less pronounced. We suggest the advisability of further studies on the possible use of memantine in the treatment of perinatal asphyxia.

In this work we utilized two distinct classical models of brain ischemia. Global forebrain ischemia in the adult Mongolian gerbils was induced by 3-minute-long bilateral occlusion of the carotid arteries [34]. The rat model of perinatal asphyxia consists of submitting PND7 rats to unilateral carotid ligation combined with normobaric hypoxia, as was initially introduced by Rice *et al*. [55]. We have previous experience in using them in studies concerning induced tolerance to brain ischemia by preconditioning or postconditioning with various stressors such

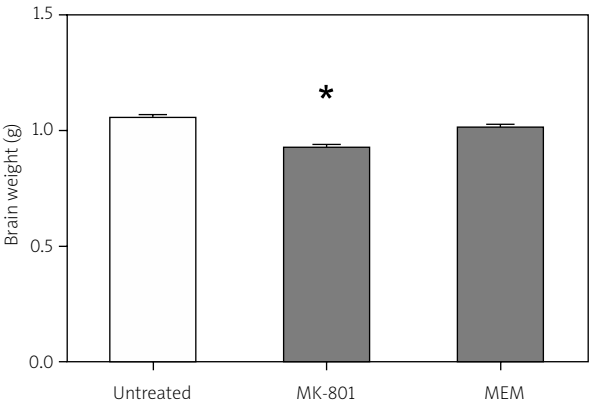

Fig. 8. The effect of NMDA receptor antagonists on brain weight. (+)MK-801 in the dose of 3 mg/kg and memantine (MEM) in the dose of 5 mg/kg were applied *i.p.* to rats at postnatal day 7. Two weeks later rats were decapitated, and brains were removed and weighed. Bars represent means ± SEM (group size: $n \geq 5$ rats per time point in each group). Significant differences from the untreated rats were tested by ANOVA followed by Tukey's multiple comparison test. *$p < 0.05$ vs. untreated.

as a sublethal short episode of ischemia or repeated hypobaric hypoxia [16,17,19]. In the gerbil model of global forebrain ischemia we used a simple and reliable method of counting the surviving neurons for the assessment of ischemia-induced loss of neurons in CA1 [16,17]. Also, the methods of evaluating brain damage induced by hypoxia-ischemia by measuring weight deficit of the ischemic hemispheres and counting the apoptotic neurons in the immature rat brain have been proven in our previous studies [16-18,30,41].

In these experiments, literature-based doses of (+)MK-801 and memantine were used. (+)MK-801 in a dose of 3 mg/kg has been previously shown to prevent neurodegeneration of CA1 pyramidal neurons in gerbils induced by bilateral carotid ligation [21]. Our previous studies demonstrated that (+)MK-801 at that dose failed to reduce the induction of brain tolerance by the ischemic preconditioning in gerbils [15]. It is known that (+)MK-801 in doses of 0.5-1 mg/kg is neuroprotective in the model of hypoxia-ischemia of PND7 rats [22, 61]. Dosing of memantine in this study in relation to its therapeutic use in practical medicine requires additional comment. Memantine from 10 mg twice daily up to 28 mg once daily has been recommended for the treatment of moderate to severe Alzheimer's disease [3]. Since memantine metabolism in rodents is known to highly exceed that of humans [4,49], the relatively high dose of memantine (5 mg/kg) that was used in our study for gerbils and immature rats has been recommended as pharmacologically relevant and equivalent of the therapeutic dose of memantine in Alzheimer's disease therapy [24]. It should be noted that the doses of (+)MK-801 and memantine applied in this study are not comparable in terms of levels of the NMDA receptor blockade. Based on the affinity for the NMDA receptor and behavioral outcomes, and on the estimated concentrations of these substances in brain, a dose of (+)MK-801 corresponding to a 5 mg/kg dose of memantine would be 0.01-0.02 mg/kg [70]. Therefore some differences observed in this study which will be discussed below could result from using not equivalent doses, not only from qualitative differences between these two agents. However, these differences are intentional. We used in this work a high dose of (+)MK-801 to determine the maximum level of neuroprotection induced by preconditioning with the NMDA receptor antagonists.

For the purposes of discussion, the results of this study concerning the induction of tolerance to ischemia by administration of NMDA receptor antagonists have been divided into two groups. One of them demonstrated that both (+)MK-801 and memantine applied 48, 76 and 92 h before test ischemia induce neuroprotection in the immature rats, but not in adult gerbils. The other set of data indicates that pretreatment of the adult gerbil and the rat pups with (+)MK-801, but not with memantine, 24 h before the ischemic insults, results in significant neuroprotection. We interpret differently these two groups of results. Then, we will discuss separately the results concerning the interference of NMDA receptor antagonists with ischemia-induced and constitutive apoptosis in the immature rat brain.

Preconditioning of the rat pups with a single episode of normobaric hypoxia was used in our study as a positive control for induced tolerance to hypoxia-ischemia. Other researchers who have also used preconditioning of immature rats with hypoxia observed protection against hypoxia-ischemia as early as after 24 h and within the next few days [60,67]. Interestingly, our data demonstrated neuroprotection, provided that preconditioning with hypoxia was applied 48, 72 or 96 h, but not 24 h, before the insult (Fig. 3A). Further studies are needed

to determine the cause of these discrepancies with the previously published literature. Nevertheless, we consider the observed pattern of development of tolerance induced by preconditioning carried out in infant rats with hypoxia as the characteristic feature of our experimental model of preconditioning. Our present data consistently showed that also memantine applied 48, 72 and 96 hours, but not 24 hours, before the insult induced neuroprotection (Fig. 3B). Also, pretreatment with (+)MK-801 2, 3 and 4 days before the insult resulted in robust protection of the immature rat brain (Fig. 3C). Consequently, we ascribe these neuroprotective effects of pretreatment of the rat pups with the NMDA receptor antagonists to the common mechanism of preconditioning and induction of tolerance to hypoxia-ischemia. Indeed, this phenomenon meets the criteria of delayed preconditioning, in which a lag between the preconditioning stimulus and development of tolerance is necessary to induce synthesis of proteins involved in neuroprotection [2,8,13,52]. Tremblay *et al*. [64] in their pioneering *in vitro* study demonstrated that administration of the protein synthesis inhibitor during the first few hours after preconditioning with (+)MK-801 prevented induction of tolerance in the primary cultures of the rat cortical neurons. The other characteristic feature of preconditioning inducing delayed tolerance against brain ischemia is the involvement of oxidative stress in triggering the neuroprotective mechanisms [52]. Consistently with that, in our experiments the free radical scavenger ebselen administered to the rat pups 30 minutes before preconditioning with memantine reversed brain tolerance to hypoxia-ischemia (Fig. 4). Resistance of the preconditioning with (+)MK-801 to the inhibition by ebselen may result from very high stress which the brain is submitted to by tonic (+)MK-801-evoked inhibition of the NMDA receptors, which could not be reversed by a single injection of ebselen.

In agreement with our previous data [15] using the gerbil model of global forebrain ischemia, in the present study robust damage to the hippocampal CA1 pyramids 14 days after 3-minute-long ischemia was observed. In contrast to the aforementioned data from the rat model of perinatal asphyxia, our results demonstrated that application of (+)MK-801 or memantine to gerbils 48, 72 and 96 h before ischemia does not induce morphological or behavioral neuroprotection (Figs. 1 and 2). Based on these results, we assume that under the conditions of this study NMDA receptor antagonists do not induce long-lasting ischemic tolerance of the hippocampal neurons in adult gerbils. It is tempting to generalize these results and to argue that resistance to preconditioning with the NMDA receptor antagonists is the characteristic feature of adult animals or of the model of global brain ischemia. However, further studies are needed to test these and other alternative explanations, including the one suggesting that a very high level of neuronal loss after 3-minute-long ischemia, which was observed in our present experiments, precluded any neuroprotective effect of tolerance.

Another interesting result obtained from the experiments in which we tested the potential of (+)MK-801 to induce tolerance of the gerbils and immature rats against the ischemic insult is the occurrence of neuroprotection when (+)MK-801, but not memantine, was applied 24 h before the insult (Figs. 1 and 3). We do not attribute that phenomenon to the tolerance to ischemia induced by preconditioning because such early and transitory neuroprotection does not correspond to the characteristics of delayed preconditioning after which tolerance to ischemia persists for several days [13]. Instead, we interpret this effect observed in gerbils and the neuroprotection obtained with (+)MK-801 (but not with memantine) administered to PND7 rats 24 h before hypoxia-ischemia (Fig. 3C) as the effect of persistent presence of (+)MK-801 in the brain and its direct inhibition of the NMDA receptors during ischemia. (+)MK-801 is known to block the channel of NMDARs for a long time even after its washing out from the extracellular space [54]. Although the time required for 50% elimination ($T_{1/2}$) of (+)MK-801 in the brain of rats has been evaluated to be at the level of 2 hours [68], behavioral studies of Lysko *et al*. [40] demonstrated prolonged effects of a single injection into Mongolian gerbils of 3 mg/kg (+)MK-801, pointing to the physical presence of this inhibitor in brain. In their studies, the hypothermic response was maintained at a maximal level for at least 24 hours. Moreover, the recovery of motor functions from severe ataxia was slow, and the time required for 50% recovery ($T_{1/2}$) of 11 hours was found [40]. Although we do not have information from the literature on the (+)MK-801 elimination half-life in the developing rat brain, Schwartz and Westerlain [57] demonstrated that the kinetics of (+)MK-801 accumulation in

the PND7 rat brain does not differ significantly from that of an adult rat [68], which may suggest that its elimination from the brain is also similar. Both direct inhibition of NMDA receptors, which are involved in brain injury caused by ischemia [62], and prolonged hypothermia in (+)MK-801-treated animals [11] may be responsible for neuroprotection. In addition, our present results obtained in the gerbil model of global brain ischemia demonstrate that (+)MK-801, which persists for a long time in the brain and induces by itself a delayed tolerance to ischemia, is not a good tool to study the participation of NMDA receptors in the mechanisms of brain ischemic preconditioning (compare [6,15,33,71]).

Our promising results, showing for the first time that *in vivo* in the developing rat brain preconditioning with (+)MK-801 induces tolerance to hypoxia-ischemia, have been overshadowed by the induction by this high-affinity NMDA receptor antagonist of constitutive apoptosis (Fig. 5A). This phenomenon has been previously demonstrated [27,47]. On the other hand, data from both *in vitro* and *in vivo* studies indicate that memantine by itself does not induce massive constitutive apoptosis in a developmentally relevant model of primary neuronal cultures [29] or in the brain of control, otherwise untreated rat pups [42]. Our present results showed that although the effectiveness of memantine applied at a therapeutic dose of 5 mg/kg in inducing constitutive apoptosis is approximately 3.5 to 5 times lower than that of (+)MK-801 (3 mg/kg), it is still considerable (Fig. 5A). The key issue was how the preconditioning with (+)MK-801 and memantine affects apoptosis induced by hypoxia-ischemia in the developing rat brain. Our present results (Fig. 5B) demonstrate that preconditioning of the immature rats with (+)MK-801 and memantine significantly and with approximately the same potency reduces ischemia-induced apoptosis in the brains of these animals. The previous studies demonstrated neuroprotection, inhibition of caspases and decrease in the number of apoptotic neurons with DNA fragmentation in the brain of immature rats treated with (+)MK-801 or memantine during or immediately after hypoxia-ischemia [37,53]. However, ours is the first report demonstrating the antiapoptotic potential of preconditioning of the immature rats with (+)MK-801 or memantine. These results are consistent with the *in vitro* findings of Tremblay *et al.* [64] that preconditioning of the primary cortical neurons with (+)MK-801 prevents staurosporine-induced apoptosis.

Due to the very well-known side effects of (+)MK-801 treatment, particularly its toxicity in the developing brain, our data presenting neuroprotective effects of preconditioning with (+)MK-801 via the induction of tolerance against ischemia are of purely cognitive significance. However, the results of our study concerning the effects of memantine may have potential practical value. Memantine administered in a therapeutic dose appeared to be equally effective as (+)MK-801 in preventing apoptosis induced by hypoxia-ischemia in the developing rat brain, being a several times weaker inducer of constitutive apoptosis. In contrast to Manning *et al.* [42], who assumed that memantine exhibits relative safety, we observed some hazardous effects of its use in neonatal rats. Memantine is widely used in adults for the treatment of dementia, particularly of the Alzheimer's type [49], and its safety has been demonstrated [63]. There have also been clinical tests evaluating the therapeutic potential of memantine in children diagnosed with developmental disorders including autism [10,48]. It appeared protective in the treatment of periventricular leukomalacia in a rat model [43] and neuroprotective in hypoxia-ischemia in PND7 rats [37]. Our present study presented a novel strategy in the therapeutic use of memantine to induce tolerance to ischemia in the developing brain. Although preconditioning may be of limited utility, there are indications that induction of tolerance to brain ischemia by postconditioning may also be an effective way of neuroprotection, as this phenomenon probably uses mechanisms of induction and expression similar to preconditioning (for a review see [13]).

In conclusion, this study demonstrates for the first time that a single injection of memantine in a therapeutic dose of 5 mg/kg or of (+)MK-801 in a high dose of 3 mg/kg induces tolerance to hypoxia-ischemia in neonatal rats, which persists for 48-96 hours and is similar to the neuroprotective effects of preconditioning with normobaric mild hypoxia. We ascribe this effect to the phenomenon of delayed preconditioning and we differentiate it from the direct neuroprotective action of (+)MK-801 which may persist for up to 24 hours after injection. However, we did not find delayed tolerance against global forebrain ischemia after injecting these NMDA receptor antagonist into Mongolian gerbils. The neuroprotective effect of pre-

treatment of the rat pups with memantine may be reversed by application of the free radical scavenger ebselen, which is in accordance with the role of preconditioning in that process. Thus, our data demonstrate that neuroprotection of the developing brain with NMDA receptor antagonists may be achieved under two different routes: by direct inhibition of these receptors during and just after the insult, or by pharmacological preconditioning and gaining induced delayed tolerance to ischemia. Moreover, we evaluated the toxicity of (+)MK-801 and memantine in the developing rat brain. Our data confirmed previous information on the significant potentiation by (+)MK-801 of constitutive apoptosis, while such an effect of memantine was considerably less pronounced. However, both (+)MK-801 and memantine equally inhibited apoptosis induced by ischemia. This indicates that memantine may be considered as a promising candidate for further studies on brain protection in perinatal asphyxia.

Acknowledgements

This study was supported by grant no. N N401 066738 from the Polish Ministry of Science and Higher Education. The expert technical assistance of Mrs Apolonia Ziembowicz is gratefully acknowledged.

Disclosure

Authors report no conflict of interest.

References

1. Baldwin HA, Jones JA, Cross AJ, Green AR. Histological, biochemical and behavioural evidence for the neuroprotective action of chlormetiazole following prolonged carotid occlusion. Neurodegeneration 1993; 2: 139-146.
2. Barone FC, White RF, Spera PA, Ellison J, Currie RW, Wang X, Feuerstein GZ. Ischemic preconditioning and brain tolerance: temporal histological and functional outcomes, protein synthesis requirement, and interleukin-1 receptor antagonist and early gene expression. Stroke 1998; 29: 1937-1950.
3. Bassil N, Thaipisuttikul P, Grossberg GT. Memantine ER, a once-daily formulation for the treatment of Alzheimer's disease. Expert Opin Pharmacother 2010; 11: 1765-1771.
4. Beconi MG, Howland D, Park L, Lyons K, Giuliano J, Dominguez C, Munoz-Sanjuan I, Pacifici R. Pharmacokinetics of memantine in rats and mice. PLOS Curr 2012 Feb 15. Edition 1. doi: 10.1371/currents.RRN1291.
5. Belousov AB. Novel model for the mechanisms of glutamate-dependent excitotoxicity: role of neuronal gap junctions. Brain Res 2012; 1487: 123-130.
6. Bond A, Lodge D, Hicks CA, Ward MA, O'Neill MJO. NMDA receptors antagonism, but not AMPA receptors antagonism attenuates induced ischemic tolerance in gerbil hippocampus. Eur J Pharmacol 1999; 380: 91-99.
7. Brainin M, Zorowitz RD. Advances in stroke: recovery and rehabilitation. Stroke 2013; 44: 311-313.
8. Burda J, Hrehorovská M, Bonilla LG, Danielisová V, Cízková D, Burda R, Némethová M, Fando JL, Salinas M. Role of protein synthesis in the ischemic tolerance acquisition induced by transient forebrain ischemia in the rat. Neurochem Res 2003; 28: 1213-1219.
9. Cheng YD, Al-Khoury L, Zivin JA. Neuroprotection for ischemic stroke: two decades of success and failure. NeuroRx 2004; 1: 36-45.
10. Chez MG, Burton Q, Dowling T, Chang M, Khanna P, Kramer C. Memantine as adjunctive therapy in children diagnosed with autistic spectrum disorders: an observation of initial clinical response and maintenance tolerability. J Child Neurol 2007; 22: 574-579.
11. Corbett D, Nurse S, Colbourne F. Hypothermic neuroprotection. A global ischemia study using 18- to 20-minth-old gerbils. Stroke 1997; 28: 2238-2243.
12. Danysz W, Parsons CG. Alzheimer's disease, β-amyloid, glutamate, NMDA receptors and memantine – searching for the connections. Br J Pharmacol 2012; 167: 324-352.
13. Dirnagl U, Becker K, Meisel A. Preconditioning and tolerance against cerebral ischaemia: from experimental strategies to clinical use. Lancet Neurol 2009; 8: 398-412.
14. Doyle KP, Simon RP, Stenzel-Poore MP. Mechanisms of ischemic brain damage. Neuropharmacology 2008; 55: 310-318.
15. Duszczyk M, Gadamski R, Ziembowicz A, Danysz W, Lazarewicz JW. NMDA receptor antagonism does not inhibit induction of ischemic tolerance in gerbil brain in vivo. Neurotox Res 2005; 7: 283-292.
16. Duszczyk M, Ziembowicz A, Gadamski R, Lazarewicz JW. Behavioral evaluation of ischemic damage to CA1 hippocampal neurons: effects of preconditioning. Acta Neurobiol Exp (Wars) 2006; 66: 311-319.
17. Duszczyk M, Ziembowicz A, Gadamski R, Wieronska JM, Smialowska M, Lazarewicz JW. Changes in the NPY immunoreactivity in gerbil hippocampus after hypoxic and ischemic preconditioning. Neuropeptides 2009; 43: 31-39.
18. Frontczak-Baniewicz M, Chrapusta SJ, Sulejczak D. Long-term consequences of surgical brain injury – characteristics of the neurovascular unit and formation and demise of the glial scar in a rat model. Folia Neuropathol 2011; 49: 204-218.
19. Gamdzyk M, Makarewicz D, Słomka M, Ziembowicz A, Salinska E. Hypobaric hypoxia postconditioning reduces brain damage and improves antioxidative defense in the model of birth asphyxia in 7-day-old rats. Neurochem Res 2014; 39: 68-75.
20. Gancia P, Pomero G. Therapeutic hypothermia in the prevention of hypoxic-ischaemic encephalopathy: new categories to be enrolled. J Matern Fetal Neonatal Med 2012; 25 Suppl 4: 94-96.
21. Gill R, Foster AC, Woodruff GN. MK-801 is neuroprotective in gerbils when administered during the post-ischaemic period. Neuroscience 1988; 25: 847-855.

22. Gilland E, Hagberg H. Is MK-801 neuroprotection mediated by systemic hypothermia in the immature rat? Neuroreport 1997; 8: 1603-1605.
23. Grabb MC, Choi DW. Ischemic tolerance in murine cortical cell culture: critical role for NMDA receptors. J Neurosci 1999; 19: 1657-1662.
24. Guadagna S, Bundgaard C, Hovelsø N, Volbracht C, Francis PT, Egebjerg J, Sotty F. Memantine potentiates hippocampal θ oscillations at a therapeutic dose in anesthetized mice: a mechanistic link to its cognitive-enhancing properties. Neuropharmacology 2012; 62: 2208-2218.
25. Guo MF, Yu JZ, Ma CG. Mechanisms related to neuron injury and death in cerebral hypoxic ischaemia. Folia Neuropathol 2011; 49: 78-87.
26. Hargreaves RJ, Hill RG, Iversen LL. Neuroprotective NMDA antagonists: the controversy over their potential for adverse effects on cortical neuronal morphology. Acta Neurochir Suppl (Wien) 1994; 60: 15-19.
27. Ikonomidou C, Bosch F, Miksa M, Bittigau P, Vöckler J, Dikranian K, Tenkova TI, Stefovska V, Turski L, Olney JW. Blockade of NMDA receptors and apoptotic neurodegeneration in the developing brain. Science 1999; 283: 70-74.
28. Ikonomidou C. Triggers of apoptosis in the immature brain. Brain Dev 2009; 31: 488-492.
29. Jantas D, Lasoń W. Anti-apoptotic effect of memantine against staurosporine- and low-potassium-induced cell death in cerebellar granule cells: a development-dependent effect. Pharmacol Rep 2009; 61: 827-937.
30. Kajta M, Makarewicz D, Ziemińska E, Jantas D, Domin H, Lasoń W, Kutner A, Łazarewicz JW. Neuroprotection by co-treatment and post-treating with calcitriol following the ischemic and excitotoxic insult in vivo and in vitro. Neurochem Int 2009; 55: 265-274.
31. Kasischke K, Ludolph AC, Riepe MW. NMDA-antagonists reverse increased hypoxic tolerance by preceding chemical hypoxia. Neurosci Lett 1996; 214: 175-178.
32. Kaste M. Stroke: advances in thrombolysis. Lancet Neurol 2013; 12: 2-4.
33. Kato H, Liu Y, Araki T, Kogure K. MK-801, but not anisomycin, inhibits the induction of tolerance to ischemia in the gerbil hippocampus. Neurosci Lett 1992; 139: 118-121.
34. Kirino T, Sano K. Selective vulnerability in the gerbil hippocampus following transient ischemia. Acta Neuropathol 1984; 62: 201-208.
35. Kitagawa K, Matsumoto M, Tagaya M, Hata R, Ueda H, Niinobe M, Handa N, Fukunaga R, Kimura K, Mikoshiba K, et al. 'Ischemic tolerance' phenomenon found in the brain. Brain Res 1990; 528: 21-24.
36. Kuszczyk M, Słomka M, Antkiewicz-Michaluk L, Salińska E, Łazarewicz JW. 1-Methyl-1,2,3,4-tetrahydroisoquinoline and established uncompetitive NMDA receptor antagonists induce tolerance to excitotoxicity. Pharmacol Rep 2010; 62: 1041-1050.
37. Liu C, Lin N, Wu B, Qiu Y. Neuroprotective effect of memantine combined with topiramate in hypoxic-ischemic brain injury. Brain Res 2009; 1282: 173-182.
38. Liu Y, Kato H, Nakata N, Kogure K. Protection of rat hippocampus against ischemic neuronal damage by pretreatment with sublethal ischemia. Brain Res 1992; 586: 121-124.
39. Lo D, Grossberg GT. Use of memantine for the treatment of dementia. Expert Rev Neurother 2011; 11: 1359-1370.
40. Lysko PG, Gagnon RC, Yue TL, Gu JL, Feuerstein G. Neuroprotective effects of SKF 10,047 in cultured rat cerebellar neurons and in gerbil global brain ischemia. Stroke 1992; 23: 414-419.
41. Makarewicz D, Duszczyk M, Gadamski R, Danysz W, Łazarewicz JW. Neuroprotective potential of group I metabotropic glutamate receptor antagonists in two ischemic models. Neurochem Int 2006; 48: 485-490.
42. Manning SM, Boll G, Fitzgerald E, Selip DB, Volpe JJ, Jensen FE. The clinically available NMDA receptor antagonist, memantine, exhibits relative safety in the developing rat brain. Int J Dev Neurosci 2011; 29: 767-773.
43. Manning SM, Talos DM, Zhou C, Selip DB, Park HK, Park CJ, Volpe JJ, Jensen FE. NMDA receptor blockade with memantine attenuates white matter injury in a rat model of periventricular leukomalacia. J Neurosci 2008; 28: 6670-6678.
44. Muir KW, Lees KR. Clinical experience with excitatory amino acid antagonist drugs. Stroke 1995; 26: 503-513.
45. Nolan JP, Neumar RW, Adrie C, Aibiki M, Berg RA, Böttiger BW, Callaway C, Clark RS, Geocadin RG, Jauch EC, Kern KB, Laurent I, Longstreth WT, Merchant RM, Morley P, Morrison LJ, Nadkarni V, Peberdy MA, Rivers EP, Rodriguez-Nunez A, Sellke FW, Spaulding C, Sunde K, Hoek TV. Post-cardiac arrest syndrome: epidemiology, pathophysiology, treatment, and prognostication. Resuscitation 2008; 79: 350-379.
46. Obrenovitch TP. Molecular physiology of preconditioning-induced brain tolerance to ischemia. Physiol Rev 2008; 88: 211-247.
47. Olney JW, Wozniak DF, Jevtovic-Todorovic V, Farber NB, Bittigau P, Ikonomidou C. Drug-induced apoptotic neurodegeneration in the developing brain. Brain Pathol 2002; 12: 488-498.
48. Owley T, Salt J, Guter S, Grieve A, Walton L, Ayuyao N, Leventhal BL, Cook EH Jr. A prospective, open-label trial of memantine in the treatment of cognitive, behavioral, and memory dysfunction in pervasive developmental disorders. J Child Adolesc Psychopharmacol 2006; 16: 517-524.
49. Parsons CG, Danysz W, Dekundy A, Pulte I. Memantine and cholinesterase inhibitors: complementary mechanisms in the treatment of Alzheimer's disease. Neurotox Res 2013; 24: 358-369.
50. Pluta R, Kocki J, Maciejewski R, Ułamek-Kozioł M, Jabłoński M, Bogucka-Kocka A, Czuczwar SJ. Ischemia signalling to Alzheimer-related genes. Folia Neuropathol 2012; 50: 322-329.
51. Pradeep H, Diya JB, Shashikumar S, Rajanikant GK. Oxidative stress – assassin behind the ischemic stroke Folia Neuropathol 2012; 50: 219-230.
52. Puisieux F, Deplanque D, Bulckaen H, Maboudou P, Gelé P, Lhermitte M, Lebuffe G, Bordet R. Brain ischemic preconditioning is abolished by antioxidant drugs but does not up-regulate superoxide dismutase and glutathion peroxidase. Brain Res 2004; 1027: 30-37.
53. Puka-Sundvall M, Hallin U, Zhu C, Wang X, Karlsson JO, Blomgren K, Hagberg H. NMDA blockade attenuates caspase-3 activation and DNA fragmentation after neonatal hypoxia-ischemia. Neuroreport 2000; 11: 2833-2836.

54. Reynolds IJ, Miller RJ. Multiple sites for the regulation of the N-methyl-D-aspartate receptor. Mol Pharmacol 1988; 33: 581-584.
55. Rice JE 3rd, Vannucci RC, Brierley JB. The influence of immaturity on hypoxic-ischemic brain damage in the rat. Ann Neurol 1981; 9: 131-141.
56. Rosamond W, Flegal K, Furie K, Go A, Greenlund K, Haase N, Hailpern SM, Ho M, Howard V, Kissela B, Kittner S, Lloyd-Jones D, McDermott M, Meigs J, Moy C, Nichol G, O'Donnell C, Roger V, Sorlie P, Steinberger J, Thom T, Wilson M, Hong Y; American Heart Association Statistics Committee and Stroke Statistics Subcommittee. Heart disease and stroke statistics-2008 update: a report from the American Heart Association Statistics Committee and Stroke Statistics Subcommittee. Circulation 2008; 117: 25-146.
57. Schwartz PH, Wasterlain CG. Determination of serum and brain concentrations of neuroprotective and non-neuroprotective doses of MK-801. J Neurol Sci 1993; 115: 26-31.
58. Scirica BM. Therapeutic hypothermia after cardiac arrest. Circulation 2013; 127: 244-250.
59. Semenov DG, Samoilov MO, Łazarewicz JW. Calcium transients in the model of rapidly induced anoxic tolerance in rat cortical slices: involvement of NMDA receptors. Neurosignals 2002; 11: 329-335.
60. Seo H, Lim KH, Choi JH, Jeong SM. Similar neuroprotective effects of ischemic and hypoxic preconditioning on hypoxia-ischemia in the neonatal rat: A proton MRS study. Int J Dev Neurosci 2013; 31: 616-623.
61. Silverstein FS, McDonald JW 3rd, Bommarito M, Johnston MV. Effects of hypoxia-ischemia and MK-801 treatment on the binding of a phencyclidine analogue in the developing rat brain. Stroke 1990; 21: 310-315.
62. Szydlowska K, Tymianski M. Calcium, ischemia and excitotoxicity. Cell Calcium 2010; 47: 122-129.
63. Thomas SJ, Grossberg GT. Memantine: a review of studies into its safety and efficacy in treating Alzheimer's disease and other dementias. Clin Interv Aging 2009; 4: 367-377.
64. Tremblay R, Chakravarthy B, Hewitt K, Tauskela J, Morley P, Atkinson T, Durkin JP. Transient NMDA receptor inactivation provides long-term protection to cultured cortical neurons from a variety of death signals. J Neurosci 2000; 20: 7183-7192.
65. Tuttolomondo A, Di Sciacca R, Di Raimondo D, Arnao V, Renda C, Pinto A, Licata G. Neuron protection as a therapeutic target in acute ischemic stroke. Curr Top Med Chem 2009; 9: 1317-1334.
66. Vanderschuren LJ, Schoffelmeer AN, Mulder AH, De Vries TJ. Dizocilpine (MK801): use or abuse? Trends Pharmacol Sci 1998; 19: 79-81.
67. Vannucci RC, Towfighi J, Vannucci SJ. Hypoxic preconditioning and hypoxic-ischemic brain damage in the immature rat: pathologic and metabolic correlates. J Neurochem 1998; 71: 1215-1220.
68. Vezzani A, Serafini R, Stasi MA, Caccia S, Conti I, Tridico RV, Samanin R. Kinetics of MK-801 and its effect on quinolinic acid-induced seizures and neurotoxicity in rats. J Pharmacol Exp Ther 1989; 249: 278-283.
69. Wachtel EV, Hendricks-Muñoz KD. Current management of the infant who presents with neonatal encephalopathy. Curr Probl Pediatr Adolesc Health Care 2011; 41: 132-153.
70. Wegener N, Nagel J, Gross R, Chambon C, Greco S, Pietraszek M, Gravius A, Danysz W. Evaluation of brain pharmacokinetics of (+)MK-801 in relation to behaviour. Neurosci Lett 2011; 503: 68-72.
71. Wrang ML, Diemer NH. MK-801 does not prevent development of ischemic tolerance in rat brain. Neuroreport 2004; 15: 1151-1155.
72. Xie J, Lu G, Hou Y. Role of excitatory amino acids in hypoxic preconditioning. Biol Signals Recept 1999; 8: 267-274.
73. Zhao H, Ren C, Chen X, Shen J. From rapid to delayed and remote postconditioning: the evolving concept of ischemic postconditioning in brain ischemia. Curr Drug Targets 2012; 13: 173-187.
74. Zhao H. Ischemic postconditioning as a novel avenue to protect against brain injury after stroke. J Cereb Blood Flow Metab 2009; 29: 873-885.

Original article

Folia Neuropathologica

Paeoniflorin attenuates Aβ_{25-35}-induced neurotoxicity in PC12 cells by preventing mitochondrial dysfunction

Jialei Li[1], Xiaoxia Ji[2], Jianping Zhang[1], Guofeng Shi[1], Xue Zhu[3], Ke Wang[3]

[1]Department of Internal Neurology, Wuxi People's Hospital, Wuxi, Jiangsu Province, [2]Department of Intensive Care Unit, Wuxi No. 2 People's Hospital, Wuxi, Jiangsu Province, [3]Key Laboratory of Nuclear Medicine, Ministry of Health, Jiangsu Key Laboratory of Molecular Nuclear Medicine, Jiangsu Institute of Nuclear Medicine, Wuxi, Jiangsu Province, China

Folia Neuropathol 2014; 52 (3): 285-290 DOI: 10.5114/fn.2014.45569

Abstract

The pathogenic mechanism of neurodegenerative brain disorder such as Alzheimer's disease (AD) has been still far from clearly understood. Previous research has identified that mitochondrial dysfunction induced by Aβ has been recognized as a hallmark in AD. Therefore, the effective agents targeting β-amyloid (Aβ)-induced mitochondrial dysfunction may be useful for the treatment or prevention of AD. In the present study, the neuroprotective effect of paeoniflorin (PF), one monoterpene glycoside isolated from the Chinese herb Radix Paeoniae alba, on Aβ_{25-35}-induced toxicity in PC12 cells was investigated for the first time. The results showed that PF could attenuate or restore the cell injury induced by Aβ_{25-35} in PC12 cells through preventing mitochondrial dysfunction, including decreased mitochondrial membrane potential, increased cytochrome c release as well as activity of caspase-3 and caspase-9. Therefore, our data provide the evidence that PF could protect PC12 cells against Aβ_{25-35}-induced neurotoxicity and might be a potentially therapeutic approach for AD in the future.

Key words: *paeoniflorin, Alzheimer's disease, β-amyloid, mitochondrial dysfunction, PC12 cells.*

Introduction

Alzheimer's disease (AD) is a neurodegenerative disorder which approximately affects 14 million people worldwide [2,6,9]. One major pathological feature of AD is the deposition of amyloid plaques in the cerebral cortex, which are mainly composed of β-amyloid (Aβ) peptides [7,13]. Studies of postmortem brains of AD patients and transgenic mouse models of AD suggest that Aβ exerts neurotoxicity by promoting oxidative stress that is believed to directly affect the mitochondrial function [4,17]. Then, mitochondrial dysfunction induced by Aβ has been recognized as a prominent and early event in AD [16,19]. Therefore, the effective agents targeting Aβ-induced mitochondrial dysfunction may be useful for the treatment or prevention of AD.

Oriental herbal medicine, with fewer side effects and better safety, has been widely investigated for drug development [3]. Paeoniflorin (PF), a monoterpene glycoside isolated from the aqueous extract of the Chinese herb *Radix Paeoniae alba*, was reported to exert wide pharmacological effects in the nervous system (Fig. 1) [1,10-12,21]. Previous studies have identified that PF could attenuate the neurotoxicity induced by β-amyloid in the animal model and

Communicating author:
Jialei Li, Department of Internal Neurology, Wuxi People's Hospital, Wuxi, Jiangsu Province, China, phone: +86 13912489660, fax: (00) 86-(0) 510-85520770, e-mail: lijialei00@gmail.com

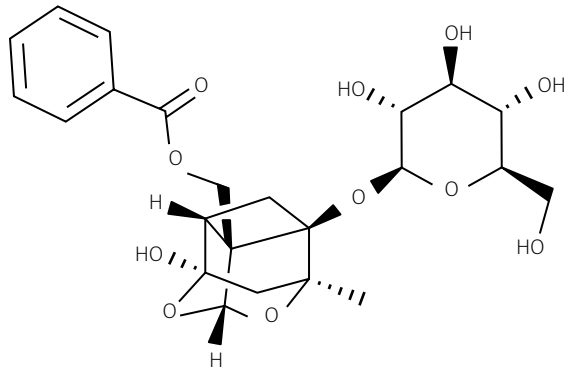

Fig. 1. Chemical structure of paeoniflorin.

might exert beneficial action for the treatment of AD [25]. However, the molecular mechanisms by which PF exerts its neuroprotective effect against β-amyloid-induced toxicity are still unclear.

In this study, we aimed to elucidate the protective effect of PF on $A\beta_{25-35}$-induced cytotoxicity in PC12 cells. Furthermore, the molecular mechanisms by which PF acted in models of neuron injury was also analyzed and this analysis focused on the mitochondrial pathway.

Material and methods

Materials and chemicals

Paeoniflorin (purity ≥ 98%, MW: 480.46) was purchased from the National Institute for the Control of Pharmaceutical and Biological Products (Beijing, China). All cell culture reagents were purchased from Gibco (Grand Island, NY, USA). $A\beta_{25-35}$, 3-(4,5-dimethylthiazol-2-yl)-2,5-diphenyltetrazolium bromide (MTT) and rhodamine 123 (Rh123) were purchased from Sigma-Aldrich (St. Louis, Mo, USA). Annexin V-FITC and PI double staining kit were purchased from PharMingen (San Diego, CA, USA). Dimethyl sulfoxide (DMSO), ribonuclease A (Rnase A), polyvinylidene fluoride (PVDF) membranes and enhanced chemiluminescence (ECL) detection kit were purchased from Beyotime (Nantong, China). Antibody against cytochrome c was obtained from Santa Cruz Biotechnology (CA, USA). Caspase-3 and caspase-9 fluorometric assay kits were obtained from BioVision (SF, USA). All other chemicals and reagents were of analytical grade.

Cell culture and treatment

The rat pheochromocytoma (PC12) cell line was obtained from the Shanghai Institute of Cell Biology, Chinese Academy of Sciences (Shanghai, China). PC12 cells were cultured in flasks at 37°C under an atmosphere of 5% CO_2/95% air in RPMI-1640 medium supplemented with 10% foetal bovine serum and 1% penicillin-streptomycin. For the experiments, the cells were detached and re-seeded in plates. After seeding, cells were pretreated with or without various concentrations of PF for 24 h, and then $A\beta_{25-35}$ (25 μM) was added to the medium for an additional 24 h.

MTT assay for cell viability

Cell viability was measured by MTT assay as described previously [17]. Briefly, after treated with the indicated drugs, 10 μL of MTT (5 mg/mL) was added to each well and incubated at 37°C for 4 h. Then, the culture medium was removed and 100 μL of DMSO was added to dissolve the formazan crystals. Absorbance was measured at 570 nm with an ELISA reader (Model 680, Bio-Rad, USA). Cell viability was expressed as a percentage of the value against the non-treated control group.

Measurement of cell apoptosis

Apoptosis of PC12 cells was examined by flow cytometry (Becton Dickinson FACS Calibur, Franklin Lakes, USA). After treated with the indicated drugs, cells were washed twice with ice-cold PBS and resuspended in 300 μL of binding buffer (Annexin V-FITC kit) containing 10 μL of Annexin V-FITC stock and 10 μL of PI. After incubation for 15 min at room temperature in the dark, the samples were analyzed by flow cytometry for the evaluation of cell apoptosis.

Measurement of mitochondrial membrane potential

Mitochondrial membrane potential (MMP) was measured by uptake of lipophilic cation Rh123. Cells were treated with the indicated drugs and incubated with 5 μM of Rh123 at 37°C for 30 min. Then, the cells were washed twice and resuspended in PBS. The cellular levels of Rh123 were analyzed by flow cytometry (Becton-Dickinson, CA, USA).

Measurement of cytochrome c release

For measurement of cytochrome c release, the cytosol and mitochondrial fractions were prepared as described previously [24]. The protein concentration of samples was determined with Bradford method

[8]. Then, the samples (50 µg) were applied to 10% SDS polyacrylamide gel and transblotted onto PVDF membranes. After blocking with 5% BSA in Tris-buffer saline (TBST) for 1 h, membranes were incubated with the primary antibody against cytochrome c overnight and followed by secondary antibody incubation for 1 h at room temperature. Protein bands were visualized by ECL detection kit.

Measurement of caspase-3 and caspase-9 activity

Fluorometric assay was used to detect the cleavage of substrate to caspase-3 or caspase-9. Cells were collected and lysed in buffer containing 50 mM 4-(2-hydroxyethyl)-1-piperazineethanesulfonic acid (HEPES) (pH 7.4), 100 mM NaCl, 2 mM ethylene diamine tetraacetic acid (EDTA), 0.1% 3 [(3-cholamidopropyl)-dimethylammonio]-1-propane sulfonate (CHAPS), 10% sucrose and 5 mM dithiothreitol (DTT). Aliquots of 6 mg of crude cell lysate were incubated with caspase-3 substrate DEVD-AFC or caspase-9 substrate LEHD-AFC at 37°C for 30 min. The activity was quantified by a spectrofluorometer with an excitation wavelength at 400 nm and an emission wavelength at 505 nm.

Statistical analysis

Biostatistical analyses were conducted with SPSS 16.0 software. All experiments were done in triplicates and the results were indicative of three independent studies. Data were presented as the mean ± SEM. Difference was considered statistically significant when $p < 0.05$.

Results

Effect of paeoniflorin on $A\beta_{25-35}$-induced cell injury

Cell viability of PC12 cells treated with the indicated drugs was evaluated with MTT assay. As shown in Figure 2, $A\beta_{25-35}$ (25 µM) exhibited a remarkably inhibitory effect on the growth of PC12 cells. However, the cytotoxic effects were attenuated by the pretreatment with PF in a dose-dependent manner.

Effect of paeoniflorin on $A\beta_{25-35}$-induced cell apoptosis

Apoptosis of PC12 cells treated with the indicated drugs was assessed by annexin V-PI dual-staining assay. The results showed that the percentage of apoptotic cells induced by $A\beta_{25-35}$ (25 µM) increased from 1.58 ± 1.52% to 42.51 ± 6.53% as compared to the control. While with the pretreatment of 2, 10 and 50 µM of CNTF, cell apoptosis induced by $A\beta_{25-35}$ (25 µM) decreased to 32.72 ± 4.48%, 22.23 ± 3.07% and 10.35 ± 3.27%, respectively (Fig. 3). These results indicated that PF could suppress $A\beta_{25-35}$-induced apoptosis in PC12 cells.

Effect of paeoniflorin on $A\beta_{25-35}$-induced loss of mitochondrial membrane potential

The change of MMP was evaluated by the fluorescence probe Rh123. As shown in Figure 4, cells exposed to $A\beta_{25-35}$ (25 µM) for 24 h markedly decreased Rh123 staining, indicating a drop in MMP which is related to mitochondrial dysfunction, while PF significantly improved $A\beta_{25-35}$-induced impairments of MMP in a dose-dependent manner.

Effect of paeoniflorin on $A\beta_{25-35}$-induced cytochrome c release

The reduction in MMP could induce a release of cytochrome c from the mitochondria to cytosol. As shown in Figure 5, $A\beta_{25-35}$ (25 µM) significantly increased the release of cytochrome c from mitochondria to cytosol. However, PF pretreatment could

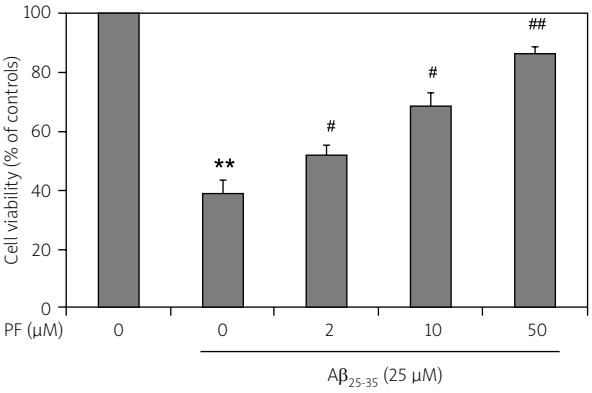

Fig. 2. Effect of PF on $A\beta_{25-35}$-induced cytotoxicity in PC12 cells. Determination of the viability of PC12 cells by the MTT assay after treatment with $A\beta_{25-35}$ (25 µM) in the absence or presence of the indicated concentrations of PF. The results are shown as mean ± SEM of three experiments and each included triplicate sets. $^{*}p < 0.05$, $^{**}p < 0.01$ vs. control; $^{\#}p < 0.05$, $^{\#\#}p < 0.01$ vs. $A\beta_{25-35}$ alone.

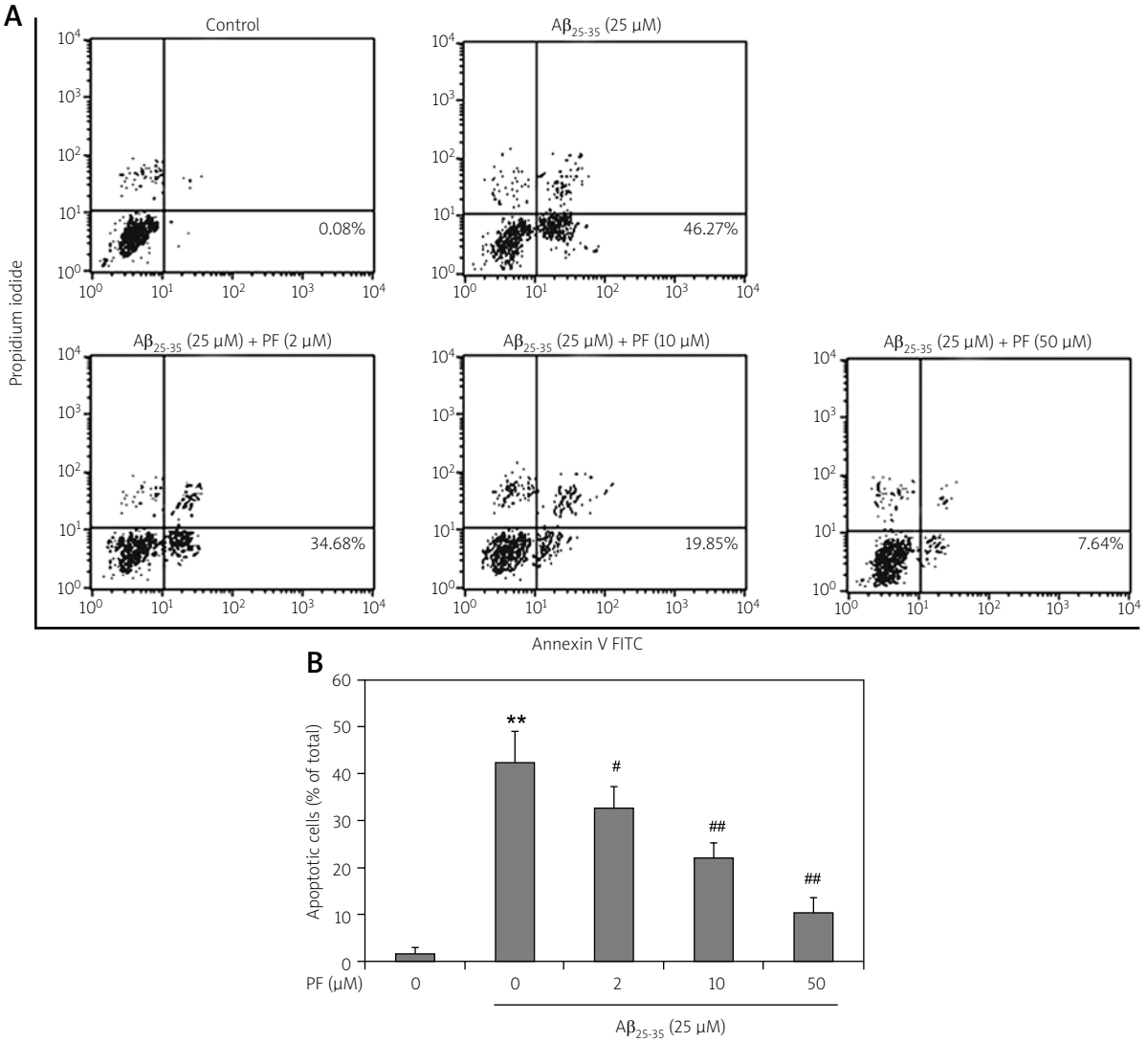

Fig. 3. Effect of PF on $A\beta_{25-35}$-induced apoptosis in PC12 cells. Determination of the apoptosis of PC12 cells by the annexin V-PI dual-staining assay after treatment with $A\beta_{25-35}$ (25 μM) in the absence or presence of the indicated concentrations of PF. **A)** Flow cytometry analysis of cell apoptosis. The dual parametric dot plots combining annexin V-FITC and PI fluorescence show the viable cell population (lower left quadrant, annexin V^-PI^-), the early apoptotic cells (lower right quadrant, annexin V^+PI^-) and the necrotic cells (upper right quadrant, annexin V^+PI^+). **B)** The percentage distribution of apoptotic cells. The results were shown as mean ± SEM of three experiments and each included triplicate sets. $^{**}p < 0.01$ vs. control; $^{\#}p < 0.05$, $^{\#\#}p < 0.01$ vs. $A\beta_{25-35}$ alone.

inhibit the release of cytochrome c in a dose-dependent manner.

Effect of paeoniflorin on $A\beta_{25-35}$-induced caspase-3 and caspase-9 activation

The release of cytochrome c could activate caspase-9, and then activate effector caspase-3. The activation status of caspase-3 and caspase-9 was further investigated when cells were treated with the indicated drugs. As shown in Figure 6, the activity of caspase-3 and caspase-9 significantly increased following $A\beta_{25-35}$ (25 μM) treatment for 24 h and which were dose-dependently reversed when cells were pretreated with PF (Fig. 6).

Discussion

More and more scientific research has identified that mitochondrial dysfunction is a hallmark of

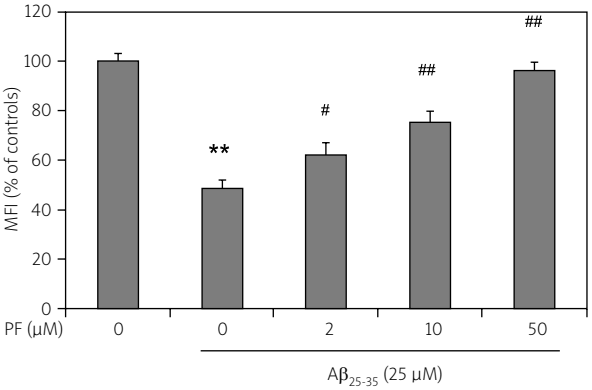

Fig. 4. Effect of PF on $A\beta_{25-35}$-induced loss of MMP in PC12 cells. Mean relative fluorescent density (MFI) of Rh123 was calculated after treatment with $A\beta_{25-35}$ (25 μM) in the absence or presence of the indicated concentrations of PF. The results are shown as mean ± SEM of three experiments and each included triplicate sets. $^{*}p < 0.05$, $^{**}p < 0.01$ vs. control; $^{\#}p < 0.05$, $^{\#\#}p < 0.01$ vs. $A\beta_{25-35}$ alone.

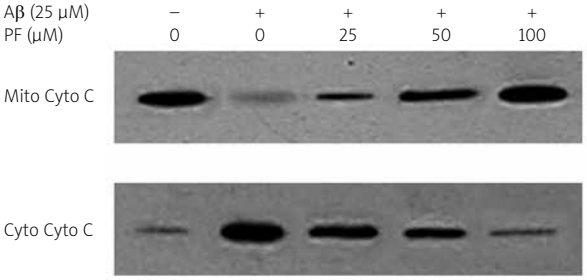

Fig. 5. Effect of PF on $A\beta_{25-35}$-induced cytochrome c release in PC12 cells. The expression level of cytochrome c in mitochondria and cytosol was assessed by western blot after treatment with $A\beta_{25-35}$ (25 μM) in the absence or presence of the indicated concentrations of PF. The results are shown as mean ± SEM of three experiments and each included triplicate sets.

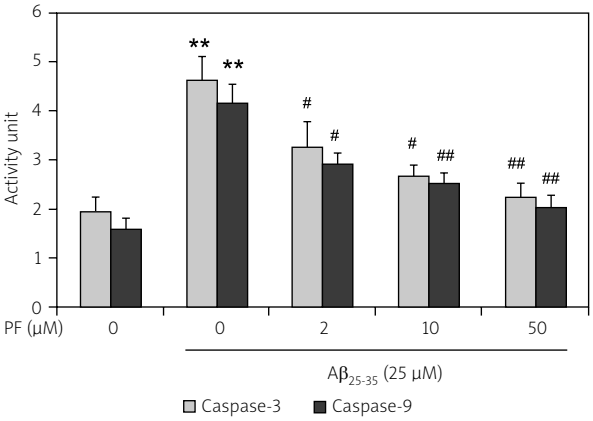

Fig. 6. Effect of PF on $A\beta_{25-35}$-induced caspase-3 and caspase-9 activation in PC12 cells. The activity of caspase-3 and caspase-9 was evaluated by fluorometric assay after treatment with $A\beta_{25-35}$ (25 μM) in the absence or presence of the indicated concentrations of PF. The results are shown as mean ± SEM of three experiments and each included triplicate sets. $^{*}p < 0.05$, $^{**}p < 0.01$ vs. control; $^{\#}p < 0.05$, $^{\#\#}p < 0.01$ vs. $A\beta_{25-35}$ alone.

Aβ-induced neuronal toxicity in AD [14,18]. Therefore, any substances that can decrease mitochondrial dysfunction may be useful for the treatment or prevention of AD. Paeoniflorin, one of components of the aqueous extract of the Chinese herb *Radix Paeoniae alba*, has recently been reported to be an active neuroprotective agent in animal models of neurodegenerative diseases [25]. To further understand the biological function of PF on the AD *in vitro* model, the present study focused on the molecular effect of PF on $A\beta_{25-35}$-induced mitochondrial dysfunction in PC12 cells.

Previous studies suggested that $A\beta_{25-35}$-induced cytotoxicity in PC12 cells was recognized as a typical model of Alzheimer's disease [5,15]. In this study, we confirmed for the first time that pretreatment with PF could markedly attenuate $A\beta_{25-35}$ (25 μM)-induced loss of cell viability in PC12 cells by MTT assay. Then, the protective effect of PF against $A\beta_{25-35}$-induced cell apoptosis was evaluated by annexin V-PI dual-staining assay. The results showed that PF pretreatment significantly reduced the percentage of apoptotic cells induced by $A\beta_{25-35}$ in PC12 cells. Furthermore, the molecular mechanism of the neuroprotective effect of PF on $A\beta_{25-35}$-induced cell apoptosis in PC12 cells was investigated.

One classification of neuronal apoptosis is based on compelling evidence that mitochondrial changes are pivotal in the cell death decision in many cases [20,22]. Our results showed that mitochondrial dysfunction is involved in $A\beta_{25-35}$-induced apoptosis in PC12 cells which includes opening of pores in cell membrane, release of cytochrome c and activation of caspases. Then, we investigated whether PF can regulate mitochondrial dysfunction induced by $A\beta_{25-35}$ in PC12 cells. The subsequent experiments revealed that pretreatment of PF could attenuate all

of these biochemical changes which are tightly associated with $A\beta_{25-35}$-induced apoptosis.

In conclusion, our results confirmed for the first time the neuroprotective effect of PF on $A\beta_{25-35}$-induced cell injury in PC12 cells by preventing mitochondrial dysfunction. The potency of PF presented here provides a rational reason for exploring its clinical efficiency.

Acknowledgements

This work is supported by grants from the National Natural Science Foundation (81300787) and the Natural Science Foundation of Jiangsu Province (BK2011168, BK2012105).

Disclosure

Authors report no conflict of interest.

References

1. Cao BY, Yang YP, Luo WF, Mao CJ, Han R, Sun X, Cheng J, Liu CF. Paeoniflorin, a potent natural compound, protects PC12 cells from MPP+ and acidic damage via autophagic pathway. J Ethnopharmacol 2010; 131: 122-129.
2. Citron M. Alzheimer's disease: strategies for disease modification. Nat Rev Drug Discov 2010; 9: 387-398.
3. Conklin KA. Dietary antioxidants during cancer chemotherapy: impact on chemotherapeutic effectiveness and development of side effects. Nutr Cancer 2000; 37: 1-18.
4. Gu XM, Huang HC, Jiang ZF. Mitochondrial dysfunction and cellular metabolic deficiency in Alzheimer's disease. Neurosci Bull 2012; 28: 631-640.
5. Hoi CP, Ho YP, Baum L, Chow AH. Neuroprotective effect of honokiol and magnolol, compounds from Magnolia officinalis, on beta-amyloid-induced toxicity in PC12 cells. Phytother Res 2010; 24: 1538-1542.
6. Holtzman DM, Morris JC, Goate A. Alzheimer's disease: the challenge of the second century. Sci Transl Med 2011; 3: 77sr71. doi: 10.1126/scitranslmed.3002369.
7. Ittner LM, Götz J. Amyloid-β and tau – a toxic pas de deux in Alzheimer's disease. Nat Rev Neurosci 2010; 12: 67-72.
8. Kruger NJ. The Bradford method for protein quantitation. In: Methods in Molecular Biology. Vol. 32. Basic protein and peptide protocols. Springer 1994, pp. 9-15.
9. Mangialasche F, Solomon A, Winblad B, Mecocci P, Kivipelto M. Alzheimer's disease: clinical trials and drug development. Lancet Neurol 2010; 9: 702-716.
10. Mao QQ, Zhong XM, Feng CR, Pan AJ, Li ZY, Huang Z. Protective effects of paeoniflorin against glutamate-induced neurotoxicity in PC12 cells via antioxidant mechanisms and Ca2+ antagonism. Cell Mol Neurobiol 2010; 30: 1059-1066.
11. Mao QQ, Zhong XM, Li ZY, Huang Z. Paeoniflorin protects against NMDA induced neurotoxicity in PC12 cells via Ca^{2+} antagonism. Phytother Res 2011; 25: 681-685.
12. Mao QQ, Zhong XM, Qiu FM, Li ZY, Huang Z. Protective effects of paeoniflorin against corticosterone-induced neurotoxicity in PC12 cells. Phytother Res 2012; 26: 969-973.
13. Mawuenyega KG, Sigurdson W, Ovod V, Munsell L, Kasten T, Morris JC, Yarasheski KE, Bateman RJ. Decreased clearance of CNS β-amyloid in Alzheimer's disease. Science 2010; 330: 1774-1774.
14. Moreira PI, Carvalho C, Zhu X, Smith MA, Perry G. Mitochondrial dysfunction is a trigger of Alzheimer's disease pathophysiology. Biochim Biophys Acta 2010; 1802: 2-10.
15. Muthaiyah B, Essa MM, Chauhan V, Chauhan A. Protective effects of walnut extract against amyloid beta peptide-induced cell death and oxidative stress in PC12 cells. J Neurosci 2011; 36: 2096-2103.
16. Pagani L, Eckert A. Amyloid-beta interaction with mitochondria. Int J Alzheimers Dis 2011; 2011: 925050.
17. Panahi N, Mahmoudian M, Mortazavi P, Hashjin GS. Effects of berberine on β-secretase activity in a rabbit model of Alzheimer's disease. Arch Med Sci 2013; 9: 146-150.
18. Sheng B, Wang X, Su B, Lee Hg, Casadesus G, Perry G, Zhu X. Impaired mitochondrial biogenesis contributes to mitochondrial dysfunction in Alzheimer's disease. J Neurochem 2012; 120: 419-429.
19. Spuch C, Ortolano S, Navarro C. New insights in the amyloid-beta interaction with mitochondria. J Aging Res 2012; 2012: 324968.
20. Sims NR, Muyderman H. Mitochondria, oxidative metabolism and cell death in stroke. Biochim Biophys Acta 2010; 1802: 80-91.
21. Sun R, Wang K, Wu D, Li X, Ou Y. Protective effect of paeoniflorin against glutamate-induced neurotoxicity in PC12 cells via Bcl-2/Bax signal pathway. Folia Neuropathol 2012; 50: 270-276.
22. Su B, Wang X, Zheng L, Perry G, Smith MA, Zhu X. Abnormal mitochondrial dynamics and neurodegenerative diseases. Biochim Biophys Acta 2010; 1802: 135-142.
23. van Meerloo J, Kaspers GJ, Cloos J. Cell sensitivity assays: the MTT assay. Cancer Cell Culture. Springer 2011, pp. 237-245.
24. Zhao S, Xu W, Jiang W, Yu W, Lin Y, Zhang T, Yao J, Zhou L, Zeng Y, Li H. Regulation of cellular metabolism by protein lysine acetylation. Science 2010; 327: 1000-1004.
25. Zhong SZ, Ge QH, Li Q, Qu R, Ma SP. Peoniflorin attentuates Aβ(1-42)-mediated neurotoxicity by regulating calcium homeostasis and ameliorating oxidative stress in hippocampus of rats. J Neurol Sci 2009; 280: 71-78.

Original paper

Folia Neuropathologica

Age-dependent neuroprotection of retinal ganglion cells by tempol-C8 acyl ester in a rat NMDA toxicity model

Michal Fiedorowicz[1,2], Robert Rejdak[1,2,3], Frank Schuettauf[1], Michal Wozniak[4], Pawel Grieb[2], Sebastian Thaler[1]

[1]Eye Hospital and Institute for Ophthalmic Research, Centre for Ophthalmology, University of Tübingen, Tübingen, Germany, [2]Department of Experimental Pharmacology, Mossakowski Medical Research Centre, Polish Academy of Science, Warsaw, Poland, [3]1st Eye Hospital, Medical University of Lublin, Lublin, Poland, [4]Chair & Department of Medical Chemistry, Medical University of Gdansk, Gdansk, Poland

Folia Neuropathol 2014; 52 (3): 291-297 DOI: 10.5114/fn.2014.45570

Abstract

Background: *The efficacy of tempol and its acyl derivative tempol-C8 as retinoprotective agents was compared in a rat model of NMDA-induced retinal ganglion cell (RGC) damage.*

Material and methods: *Tempol or tempol-C8 in different doses was administered intraperitoneally to 6 weeks old (pre-adolescent) and 9-10 weeks old (young adult) rats before and after an intravitreous NMDA injection. Retinal ganglion cell were retrogradely labeled with the fluorescent tracer hydroxystilbamidine and RGC counting was performed on retinal flatmounts.*

Results: *Intravitreal NMDA reduced RGC counts by about 90%, independently of age ($p < 0.001$). In pre-adolescent animals tempol-C8, but not tempol unmodified, showed a significant, dose-dependent RGC rescue effect, with peak activity at 5.8 µmol/kg ($p < 0.001$). In young adult animals, however, no neuroprotective effect was found for either tempol or tempol-C8.*

Conclusions: *In contrast to tempol itself, tempol-C8 acyl ester was neuroprotective in pre-adolescent rats in the NMDA-induced RGC damage model. Therefore, neuroprotection by tempol acyl esters seems to be superior to that of tempol under certain conditions.*

Key words: *tempol, tempol acyl ester, NMDA, ganglion cell, neuroprotection.*

Introduction

Retinal ganglion cell loss is a feature of several important chronic disorders of the eye, including glaucoma, ischemia, and diabetic retinopathy. Several pathways modifying the course of this selective neuronal cell death have been identified in the last decades. The exact mechanisms still remain unclear, but excitotoxicity appears to play an important role. Anti-excitotoxic drugs have been shown to act neuroprotectively in animal models of ocular hypertension and ischemia [3,9].

Antioxidant enzymes play a key role in defending cells against free radical toxicity; superoxide dismutases (SOD), for example, catalyze the decomposition (dismutation) of the superoxide anion into hydrogen peroxide. Superoxide anion dismutation is crucial to free radical defense and limits the gen-

Communicating author:
Dr. Sebastian Thaler, Centre for Ophthalmology, University of Tübingen, Schleichstrasse 12, 72076 Tübingen, Germany, phone: +49 7071 29 83721, fax: +49 7071 29 5018, e-mail: sebastian.thaler@uni-tuebingen.de

eration of highly reactive species such as hydroxyl radical ($OH^{\bullet}$) or peroxynitrite ($ONOO^{-}$). *In vitro* and *in vivo* experiments have demonstrated that antioxidant enzyme mimetics – small, non-protein molecules with catalytic properties similar to those of enzymes – can improve oxidative stress defenses. A well-known SOD mimetic in this respect is tempol (4-hydroxy-2,2,6,6-tetramethylpiperidinyl-1-oxyl), a stable nitroxide radical. Tempol is highly cell-permeable and easily crosses the blood brain barrier [14]. It has been shown previously both *in vitro* and *in vivo* to protect neuronal cells in models of brain trauma, ischemic stroke, and Parkinson's disease [1], all of which are neurodegenerative conditions that share many similarities with retinal neurodegenerative disorders such as glaucoma. In an *in vitro* model of retinal ganglion cell (RGC) damage via TNF-α and hypoxia, tempol significantly improved RGC survival after the onset of mitochondrial damage [21]. Tempol and its derivative tempol hydroxylamine also acted neuroprotectively in models of light damage [26]. Unfortunately, tempol is effective only in relatively high doses; some authors have reported effective doses of $\geq$ 100 mg/kg body weight in *in vivo* situations [18]. Such high doses in conscious animals have been reported to trigger serious side effects, including seizures, hypotension, and agitation [7].

Increased tempol effectiveness can be achieved by attaching an "address molecule" to tempol that will direct it to sites of free radical generation. An example of this might be mitochondria-targeted TEMPO conjugates with hemigramicidin as an "address molecule" [6]. However, free radicals can be generated not only in mitochondria but also in cell membranes, for example in the plasma respiratory chain called plasma membrane oxidoreductase (PMOR), which is also present in neuronal tissue [27]. We therefore conjectured that adding a lipophilic "address molecule" could increase both the amount and neuroprotective efficacy of tempol in membranes. Recently, we were able to show that one such tempol derivative, tempol-C8 acyl ester, provides RGC neuroprotection in lower doses than unmodified tempol in a rat partial optic nerve crush (PONC) model [22].

The purpose of the present study was to compare the efficacy of tempol and its acyl derivative tempol-C8 as retinoprotective agents in the excitotoxicity model of N-methyl-D-aspartate (NMDA)-induced RGC damage in pre-adolescent and young adult rats.

Material and methods

Animals

Brown Norway rats (Charles River, Wilmington, MA), body weight 100-120 g (6 weeks of age – "pre-adolescent") and 190-210 g (9-10 weeks of age – "young adult") were housed under a 12-hour light-dark cycle. The treatment of the animals was in accordance with the ARVO Statement for the Use of Animals in Ophthalmic and Vision Research and was approved and monitored by the respective authorities (Regierungspräsidium Tübingen).

Intravitreal injection

The rats were anesthetized with an intraperitoneal injection of chloral hydrate (7%, 6 ml/kg body weight). Local anesthesia in the form of eye drops (oxybuprocaine) was also applied. 2 µl of NMDA solution (10 mM in 0.2 phosphate buffered saline [PBS], pH 7.2; Sigma-Aldrich, Steinheim, Germany) were intravitreally injected into the posterior side of the globe, 1 mm behind the limbus, with a heat-pulled glass capillary connected to a microsyringe (Drummond Scientific, Broomall, PA) under direct observation through the microscope. The eye volume was estimated to be about 20 µl, leading to a final intraocular NMDA concentration of 1 mM. Antibiotic eye drops (ofloxacin) were applied directly after the injection. Any rat that exhibited postoperative complications such as lens damage, retinal hemorrhage, retinal detachment, or vitreous hemorrhage was excluded from the study. Contralateral eyes served as control eyes and were injected with PBS (NMDA vehicle).

Treatment

Either tempol (Sigma-Aldrich, Steinheim, Germany) in doses of 116 and 290 µmol/kg (20 and 50 mg/kg bw) or tempol-C8 (synthesized by M. Wozniak as described previously [22]) in doses of 0.58, 2.9, 5.8, 29, and 58 µmol/kg (molar equivalents of tempol 0.1, 0.5, 1, 5, and 10 mg/kg bw) was administered intraperitoneally twice before NMDA injection (24 h and 30 min), and then once daily for 6 consecutive days. Control rats were treated with tempol vehicle (5% ethanol in PBS, pH 7.2).

Quantification of retinal ganglion cells

Retrograde labeling of retinal ganglion cells was performed as described previously [25]. Briefly, 5 days after NMDA injection the animals were anesthetized

as described above, and 7 µl of the fluorescent tracer hydroxystilbamidine methane sulfonate (Molecular Probes, Eugene, OR) was injected stereotaxically into each superior colliculus. Two days after labeling (i.e. 7 days after NMDA injection), the animals were sacrificed with CO_2, the eyes were enucleated, and the retinas were dissected, flat-mounted on cellulose nitrate filters (pore size 60 µm; Sartorius, Long Island, NY), and fixed in 2% PFA for 30 min. Visualization of RGC was performed immediately by fluorescence microscopy. Images obtained using a digital imaging system (Image-Pro 3.0, Media Cybernetics Inc., Silver Spring, MD) connected to a microscope were coded and analyzed in a masked fashion by an observer who was unaware of the treatment scheme. Counts taken in 12 distinct areas of 62,500 µm^2 each per retina were added and expressed as cell density (cells per square millimeter; mean ± SE), as described in detail previously [23].

Statistical analysis

Statistical analysis was performed using GraphPad Prism version 5.04 for Windows (GraphPad Software, San Diego, CA, USA). Kruskal-Wallis non-parametric ANOVA was used followed by Dunn's multiple comparison *post hoc* test. Differences were regarded significant when $p < 0.05$. Unless stated otherwise, the data are presented as means with respective standard errors.

Results

NMDA vehicle-treated animals

The average density of RGC in vehicle (PBS)-treated animals was 2342.1 ± 78.0. There was no significant difference between pre-adolescent and young adult rats ($p > 0.05$). Neither tempol nor tempol-C8 treatment significantly affected RGC numbers in vehicle-treated animals.

NMDA-injected animals

NMDA injection reduced RGC counts by around 90%, i.e. to 278.1 ± 12.1 ($n = 8$, $p < 0.001$). There was no significant difference between pre-adolescent and young adult rats ($p > 0.05$).

Tempol-treated animals

Tempol treatment exerted no significant protective effect against NMDA-induced RGC loss in any dose tested (up to 50 mg/kg BW) ($p > 0.05$). There were no significant differences between the pre-adolescent and young adult rat groups ($p > 0.05$) (Fig. 1).

Tempol-C8-treated animals

Tempol acyl ester tempol-C8 partially rescued RGC against NMDA-induced cell loss, but only in pre-adolescent animals. The most effective dose was 5.8 µmol/kg BW (i.e. equivalent of 1 mg of tempol/kg BW). Tempol-C8 treatment increased RGC numbers after NMDA to a level 63% higher than that of untreated control animals (452.8 ± 16.4, $p < 0.001$). Other concentrations which were tested did not increase RGC counts significantly (336.8 ± 20.8; 354.4 ± 28.7 and 261.2 ± 16.1 for 2.9, 29 and 58 µmol/kg doses respectively, $p > 0.05$ for all groups vs. controls). Tempol-C8 did not result in any significant differences in RGC counts in the young adult animals after NMDA compared to the control animals (322.9 ± 15.7; 318.4 ± 9.8; 330.1 ± 27.5; 232.9 ± 4.3 for 0.58, 2.9, 5.8 and 29 µmol/kg doses respectively, $p > 0.05$ for all groups) (Fig. 2).

Discussion

In this study intravitreous NMDA led to a massive RGC loss after one week, in accordance with previous studies of our group and others [10,22,24]. Against this background we tested the neuroprotective effects of the free radical scavenger tempol and its acyl ester tempol-C8 in a rat NMDA-induced RGC damage model. Both compounds were shown previously to provide neuroprotection to RGC in a rat PONC model [22,24]. Li *et al*. have suggested that RGC death after NMDA displays signs of apoptosis similar to that of RGC death after PONC [10]. It was, therefore, reasonable to assume that these two models may share similarities concerning the nature of RGC damage, although with differences in the onset and course. However, both models have their limitations and exhibit different aspects of glaucomatous degeneration in the form of mechanical or intrinsic activation of neurodegeneration. PONC simulates particularly a mechanical onset of optic nerve damage in glaucomatous neuropathy, while the NMDA toxicity model described here reflects more the excitotoxic aspect of glaucoma, whose significance is still under discussion [17,20]. Nevertheless, both models produce selective and pronounced loss of RGC within a relatively short time (days-weeks).

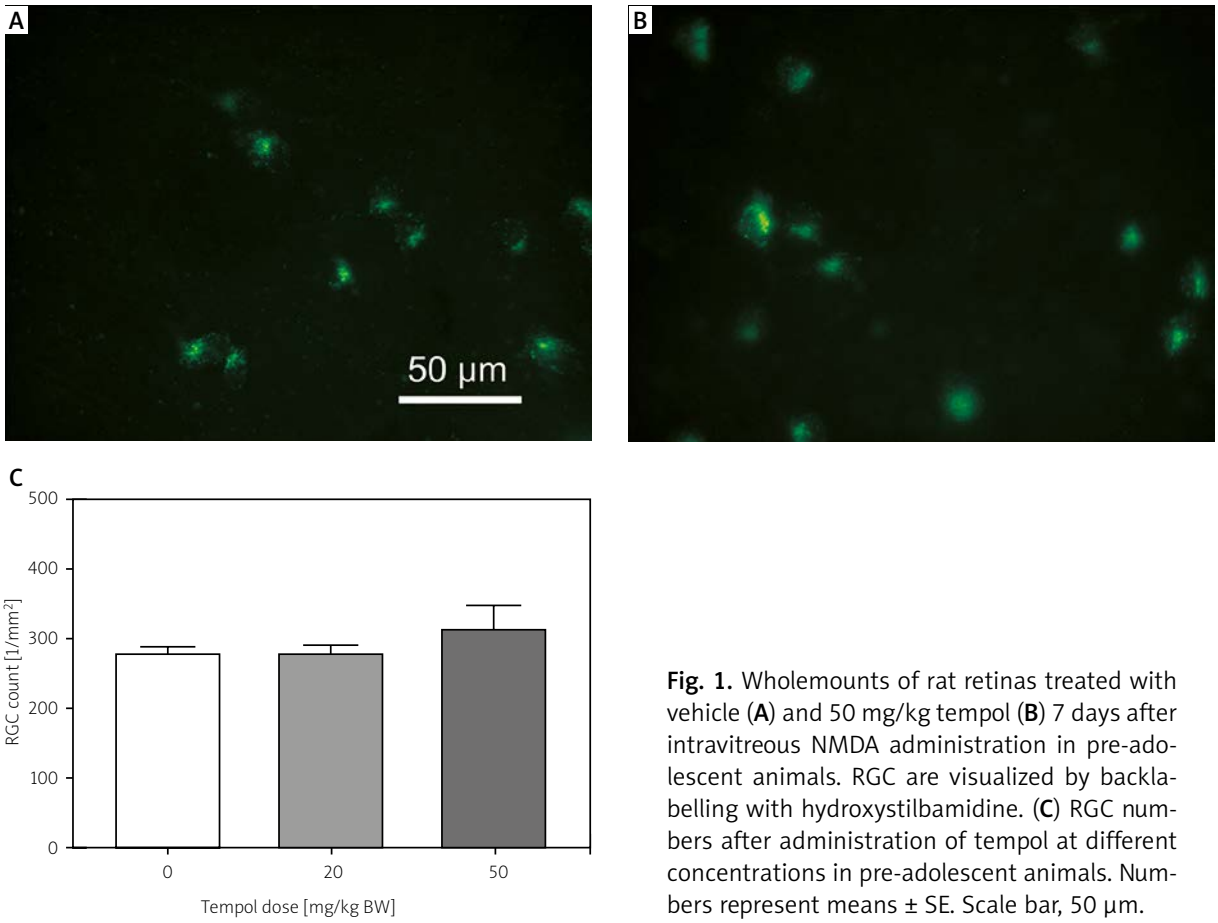

Fig. 1. Wholemounts of rat retinas treated with vehicle (**A**) and 50 mg/kg tempol (**B**) 7 days after intravitreous NMDA administration in pre-adolescent animals. RGC are visualized by backlabelling with hydroxystilbamidine. (**C**) RGC numbers after administration of tempol at different concentrations in pre-adolescent animals. Numbers represent means ± SE. Scale bar, 50 µm.

Surprisingly, and in contrast to PONC, tempol in the doses used did not show any protection toward RGC in the NMDA toxicity model. This stands partly in contrast with a previous study of El-Remessy *et al*. [5], who found that intravitreal injection of tempol (0.4 mg/eye) diminished TUNEL staining in the ganglion cell layer and the inner nuclear layer (ganglion cell layer – GCL, inner nuclear layer – INL) when coadministered with 200 nmol of NMDA per eye (i.e. 2 µl of 100 mM NMDA). Tempol also diminished malondialdehyde and nitrotyrosine staining. However, there were significant differences in the experimental settings. The model utilized by El-Remessy *et al*. used a 10-times higher concentration of NMDA than was the case in our experiments. Furthermore, El-Remessy *et al*. administered tempol intravitreally and at the same time as NMDA, which includes the possibility of direct interaction. The intravitreal concentration of tempol in the eye might be even 1000-fold higher than in our experiments after intraperitoneal tempol administration. A much higher concentration of systemic tempol might have had a neuroprotective effect in our model as well, but we did not test it because we expected prohibitive systemic side effects [7].

We found that tempol-C8, a tempol acyl ester previously shown to be more effective than tempol in a rat model of PONC, was also effective in the NMDA toxicity model. However, in our experiments tempol-C8 was effective only in pre-adolescent animals, despite the fact that NMDA-induced damage to RGC did not depend on animal age. We suppose that the resistance of older animals to tempol-C8 may mirror different mechanisms engaged in the excitotoxic damage evoked by NMDA in the pre-adolescent and young adult rats.

Dramatic age-related changes of vulnerability to excitotoxicity have been observed in cultured hippocampal neurons within 35 days after birth [13]. In cortical slices glutamate-induced reactive oxygen species (ROS) formation and lactate dehydrogenase release (a marker of cell death) were significantly higher in 80-day-old rats than in 21-day-old rats [8].

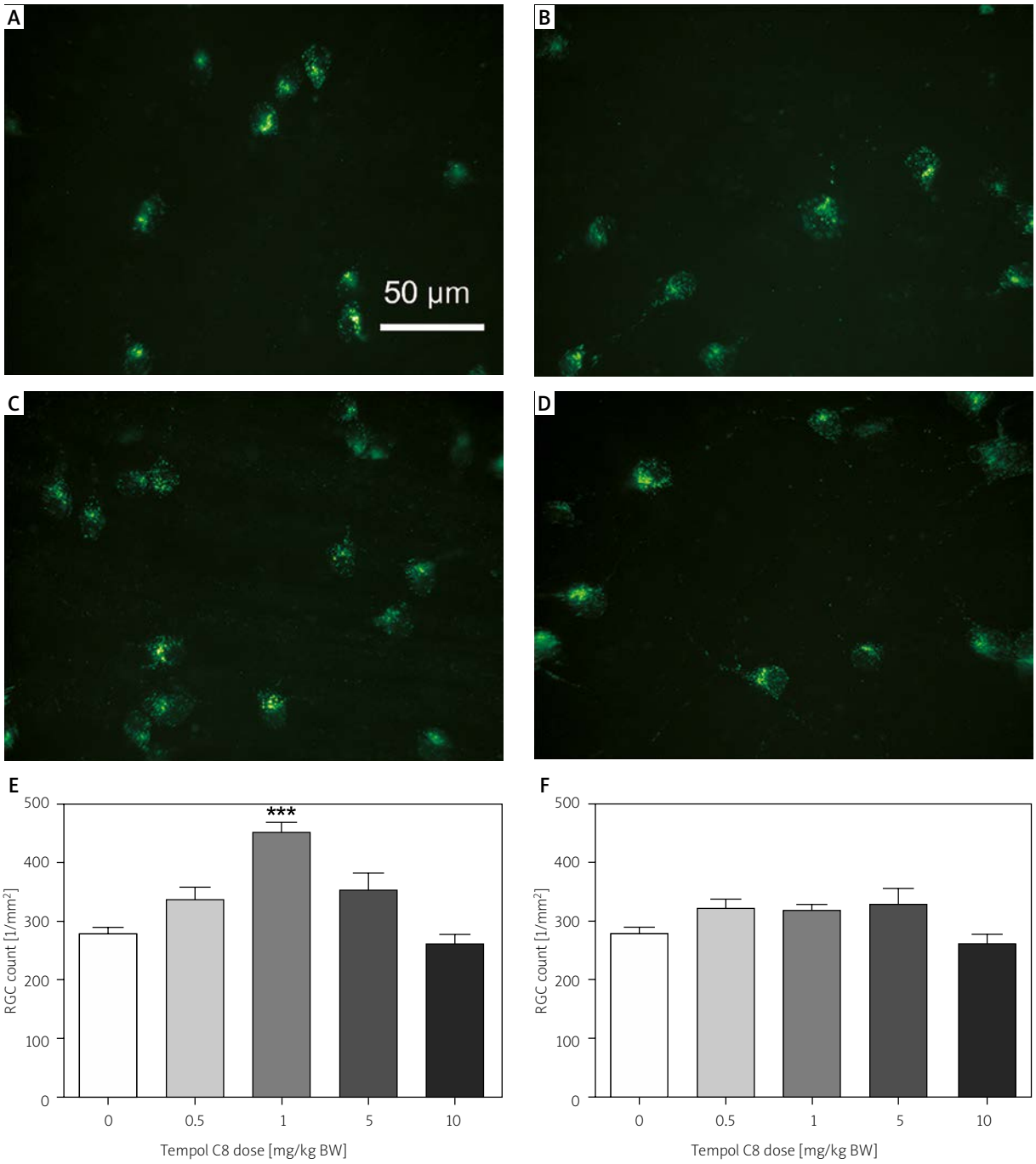

Fig. 2. Upper panel: Wholemounts of rat retinas treated with vehicle (**A, B**) or tempol-C8 1 mg/kg BW (**C, D**) in pre-adolescent (**A, C**) or young adult (**B, D**) animals. Lower panel: RGC numbers after administration of tempol-C8 at different concentrations in pre-adolescent (**E**) and young adult (**F**) animals. Tempol-C8 concentrations are given in molar equivalents of tempol. Numbers represent means ± SE. ***$p < 0.001$, Scale bar, 50 µm.

It is also well established that various receptors contribute to glutamate toxicity, depending on the developmental stage, as has been shown in cortical slices [19] and in RGC [2].

The age-dependent changes in excitotoxic insult vulnerability may be calcium-dependent [8]. Glutamate-induced calcium currents are similar in young and adult neurons from rat cortical slices [8] and

in isolated mouse RGC [11]. However, Mann *et al*. reported a dramatic difference in calcium buffering capacities between early postnatal and adult RGC. The difference seems to appear at the level of the mitochondria [13]. These differences are possibly due to the existence of cytosolic and mitochondrial nitric oxide synthase (NOS). Mitochondrial NOS mediates decreased vulnerability of young neurons to NMDA, and cytosolic NOS contributes to NMDA toxicity in mature neurons [11]. It may be of relevance that male rats display signs of sexual maturation between 40 and 60 days of age [4]; therefore our pre-adolescent rats presumably were sexually immature.

In our study, tempol-C8 was effective only in one of the tested doses, equivalent to tempol 1 mg/kg BW. It is known that SOD and its mimetics including tempol exert pro-oxidative effects in high doses (10^{-4}-10^{-2} M) [15]. Inefficacy of higher tempol doses may be analogous to the previously described decrease of SOD cytoprotective activity at higher levels of the enzyme [16].

In summary, we have shown that lipophilic tempol-C8 is a potent neuroprotectant in NMDA-induced RGC damage in rats, effective at a relatively low concentration, at which unmodified tempol is ineffective. However, the neuroprotective effect of tempol-C8 was found only in 6 weeks old, presumably sexually immature, rats. Whereas the issue of age dependency of free radical toxic effects on retinal ganglion cells needs further research, these results underscore the necessity of using older animals in experiments that model diseases with age as a significant risk factor.

Acknowledgements

M. Fiedorowicz received support from the Kerstan Foundation in the form of a research fellowship. S. Thaler and F. Schuettauf were supported by a grant from the Neuroophthalmologische Gesellschaft, Tübingen, Germany. M. Wozniak was supported by a grant from the Polish Ministry of Science within the project ref. ST46.

Disclosure

Authors report no conflict of interest.

References

1. Beit-Yannai E, Zhang R, Trembovler V, Samuni A, Shohami E. Cerebroprotective effect of stable nitroxide radicals in closed head injury in the rat. Brain Res 1996; 717: 22-28.
2. Cady C, Evans MS, Brewer GJ. Age-related differences in NMDA responses in cultured rat hippocampal neurons. Brain Res 2001; 921: 1-11.
3. Chaudhary P, Ahmed F, Sharma SC. MK801-a neuroprotectant in rat hypertensive eyes. Brain Res 1998; 792: 154-158.
4. Clark BR, Price EO. Sexual maturation and fecundity of wild and domestic Norway rats (Rattus norvegicus). J Reprod Fertil 1981; 63: 215-220.
5. El-Remessy AB, Khalil IE, Matragoon S, bou-Mohamed G, Tsai NJ, Roon P, Caldwell RB, Caldwell RW, Green K, Liou GI. Neuroprotective effect of (-)Delta9-tetrahydrocannabinol and cannabidiol in N-methyl-D-aspartate-induced retinal neurotoxicity: involvement of peroxynitrite. Am J Pathol 2003; 163: 1997-2008.
6. Fink MP, Macias CA, Xiao J, Tyurina YY, Delude RL, Greenberger JS, Kagan VE, Wipf P. Hemigramicidin-TEMPO conjugates: novel mitochondria-targeted antioxidants. Crit Care Med 2007; 35: S461-S467.
7. Hahn SM, Sullivan FJ, DeLuca AM, Bacher JD, Liebmann J, Krishna MC, Coffin D , Mitchell JB. Hemodynamic effect of the nitroxide superoxide dismutase mimics. Free Radic Biol Med 1999; 27: 529-535.
8. Kannurpatti SS, Sanganahalli BG, Mishra S, Joshi PG, Joshi NB. Glutamate-induced differential mitochondrial response in young and adult rats. Neurochem Int 2004; 44: 361-369.
9. Lam TT, Siew E, Chu R, Tso MO. Ameliorative effect of MK-801 on retinal ischemia. J Ocul Pharmacol Ther 1997; 13: 129-137.
10. Li Y, Schlamp CL, Nickells RW. Experimental induction of retinal ganglion cell death in adult mice. Invest Ophthalmol Vis Sci 1999; 40: 1004-8.
11. Mann M, Haq W, Zabel T, Guenther E, Zrenner E, Ladewig T. Age-dependent changes in the regulation mechanisms for intracellular calcium ions in ganglion cells of the mouse retina. Eur J Neurosci 2005; 22: 2735-2743.
12. Marks JD, Boriboun C, Wang J. Mitochondrial nitric oxide mediates decreased vulnerability of hippocampal neurons from immature animals to NMDA. J Neurosci 2005; 25: 6561-6575.
13. Marks JD, Bindokas VP, Zhang XM. Maturation of vulnerability to excitotoxicity: intracellular mechanisms in cultured postnatal hippocampal neurons. Brain Res Dev Brain Res 2000; 124: 101-116.
14. Mitchell JB, Samuni A, Krishna MC, DeGraff WG, Ahn MS, Samuni U, Russo A. Biologically active metal-independent superoxide dismutase mimics. Biochemistry 1990; 29: 2802-2807.
15. Offer T, Russo A, Samuni A. The pro-oxidative activity of SOD and nitroxide SOD mimics. FASEB J 2000; 14: 1215-1223.
16. Omar BA, Gad NM, Jordan MC, Striplin SP, Russell WJ, Downey JM, McCord JM. Cardioprotection by Cu,Zn-superoxide dismutase is lost at high doses in the reoxygenated heart. Free Radic Biol Med 1990; 9: 465-471.
17. Rejdak R, Zarnowski T, Turski WA, Kocki T, Zagorski Z, Zrenner E, Schuettauf F. Alterations of kynurenic acid content in the retina in response to retinal ganglion cell damage. Vision Res 2003; 43: 497-503.
18. Rosales MA, Silva KC, Lopes de Faria JB, Lopes de Faria JM. Exogenous SOD mimetic tempol ameliorates the early retinal changes reestablishing the redox status in diabetic hypertensive rats. Invest Ophthalmol Vis Sci 2010; 51: 4327-4336.

19. Sanganahalli BG, Joshi PG, Joshi NB. NMDA and non-NMDA receptors stimulation causes differential oxidative stress in rat cortical slices. Neurochem Int 2006; 49: 475-480.
20. Schuettauf F, Vorwerk C, Naskar R, Orlin A, Quinto K, Zurakowski D, Dejneka NS, Klein RL, Meyer EM, Bennett J. Adeno-associated viruses containing bFGF or BDNF are neuroprotective against excitotoxicity. Curr Eye Res 2004; 29: 379-386.
21. Tezel G, Yang X. Caspase-independent component of retinal ganglion cell death, in vitro. Invest Ophthalmol Vis Sci 2004; 45: 4049-4059.
22. Thaler S, Fiedorowicz M, Grieb P, Wypych Z, Knap N, Borowik T, Zawada K, Kaminski J, Wozniak M, Rejdak R, Zrenner E, Schuettauf F. Neuroprotective effects of tempol acyl esters against retinal ganglion cell death in a rat partial optic nerve crush model. Acta Ophthalmol 2011; 89: e555-e560.
23. Thaler S, Choragiewicz TJ, Rejdak R, Fiedorowicz M, Turski WA, Tulidowicz-Bielak M, Zrenner E , Schuettauf F, Zarnowski T. Neuroprotection by acetoacetate and beta-hydroxybutyrate against NMDA-induced RGC damage in rat-possible involvement of kynurenic acid. Graefes Arch Clin Exp Ophthalmol 2010; 248: 1729-1735.
24. Thaler S, Fiedorowicz M, Rejdak R, Choragiewicz TJ, Sulejczak D, Stopa P, Zarnowski T, Zrenner E, Grieb P, Schuettauf F. Neuroprotective effects of tempol on retinal ganglion cells in a partial optic nerve crush rat model with and without iron load. Exp Eye Res 2010; 90: 254-260.
25. Thaler S, Rejdak R, Dietrich K, Ladewig T, Okuno E, Kocki T, Turski WA , Junemann A, Zrenner E, Schuettauf F. A selective method for transfection of retinal ganglion cells by retrograde transfer of antisense oligonucleotides against kynurenine aminotransferase II. Mol Vis 2006; 12: 100-107.
26. Wang M, Lam TT, Fu J, Tso MO. TEMPOL, a superoxide dismutase mimic, ameliorates light-induced retinal degeneration. Res Commun Mol Pathol Pharmacol 1995; 89: 291-305.
27. Wright MV, Kuhn TB. CNS neurons express two distinct plasma membrane electron transport systems implicated in neuronal viability. J Neurochem 2002; 83: 655-664.

Folia Neuropathologica

Adult sublingual schwannoma with angioma-like features and foam cell vascular change

Sarah Taconet[1,2], Philippe Gorphe[3], Adriana Handra-Luca[1,2]

[1]Universite Paris Nord Sorbonne Cite, Bobigny, [2]Service d'Anatomie Pathologique, APHP Avicenne, Bobigny, [3]Service Oto-Rhino-Laryngologie et Chirurgie Cervico-Faciale, APHP Avicenne, Bobigny, France

All authors contributed equally and should be considered as first author.

Folia Neuropathol 2014; 52 (3): 298-302 DOI: 10.5114/fn.2014.45571

Abstract

Schwannomas are benign, slow-growing neoplasms of the neural sheaths. They occur rarely in a sublingual location; 9 cases have been reported to our knowledge. We aimed to report the case of a sublingual schwannoma with peculiar morphological features. A 23-year-old woman presented for a right sublingual mass, clinically diagnosed as a vascular malformation. A pleomorphic adenoma was suggested by cytology examination. The diagnosis of schwannoma was made on the resected specimen. The tumour, measuring 4.1 cm, showed several angioma-like vessel agglomerates and macrophage thickening of the intratumour vessel wall. Tumour cells expressed diffusely S100 protein, as well as CD56 and podoplanin. In conclusion, we report the case of a sublingual schwannoma, of peculiar morphology, with presence of pseudo-angioma aggregates and foam cell thickening of the vessel wall, features which were of clinical relevance.

Key words: *schwannoma, salivary gland, sublingual, differential diagnosis, angioma, macrophage, podoplanin/D2.40, NCAM/CD56, CD68.*

Introduction

Schwannomas are benign slow-growing neoplasms of the neural sheaths. They occur rarely in a sublingual location; 9 cases have been reported to our knowledge [1,3,6,7,9,10,12-15]. In only one of the reported cases the schwannoma was intraglandular [10]. The diagnosis is made on the surgical specimen, after surgical resection, possibly due to their rarity in this setting and to nonspecific clinical complaints [1,3,6,7,9,10,12-15]. Similarly to schwannomas in other locations, tumour cells express the S100 protein, neuron-specific enolase, and vimentin [13].

We report a case of a sublingual schwannoma, peculiar by the presence of angioma-like vessel agglomerates and macrophage thickening of the intratumour vascular wall.

Case report

A 23-year-old woman presented with a 2-year history of a slow-growing mass of the right sublingual space, clinically diagnosed as a vascular malformation. Clinical examination revealed a firm, mobile mass. There was no adenopathy or nerve deficit. Familial and personal medical histories did not reveal any disease except concomitant cystitis.

Communicating author:
Adriana Handra-Luca, MD, PhD, Service d'Anatomie Pathologique, APHP Avicenne, Universite Paris Nord Sorbonne Cite, 125, rue de Stalingrad, 93000 Bobigny, France, phone: +33 1 48955555, ext. 2047/5601, fax: +33 1 48955602, e-mail: adriana.handra-luca@avc.aphp.fr

At ultrasound examination, there was a heterogeneous, well-limited and well-vascularised sublingual mass. On magnetic resonance imaging (MRI), the tumour was located in the anterior third of the mouth floor, in a sublingual location, pushing the submandibular gland and the mylohyoid muscle, and in contact with the right horizontal branch of the mandible. The tumour was heterogeneous with central zones of T2 hypersignal. A moderate heterogeneous increase occurred after gadolinium injection. Fine-needle aspiration cytology analysis showed non-specific microscopic aspects with abundant haemorrhage, eosinophilic material, lymphocytes and epithelial-like cells. The suggested diagnosis was pleomorphic adenoma. The tumour with the contacting right submandibular gland was surgically resected. Perioperatively, the tumour was well limited by a capsule, of firm consistency. The hypoglossal and lingual nerves did not show direct attachment to the tumour, and were preserved.

Macroscopically, the tumour was well limited, encapsulated and measured 4.1 × 3.5 × 3.5 cm. At microscopic examination, this tumour consisted of proliferating spindle cells, with frequent dense cellular zones of palisading of Antoni A pattern, and rarely with epithelioid features (Fig. 1). Cells showed nuclear atypia with a conserved nuclear : cytoplasmic ratio. Vessels were numerous, focally densely packed in multiple clusters without interspersed tumour cells, with a pseudo-angioma pattern, randomly disposed within the tumour (Fig. 1). Most vessels were thin walled, of capillary type, large, medium and small sized or having a cavernomatous aspect. Several haemorrhagic zones were also observed. Hyaline vascular parietal change was rare, as were reactive lymphocytes. Several thin-walled vessels, mainly medium-sized vessels, showed thrombosis. Some of these vessels, as well as several non-thrombotic thin-walled medium- or small-sized vessels, contained layers of subendothelial foamy macrophages (Fig. 1). In the latter vessels, the endothelial lining was continuous, focally hyperplastic/regenerative. Small sheets of foamy macrophages were observed, less frequently between tumour cells, mainly in oedematous zones. These foamy cells did not contain haemosiderin pigment. Submandibular gland parenchyma was normal, without vascular abnormality, with several millimetric sebaceous foci. Salivary gland lobules were present in a pericapsular location. At 6 months post-operatively, the patient was well, without recurrence, other tumour or nerve deficit.

An immunohistochemical study on tumour tissue sections was performed with XT Benchmark and Benchmark Ventana automates (avidin-biotin complex method) with antibodies directed against the following proteins: calretinin (Dako, clone DAK Calret1, 1/100), CD31 (Dako, clone JC70A, 1/20), CD34 (Dako, QBEnd-10, dilution 1/25), CD56 (Novocastra, NCL-L-CD56-1B6, dilution 1/100), CD68 (Dako, clone PG-M1, dilution 1/50), podoplanin (Dako, clone D2-40, dilution 1/100), CD117 (Novocastra, NCL-L-CD117, dilution 1/40), chromogranin (Dako, clone DAK-A3, dilution 1/200), cytokeratin AE1/3 (Dako, clone AE1/AE3, dilution 1/100), desmin (Dako, clone D33, dilution 1/100), EMA (Dako, clone E29, dilution 1/50), neuron-specific enolase (Dako, clone BBS/NC/VI-H14, dilution 1/400), S100 protein (Dako, polyclonal, dilution 1/1500), smooth muscle actin (Dako, clone 1A4, 1/400), and synaptophysin (Dako, clone SY38, dilution 1/20).

Tumour cells expressed the S100 protein (Fig. 1), neuron-specific enolase diffusely, as well as synaptophysin. We also observed focal, cytoplasmic tumour cell expression of podoplanin, CD56 and CD68. The CD31 was expressed in the endothelial lining of intratumour vessels (Fig. 1), which showed focally an irregular layer of smooth muscle actin positive cells. Desmin was expressed only in the wall of sparse, large vessels in the pericapsular tumour zone. Podoplanin was expressed very focally in the lining cells of a cavernomatous space. Subendothelial foamy macrophages, as well as macrophages in xanthomatous foci, strongly expressed CD68. They also expressed CD31, less intensely than endothelial cells (Fig. 1).

Discussion

We report the case of a schwannoma of rare location, sublingual, showing several morphological peculiarities of clinical relevance, this tumour being unusual due to the presence of angioma-like aggregates and subendothelial foamy macrophage accumulations.

Schwannomas are benign tumours, extremely rare in a sublingual location, 9 cases being reported since 1960 to our knowledge [1,3,6,7,9,10,12-15] (Table I). In the 8 reported cases with available data for review, there is a female gender prevalence of 5 : 3 (women : men). Patient's median age is 52 years,

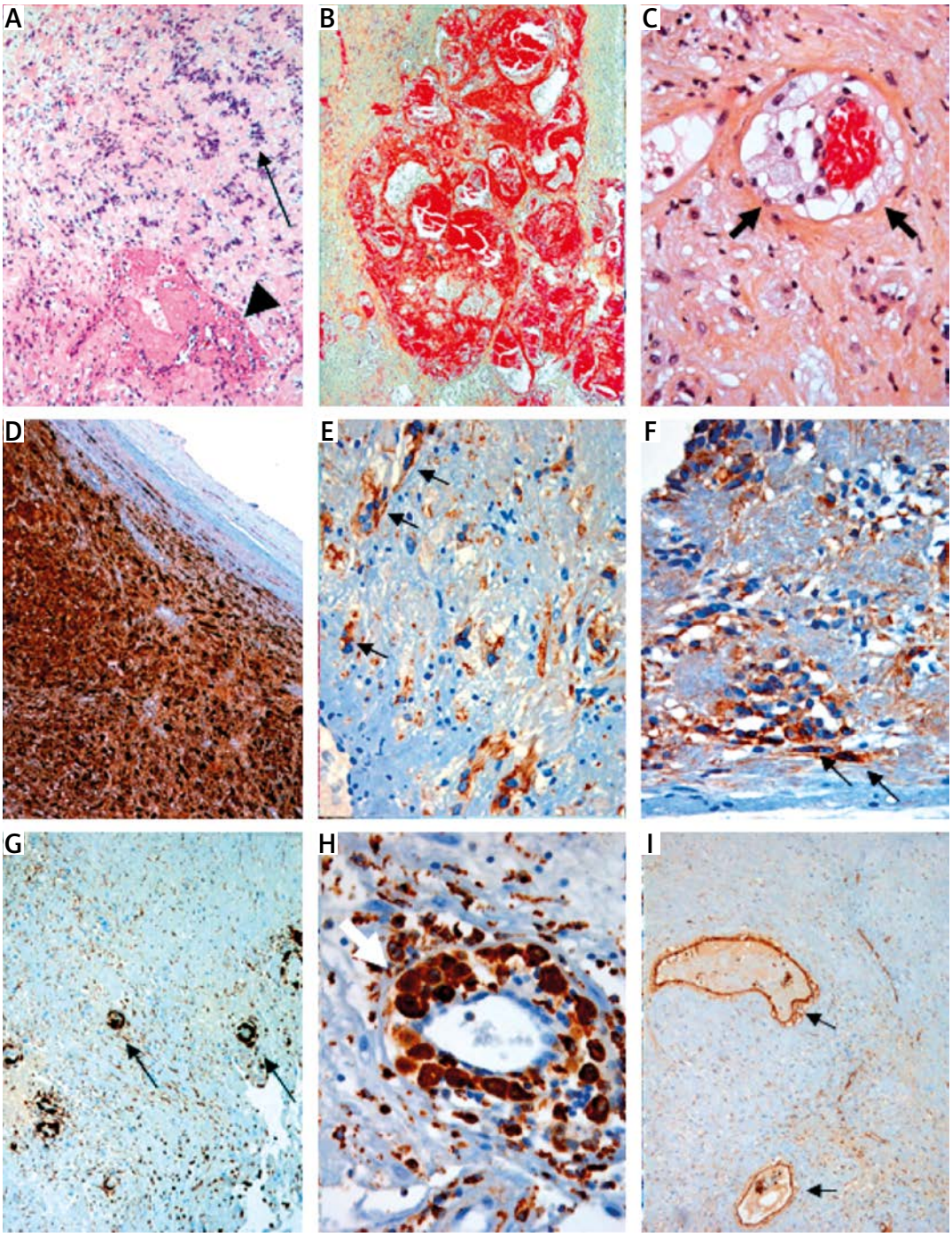

Fig. 1. Microscopic features of sublingual schwannoma. The tumour showed palisading Antoni A zones with spindle cells (**A** – arrow, haematoxylin and eosin stain, original magnification ×10) and thrombosis in vascular cavities (**A** – arrowhead). Intratumour angioma-like vascular aggregates composed of several thin-walled vessels were also observed (**B** – haematoxylin and eosin stain, original magnification ×10). Tumour cells expressed diffusely the S100 protein (**D** – original magnification ×20) and focally CD56 (**E** – arrows, original magnification ×40) and podoplanin (**F** – arrows, original magnification ×40). Foamy macrophages (**C** – arrows, haematoxylin and eosin stain ×40), CD68 positive were observed in the vessel wall, in subendothelial location (**G** – arrows, original magnification ×20, and **H**, original magnification ×40). Endothelial cells were strongly positive for CD31, which was also expressed by subendothelial macrophages, less intensely (**I** – arrows, original magnification ×10).

Table I. Reported cases of sublingual schwannomas

Author, year	Age	Gender	Tumour size (cm)	Nerve of origin	Cytology diagnosis	Peculiarity
Okada, 2012 [10]	70	female	2.3	NI		
Pattani, 2010 [12]	63	male	4.4	mylohyoid nerve	pleomorphic adenoma	
Kawakami, 2004 [6]	49	female	3.2	lingual nerve		cystic degeneration
Arda, 2003 [1]	34	female	5	sublingual nerve	inconclusive	
Ogawa, 2001 [9]	72	female	5.3	hypoglossal nerve		multifocal tumour
Drevelengas, 1998 [3]	55	male	4.5	hypoglossal nerve		
Lee, 1994 [7]	20	female	5	NI		
Sengupta, 1975 [14]	NA	NA	NA	NA		
Swanson, 1960 [15]	20	male	12	NI	non-contributory	multifocal tumour

NA – non-available, NI – non-identifiable

ranging from 20 to 72 years. Only 2 patients were younger than 25 years, similarly to our patient. In the reported cases, the lesion was painless and treatment consisted of surgery. The diagnosis of schwannoma was made after the resection specimen analysis. The median tumour size was of 4.75 cm, varying between 2.3 [10] and 12 cm [15]. Rarely tumours can be multifocal/multinodular [10,15]. The nerve of origin remains relatively frequently unidentified, in the reported sublingual schwannomas in 3 out of the 8 cases with available data (Table I). Similarly to the case reported by Pattani *et al*. [12], the nerve of origin in our case was probably the mylohyoid nerve, although we did not detect a direct connection to the tumour, as they did. In our case, this hypothesis was sustained by the lack of hypoglossal palsy, of dry mouth and change in salivary flow. Moreover, the hypoglossal and lingual nerves appeared normal at preoperative examination.

The presence of several intratumour angioma-like vessel aggregates along with the fibrous, oedematous change and haemorrhage were of clinical relevance, the tumour being initially diagnosed clinically as a vascular malformation. Moreover, presence of a prominent intratumour vascular component is related to an increased haemorrhagic risk at fine needle aspiration or operative manipulation [5]. The origin of such an intratumour vascular component is still debated as to whether it is of angioma or malformation type, part of a composite tumour or of angioma-like vascular change in the stroma [5].

Interestingly, in both our case and the sublingual schwannoma reported by Pattani *et al*. [12], the preoperative cytological features suggested a pleomorphic adenoma. The MRI features may also suggest a pleomorphic adenoma [7]. In all these cases of sublingual schwannoma, only the standard histological examination of the surgically resected tumour allowed the precise tumour type to be established and the schwannoma diagnosed.

The present case was unusual not only due to the presence of pseudoangiomatous vascular aggregates but also due to the presence of intratumour vascular lesions. These lesions consisted of an accumulation of subendothelial, CD68-positive, xanthomatous, foamy macrophages. Rarely such cells formed small sheets between tumour cells, described as related to long evolution of degenerative changes. To our knowledge, in the English language medical literature, presence of intratumour xanthomatous foci has been specifically reported in a few intracranial schwannomas as well as in two extracranial schwannomas, of perihepatic and thoracic locations [2,8]. Patients did not have a history of metabolic condition but had contrast substance injection for imaging procedures, similarly to our patient. The subendothelial accumulations of macrophages we have observed in our case are peculiar, but possibly belong to the same spectrum of such xanthomatous

lesions. The hypothesis of a contrast-substance vascular reaction is sustained by the presence, in some of the vessels, of focal disruption and damage of the vascular endothelial lining with thrombosis, by the lack of personal or familial history of metabolic disease, and by the lack of similar deposits in the normal submandibular gland that we could examine. However, we cannot completely eliminate the possibility of degenerative changes related to a long evolution of the tumour or changes related to fine needle puncture. Abundant xanthomatous changes may result in intratumour heterogeneity on the CT scan, similarly to other schwannoma changes such as cellularity, cystic degeneration or collagen deposition [8].

Although eight cases of sublingual schwannomas have been reported, only three have been studied for S100 protein [1,3,7], one of which has also been studied for neuron specific enolase, vimentin and Ki67 [1]. Tumour cells in our case expressed the S100 protein and neuron-specific enolase. Interestingly, we also observed focal tumour expression of CD56 and of podoplanin, both proteins having been already reported in schwannomas of other location [11]. While CD56 interferes with calcium-independent homophilic cell-cell binding [11], the role of podoplanin-positive schwannoma tumour cells remains incompletely understood, possibly interfering with occurrence of oedema. Indeed this protein has been reported to interfere with the regulation of inner ear fluid pressure of D2.40 positive periductal connective tissue cells [4].

In conclusion, we report a rare case of sublingual schwannoma, peculiar due to stromal angioma-like features, which might be relevant for clinical and imaging preoperative diagnosis.

Acknowledgements

We thank Isabelle Alexandre, Emilie Weber, Viviane Bodiguel, Emmanuel Sauce, and Didier Dunghi for technical and administrative support as well as Dr. Marcela Albiter, Dr. Claude Bigorne, Dr. Frederique Larousserie and Prof. Anne Couvelard for constructive discussion. The authors thank Pascal Cusenier for help with reference research.

Disclosure

Authors report no conflict of interest.

A new case of sublingual schwannoma occuring in an adult patient (Yamamoto et al.) was published since the acceptance of this manuscript.

References

1. Arda HN, Akdogan O, Arda N, Sarikaya Y. An unusual site for an intraoral schwannoma: A case report. Am J Otolaryngol 2003; 24: 348-350.
2. Cohen LM, Schwartz AM, Rockoff SD. Benign schwannomas: pathologic basis for CT inhomogeneities. AJR Am J Roentgenol 1986; 147: 141-143.
3. Drevelengas A, Kalaitzoglou I, Lazaridis N. Sublingual hypoglossal neurilemmoma. Case report. Aust Dent J 1998; 43: 311-314.
4. Hultgård-Ekwall AK, Mayerl C, Rubin K, Wick G, Rask-Andersen H. An interstitial network of podoplanin-expressing cells in the human endolymphatic duct. J Assoc Res Otolaryngol 2006; 7: 38-47.
5. Kasantikul V, Netsky MG. Combined neurilemmoma and angioma. Tumor of ectomesenchyme and a source of bleeding. J Neurosurg 1979; 50: 81-87.
6. Kawakami R, Kaneko T, Kadoya M, Matsushita T, Fujinaga Y, Oguchi K, Kurashina K. Schwannoma in the sublingual space. Dentomaxillofac Radiol 2004; 33: 259-261.
7. Lee ES, Choi SC, Park TW, You DS. Schwannoma of the sublingual gland. Korean J Oral Maxillofacial Surg 1994; 24: 461-467.
8. Nagafuchi Y, Mitsuo H, Takeda S, Ohsato K, Tsuneyoshi M, Enjoji M. Benign schwannoma in the hepatoduodenal ligament: report of a case. Surg Today 1993; 23: 68-72.
9. Ogawa T, Kitagawa Y, Ogasawara T. A multifocal neurinoma of the hypoglossal nerve with motor paralysis confirmed by electromyography. Int J Oral Maxillofac Surg 2001; 30: 176-178.
10. Okada H, Tanaka S, Tajima H, Akimoto Y, Kaneda T, Yamamoto H. Schwannoma arising from the sublingual gland. Ann Diagn Pathol 2012; 16: 141-144.
11. Park JY, Park H, Park NJ, Park JS, Sung HJ, Lee SS. Use of calretinin, CD56, and CD34 for differential diagnosis of schwannoma and neurofibroma. Korean J Pathol 2011; 45: 30-35.
12. Pattani KM, Dowden K, Nathan CO. A unique case of a sublingual-space schwannoma arising from the mylohyoid nerve. Ear Nose Throat J 2010; 89: E31-33.
13. Rosai J. Rosai and Ackerman's Surgical Pathology. 10th ed. Elsevier Sanders Mosby, New York 2011.
14. Sengupta P, Sarkar SK, Niyogi SK. Sublingual neurilemmoma. J Indian Med Assoc 1975; 64: 238-240.
15. Swanson AE, White JB. The unusual occurrence of a large sublingual neurilemmoma. Oral Surg Oral Med Oral Pathol 1960; 13: 1163-1166.

The 12th International Symposium

MOLECULAR BASIS OF PATHOLOGY AND THERAPY IN NEUROLOGICAL DISORDERS

November 20-21, 2014

Warsaw, Poland

ORGANIZERS

Mossakowski Medical Research Centre, Polish Academy of Sciences,
Polish Academy of Sciences, Division V Medical Sciences,
Committee of Physiological and Pharmacological Sciences
and Committee of Neurobiology

SCIENTIFIC COMMITTEE

Elzbieta Salinska-Chairperson
Leonora Buzanska
Krystyna Domanska-Janik
Jerzy Lazarewicz
Andrzej W. Lipkowski
Barbara Lukomska
Lidia Struzynska
Barbara Zablocka
Teresa Zalewska
Magdalena Zielinska

MAZOWIECKI KLASTER PEPTYDOWY

Projekt współfinansowany przez Unię Europejską, ze środków Europejskiego Funduszu Rozwoju Regionalnego
w ramach Regionalnego Programu Operacyjnego Województwa Mazowieckiego 2007-2013.

SPONSORS:

ANIMA LAB
wyposażenie zwierzętarni i laboratoriów • modele zwierzęce

biogenet

BIOKOM
www.biokom.com.pl

BIO-RAD

CELLLAB

eppendorf

IMMUNI
WWW.IMMUNIQ.PL

Lab-JOT®


SYMBIOS LIFE SCIENCES

WYATT
TECHNOLOGY EUROPE

ZEISS

The growth and regeneration of axons: an *in vitro* model for studying interactions in 3D

Gerardo-Nava J.[1], Hodde D.[1], Katona I.[1], Bozkurt A.[2], Grehl T.[3], Steinbusch H.W.M.[4], Weis J.[1], Brook G.A.[1]

[1]Institute of Neuropathology, Uniklinik RWTH Aachen, Aachen 52074, Germany
[2]Department of Plastic, Hand and Burns Surgery, Uniklinik RWTH Aachen University, Aachen, Germany
[3]Department of Neurology, Ruhr-University Bochum, BG-Kliniken Bergmannsheil GmbH, Bochum 44789, Germany
[4]Department of Translational Neuroscience, Maastricht University Medical Center, Maastricht, The Netherlands

Investigations of the factors influencing mammalian axonal growth and regeneration are currently addressed using a range of *in vitro* and *in vivo* models. The *in vitro* models often employ relatively simple 2D culture systems (or the more recent development of axon diodes in micro-fluidics [5,6]) and present the advantage of ready access, manipulation and visualization of the axons and the environment in which they are growing. The *in vivo* models employ relatively expensive laboratory animals and present the advantage of studying axon growth in a more natural 3D environment of supporting cells and extracellular matrix. Our earlier *in vitro* attempts to demonstrate the support of axon regeneration by 3D bioengineered scaffolds involved the use of explanted dorsal root ganglia (DRG) obtained from adult rats [2,3]. This approach has been useful for demonstrating the influence of the scaffold on the properties of glial cell adhesion, proliferation, migration and process extension as well as on axon regeneration and orientation of growth. However, such studies were limited sensory neurons which are easy to dissect and can be maintained in culture for extended periods of time. However, patterns of DRG axonal growth do not necessarily reflect those that may be demonstrated would be expected by motor axons: differences in axonal growth between the motor and sensory neurons (in both *in vivo* and *in vitro* models) have been demonstrated by others in response to specific cellular and molecular cues, including differences when presented with environments containing a range of growth factors [1]. Such differences highlight the value of assays capable of evaluating neuron subtype-specific responses to their environment. Here, we describe the use of the *in vitro* organotypic spinal cord slice preparation for the investigation of motor axon regeneration from early post natal (P7-P9) rat pups and demonstrate the influence of scaffold microstructure on the trajectories the axons (for a complete description see Gerardo-Nava and colleagues [4]). To date, *in vitro* investigations of such motor axon-3D scaffold interactions remain poorly characterized, largely due to the difficulties of culturing motor neurons (MN) for extended periods *in vitro*. The organotypic spinal cord slice preparation has the advantage of studying motoneurons in a relatively normal cellular niche of the ventral horn gray matter in which their survival and axonal regeneration can be maintained for many weeks or even months.

The rat pup spinal cords were rapidly isolated in ice-cold Gey's balanced salt solution and the dura mater and superficial blood vessels carefully removed. The lumbar spinal cord was sectioned transversely (350 µm thick) with a McIlwain tissue chopper and the slices transferred to Millicell membrane inserts where previously dissected ventral roots or biomaterials (fibrin hydrogel or orientated collagen scaffold, Matricel GmbH) could be carefully apposed to the ventral surface of the slices (as described by Vyas and colleagues [7]). The preparations were then maintained in an incubator at 37°C with 5% CO_2.

Myelin clearance within the explanted ventral roots was rapid with the events following a similar pattern to that already described for Wallerian degeneration *in vivo*. By 7-14 days in culture, axons regenerated for substantial distances along the explanted nerve root, with most axons following a trajectory within the root itself. The interactions between regenerating motor axons and Schwann cells revealed different stages of maturity from simple, initial axon-Schwann cell contacts, to the ensheathment and the formation of compact myelin surrounded by basal lamina. A similar sequence of events could also be seen within the longitudinally orientated porous framework of the collagen scaffold, however, these interactions took place between migrating Schwann cells (from the residual root stumps remaining at the ventral surface of the slice) and the regenerating motor axons which formed longitudinally orientated fascicles. Although similarly extensive Schwann cell migration and axon growth was also supported by the fibrin hydrogel, the trajectory of both cells and axons followed the surface of the hydrogel rather through it.

Although the organotypic spinal cord preparation is capable of reproducing many of the events taking place in PNS Wallerian degeneration with subsequent axonal regeneration, the model has clear limitations, including the lack of any functioning vasculature, an incomplete immune system and the absence of appropriate end organ targets for the regenerating motor axons. However, despite these limitations, the model affords a number of significant advantages over assays that attempt to employ cultures of freshly isolated embryonic motor neurons (or cells lines), or studies involving laboratory animals. These include the simplicity and ease of preparation, the length of time such preparations can be maintained and the financial and ethical benefits of reducing the number of animals required to perform such studies. The model thus represents, in our opinion, an excellent platform for inves-

tigating how regenerating motor axons interact with any 3D growth-promoting environment and can be used as a cost-effective means of screening or assaying bioengineered scaffolds or the mechanism of action of drugs and bioactive agents that modify axon growth and regeneration.

References

1. Allodi I, Guzmán-Lenis MS, Hernàndez J, Navarro X, Udina E. In vitro comparison of motor and sensory neuron outgrowth in a 3D collagen matrix. J Neurosci Methods 2011; 198: 53-61.
2. Bozkurt A, Brook GA, Moellers S, Lassner F, Sellhaus B, Weis J, Woeltje M, Tank J, Beckmann T, Fuchs P, Olde Damink L, Schügner F, Heschel I, Pallua N. In-vitro assessment of axonal growth using dorsal root ganglia (DRG) explants in a novel 3D collagen matrix. Tissue Engineering 2007; 13: 2971-2979.
3. Bozkurt A, Deumens R, Beckmann C, Olde Damink L, Schügner F, Heschel I, Selhaus B, Weis J, Jahnen-Dechent W, Brook GA, Pallua N. In vitro cell alignment obtained with a Schwann cell enriched microstructured nerve guide with longitudinal guidance channels. Biomaterials 2009; 30: 169-179.
4. Gerardo-Nava J, Hodde D, Katona I, Bozkurt A, Grehl T, Steinbusch HW, Weis J, Brook GA. Spinal cord organotypic slice cultures for the study of regenerating motor axon interactions with 3D scaffolds. Biomaterials 2014; 35: 4288-4296.
5. Kim Y, Karthikeyan K, Chirvi S, Dave DP. Neuro-optical microfluidic platform to study injury and regeneration of single axons. Lab Chip 2009; 9: 2576-2581.
6. Peyrin JM, Deleglise B, Saias L, Vignes M, Gougis P, Magnifico S, Betuing S, Pietri M, Caboche J, Vanhoutte P, Viovy JL, Brugg B. Axon diodes for the reconstruction of oriented neuronal networks in microfluidic chambers. Lab Chip 2011; 11: 3663-3673.
7. Vyas A, Li Z, Aspalter M, Feiner J, Hoke A, Zhou C, O'Daly A, Abdullah M, Rohde C, Brushart TM. An in vitro model of adult mammalian nerve repair. Exp Neurol 2010; 223: 112-118.

Use of induced pluripotent stem cells – derived neurons for disease modeling

Liszewska E.[1*], Rydz K.[1], Kotulska K.[2], Jozwiak S.[2], Jaworski J.[1*]

[1]International Institute of Molecular and Cell Biology, Warsaw, Poland
[2]The Children's Memorial Health Institute, Warsaw, Poland
*Correspondence should be addressed to eliszewska@iimcb.gov.pl, jaworski@iimcb.gov.pl

Yamanaka's breakthrough discovery of cell reprogramming, awarded with the Nobel Prize in Physiology or Medicine in 2012, showed that the fate of differentiated somatic cells is not definitively defined and can be changed [14,15]. Yamanaka's strategy relied on over expression of transcription factors required for pluripotency such as Oct4 (octamer-binding transcription factor 4), Klf4 (Krueppel-like factor 4), Sox2 (sex determining region Y-box 2), and c-Myc [14,15] in differentiated cells (e.g., fibroblasts). Cells modified in that way change their morphology to embryonic stem cell-like one, start expressing genes, normally only active in cells of the embryonic node, in the early stages of embryonic development and can be differentiated in all cell types characteristic of the three germ layers, including those that morphology and profile of protein produced resembled neurons. Therefore they were called induced pluripotent stem cells (iPSC).

While virus-based reprogramming technology is currently one of several options [1,17], it is still the most popular one and gives researchers an easy access to human cells that were previously unavailable or difficult to achieve, such as neural stem cells or different types of neurons [3,5,7,8,13]. In addition to reprogramming followed by differentiation, recently a new technology of direct change, both *in vitro* and *in vivo*, of differentiated cells (fibroblasts, astrocytes) to neurons (transdifferentiation) emerged [12,16]. An immediate consequence of these technologies was development of a number of cellular models of the nervous system diseases. These models are used both to explore the cellular mechanisms of these diseases and for the development of new pharmacological strategies as well as nuclease based correction of genetic defects.

Thus far, induced pluripotent stem cell-derived neurons (iPSC-N) and induced neurons (IN) have been already obtained from patients with several neurological disorders including neurodegenerative diseases (e.g., amyotrophic lateral sclerosis [ALS], Parkinson's [PD], Alzheimer's [AD] and Huntington's disease [HD], neurodevelopmental diseases (e.g., fragile X syndrome, Rett syndrome) and psychiatric disorders (e.g., schizophrenia) [3,5,7,8,13]. In majority of cases researchers' efforts focused on reproducing basic cellular features of selected diseases. Yet, in few cases new interesting observations concerning disease mechanism have been made and schizophrenia, ALS and PD can serve as good examples. Brennand *et al.* [2] using schizophrenic patients' iPSC-N revealed disturbed dendritic arbor morphology and decreased synaptic connectivity. In iPSC-N derived from ALS patients carrying mutations in *TDP-43* (*TAR DNA-binding protein 43*), Egawa *et al.* [6] discovered that changes in RNA metabolism likely underlay sensitivity of these cells to oxidative stress. Last but not least, Belmonte group discovered new feature of PD caused by *LRRK2* (*leucine-rich repeat kinase 2*) mutations, namely death of neuroprecursors, which may explain cognitive dysfunctions observed in course of PD [10]. It is worth stressing that most ambitious projects assume the use of iPSC-N to search for new drugs. Although this type of exploration requires testing hundreds of thousands of substances, pre-

viously published work focused on testing only a few substances at the same time [2,6,11]. Yet, it should be stressed that some of these studies brought interesting results, e.g. use of anacardic acid for protecting ALS-derived iPSC-N against arsenate induced cell death [6].

Among the diseases that have not been yet modeled with use of iPSC-N is Tuberous sclerosis (TSC). TSC is a developmental disease caused by mutations in genes encoding either hamartin or tuberin and manifested by tumor development, epilepsy and autism [4]. On the cellular level the major characteristic of this disease are hypertrophy and mTOR signaling hyperactivation [9]. While the hyperactivation of the mTOR pathway is considered as one of the major causes of the pathology it is not clear what molecular mechanisms downstream of this multitask homeostatic kinase are involved in TSC development. Using overexpression of Oct4, Klf4, Sox2 and c-Myc we established several iPSC lines from patients with mutations in *TSC1*, which were differentiated to iPSC-N (FENS Abstract, Volume 6, p093.06, 2012). The TSC patient-derived iPSC-N are characterized by hypertrophy, disturbed overall morphology and increased mTOR activity (e.g., increased phosphorylation of ribosomal protein S6). Thus, we show that these iPSC-N recapitulate major cellular defects observed in TSC patients and therefore can be used for further search for molecular mechanisms contributing to TSC development.

This work has been financed by ERA-NET NEURON/06/2011 "AMRePACELL" (co-financed by NCBiR) to JJ and Homing Plus programme (HOMING PLUS/2012-5/6) of the Foundation for Polish Science, cofinanced from the European Union under the European Regional Development Fund to EL.

References

1. Bayart E, Cohen-Haguenauer O. Technological overview of iPS induction from human adult somatic cells. Curr Gene Ther 2013; 13: 73-92.
2. Brennand KJ, Simone A, Jou J, Gelboin-Burkhart C, Tran N, Sangar S, Li Y, Mu Y, Chen G, Yu D, McCarthy S, Sebat J, Gage FH. Modelling schizophrenia using human induced pluripotent stem cells. Nature 2011; 473: 221-225.
3. Chailangkarn T, Acab A, Muotri AR. Modeling neurodevelopmental disorders using human neurons. Curr Opin Neurobiol 2012; 22: 785-790.
4. Curatolo P, Bombardieri R, Jozwiak S. Tuberous sclerosis. Lancet 2008; 372: 657-668.
5. Dolmetsch R, Geschwind DH. The human brain in a dish: the promise of iPSC-derived neurons. Cell 2011; 145: 831-834.
6. Egawa N, Kitaoka S, Tsukita K, Naitoh M, Takahashi K, Yamamoto T, Adachi F, Kondo T, Okita K, Asaka I, Aoi T, Watanabe A, Yamada Y, Morizane A, Takahashi J, Ayaki T, Ito H, Yoshikawa K, Yamawaki S, Suzuki S, Watanabe D, Hioki H, Kaneko T, Makioka K, Okamoto K, Takuma H, Tamaoka A, Hasegawa K, Nonaka T, Hasegawa M, Kawata A, Yoshida M, Nakahata T, Takahashi R, Marchetto MC, Gage FH, Yamanaka S, Inoue H. Drug screening for ALS using patient-specific induced pluripotent stem cells. Sci Transl Med 2012; 4: 145ra104.
7. Han SS, Williams LA, Eggan KC. Constructing and deconstructing stem cell models of neurological disease. Neuron 2011; 70: 626-644.
8. Koch P, Kokaia Z, Lindvall O, Brustle O. Emerging concepts in neural stem cell research: autologous repair and cell-based disease modelling. Lancet Neurol 2009; 8: 819-829.
9. Kwiatkowski DJ. Tuberous sclerosis: from tubers to mTOR. Ann Hum Genet 2003; 67: 87-96.
10. Liu GH, Qu J, Suzuki K, Nivet E, Li M, Montserrat N, Yi F, Xu X, Ruiz S, Zhang W, Wagner U, Kim A, Ren B, Li Y, Goebl A, Kim J, Soligalla RD, Dubova I, Thompson J, Yates J, 3rd, Esteban CR, Sancho-Martinez I, Izpisua Belmonte JC. Progressive degeneration of human neural stem cells caused by pathogenic LRRK2. Nature 2012; 491: 603-607.
11. Marchetto MC, Carromeu C, Acab A, Yu D, Yeo GW, Mu Y, Chen G, Gage FH, Muotri AR. A model for neural development and treatment of Rett syndrome using human induced pluripotent stem cells. Cell 2010; 143: 527-539.
12. Niu W, Zang T, Zou Y, Fang S, Smith DK, Bachoo R, Zhang CL. In vivo reprogramming of astrocytes to neuroblasts in the adult brain. Nat Cell Biol 2013; 15: 1164-1175.
13. Robinton DA, Daley GQ. The promise of induced pluripotent stem cells in research and therapy. Nature 2012; 481: 295-305.
14. Takahashi K, Tanabe K, Ohnuki M, Narita M, Ichisaka T, Tomoda K, Yamanaka S. Induction of pluripotent stem cells from adult human fibroblasts by defined factors. Cell 2007; 131: 861-872.
15. Takahashi K, Yamanaka S. Induction of pluripotent stem cells from mouse embryonic and adult fibroblast cultures by defined factors. Cell 2006; 126: 663-676.
16. Vierbuchen T, Ostermeier A, Pang ZP, Kokubu Y, Sudhof TC, Wernig M. Direct conversion of fibroblasts to functional neurons by defined factors. Nature 2010; 463: 1035-1041.
17. Zhou YY, Zeng F. Integration-free methods for generating induced pluripotent stem cells. Genomics Proteomics Bioinformatics 2013; 11: 284-287.

Biogenesis, transport and degradation of mitochondrial proteins

Chacinska A.

International Institute of Molecular and Cell Biology, Warsaw, Poland

Mitochondria play an important role in variety of metabolic and regulatory processes and their dysfunction leads to life threatening disorders. About 1000-1500 proteins are needed to build this essential organelle. The large majority of mitochondrial proteins is synthesized on the cytosolic ribosomes, and after completion of their synthesis must

be properly targeted to mitochondria. After synthesis, precursors of mitochondrial proteins are directed to the TOM complex and subsequently to specific mitochondrial import machineries that are responsible for their sorting. Proteins destined to the intermembrane space of mitochondria follow the mitochondrial intermembrane space import and assembly (MIA) pathway. The MIA pathway provides an efficient and redox-dependent mechanism for trapping substrate proteins in the intermembrane space of mitochondria. The cytosolic steps that precede mitochondrial import have not been well understood. We identified a role for the ubiquitin-proteasome system in the biogenesis of the intermembrane space proteins. The ubiquitin-proteasome system persistently removes a fraction of intermembrane space proteins under physiological conditions, acting as a negative regulator in the biogenesis of this class of proteins. Moreover, based on unbiased proteomic approaches, we discovered that mitochondria play a role in the regulation of cellular protein homeostasis.

Mechanisms of neuroprotection by ischemic preconditioning: synaptic and mitochondrial modifications

Perez-Pinzon M.

Department of Neurology, University of Miami, Miller School of Medicine, Miami, USA

Ischemic Preconditioning (IPC) has been shown to be a robust neuroprotective approach to protect against cerebral ischemia. IPC is modelled when tissues are exposed to mild ischemic insults and after a period of recovery they become highly resistant to a subsequent, more lethal ischemic insult. My laboratory has demonstrated that the ischemic tolerance that ensues following IPC occurs at the level of mitochondria and by modifications in synaptic function. Mitochondria are key players in ischemic/reperfusion injury hours to days following cerebral ischemia and thus an important target for IPC-induced neuroprotection. Excitotoxicity following cerebral ischemia plays a major role in the pathology that ensues following cerebral ischemia. This presentation will summarize several signaling pathways involved in mitochondrial and synaptic neuroprotection against ischemia following IPC.

These studies were supported by National Institutes of Health Grants NS45676-01, NS054147-01 and NS34773.

Two faces of ER stress-from cancer to neurodegenerative diseases

Piwocka K.[1], Kusio-Kobialka M.[1], Dudka-Ruszkowska W.[1], Brewinska-Olchowik M.[1], Krysa W.[2], Rakowicz M.[2], Stepniak I.[2], Sulek A.[2]

[1]Nencki Institute of Experimental Biology, Warsaw, Poland
[2]Institute of Psychiatry and Neurology, Warsaw, Poland

Endoplasmic reticulum (ER) is the site where proteins folding and assembly occurs. A number of stimuli, such as perturbations in calcium homeostasis or redox state, accumulation of misfolded proteins, glucose deprivation, and altered glycosylation disrupts ER homeostasis and induces ER stress. Mild chronic ER stress allows for adaptation and leads to permanent changes in cellular function and activation of pro-survival mechanisms, whereas excessive stress activates cell death execution. The balance between adaptation *versus* cell death has a tremendous physiological importance. The UPR (Unfolded Protein Response) activates three signaling branches participating in regulation between survival and apoptosis upon ER stress. Activation of the ER stress signalling can play an opposite role in cancer and neurodegenerative diseases. In cancer, activation of the UPR response plays predominantly a prosurvival and protective role, but can also correlate with induction of cell death. Previously, the cytoprotective function was mostly correlated with solid tumors. However, we showed that mild ER stress and one of the UPR branches are activated in chronic myeloid leukemia cells, and are connected with the disease progression and resistance to imatinib therapy. Attenuation of this pathway in CML cells led to inhibition of proleukemic signaling, apoptosis and increased sensitivity to imatinib. On the other hand, disturbed levels of endoplasmic reticulum stress (ER) markers were already observed in post-mortem brains, mouse models and cell cultures derived from patients with Alzheimer's (AD), Parkinson's or Huntington's disease (HD), highlighting the role of ER stress in the neurodegeneration. Moreover, targeting the UPR elements seems to be an interesting strategy to prevent loss of neurons. It was also reported that UPR proteins are activated in blood cells of AD patients, suggesting that peripheral cells may serve as a model to study the disease pathophysiology. In HD mutated huntingtin aggregates provoke ER stress and the UPR. We performed pilot studies to verify the hypothesis that level of some ER stress mediators may serve as a peripheral biomarker in HD patients, correlating to disease stage and number of CAG repetitions in carriers of CAG expansion in *HTT locus*. We assume that pathophysiological processes appear in HD prior to clinical manifestations, and this study was done to look for the biomarkers correlating to the disease

progression and indicators of the compensative mechanisms efficiency in asymptomatic subjects. Understanding the complexity of ER stress response in cancer and neurodegeneration is necessary and may help to improve current, and discover novel therapeutic strategies.

This work was supported by grants 2011/01/B/NZ3/02145 and 2013/10/E/NZ3/00673 from the National Science Centre in Poland.

Astrocytes ER Ca^{2+} signalling and its pathological relevance

Verkhratsky A.

The University of Manchester, Manchester, United Kingdom

The evolution of the central nervous system (CNS) resulted in an appearance of highly specialised neuronal networks optimised for rapid information transfer. In the course of this specialisation neuronal cells lost their metabolic independence and the ability to survive in the absence of homeostatic systems. These homeostatic systems, represented by neuroglia regulate all aspects of CNS function in physiological and pathological conditions. The neurological diseases should be therefore considered as primary gliopathologies, which determine the progression and outcome of neuropathological process. Glial function is intimately regulated by cellular calcium signalling that underlies the specific form of "glial calcium excitability". Glial Ca^{2+} signals are triggered by activation of multiple receptors, and are primarily driven by Ca^{2+} release from the endoplasmic reticulum. In this review we summarise the role of glial calcium signalling in various forms of pathological processes including neurological and psychiatric disorders and neurodegeneration.

Who is running your gut? The gut-brain axisin brain metastasis formation by polychlorinated biphenyls

Toborek M.

Department of Biochemistry and Molecular Biology, University of Miami School of Medicine, USA

The gut microbiome is a dynamic bacterial community that interacts with the host and closely relates to human health by regulating energy metabolism and immune functions. Each host has a unique composition of gut microbiota, which implies highly individual responses to environmental stressors and suggests a role for gut microbiota in future personalized health strategies. However, the influence of the microbiome on the toxicity of environmental pollutants and its role in risk assessment are largely unknown. In addition, there is an emerging interest in the role of behavioral factors in modulating toxicity of environmental pollutants. While the role of nutrition has been explored, the impact of exercise on the health effects of toxicants is not known. Because exercise can influence the outcomes of disorders known to be associated with alterations of the gut microbiome, we hypothesized that physical activity may affect the composition of the gut microbiota and thus influence the impact of environmental toxicants. In order to address this hypothesis, we investigated the effects of polychlorinated biphenyls (PCBs) and exercise on the composition and structure of the gut microbiome. In addition, we related these results to PCB-induced development of brain metastases [1,2]. Mice exercised voluntarily for 5 weeks, followed by the exposure to a mixture of environmentally relevant PCB congeners (PCB153, PCB138 and PCB180) for 48 h. The microbiome was assessed by determination of 16S rRNA. Oral exposure to PCBs disrupted the integrity of the gut barrier function and significantly altered the abundance of the gut microbiome primarily by decreasing the levels of Proteobacteria. The activity level correlated with a substantial shift in abundance, biodiversity, and microbiome composition. Importantly, exercise attenuated PCB-induced changes in the gut microbiome. Oral exposure to PCBs facilitated the development of brain metastases, the effects that was attenuated by exercise. This study provides the first evidence that oral exposure to PCBs can induce substantial changes in the gut microbiome, which may then influence their systemic toxicity. Importantly, these changes can be attenuated by behavioral factors, such as voluntary exercise.

References

1. Choi JJ, Eum SY, Rampersaud E, Daunert S, Abreu MT, Toborek M. Exercise attenuates PCB-induced changes in the mouse gut microbiome. Environ Health Perspect 2003; 121: 725-730.
2. Sipos E, Chen L, Andras IE, Wrobel J, Zhang B, Pu H, Park MS, Eum SY, Toborek M. Proinflammatory adhesion molecules facilitate polychlorinated biphenyl-mediated enhancement of brain metastasis formation. Toxicol Sci 2012; 126: 362-371.

Uptake and toxicity of metal containing nanoparticles in brain cells

Dringen R.

Centre for Biomolecular Interactions Bremen, University of Bremen, PO. Box 330440, D-28334 Bremen, Germany
Centre for Environmental Research and Sustainable Technology, University of Bremen, Leobener Straße, D-28359 Bremen, Germany

Metal-containing nanoparticles (NPs) have gained considerable interest during the last decade due to their exciting properties as antibacterial agents, for consumer products as well as for technical applications and diagnostics. Due to their frequent use, the likelihood that brain cells will encounter such NPs has strongly increased. To investigate potential adverse effects of NPs on brain cells, we have studied the biocompatibility, the uptake and the metabolism of metal-containing NPs such as iron oxide NPs (IONPs), copper oxide NPs (CuONPs) and silver NPs (AgNPs) on cultured primary brain cells. Cultured astrocytes, neurons and microglial cells accumulated IONPs efficiently in a time-, concentration- and temperature-dependent manner. However, despite of an accumulation of large amounts of iron in IONP-treated astrocytes and neurons, the viability of these brain cells was not compromised. In contrast, accumulated IONPs were toxic for microglial cells, most likely due to the rapid uptake and transfer of the IONPs into the lysosomal compartment which facilitates the liberation of iron ions from the accumulated particles. The presence of fetal calf serum in the incubation medium strongly decreased the rate of IONP uptake into brain cells. While some inhibitors of endocytotic pathways lowered IONP accumulation in serum-containing medium, these inhibitors did not affect the rapid IONP accumulation in serum-free conditions. Astrocytes that had been exposed to IONPs for only 4 h remained viable for up to 7 days, hardly releasing any iron during this incubation period and showed a transient appearance of reactive oxygen species and a strong upregulation of the iron storage protein ferritin. Similarly, AgNP-treated astrocytes were not compromised in their viability and increased their content of metal-storing metallothioneins. These data demonstrate that cultured brain astrocytes deal well even with large amounts of iron or silver that are accumulated as IONPs or AgNPs. In contrast, the treatment of cultured astrocytes with CuONPs caused severe oxidative stress-mediated toxicity that was prevented by copper chelators, suggesting that rapid liberation of copper from accumulated CuONPs is involved in the observed toxicity of these NPs to astrocytes. These data demonstrate that different brain cell types differ in their vulnerability to one type of metal-containing NPs and that NP toxicity on a given type of brain cells strongly depends on the content of applied NPs.

Impairment of glutamine/glutamate-γ-aminobutyric acid cycle in manganese toxicity in the central nervous system

Sidoryk-Wegrzynowicz M.

Cambridge Centre of Brain Repair, University of Cambridge, Cambridge, United Kingdom

Manganese (Mn) is an essential trace element that is required for maintaining the proper function and regulation of many biochemical and cellular reactions. Despite its essentiality, at excessive levels Mn is toxic to the central nervous system (CNS). The overdose accumulation of Mn in specific brain areas, such as the substantia nigra, the globus pallidus and the striatum, triggers neurotoxicity resulting in a neurological brain disorder, referred to as manganism. Mn toxicity is associated with the disruption of glutamine (Gln)/glutamate (Glu) GABA cycle (GGC). The GGC represents a complex process, since Gln efflux from astrocytes must be met by its influx in neurons. Mn toxicity is associated with the disruption of both of these critical points in the cycle. In cultured astrocytes, pre-treatment with Mn inhibits the initial net uptake of Gln in a concentration-dependent manner. Mn added directly to primary culture of astrocytes induces deregulation in the expression of SNAT3, SNAT2, ASCT2 and LAT2 transporters and significantly decreases in Gln uptake mediated by the transporting Systems N and ASC, and a decrease in Gln efflux mediated by Systems N, ASC and L. Further, Mn disrupts Glu transporting systems leading to both a reduction in Glu uptake and elevation in extracellular Glu levels. Interestingly, there appear to be common signaling targets of Mn in GGC cycling in glial cells. Namely, the PKC signaling is affected by Mn in glutamine and glutamate transporters expression and function. Additionally, Mn deregulates GS expression and activity. Those evidences could triggers depletion of glutamine synthesis/metabolism in glia cells and consequently diminish astrocytic-derived glutamine, while disruption of Glu removal/transport can mediate dyshomeostasis in neurotransmission of functioning neurons. Here we highlight the mechanistic commonalities inherent to Mn-neurotoxicity related to the astrocyte pathology and GGC impairment.

Cadmium as a pro-inflammatory factor. Chosen cadmium neurotoxicity issues

Olszowski T.

Department of Hygiene and Epidemiology, Pomeranian Medical University, Szczecin, Poland

Cadmium belongs to the environmental toxins that constitute nowadays a serious problem for public health. The aim of this paper is to summarize the existing state of knowledge on the effects of cadmium on selected inflammatory mediators and markers, such as NF-κB, AP-1, IL-6, TNF-α, IL-1β, IL-8, MPO, iNOS, MMPs, COX-2, PGE_2, ICAM-1, VCAM-1, PECAM-1 and CRP in humans and rodents, both *in vitro* and *in vivo*. Moreover, the results of the author's original research on the effects of cadmium on COX-1 and COX-2 gene, protein expression and enzymatic activity in THP-1 macrophages are presented. In addition, the literature review as regards the neurotoxic effects of cadmium in humans and rodents is discussed. The effects on oxidative stress, interference with calcium, interaction with other metals, the impact on neurotransmitters, apoptosis induction, estrogen-like effects and epigenetic modification may be the mechanisms underlying cadmium neurotoxicity.

New mechanisms of GPCRs function: regulation by protein-protein interaction

Georgoussi Z.

Institute of Biosciences and Applications, Laboratory of Cellular Signaling and Molecular Pharmacology, National Centre for Scientific Research "Demokritos", 15310 Ag. Paraskevi, Athens, Greece

Evidence has demonstrated that G protein coupled receptors (GPCRs) can physically interact with a variety of accessory proteins, confirming that signal transduction of these receptors is not restricted to heterotrimeric G protein activation. Such interactions can alter the effectiveness of agonist-driven cell signalling, determine the signals generated and alter the trafficking, targeting, fine tuning and cellular localization of these receptors by providing a scaffold that links the receptors to the cytoskeletal network (Georgoussi *et al.* 2013). Opioid receptors which belong to GPCRs modulate a variety of physiological responses in the nervous system through activation of a diverse array of effector systems ranging from adenylyl cyclase, ion channels to other signalling intermediates. Opioid administration causes activation of several transcription factors, including CREB, NF-κB, STAT3 and STAT5A/B (Tso and Wong 2003; Mazarakou and Georgoussi 2005; Georganta *et al.* 2010). Such parallel manifestations of opioid receptor function suggest that these receptors are involved in different signaling circuits that lead to alterations in target gene expression in a pleiotropic fashion.

In the present study emphasis will be given to unconventional interacting partners of the μ- and δ-opioid receptors opioid receptors such as the regulators of G protein signalling (RGS) proteins and STAT5B. Evidence will be presented on which RGS proteins opioid receptors interact; how RGS4 and RGS2 confer selectivity to the receptors to choose a specific subset of G proteins; how activation of opioid receptors result in recruitment of RGS proteins to the plasma membrane; and how RGS proteins exert a differential modulatory effect in ERK1,2 phosphorylation, agonist-driven inhibition of adenylyl cyclase and the internalization fate of opioid receptors. Moreover evidence will be presented on how STAT5B associates with the δ-opioid receptor and forms selective pairs with selective Gα and Gβγ subunits and RGS proteins; and how activation of the δ-opioid receptor with selective agonists promotes a multi-component signaling complex involving the STAT5B transcription factor and other signaling intermediates to mediate neuronal survival and neurite outgrowth. Understanding the mechanism of intercellular communication via G-protein-mediated signalling pathways in the nervous system is crucial for normal brain development and regulation of adult neural processes. Thus, defining the molecular determinants that control opioid receptor signaling is important to address problems related to phenomena such as pain perception, tolerance and dependence that occur upon chronic opiate administration and define whether disruption of such interactions may contribute to the pathophysiology of nervous system related disorders and to .the development of novel therapeutic strategies.

This work was supported by the EU «Normolife» (LSHC-CT2006-037733) and the GSRT, Excellence II grant 3722, "NO-ALGOS". Z.G participates in the European COST Action CM1207 (GLISTEN).

The role of opioid peptides under neuropathic pain

Mika J.

Department of Pain Pharmacology, Institute of Pharmacology, Polish Academy of Sciences, Cracow, Poland

Despite many advances, our understanding of the involvement of endogenous opioid peptides in the develop-

ment of neuropathic pain, is not fully understood. Many recent studies show, that microglia cells play a crucial role in the maintenance of neuronal homeostasis, therefore pain may now be considered as neuro-immune disorder. The microglial production of immune factors is believed to play an important role in nociceptive transmission and opioids effectiveness. Endogenous opioidergic neurotransmission is found throughout the brain and spinal cord and appears to influence many nervous system functions, including nociception. Paradoxaly opioids can induce both, analgesia and algesia. It has recently been hypothesized that the imbalance between the pro- and anti-nociceptive activity of peptides generated from opioid prohormones is leading to the development of chronic pain. Our studies show that minocycline reduced prodynorphin mRNA levels that were previously elevated in the spinal cord and/or dorsal root ganglia following sciatic nerve injury. Moreover, the repeated administration of minocycline enhanced the analgesic effects of low-dose dynorphin (0.15 nmol) and prevented the development of flaccid paralysis following high-dose dynorphin administration (15 nmol), suggesting a neuroprotective effect. Minocycline diminished the dynorphin(15 nmol)-induced upregulation of expression of IL-1β and IL-6 within the spinal cord. These results suggest an important role of these proinflammatory cytokines in the development of the neurotoxic effects of dynorphin. Additionally, our study of primary microglial cell culture confirmed the presence of μ- and κ-opioid receptors. Further, we provide the first evidence for the lack of δ-opioid receptors on microglial cells. Interestingly, the analgesic effect of δ-opioid receptor ligands (DPDPE, deltorphine II) in neuropathic pain is not diminished in contrast to other opioid receptor ligands (morphine, DAMGO, U50.488H, SNC80). In conclusion, our results underline the importance of neuro-glial interactions as evidenced by the involvement of IL-1β and IL-6 and the minocycline effect in dynorphin-induced toxicity, which suggests that drugs, that alter the prodynorphin system could be used to a better control of neuropathic pain. Our results suggest, that δ-opioid receptor agonists analgesia is different from analgesia induced by μ- and κ-opioid receptors because it does not dependent on injury-induced microglial activation. Therefore, δ-opioid receptor agonists appear to be the best candidates for new drugs to treat neuropathic pain.

NCN grants 2011/03/B/NZ4/00042 and 2012/06/A/NZ4/00028.

Peptides in neurological disorders

Nyberg F.

Department of Pharmaceutical Biosciences, Uppsala University, Sweden

This presentation addresses past and current research on various neuropeptides that have been implicated in neurological complications, including drug addiction, chronic pain, cognitive disiorders, anxiety, and brain injury. However, considering the large and even increasing number of identified neuroactive peptides, it is necessary to limit this presentation to a few peptides or peptide systems, which have received particular attention in relation to these items. Among these are the opioid peptides, the tachykinins, calcitonin gene-related peptide (CGRP), and peptides belonging to the endocrine system. Most of these neuropeptides are not only involved in pain processing and drug addiction but are aso involved in the endogenous mechanisms of regulating memory and cognitive function. Also many of these neuroactive peptides are affected and dysregulated at injury to the central nervous system (CNS). The presentation also highlight some new aspects regarding the possibility to use endocrine peptides to counteract and repair brain damages induced by addictive drugs and CNS injuries. It does not endeavor to fully cover the field but it does aim to give an idea of how various neuropeptides may be involved in the control of various neurobehavior and how peptidergic systems are affected during various diseases related to the CNS.

Peptides in angiogenesis. Development of peptidomimetic inhibitors of VEGF co-receptor NRP-1

Tymecka D.[1], Fedorczyk F.[1], Niescioruk A.[1], Grabowska K.[1], Puszko A.[1], Sosnowski P.[1], Wilenska B.[1], Witkowska E.[1], Perret G.Y.[3], Starzec A.[†3], Misicka A.[1]

[1]Faculty of Chemistry, Biological and Chemical Research Center, University of Warsaw, Warsaw, Poland
[2]Mossakowski Medical Research Centre, Polish Academy of Sciences, Warsaw, Poland
[3]Universite Paris 13, Li2P EA 4222, Bobigny, France

Angiogenesis, the growth of new capillary blood vessels from existing ones, is an important physiological process in embryogenesis, wound healing and reproduction. In cancer, angiogenesis permits to develop a network of intra tumour blood vessels supplying oxygen and nutrients thus enhancing tumour growth. Therefore, compounds blocking

angiogenesis could be prospective antitumour drugs, but so far only a few angiogenesis inhibitors are used in the clinic for the treatment of cancer.

One of the most important growth factors involved in angiogenesis process is vascular endothelial growth factor-165 ($VEGF_{165}$). $VEGF_{165}$ signal is transduced via VEGF receptors and significantly enhanced by association with co-receptor NRP-1. Moreover, overexpression of NRP-1 was found in different malignant cancer tissues. All these findings suggest that NRP-1 could be involved in pathological angiogenesis and inhibitors of NRP-1 have considerable potential as novel antiangiogenetic and cancer therapeutics.

As a starting point for our study of searching for antiangiogenic peptidomimetics we utilized a heptapeptide ATWLPPR (A7R). It was shown that A7R binds to NRP-1 and selectively inhibits $VEGF_{165}$ binding to NRP-1, and *in vivo* treatment with A7R resulted in decreasing breast cancer angiogenesis and growth [3]. The detailed studies have shown the importance of C-terminal arginine and that its shortest sequence preserving inhibitory activity is the *C*-terminal tetrapeptide LPPR [2].

This presentation reports structure-activity relationship studies of the tetrapeptide LPPR in order to understand the structural determinants for inhibition of binding $VEGF_{165}$ to NRP-1 by this tetrapeptide and to develop more resistant to enzymatic degradation peptidomimetic NRP-1 inhibitors. These compounds may serve as tools for the study of NRP-1 biology and provide a point of departure for development of more potent anti-NRP-1 drugs in the future [1].

This work was supported by NCN grant no N 204 350940. Project was carried out with the use of CePT infrastructure cofinanced by the European Union – the European Regional Development Fund within the Operational Programme "Innovative economy" for 2007-2013.

References

1. Misicka-Kesik A, Tymecka D, Fedorczyk B, Wilenska B, Sosnowski P, Witkowska E, Ladam P, Perret G, Starzec A. Polish Patent Application, P.405129.
2. Starzec A, Ladam P, Vassy R, Badache S, Buchemal N, Navaza A, Herve du Penhoat C, Perret GY. Structure-function analysis of the antiangiogenic ATWLPPR peptide inhibiting VEGF(165) binding to neuropilin-1 and molecular dynamics simulations of the ATWLPPR/neuropilin-1 complex. Peptides 2007; 28: 2397-2402.
3. Starzec A, Vassy R, Martin A, Lecouvey M, Di Benedetto M, Crepin M, Perret GY. Antiangiogenic and antitumor activities of peptide inhibiting the vascular endothelial growth factor binding to neuropilin-1. Life Sci 2006; 79: 2370-2381.

Stroke-induced neurogenesis

Kokaia Z.

Stem Cell Center, Lund University, Sweden

Stroke is caused by occlusion of a cerebral artery, which gives rise to focal ischemia with irreversible injury in a core region and partially reversible damage in the surrounding penumbra zone.

Stroke is the leading cause of disability in adult humans in developed countries. After ischemic stroke neurons are rapidly damaged and usually die but cellular loss can occur hours and days thereafter. Stroke increases stem cell proliferation in the subventricular zone (SVZ) and the generated neuroblasts migrate to the stroke-damaged area of the brain where they become mature neurons. This process may continue for several months and produce a significant number of new, functional neurons. The evidence of increased neuroblast production after stroke has also been demonstrated in human brain. A bulk of experimental evidence supports the idea that the stroke-damaged adult brain makes an attempt to repair itself by producing new neurons also in areas where neurogenesis does not normally occur, e.g., striatum and cerebral cortex. Knowledge about mechanisms regulating the different steps of neurogenesis after stroke is rapidly increasing but still incomplete. The functional consequences of stroke-induced neurogenesis and the level of integration of the new neurons into existing neural circuitries are poorly understood. In order to have a substantial impact on the recovery after stroke, this potential mechanism for self-repair needs to be markedly enhanced, primarily by increasing the survival and differentiation of the generated neuroblasts. Moreover, for efficient repair, optimization of neurogenesis most likely needs to be combined with promotion of other endogenous neuroregenerative responses, e.g., protection and sprouting of remaining mature neurons, and transplantation of stem cell-derived neurons and glia cells.

Injury-induced neurogenesis in the adult striatum

Magnusson J.P.[1], Göritz C.[1], Tatarishvili J.[2], Smith E.M.K.[3], Kokaia Z.[2], Lindvall O.[2], Frisén J.[1]

[1]Department of Cell and Molecular Biology, Karolinska Institute, SE-171 77, Stockholm, Sweden
[2]Wallenberg Neuroscience Center, Lund Strategic Research Center for Stem Cell Biology and Cell Therapy, Lund University Hospital, SE-221 84 Lund, Sweden
[3]Division of Translational Cancer Research, Lund University, SE-223 63 Lund, Sweden

The adult brain is not good at repairing itself. After brain injury, functional recovery is generally restricted to behavioral compensation and rewiring of spared circuits and there is very limited, if any, replacement of dead neurons. In the adult mammalian brain, neuron-producing stem cells do exist in two spatially restricted regions, the dentate gyrus of the hippocampus and the subventricular zone lining the lateral ventricles. These stem cells are important for normal brain function and their primary role does not seem to be to repair injuries; however, the discovery of these cells has garnered much speculation about whether the brain's inherent capacity to make new neurons can be harnessed to improve functional recovery after injury. It is likely that a detailed understanding of the mechanisms that govern adult neurogenesis will be crucial if this prospect is to become reality. The striatum has recently emerged as a brain region that sustains neurogenesis into adulthood in humans; in addition, this region is known to support injury-induced neurogenesis in animal models of stroke. In my talk, I will discuss recent findings regarding the extent, origin and molecular mechanisms governing stroke-induced neurogenesis in the striatum – results that highlight a previously unknown level of plasticity in the adult brain.

Poster session I

|A1|

Intervertebral disc regeneration with the use of autologous population of chondrocytes and its analysis in terms of morphology and activities

Abaaslam F.[1], Wluka A.[2], Głowacki M.[1], Czernicki Z.[1], Lipkowski A.W.[2]

[1]Department of Neurosurgery, Mossakowski Medical Research Centre, Polish Academy of Sciences, Warsaw, Poland
[2]Department of Neuropeptides, Mossakowski Medical Research Centre, Polish Academy of Sciences, Warsaw, Poland

Introduction: Lumbosacral spine pains affect nearly 80% of the population. In the last two decades various biological methods aimed at treatment of the intervertebral disc diseases have been developed. Out of all methods, the cell therapy based on the transplantation of autologous chondrocyte cells seems promising. This procedure stimulates the matrix production, increases the population of chondrocytes and equates the disturbed balance within the disc.

The aim of the study was to establish the best method of obtaining chondrocytes for autologous cell transplantations in cases of intervertebral disc diseases. This project takes into account the duration of the disease, the place of collecting the material from the disc, the quantity of the collected material and the degree of destruction of the intervertebral disc, in order to derive the optimal, autologous material to be administered to the intervertebral space during operation.

Material and methods: The population of the study consisted of 47 patients whose age ranged from 18 to 40. Those patients were diagnosed with a single-level lumbar degenerative disc disorder on the basis of clinical and MRI examinations. The research topic of the present study dealt with the chondrocyte cells culture derived from the intervertebral disc by means of a single-level discectomy at L4-S1 levels. The analysis also included the target material removed from the intervertebral disc.

Results: The study revealed that the transplantation of cultured cells produced a good radiological and clinical effect. Tests in confocal microscope showed good integration of transplanted cells with the matrix and their correct activity. It was observed that the relation between the production of typical components of the matrix-collagen I, II, III, IV, proteoglycans, aggrecans and anomalous for the matrix-collagen type IV in the initial material was appropriate.

Conclusions: The conducted examinations show that the transplantation of chondrocyte cells derived from the culture to the previously operated intervertebral space suppresses degenerative processes of the disc and influences its recreation. Tests in the light and confocal microscope indicate a good integration of transplanted cells with the matrix and their correct productive activity as the production of typical components of the matrix-collagen I, II, III, IX, proteoglycans and aggrecans and anomalous for the matrix-collagen type I. The examination of the matrix-collagen type D could be the subject for future research. Such research might verify the role of this collagen in a healthy nucleus pulposus, and its functions in both processes of degeneration and regeneration of the intervertebral disc. To conclude, lack of inflammatory processes and other clinical complications after the transplantation of cells derived from the autologous chondrocytes culture show that this procedure is safe and beneficial for patients.

|A2|

Adhesion to the endothelial wall – the crucial step of cell homing into the tissue after their systemic transplantation

Andrzejewska A.[1], Nowakowski A.[1], Janowski M.[1,2,3], Koniusz S.[1], Walczak P.[3], Grygorowicz T.[4], Jablonska A.[1,2], Lukomska B.[1]

[1]NeuroRepair Department, Mossakowski Medical Research Centre, Polish Academy of Sciences, Warsaw, Poland
[2]Cellular Imaging Section and Vascular Biology Program, Institute for Cell Engineering, the Johns Hopkins University School of Medicine, Baltimore, Maryland, USA
[3]Russel H. Morgan Vascular Biology Program, Division of MR Research, The Johns Hopkins University School of Medicine, Baltimore, USA
[4]Laboratory of Advanced Microscopy Techniques, Mossakowski Medical Research Centre, Polish Academy of Sciences, Warsaw, Poland

Application of mesenchymal stromal cells (MSCs) is a new and promising approach for the treatment of neurological disorders. The success of clinical application of MSCs relies upon the efficient recruitment of these cells into appropriate tissues. Systemic infusion of MSCs is preferred as a minimally invasive method of transplantation however cell migration from the vasculature into injured brain is inefficient. Leukocytes, circulating in the blood are known for their ability to migrate through the endothelial wall into surrounding tissues and this is a multi-step process that includes rolling and adhesion to the endothe-

lial cells. Initial capture of the leukocytes on the endothelium is promoted by the adhesion proteins i.e. selectins and integrins present on the leukocyte cell surface, interacting with their specific ligands expressed on activated endothelial cells. We hypothesize that the overexpression of $\alpha 4\beta 1$ (VLA-4) integrin in MSCs will enhance their migration towards ischemic brain regions after systemic transplantation.

Material and methods: Human bone marrow mesenchymal stromal cells (hBM-MSCs) (Lonza) were employed. Overexpression of $\alpha 4$ subunit of VLA-4 in hBM-MSCs was obtained by mRNA-ITGA4 based transfection. The naïve (non-transfected) and modified (mRNA-ITGA4 transfected) hBM-MSCs were labelled with iron nanoparticles coupled with Rhodamine-B (Molday, BioPAL) and used in microfluidic assays with microchannels coated with TNF-α activated rat brain endothelial cell line (RBE-4). The experiments with microfluidic device are based on the use of special microchannels, where laminar flow mimics physiological blood flow *in vivo*. Microchannels are covered with endothelial cells in the way that seeded cells resemble physiological blood vessel wall by their shape and diameter. The hBM-MSCs are forced to pass through microchannels with the flow and their interactions and adhesion rate to endothelial cells layer are assessed. The systemic transplantation of 10^5 naïve hBM-MSCs labelled with iron nanoparticles into internal carotid artery of ouabain-induced stroke rat was observed using MRI. The displaying was performed during the cells infusion and the day after surgery.

Results and conclusions: During the *in vitro* observation naïve hBM-MSCs interacted with rat endothelial cells. After pressure-driven perfusion of hBM-MSCs through the microfluidic channels even naïve cells were found to roll and be captured at the surface of endothelial cell layer. The effect of $\alpha 4\beta 1$ overexpression in MSCs on endothelial adhesion is currently being investigated. The model of microfluidic assay is a useful tool that can be used to assess the adherent properties of engineered hBM-MSCs before their intravenous or intra-arterial transplantation. The *in vivo* MRI research revealed a huge loss of transplanted hBM-MSCs the day after surgery in comparison to their amount observed directly after transplantation. This may be caused by their weak adhesiveness. We hope that our further study will show both *in vitro* and *in vivo* enhanced adherent properties of engineered hBM-MSCs.

Supported by a NCR&D grant No 101 in ERA-NET NEURON project: "MEMS-IRBI".

|A3|

Hypoxic ventilatory response after central dopamine receptor blockade in rat model of Parkinson's disease

Andrzejewski K.[1], Budzinska K.[1], Kaczynska K.[2]

[1]Department of Respiratory Research, Mossakowski Medical Research Centre, Polish Academy of Sciences, Warsaw, Poland
[2]Laboratory of Respiratory Reflexes, Mossakowski Medical Research Centre, Polish Academy of Sciences, Warsaw, Poland

Parkinson's disease (PD) patients apart from motor dysfunctions exhibit also respiratory disturbances such as: dyspnea, restrictive pulmonary function, respiratory dysrhythmias, upper airway dysfunction. Our study was aimed to investigate the effect of impairment of nigrostriatal dopaminergic system on resting breathing and hypoxic ventilatory response in experimental model of PD. Further, the involvement of central dopamine D_2 receptors in the hypoxic ventilatory response was examined. In our experiments we used neurotoxin 6-hydroxydopamine (6-OHDA) model with unilateral, double injection into the right medial forebrain bundle (MFB).

The experiments were performed on adult Wistar rats microinjected with 6-OHDA or vehicle according to the stereotaxic coordinates. Ventilatory parameters: tidal volume, minute ventilation, and frequency of breathing were measured in conscious rats with the use of whole body plethysmograph apparatus before and two weeks following the lesion. Changes in body weight and behavioral cylinder test were evaluated at the same time points and compared with the results obtained in sham-operated animals. Effects of centrally acting dopamine D_2 receptor antagonist, haloperidol (1 mg/kg *i.p.*), on ventilatory responses during resting breathing and exposure to hypoxia (8%) were studied before and after 6-OHDA injection.

Two weeks after 6-OHDA treatment the cylinder test displayed limb use asymmetry. Body weight showed lesser increase in comparison to the sham-operated animals. No effect of nigrostriatal pathway degeneration to the resting normoxic respiration was observed. Injection of 6-OHDA caused increase in tidal volume and decrease in respiratory rate during respiratory response to hypoxia with no alteration in minute ventilation. Haloperidol treatment in intact animals evoked significant increase in V_T stimulation in response to hypoxia. Fourteen days after lesion the effect of haloperidol injection was not observed.

In conclusion, stimulatory action of haloperidol via D_2 central dopamine receptor on tidal volume in reaction to hypoxia suggests inhibitory involvement of central dopamine to hypoxic ventilatory response. Augmentation of tid-

al volume response to hypoxia present after lesion in the MFB area, resulted from a deficit of dopamine connected with degeneration of dopaminergic neurons evoked by 6-OHDA treatment.

|A4|

The influence of dopaminergic system lesion and repeated administration of pramipexole and imipramine on BDNF and trkB mRNAs expression

Berghauzen-Maciejewska K., Wardsa J., Glowacka U., Kuter K., Mroz B., Ossowska K.

Department of Neuropsychopharmacology, Institute of Pharmacology, Polish Academy of Sciences, Cracow, Poland

Motor dysfunctions in Parkinson's disease (PD) are frequently preceded by comorbid depression. Emerging pieces of evidence suggest that BDNF alterations are associated with neurodegenerative and neuropsychiatric disorders. Postmortem studies in depressed patients showed reduced expression of mRNA and protein levels of BDNF in hippocampus (HIP) and prefrontal cortex, as well as in the serum and plasma of patients (suicide) with depression. The above effects were reversed by administration of different classes of antidepressant drugs. Similar results were observed in animal models of stress and depression.

Clinical studies indicate that adopamine D3/D2 receptor agonist – pramipexole (PRA) is the most effective compound in the treatment of depression in PD. The action of classical tricyclic antidepressant drug – imipramine (IMI) in PD patients is controversial. This drug causes a number of side-effects, including sedation and may even worsen the condition of patients.

The aim of the present study was to search for the mechanisms involved in the "depressive-like" behavior in an animal model of depression in the preclinical phase of PD.

Male Wistar rats were bilaterally injected with 6-OHDA (15 µg/2.5 µl) into the ventral striatum (vSTR). IMI was injected *i.p.* (10 mg/kg) once a day and PRA *s.c.* (1 mg/kg) twice a day for two weeks. On the 15th day after the surgery (24 h after the last drug injection) the forced swimming test (FST) and motility were examined. After decapitation the BDNF and trkB mRNAs were investigated using in situ hybridization.

The lesion of vSTR induced by 6-OHDA was moderate (ca. 50% of STR dopamine level), increased immobility in FST, but did not influence motility of rats suggesting "depressive-like" changes without motor disturbances. PRA, but not IMI, shortened the immobility in FST in lesioned rats. 6-OHDA administration reduced the BDNF and/or trkB mRNAs in HIP, amygdala and habenula, while IMI reversed the lesion effect in the dentate gyrus of HIP. PRA consistently reduced the BDNF and trkB mRNAs in mesolimbic and nigrostriatal systems in lesioned animals.

These results seem to indicate that the presymptomatic dopaminergic lesion may induce "depressive-like" symptoms which are reversed by PRA but not by IMI. The PRA-induced reduction of BDNF-trkB signaling pathway may be related to its clinical efficacy.

|A5|

The *N*-terminal portion of mitofusin 2 inhibits proliferation of cells

Boratynska-Jasinska A.[1]*, Kawalec M.[1]*, Beresewicz M.[1], Kabzinska D.[2], Zablocka B.[1]

[1]Molecular Biology Unit, Mossakowski Medical Research Centre, Polish Academy of Sciences, Warsaw, Poland
[2]Neuromuscular Unit, Mossakowski Medical Research Centre, Polish Academy of Sciences, Warsaw, Poland
*These authors contributed equally to this work.

Mitofusin 2 (Mfn2) is a nuclear encoded protein involved in mitochondrial fusion. It has two *C*-terminal transmembrane domains that anchor Mfn2 in the mitochondrial outer membrane, while both the *NH2*- and *COOH*-terminal ends are exposed to cytoplasm.

Proper mitochondrial function is maintained by mitochondrial dynamics that is the balance between mitochondrial fusion and fission. Disruption of this balance, resulting in excessive mitochondrial fission has been suggested to have a role in apoptosis activation by facilitation of Bax insertion and activation in mitochondria. It has been known for a long time that mutations in MFN2 gene are associated with Charcot-Marie-Tooth disease type 2A (CMT2A). On the other hand, a recent cancer studies have shown that Mfn2 may be responsible for inhibition of cell proliferation. Over-expression of Mfn2 protein has an anti-proliferative effect in hepatoma cells and exerts pro-apoptotic effect in hepatocellular carcinoma cells. It has also been shown that the expression of Mfn2 gene is reduced in actively proliferating cancer cells. On this basis, we decided to study the influence of Mfn2 mutations on mouse embryonic fibroblasts (MEFs) viability. We tested here: (i) proliferation rate of MEFs: wild type MEF (MEFwt) and Mfn2-null MEF ($MEF^{Mfn2-/-}$); (ii) the effect of over-expres-

sion of wild type human Mfn2 gene and (iii) the effect of over-expression of mutated (R400X and R250W) Mfn2. These mutations were detected in Polish patients diagnosed with CMT2A. In this study we observed that depletion of Mfn2 gene in $MEF^{Mfn2-/-}$ increased proliferation rate, significantly reducing their doubling time in comparison to MEFwt. We found that over-expression of wild type Mfn2 gene in these knock-out cells decreased their growth rate to that observed in wild type MEF. Interestingly, the expression of R400X Mfn2 mutant in $MEF^{Mfn-2/-2}$ resulted in further elongation of doubling time of $MEF^{Mfn-2/-2}$. Additionally, by Western Blot, we showed that the mutation R400X generates truncated, 45 kDa, *N*-terminal part of mitofusin 2. Such a protein does not possess transmembrane domains located downstream of HR1 region and thus should not influence fusion of mitochondria. Taken together, these findings indicate that Mfn2 has a significant anti-proliferative effect in MEF cells and this function is mainly exerted by *N*-terminal part of the protein without engagement of its mitochondrial fusion activity.

This project was supported by NSC grant NN402474640.

|A6|

Neuroprotective effects of metabotropic glutamate receptors group II (mGluR2/3) agonists preconditioning in animal model of birth asphyxia: Investigations into molecular mechanisms

Bratek E., Ziembowicz A., Salinska E.

Department of Neurochemistry, Mossakowski Medical Research Centre, Polish Academy of Sciences, Warsaw, Poland

Hypoxic-ischemic encephalopathy is an abnormal neurobehavioral state in which the predominant pathogenic mechanism is impaired cerebral blood flow that may result in neonatal death or be manifested later as cerebral palsy or mental deficiency. Recent investigations have not provided us with promising neuroprotective compounds to reduce perinatal hypoxic-ischemic (HI) brain injury and there is a growing interest in engaging endogenous neuroprotective mechanisms. mGluR2/3 activation before or after ischemic insult results in neuroprotection and the exact mechanism of this effect is not clear. The aim of proposed study is to investigate whether mGluR2/3 activation before or after hypoxia-ischemia reduces brain damage and if induced ischemic tolerance acts through activation of antioxidant enzymes and decrease of oxidative stress. We used an animal model of hipoxia-ischemia (H-I) on 7-day old rat pups. Animals were anesthetized and the left common carotid artery was isolated and double – ligated and then cut between the ligatures. After completion of the surgical procedure the pups were subjected to hypoxia (7.2-7.4% oxygen in nitrogen for 75 min at 35°C). Control pups were sham-operated (anaesthetized and left c.c.a. dissected, but not ligated). Animals were injected intra peritoneal with specific mGluR2 (LY 379268) and mGluR3 (NAAG) agonists 24 and 1 hour before H-I (5 mg/kg of body weight). Weight deficit of the ischemic brain hemisphere, radical oxygen specied (ROS) content, activity of antioxidant enzymes (superoxide dismutase – SOD, glutatione peroxidase – GPx, catalase – CAT) and level of reduced glutatione (GSH) were measured.

Our results show a neuroprotective effect of mGluR 2/3 agonists. Both agonists decreased tissue weight loss in ischemic hemisphere independently on the time of application (from 40% in H-I to 10-20% in treated). H-I resulted in increased activity of SOD in the injured hemisphere, which was further potentiated by mGluR2/3 agonists application 1 h before H-I. The activity of glutathione peroxidase (GPX) was also increased by H-I and its activity was potentiated by both agonists. The decrease by H-I GSH level observed in ischemic hemisphere was not observed after agonists application, the effect was better expressed when agonists were administered 1 h before H-I. However, CAT activity was positively modulated only by mGluR2 agonist – LY379268. Our results show that both mGluR2/3 antagonists reduce ROS level in the injured hemisphere (HI).

Conclusions: The results show that activation of mGluR2 and mGluR3 before H-I insult triggered neuroprotective mechanisms, which probably partly engage defense against oxidative stress by activation of antioxidant enzymes. The effect is more distinct when agonists are applied in a short time before H-I.

This work was made under MMRC-KNOW 2013-2017 project.

|A7|

Photic modulation of infra slow oscillatory activity in the intergeniculate leaflet of the rat model of absence epilepsy

Chrobok L., Palus K., Orlowska-Feuer P., Lewandowski M.H.

Department of Neurophysiology and Chronobiology, Institute of Zoology, Jagiellonian University, Cracow, Poland

The intergeniculate leaflet of the thalamus (IGL) is a small retinorecipient brain nucleus participating in the regulations of circadian functions. The IGL consists of at least two GABAergic neuronal populations expressing either neuropeptide Y (NPY) or enkephalin (ENK). NPY-positive cells project to the main rhythm generator – the suprachiasmatic nucleus (SCN), whereas ENK-positive cells send their axons to the contralateral IGL. ENK-postive neurons were shown to receive direct retinal input and generate action potentials in an infra slow oscillatory (ISO) manner with a period of multiseconds during *in vivo* recordings. This characteristic pattern of activity consists of two phases: intraburst, with the high firing rate, and extraburst, in which the neuron is quiet. Interestingly, ISO depends on the contralateral retina activity, as it is completely abolished by its deactivation and is only present under photopic conditions.

Absence epilepsy (AE) is characterised by the presence of spike-wave discharges (SWDs) in EEG. WAG/Rij rats, used in the present study, are well established model of AE. This neurological disease is often connected with retinal pathologies and sleep-wake cycle abnormalities. The occurrence of SWDs is modulated by the circadian timing system. The aim of the present study was to verify the presence of ISO activity in the IGL of WAG/Rij rats and whether it is modulated by light.

The experiments were performed on urethan-anaesthetised male WAG/Rij rats by using *in vivo* single-unit extracellular recordings with simultaneous ECoG measurements. ECoG electrode was placed above the frontal cortical area, whereas the recording electrode was placed in the IGL. Experimental protocol consisted of two stages. First, the baseline ISO activity was recorded in the IGL, during REM- and NREM-like phases of urethan sleep. Next, the light was turned off and the activity of the tested neuron was recorded for at least the duration of both phases.

Obtained results confirmed the presence of infra slow oscillatory activity in the IGL of WAG/Rij rats. The period of oscillations was in the range of multiseconds. The characteristic of oscillations was comparable to ISO activity described previously in the IGL of Wistar rats. Two phases of oscillations: intra- and extra-bursts, were clearly distinguishable. In contrast to Wistar rats, all of the recorded ISO neurons remained active during the dark conditions. The features of oscillations, such as the period and mean intra- and extra-burst activity were strongly influenced by light. Namely, the period was shortened and activity was decreased. The relationship between the ISO activity and phases of urethane sleep was observed.

We hypothesise that this response to light of ISO neurons in the IGL may be due to both: abnormalities at the level of the retina and disinhibition of the IGL network itself. Our parallel *in vitro* patch clamp studies indicate that the IGL's GABAergic synaptic transmission in WAG/Rij rats is down-regulated. Based on the acquired results, further studies on the IGL of WAG/Rij can serve as a novel insight into absence epilepsy.

Supported by the Ministry of Science and Higher Education project "Diamentowy grant III" K/PMI/000190, 2014-2017.

|A8|

Neuroprotective potential of KU55933, an inhibitor of ATM kinase, against hydrogen peroxide- and doxorubicin-induced cell death in human neuroblastoma SH-SY5Y cells

Chwastek J., Jantas D., Lason W.

Department of Experimental Neuroendocrinology, Institute of Pharmacology, Polish Academy of Sciences, Cracow, Poland

The experimental data collected during the recent years point to additional functions of ATM (ataxia-telangiectasia mutated) kinase apart its involvement in DNA repair system. Since the engagement of this protein in regulation of cellular response to oxidative stress, insulin signaling and mitochondrial homeostasis has been suggested, it started to be the subject of research in diabetes, cancer and neurodegenerative diseases. In order to widen the knowledge about the role of ATM kinase in neurodegeneration, in the present study we tested the effect of pharmacological inhibition of ATM kinase by specific inhibitor KU55933 on cell death of human neuroblastoma SH-SY5Y cells, induced by oxidative stress (hydrogen peroxide) and pro-apoptotic factors – staurosporine and doxorubicin (Dox). The data showed that KU55933 (0.01-20 μM) being not toxic when given alone to undifferentiated (UN-) and retinoic acid (RA-)-differentiated SH-SY5Y

cells, partially attenuated the cell death induced by hydrogen peroxide in both cell types (about 19-25%), as was confirmed by MTT reduction assay. The protection evoked by KU55933 against oxidative stress-evoked cell damage was relatively higher in RA-SH-SY5Y, comparing to UN-SH-SY5Y, when given the effective concentrations (0.1-10 μM and 0.1-1 μM for RA- and UN-SH-SY5Y cells, respectively). Moreover, KU55933 (0.1-10 μM) almost completely blocked the cell damage induced by Dox in RA-SH-SY5Y, being only slightly protective in UN-SH-SY5Y cells (1 μM with 10% protection). In contrast, KU55933 (0.01-10 μM) did not affect cell damage evoked by staurosporine in both cell types. Further studies showed, that KU55933 completely blocked the Dox-induced caspase-3 activity in both, UN- and RA-SH-SY5Y cells, whereas did not change the hydrogen peroxide-evoked increase in this enzyme activity. The higher neuroprotective effectiveness of KU5593 in RA- vs. UN-SH-SY5Y was not related to changes in ATM mRNA abundance since we did not observe any significant differences in *Atm* gene expression between both cell types as was confirmed by quantitative PCR method. Finally, we demonstrated that KU5593 at higher concentration (20 μM) significantly increased the cell death induced by hydrogen peroxide, doxorubicin and staurosporine but only in UN-SH-SY5Y cells. Altogether our data point to neuroprotective potential of ATM kinase inhibitor, KU55933 against hydrogen peroxide- and doxorubicin-evoked injury in SH-SY5Y cells with engagement of caspase-3 inhibition only in the latter one. Moreover, the results showed better usefulness of retinoic acid-differentiated SH-SY5Y cells over undifferentiated one for further study of the mechanisms of ATM kinase inhibition-mediated neuroprotection.

The study was supported by statutory funds of the Institute of Pharmacology, Polish Academy of Sciences.

|A9|

Alteration of sphingosine kinase 1 by amyloid beta (1-42) and its implication in cell death

Cieslik M., Czapski G.A., Strosznajder J.B.

Department of Cellular Signaling, Mossakowski Medical Research Centre, Polish Academy of Sciences, Warsaw, Poland

Sphingosine kinase (SphK) is a key enzyme involved in maintaining sphingolipid rheostat in the brain. Deregulation of sphingolipid metabolism has been associated with accumulation of amyloid beta (Aβ) peptides and could play a crucial role in pathogenesis of Alzheimer's disease (AD). Sphingolipids are main constituents of lipid rafts and important regulators of the activity of secretase β (BACE) and Aβ liberation from its precursor protein.

The aim of this study was to investigate the role of extracellular $A\beta_{1-42}$ peptides in regulation of SphK expression and activity. Moreover, the question arose what kind of molecular events, regulated by SphK and $A\beta_{1-42}$, are responsible for cells survival or death.

In this study rat pheochromocytoma (PC12) cells were subjected for 24 and 96 h to $A\beta_{1-42}$ oligomers (1 μM) or to SphK inhibitor (SKI II 10 μM) and other pharmacological compounds. The experiments were performed using biochemical, spectrophotometric and qRT-PCR methods.

Our data indicated that $A\beta_{1-42}$ induced time-dependent alteration of SphK1 expression and activity. Exposure to $A\beta_{1-42}$ for 24 h enhanced SphK activity, but after 96 h the activity was significantly reduced. Similar changes were observed for the mRNA level of Sphk1 gene, but the expression of Sphk2 gene was not changed. Both $A\beta_{1-42}$ and SKI II evoked time-dependent cell death. The level of free radicals was negatively correlated with cell viability. These two compounds evoked up-regulation of the expression of antioxidative enzymes, catalase and superoxide dismutase. The significant increase in the level of apoptosis inducing factor (AIF) that could be involved in antioxidative defence in mitochondria was also observed. Moreover $A\beta_{1-42}$ and SKI II evoked reduction of glycogen synthase kinase-3β (Gsk-3β) immunoreactivity and altered the balance between pro- and anti-apoptotic proteins. Exposure of cells to $A\beta_{1-42}$ or SKI II resulted in the increase in gene expression for pro-apoptotic BAX protein and in decrease of anti-apoptotic Bcl-xL and Bcl-2 proteins. Several pharmacologically active compounds were then investigated for their cytoprotective effects against $A\beta_{1-42}$-evoked cytotoxicity, but only α-pifithrin (20 μM), an anhibitor of p53 protein, protected cells against death.

Our data indicated that inhibition of SphK, by the alteration of sphingolipid rheostat, may be the trigger of apoptotic signaling evoked by Alzheimer's $A\beta_{1-42}$ peptides.

Our study was supported by a Grant of NSC 2013/09/B/NZ3/01350.

|A10|

The effects of maternal immune activation on the behavior of rat offspring: a focus on changes in postsynaptic proteins – Shank

Cieslik M.[1], Kudlik M.[1], Boguszewski P.[2], Adamczyk A.[1]

[1]Department of Cellular Signaling, Mossakowski Medical Research Centre, Polish Academy of Sciences, Warsaw, Poland
[2]Department of Neurophysiology, Laboratory of Limbic System, Nencki Institute of Experimental Biology, Polish Academy of Sciences, Warsaw, Poland

Autism spectrum disorders (ASDs) are neurodevelopmental diseases characterized by two core symptoms, impaired social interactions and communication, and ritualistic or repetitive behaviors. Recent human genetic studies indicate that genes identified as altered in individuals with ASDs often encode synaptic proteins. Shank family proteins (Shank1, Shank2, and Shank3), that belong to synaptic scaffolding proteins, are involved in the regulation of morphological and functional maturation of dendritic spines and synapse formation. These proteins interact with NMDA receptor and metabotropic glutamate receptor complexes in the postsynaptic density (PSD). Previous data indicated that mutation in *SHANK1* contributes to the symptoms of autism. In Shank1(–/–) mice impaired communication characterized by low levels of ultrasonic vocalizations, as compared to wildtype Shank1(+/+) littermate controls, was observed.

Both epidemiological and biochemical evidence suggests that occurrence of ASD may be linked to immune perturbations that took place during fetal development. Therefore, "maternal immune activation" (MIA) model, where the research is carried out in offspring from female rodents subjected to an immune stimulus during early pregnancy, is commonly used as animal models of ASD. The present experiments were performed using male offspring of Wistar rats treated intraperitoneally with saline or lipopolysaccharide (LPS, 100 µg/kg) on gestational day 9.5, to mimic a bacterial infection. Autism-associated behaviors and the function of postsynaptic proteins Shank were examined in the offspring of the treated animals. Behavioral tests were conducted to assess social communication, motions and anxiety, play behaviors, as well as learning and memory. Data analysis was carried out exclusively on male rats. Gene expression and protein level of Shank was analyzed using quantitative Real-Time RT-PCR and Western blot methods, respectively. We observed that male offspring from LPS-treated animals showed impaired communication (expressed by ultrasonic vocalization on postnatal day 9-13, PND 9-13). Moreover, in the spontaneous alternation (T-maze) test, adult male offspring (PND 40-50) from LPS-treated mothers showed impaired learning and memory function. The motions and anxiety responses (Open space test, PND 40-50) and play behaviors (Tickling, PND 40-50) were not altered. When the experimental animals have reached adulthood, the changes in the expression of *SHANK1, SHANK2* and *SHANK3* was investigated. The data showed the down-regulation of *SHANK1* and *SHANK2* expression in the cerebral cortex, without changes in *SHANK3* expression in all analyzed brain structures. Summarizing, our findings indicate that offspring from mothers subjected to immune stimulation during gestation show an impaired communication and dysregulation of synaptic proteins belonging to Shank family. The lower expression of Shank proteins may lead to profound alterations in synaptic function and social behavior.

Supported from IMDIK statutory theme 17.

|A11|

Effect of prenatal stress on spleen cytokine production in female offspring

Curzytek K., Duda W., Kubera M.

Department of Experimental Neuroendocrinology, Institute of Pharmacology, Polish Academy of Sciences, Cracow, Poland

Numerous studies have shown that stressful events occurring in early life have a powerful influence on the development of the central nervous system. Prenatal stress also modifies the immune response of the offspring. It is known that chronic activation of immune-inflammatory pathway play an important role in the pathophysiology of depression. The spleen, as a crucial component of the immune system, can produce a lot of agents i.e. cytokines, chemokines and neurotrophic factors. Proinflammatory cytokines and chemokines produced by the spleen can enhance depressive-like behaviours via influencing synaptic transmission and neuronal plasticity. The aim of present study was to evaluate the disrupting effect of prenatal stress on spleen releasing cytokines and other factors in female offspring.

Pregnant Sprague-Dawley rats were subjected daily to three stress sessions (immobilization) from day 14 of pregnancy until delivery. At 4 months of age, adult female offspring of control and stressed rat dams were subjected to behavioural testing (forced swim test). After other behavioural tests (i.e. locomotor activity, elevated plus

maze test), animals were killed by rapid decapitation and the brain tissue and organs were dissected. Spleen derived cells were cultured with concavalin A (Con A, 2.5 μg/ml) for 24 hours, and supernatants were collected. The level of spleen cytokines was measured by RayBio Rat Cytokine Antibody Array – the protein array system. Our studies showed that prenatal stress caused increased ability of splenocytes to produce Fas-ligand, fractalkine, granulocyte-macrophage colony-stimulating factor (GM-CSF), monocyte chemoattractant protein-1 (MCP-1), tumor necrosis factor (TNF)-α and decreased to produce interleukin (IL)-1α, IL-10, IL-6 and tissue inhibitor of metalloproteinase-1 (TIMP-1). Our studies revealed that prenatal stress significantly changed secretory spleen functions, that can be crucial in disturbance of homeostasis in central nervous system.

The study was supported by Grant POIG.01.01.02-12-004/09 (DeMeTer).

|A12|

Cyclin dependent kinase 5 and its modulatory role in transcription of inflammation-related genes in the brain. Relevance to pathomechanism of Alzheimer's disease

Czapski G., Wilkaniec A., Gassowska M., Strosznajder J.B., Adamczyk A.

Department of Cellular Signalling, Mossakowski Medical Research Centre, Polish Academy of Sciences, Warsaw, Poland

Epidemiological and genetic studies demonstrated an important role of inflammatory reaction in the pathomechanism of Alzheimer's disease (AD), but the precise course of immune system activation and characterization of regulatory processes have not been fully elucidated. In this study we focused on the role of Cyclin dependent kinase 5 (Cdk5) in inflammatory signaling. Cdk5 is serine/threonine kinase that is involved in regulation of neuronal development and function. Moreover, it has been implicated in pathomechanism of AD and other neurodegenerative disorders. Overactivation of Cdk5 has deleterious effects on neuronal cells, leading to hyperphosphorylation of MAP tau, which is responsible for microtubule destabilization and impairment of axonal transport. Additionally, inhibition of this enzyme was proposed to be a prospective strategy preventing neurodegeneration.

The aim of this study was to analyze the role of Cdk5 in neuroinflammatory signaling in animal model of AD. Adult male mice C57BL6 received single intracerebroventricular injection of $A\beta_{1-42}$ oligomers (1 nmol). Lipopolysaccharide (LPS) was administered intraperitoneally (ip.) to evoke activation of inflammatory reaction. Roscovitine (50 mg/kg b.w.) was applied *i.p.*, as an inhibitor of Cdk5. Alterations of gene transcription were analyzed using real-time RT-PCR. The level and phosphorylation of proteins was examined by Western blotting (WB) and by using multiplexed cytometric bead array (CBA).

Our results demonstrated that LPS-induced neuroinflammatory processes evoked rapid increase in phosphorylation of tau protein at Ser396 in hippocampus. In parallel, we observed enhanced phosphorylation of Glycogen synthase kinase-3β (Gsk-3β) at Ser9, indicating inhibition of this tau-kinase. However, the rise of phosphorylation of Cdk5 and acceleration of Calpain-dependent p25 formation suggested that overactivation of Cdk5 may be responsible for hyperphosphorylation of tau protein during neuroinflammation. By using an animal model of AD we have found that Aβ peptides evoked activation of Cdk5 via p25 formation and by enhancement of Cdk5 phosphorylation at Tyr15. Moreover, administration of Aβ induced rapid increase in expression of proinflammatory genes for Tnfa and Il1b, Il6, and concomitant rise in mRNA level for anti-inflammatory Il10. Additionally, an increase in the level of mRNA for Nos2 was observed, suggesting activation of nitrosative/oxidative processes in hippocampus. By using WB and CBA methods we have found that Roscovitine significantly affected Aβ-induced inflammatory signaling in brain. Pre-treatment with Roscovitine reduced the level of Il1b in the mouse hippocampus 3 h after administration of Aβ.

Our results demonstrated for the first time that inhibition of Cdk5 significantly affects Aβ-evoked expression of inflammation-related genes in mouse hippocampus. These data indicate the critical role of Cdk5 in regulation of acute neuroinflammatory signaling in the brain.

Supported by a grant from The National Science Centre 2011/03/B/NZ3/04549.

|A13|

Involvement of huntingtin associated protein 1 in regulation of SOCE in medium spiny neurons from transgenic YAC128 mice model of Huntington's disease

Czeredys M.[1], Maciag F.[1,2], Kuznicki J.[1]

[1]International Institute of Molecular and Cell Biology in Warsaw, Laboratory of Neurodegeneration, Warsaw, Poland
[2]Warsaw University of Technology, Faculty of Chemistry, Warsaw, Poland

Huntington's disease (HD) is a hereditary neurodegenerative disease caused by the expansion of a polyglutamine stretch in the huntingtin (HTT) protein, and characterized by dysregulated calcium homeostasis (Gaicomello *et al*. 2013). One of the mechanisms that regulate calcium homeostasis is store-operated Ca^{2+} entry (SOCE). It is a process in which the depletion of Ca^{2+} stores in the endoplasmic reticulum (ER) induces Ca^{2+} influx from the extracellular space. The Ca^{2+} sensor's stromal interaction molecules 1 and 2 (STIM1 and STIM2) detect changes in Ca^{2+} concentration in the ER. In response to Ca^{2+} depletion, they rearrange into punctate structures by interacting with ORAI calcium channels in plasma membrane (PM). These structures force ER membranes toward PM and activate members of the Orai family (Orai1, Orai2, and Orai3). This results in Ca^{2+} entry by these channels (Frischauf *et al.*, 2008). The mechanism by which mutated HTT affects SOCE is unknown. Therefore, we assessed alterations of Ca^{2+} signalosome in the striatum of a transgenic YAC128 mouse, a model of HD. We found that in medium spiny neurons (MSN) from these mice, the activity of SOCE was enhanced about 25%, which confirmed previous results of Wu (2011). This could be explained by increased expression of huntingtin-associated protein 1 (Hap1) mRNA and Hap1 protein in the striatum of YAC128 mice (Czeredys *et al.* 2013) and may explain data of Wu *et al.* (2011) and Tang *et al.* (2003, 2004). In this work we are investigating the involvement of Hap1 in the regulation of SOCE in neurons from YAC128 mice. Using western blot we found that Hap1 protein is specific for MSN neurons, and was not found in primary cultures of astrocytes. We prepared constructs in lentiviral system for Hap1 overexpression in HEK293 cells. We are now analyzing if the increased level of Hap1 affects SOCE in HD neurons.

|A14|

Ceramide and sphingosine-1-phosphate the critical regulator of the PI3-K/Akt/GSK-3β signaling pathway and cell fate

Czubowicz K., Strosznajder R.P.

Laboratory of Preclinical Research and Environmental Agents, Department of Neurosurgery, Mossakowski Medical Research Centre, Polish Academy of Sciences, Warsaw, Poland

Bioactive sphingolipis: ceramides, sphingosine and sphingosine-1-phosphate (S1P) are crucial regulators of cell survival and death. S1P promotes cell proliferation and viability acting as primary and secondary messenger and exerts its effect by binding to five specific G protein coupled-receptors (S1PR1-5). Its precursors ceramide/sphingosine activate the pro-apoptotic pathways. The relationship between these sphingolipids and pro-survival pathway regulated by PI3-kinase/Akt is till now not fully elucidated. The PI3-K/Akt mediates a wide range of cellular functions, including cell proliferation, survival and cell metabolism. Alteration of ceramide/S1P biostat and signaling is implicated in brain ischemia, cancer, and also neurodegenerative diseases including Alzheimer's disease.

The aim of this study was to investigate the role of S1P in molecular mechanisms of neuronal cells death in the model of oxidative stress evoked by cell-permeable C2-ceramide. The experiments were carried out on human neuroblastoma SH-SY5Y cells, using spectrometric and immunochemical methods. Our study indicated that C2-ceramide (25 μM) inhibited the pro-survival PI3-K/Akt pathway followed by activation of glycogen synthase kinase-beta (GSK3β). Moreover, after ceramide treatment we observed the lower phosphorylation of pro-apoptotic Bad protein. Conversely, exogenously added S1P (1 μM) increased the viability of neuronal cells through S1PR (1, 3) receptors-dependent mechanism as was demonstrated by us using specific receptors antagonists (W123 and VPC23019). In addition S1P and the agonist of S1P receptor(s) (SEW2871 and pFTY720) increased the activity of PI3-K/Akt. Furthermore, it was revealed that S1P enhanced the phosphorylation of Bad protein. Summarizing, our data indicate that modulation of S1P receptor(s) signaling may offer therapeutic strategy in treatment of neurodegenerative diseases characterized by accumulation of ceramides.

Supported by statutory budget of MRC theme no. 1.

|A15|

Neuroprotective potential of neuropeptide Y receptor agonists in ischemic *in vitro* model

Domin H.[1], Jantas D.[2], Smialowska M.[1]

[1]Department of Neurobiology, Institute of Pharmacology, Polish Academy of Sciences, Cracow, Poland
[2]Department of Experimental Neuroendocrinology, Institute of Pharmacology, Polish Academy of Sciences, Cracow, Poland

Much of evidence indicates that neuropeptide Y (NPY) and Y receptors agonists may have neuroprotective potential against excitotoxic damage, however little is known about their effect in ischemic neurodegenerations. Our previous studies demonstrated that Y2 receptor agonist, NPY 13-36, given intracerebroventricularly 30 min after the onset of ischemia, significantly diminished the infarct volume in the rat transient middle cerebral artery occlusion (MCAO) model. The present study was aimed at investigating the role of Y1, Y2 and Y5 receptors in neuroprotection in primary neuronal cortical cultures, exposed to oxygen-glucose deprivation (OGD) for 3h as an *in vitro* ischemic injury paradigm. Therefore we evaluated the effects of YR agonists (0.01-1 μM) such as Y2R agonist (NPY 13-36), Y5R agonist [cPP$^{1-7}$, NPY$^{19-23}$, Ala^{31}, AiB^{32}, Gln^{34}]-hpp or Y1R agonist [Leu^{31}, Pro^{34}]-NPY on ischemia-induced LDH release and MTT reduction in the cortical cultures 24 h after the termination of OGD. The YR agonists were applied twice: just before the start of OGD and immediately after the end of OGD, or once: 30 min or 1 h after the termination of OGD. It was found that double application of the Y2R or the Y5R agonists significantly attenuated neurotoxicity. Of particular importance is the finding that those Y2R or Y5R agonists, given once 30 min after OGD also significantly decreased ischemic injury. The neuroprotective effects of Y2R or Y5R agonists were inhibited by corresponding antagonists to those receptors. No protection was found after the Y1 receptor agonist. We also observed a significant induction of calpains after OGD, evidenced by an increase in spectrin alpha II 145 kDa cleavage product, and that effect was diminished by double application of Y2R agonist, NPY 13-36, but not by Y5R agonist. In conclusion, our results indicate that particularly Y2 receptors may play an important role in the attenuation of damage after ischemia.

The study was supported by grant No. N N401 091037 from MS&HE and by funds for statutory activity of the Institute of Pharmacology, Polish Academy of Sciences, Cracow, Poland.

|A16|

Genetic variants and oxidative stress in peripheral lymphocytes of the patients with Alzheimer's disease

Dorszewska J.[1], Oczkowska A.[1], Prendecki M.[1], Florczak-Wyspianska J.[2], Dezor M.[1], Karlikowska M.[1,3], Postrach I.[1], Kozubski W.[2]

[1]Laboratory of Neurobiology, Department of Neurology, Poznan University of Medical Sciences, Poznan, Poland
[2]Chair and Department of Neurology, Poznan University of Medical Sciences, Poznan, Poland
[3]University College of London, London, United Kingdom

Alzheimer's disease (AD) leads to generation of β-amyloid (Aβ) and oxidative stress. Oxidative stress and apolipoprotein E (ApoE) are associated with DNA damage, which leads to apoptosis induction e.g. in cells expressing wild-type p53. The *TP53* gene is found to be the most frequently mutated gene in human tumor cells. Post-mortem studies have indicated that patients diagnosed with a brain tumor also had unreported signs of AD. In AD, apoptosis can also be induced by the immune system elements, e.g. tumor necrosis factor alpha (TNF-alpha). 8-Oxoguanine DNA glycosylase 1 (OGG1) is a main DNA repair enzyme that excises of 8-oxo-2'-deoxyguanosine (8-oxo2dG) from DNA.

The purpose of this study was to analyze the mutation status in highly conservative exon 7 of *TP53* gene and *APOE* genotypes and the extent of oxidative DNA damage (8-oxo2dG), and expression of p53, OGG1 and TNF-α protein levels in peripheral lymphocytes of AD patients and controls.

The studies were conducted on 31 patients with AD, including 18 women and 13 men aging 52-85 years. The control group included 31 individuals, 18 women and 13 men aging 40-83 years. The *TP53* exon 7 was analyzed by DNA sequencing. The *APOE* genotyping analysis was carried out with the use of Real-Time PCR and DNA sequencing. The levels of 8-oxo2dG were determined using HPLC/EC/UV (high-pressure liquid chromatography system with electrochemical and UV detection) technique. The p53, OGG1 and TNF-α protein levels were analyzed by Western blotting.

Our studies on the sequencing of *TP53* exon 7 revealed the presence of two various mutations only in AD patients, a missense mutation C748A (3.4%) present in an *APOE* ε3/ε4 alleles carrier and a silent mutation C708T (20.1%) in AD patients with various *APOE* genotypes, ε2/ε3, ε3/ε3, ε3/ε4. Only a person (control subject and AD patient) with one or two alleles of *APOE* ε2 had few times higher level of 8-oxo-2dG compared to non-carriers of this allele. Moreover, in AD patients with *APOE* ε2/ε3 genotype and a missense

mutation of *TP53* gene (15 times) and a silent mutation of *TP53* gene (2 times) the level of 8-oxo2dG was higher than in patients without analyzed *TP53* gene mutations. However, in the controls with *APOE* ε3/ε4 genotype the level of 8-oxo2dG and OGG1 was nearly twice higher compared to subjects with the *APOE* ε3/ε3 genotype. In contrast, in AD patients with *APOE* ε3/ε4 genotype 8-oxo2dG level was 1.5 times lower than in patients with *APOE* ε3/ε3 genotype, although the level of OGG1 in both AD groups was decreased compared to the appropriate controls. In the controls and AD, p53 and TNF-α protein levels were similar, regardless of *APOE* genotype.

It appears that especially *APOE* ε2 and ε4 together with *TP53* gene mutations may be associated with the development of oxidative stress in AD.

|A17|

Cytotoxic effects of zinc on cholinergic SN56 neuroblastoma and C6 astroglia cells

Dys A., Ronowska A., Gul-Hinc S., Klimaszewska-Lata J., Szutowicz A., Bielarczyk H.

Department of Laboratory Medicine, Medical University of Gdansk, Gdansk, Poland

Zinc excess in the synaptic cleft may be one of early pathologic signals triggering chronic neurodegenerative events. The aim of this work was to find relationships between Zn accumulation and integrity of cholinergic and astroglial cells. Exposition of cAMP/RA-differentiated (DC) and nondifferentiated (NC) cholinergic SN56 neuroblastoma cells and astroglial C6 cells to Zn yielded its concentration dependent accumulation. Zn accumulation caused concentration-dependent death of both, neuronal and astroglial cells. After 24 h exposition of SN56 cells to 0.15 mmol/L Zn, their mortality was equal to 35% and 50% at cation levels equal to 4.0 and 5.5 nmol/mg protein for NC and DC, respectively. In these conditions, the mortality of astroglial cells was close to 1-2% only, at intracellular Zn levels of 1.6 and 2.1 nmol/mg protein for NC and DC, respectively. Higher, about 0.25 mmol/L Zn concentration was required to evoke mortality of astroglial cells, similar to those seen in neuronal cells. In such conditions Zn levels in astroglia were about 6.4 and 27.0 nmol/mg protein, respectively. The lower accumulation of Zn in astroglial cells C6 than in neuronal cells SN56 may be due to the less density of voltage-gated calcium channels and higher density of ZnT1. In neuronal cells, Zn caused a decrease of mitochondrial Ca^{2+} content and increased level of Ca^{2+} in the cytoplasmic compartment, which may be one of the mechanisms of Zn-dependent increase in mortality of cholinergic neurons. In this study we examined the effects of accumulation of Zn in cholinergic neurons and adjacent astrocytes on activity of enzymes involved in energy metabolism, including PDHC, aconitase and IDH. One day culture of neuronal cells SN56 with 0.15 mmol/L Zn caused about 60% suppression of PDHC and aconitase activities. In these conditions we observed no changes in activity of these enzymes in astroglial cells. In C6, such as 0.22 mmol/L Zn concentration caused 60% and 50% inhibition of aconitase and IDH activities, respectively. The high susceptibility of cholinergic neurons and a relative high resistance of astrocytes to neurodegeneration, induced by cytotoxic concentration of zinc, may be caused by the higher inhibition of neuronal aconitase and PDHC activities. The inhibition of these enzymes reduces the synthesis of acetyl-CoA, and the flow rate of the tricarboxylic acid cycle, which leads to a decrease in ATP synthesis and cell damage. These results indicate, that zinc overload that leads to the disturbance of energy metabolism may be one of the causes of early damage of neuronal cells yielding to the development of neurodegenerative diseases.

Supported by MWiSW St57 and MN 01-0108/08 MUG projects.

|A18|

Neuroprotective effects of memantine, hyperbaric oxygen or hypobaric hypoxia do not add up when applied together in 7-day-old rat hypoxia-ischemia model

Gamdzyk M., Ziembowicz A., Salinska E.

Department of Neurochemistry, Mossakowski Medical Research Centre, Polish Academy of Sciences, Warsaw, Poland

Despite major advances in monitoring technology and knowledge of fetal and neonatal pathologies, perinatal asphyxia or, more appropriately, hypoxic-ischemic encephalopathy (HIE), remains a serious condition that causes significant mortality and long-term morbidity. In our previous studies we proved that hyperbaric oxygen (HBO) and hypobaric hypoxia postconditioning (HH) reduce brain damage in experimental model of neonatal hypoxia-ischemia by over 60%. The aim of present study was to evaluate the effect of NMDA receptor (NMDAR) antagonist

memantine, and memantine combined with HBO or HH on neonatal hypoxic-ischemic (HI) brain injury.

We used an established 7-day postnatal rat model of hypoxia-ischemia. Briefly, the ipsilateral common carotid artery of a rat pup is exposed and ligated. The contralateral artery is left intact. The animal is then subjected to a period of hypoxia at normal atmospheric pressure (7.7% O_2 for 75 min at 35.5°C). HBO (2.5 ATA) or HH (0.5 ATA) were applied 1 or 6 h after H-I for 60 min. Memantine in dose of 20 mg/kg of body weight was applied 15 min before HBO or HH. These treatments were repeated for 3 following days.

Memantine applied 1 or 6 h after H-I reduced ipsilateral hemisphere weight loss from 39.2% to 19.3% and 26.8%, respectively. Memantine combined with HBO decreased brain weight loss to 25% and 28.2%, when applied 1 and 6 h after H-I, respectively. Similarly, memantine combined with HH decreased weight loss to 21.9% and 28.8%.

Memantine applied 1 or 6 h after H-I reduced number of TUNEL-positive cells in ipsilateral hemispheres by 62 and 58%, respectively. Memantine combined with HBO or HH decreased number of positive cells by 21% and 10% (HBO), and 39% and 36% (HH), respectively. Memantine combined with HBO or HH caused protection, but the effect was less significant than effect of memantine used alone.

Our results show that HBO and HH do not increase protection caused by memantine alone. It is possible that HBO and HH, which are means of manipulation of oxygen concentration, modulate NMDAR activity and alter balance between synaptic and extrasynaptic NMDAR activity when applied in combination with memantine. There is some data showing that high dose of memantine can block not only damaging extrasynaptic activity, but also normal synaptic transmission, which interferes with pro-survival protective pathways dependent on synaptic activity, causing detrimental effects leading to cell death, which was visualized by TUNEL staining. This effect could be strengthened or triggered by HBO and HH, which would explain why memantine alone was more neuroprotective.

This project was funded by the National Science Centre based on decision no. DEC-2012/07/N/NZ4/02072.

|A19|

Pre-chiasmatic subarachnoid hemorrhage leads to tight junction disassemblance and enhanced neurodegeneration in experimental rat brain

Gendosz D., Liskiewicz A., Jedrzejowska-Szypulka H., Lewin-Kowalik J.

Medical University of Silesia, School of Medicine, Chair and Department of Physiology, Katowice, Poland

Aims: Our aim was to develop model of arterial bleeding into the pre-chiasmatic cistern resembling subarachnoid hemorrhage (SAH) from aneurysm rupture in the anterior part of the circle of Willis and to explore different aspects of its effect upon adjacent as well as distant areas of rat brain and extracellular.

Methods: Pre-chiasmatic SAH (pSAH) was produced by injection of 200 μL of fresh autologous arterial blood into pre-chiasmatic cistern in rat brain. 24 hrs following the surgery, animals were perfused transcardially and whole brains were collected. Brains were coronally cryosectioned and stained with Fluoro Jade C (FJC) and immunostained to visualize cleaved caspase 3, GFAP, zonulin-1, occludin-1 and claudin-5.

Results: We found numerous FJC positive neurons around the site of blood application as well in more distant areas and its number was especially high in neocortex and hippocampus. Distribution of caspase 3 positive cells was similar to that for FJC. To examine the presence of astrogliosis we carried out GFAP staining. We found numerous astrocytes with morphological alterations characteristic for their activation: thick processes and enlarged cell bodies. Another observations acquired from immunostaining reactions against proteins building tight junctions of BBB suggest their degradation after SAH comparing to controls.

Conclusions: Obtained results indicate that administration of arterial blood directly to pre-chiasmatic cistern leads to neuronal damage and stimulation of astrogliosis not only in the vicinity of injection site but also in more distant regions like somatosensory cortex and hippocampus. Moreover obtained results suggest also SAH crucial role in tight junction proteins degradation.

|A20|

The influence of kissorphin (KSO) on the expression of sensitization to hyperlocomotor effect of morphine and ethanol in mice

Gibula-Bruzda E.[1], Kotlinska J.H.[1], Trzcinska R.[2], Silberring J.[2,3]

[1]Department of Pharmacology and Pharmacodynamics, Medical University, Lublin, Poland
[2]Centre of Polymer and Carbon Materials, Polish Academy of Sciences, Zabrze, Poland
[3]Faculty of Materials Science and Ceramics, AGH University of Science and Technology, Cracow, Poland

Drug reward and phenomenon of sensitization play a crucial role in the development of drug dependence. It has been proposed that sensitization exhibits an important function in the etiology and maintenance of drug seeking behavior as well as in relapse to this behavior after a period of drug abstinence (Robinson and Berridge 1993; Stewart and Badiani 1993). The endogenous brain opioid system is believed to play an important role in mediating reward effects of many psychostimulants. Therefore the aim of the present study was to investigate whether a novel derivate of kisspeptin-10 with affinity to NPFF receptors – kissorphin (KSO) (Tyr-Asn-Trp-Asn-Ser-Phe-NH_2) affects the acute hyperlocomotor effect of morphine (10 mg/kg, *s.c.*) and ethanol (2.4 g/kg, 20% w/v, *i.p.*), and influences the expression of morphine- and ethanol-induced sensitization to their hyperlocomotor effects. Sensitization to the hyperlocomotor effect of ethanol and morphine was induced according to the previously established methods (Kotlinska *et al.* 2007).

Our study indicated that acute administration of KSO (1, 3 and 10 nmol/300 µl, intravenously (*i.v.*) inhibited the expression of morphine- and ethanol-induced sensitization at all used doses. Furthermore, KSO inhibited the acute hyperlocomotor effect of morphine at doses of 3 and 10 nmol/300 µl and acute hyperlocomotor effect of ethanol at the dose of 10 nmol/300 µl. KSO, given alone, did not change the locomotor activity of mice. In conclusion, our experiments indicated that KSO attenuated the acute morphine and ethanol hyperlocomotor effect and the expression of sensitization to the hyperlocomotor effect of morphine and ethanol. Therefore we anticipate that KSO may be involved in both of these effects and may reveal anti-opioid activity.

|A21|

Role of astrocytes in nigrostriatal system degeneration. HPLC analysis of dopamine and its metabolites after glia and neurons dysfunction

Glowacka U., Olech L., Kuter K.

Department of Neuropsychopharmacology, Institute of Pharmacology, Polish Academy of Sciences, Cracow, Poland

Objectives: Our aim was to investigate if prolonged energetic dysfunction of astrocytes would induce dysfunction of dopaminergic neurons in substantia nigra (SN) and striatum (STR), or influence dopaminergic neurotransmission changed by selective anti-dopaminergic toxin injection.

Background: The degeneration of dopaminergic neurons in SN is underlying cause of movement disorders observed in Parkinson's disease (PD). The role of astrocytes supporting those neurons in both energetic an trophic way is still unrecognized. It is probable that prolonged dysfunction of astrocytes could increase dopaminergic neurons vulnerability.

Material and methods: We have prepared PD rat model of selective nigrostriatal dopaminergic system degeneration by intracerebral, stereotaxic injection of 3 µg/3 µl 6-hydroxydopamine (6-OHDA) into medial forebrain bundle (MFB). Astrocytes dysfunction was induced by 7-days constant infusion of fluorocitrate (FC, 0.5 µl/hr) into SNc using osmotic ALZET minipumps. Control animals received solvent (0.2% ascorbic acid) into MFB and blank cannulas into SNc. Animals were sacrificed 1 or 4 weeks later. HPLC-EC analysis of DA, its metabolites and turnover rates in SN and STR was performed.

Results: Selective dopaminergic neurons lesion caused decrease in DA, DOPAC and 3-MT levels in STR and SN already after one week, and after 4 weeks this decrease further progressed. Increased turnover rates suggested compensatory mechanisms in STR. Induced metabolic dysfunction of astrocytes in SN caused decrease in DA level in STR, only after one week. No change in DA was observed in SN, but its metabolites DOPAC and HVA increased significantly after 7 days, and returned to almost control levels after 4 weeks. Double (glial and neuronal) dysfunction enhanced DA and metabolites decreases in STR after one week, but no further aggravation with time was detected. No enhancement of deficits was visible in SN, probably due to increased DA metabolism and turnover.

Conclusions: We conclude that astrocytes dysfunction seriously influences DA metabolism and accelerates dopa-

minergic transmission breakdown after neuronal degeneration.

The study was supported by the NCN grant nr 2012/05/B/NZ4/02599.

|A22|

Influence of caffeine and selective antagonists of adenosine A_1 and A_{2A} receptors on DA and 5-HT release induced by MDMA in the mouse striatum

Gorska A.M., Golembiowska K.

Department of Pharmacology, Institute of Pharmacology, Polish Academy of Sciences, Cracow, Poland

MDMA (3,4-methylenedioxymethamphetamine) used recreationally is the main component of ecstasy tablets which also contain another psychostimulants such as caffeine (CAF) to gain stronger effect. Amphetamines cause an increase in motor activity, anxiety, aggression. Their chronic use can lead to mental disorders like schizophrenia or depression and may influence progression of neurodegenerative diseases.

The pharmacological action of amphetamines is directed primarily at neurotransmitter systems: catecholamines – dopamine (DA), norepinephrine (NA) and serotonin (5-HT). Amphetamines cause increase in monoamines level in the synaptic cleft by blocking their reuptake and inhibit their inactivation through monoamine oxidase A and B. CAF is a weak stimulant without abuse properties. It abolishes mental fatigue and improves thinking. Pharmacological mechanism of CAF is based on blockade of adenosine A_1 and A_{2A} receptors which may affect neurotransmitter release. Our earlier data have shown that CAF (10 mg/kg) given together with MDMA (20 or 40 mg/kg) potentiated stimulatory effect of MDMA on extracellular level of DA and 5-HT in the mouse striatum.

In the present study we aimed to understand, if potentiating effect of CAF on DA and 5-HT release produced by MDMA occurs via blockade of adenosine A_1 and A_{2A} receptors.

All experiments were conducted on wild-type male mice from the breeding in the Institute of Pharmacology, PAS, weighing 20-35 g. Animals were anaesthetized with ketamine (7.5 mg/kg) and xylazine (1 mg/kg) and a vertical microdialysis probes were implanted into the striatum (AP: +1.0, L: +1.8, V: –3.8). The following drugs were injected intraperitoneally: MDMA (20 or 40 mg/kg), CAF (10 mg/kg), KW-6002 (1.25 or 2.5 mg/kg), DPCPX (1.25 or 2.5 mg/kg). The extracellular concentration of DA, 5-HT and extraneuronal DA metabolite, 3-methoxytyramine (3-MT) was quantified by HPLC with coulochemical detection.

Both adenosine A_1 and A_{2A} receptor antagonists, similarly to CAF, enhanced DA and 5-HT release induced by MDMA. However, adenosine A_1 receptor antagonist only weakly influenced DA and 5-HT release induced by MDMA. To the contrary, adenosine A_{2A} receptor antagonist markedly increased effect of MDMA on DA and 5-HT release. It can be speculated that effect of CAF on MDMA-induced release of DA and 5-HT in the mouse striatum is mediated mainly by adenosine A_{2A} receptors.

Supported by grant from National Centre of Science (NCN) no 2013/11/N/NZ7/00740.

|A23|

Involment of calcium channels and receptors in neuronal soce

Gruszczynska-Biegala J.[1], Sladowska M.[1,2], Kuznicki J.[1]

[1]International Institute of Molecular and Cell Biology, Warsaw, Poland
[2]Undergraduate student from the Warsaw University of Life Sciences – SGGW, Warsaw, Poland

Changes in the intracellular calcium (Ca^{2+}) concentration are considered to be one of the crucial signalling pathways in cells. Increased concentration of Ca^{2+} in cytoplasm is caused by influx from extra- or intracellular sources of Ca^{2+}. In non-excitable cells, such as lymphocytes, store-operated calcium channels (SOCCs) are the primary pathway for the Ca^{2+} influx. The extracellular Ca^{2+} influx through the tightly regulated SOCCs in the plasma membrane (PM) is the basis of the store-operated Ca^{2+} entry (SOCE). The process relies on refilling the cytoplasm and the endoplasmic reticulum (ER) with Ca^{2+} after their IP_3-dependent release to the cytoplasm. The key proteins involved in this process are sensors of Ca^{2+} located in ER (STIM1 and STIM2) and the Ca^{2+} channel-forming protein (ORAI1) present in the PM. Interaction between these proteins leads to formation of complexes, visible under the fluorescent microscopy as puncta, and results in entry of Ca^{2+} into the cytoplasm. Ca^{2+} is then transported to ER by the activity of the Ca^{2+}-ATPase of SERCA pump, which refills ER stores. In contrast to non-excitable cells, Ca^{2+} homeostasis in neurons is maintained primarily by voltage-gated calcium channels (VGCCs) as well as ion exchangers or

various receptors (e.g. metabotropic and ionotropic glutamate receptors). Recent studies demonstrate that SOCE also occurs in neurons. Our earlier data indicate that both STIMs are involved in calcium homeostasis in neurons, but each plays a distinct role in SOCE (Gruszczynska-Biegala *et al.*, PLoS ONE 2011) and can form complexes with endogenous ORAI1 (Gruszczynska-Biegala and Kuznicki, J Neurochem 2013). Recently, SOCE has become a subject of intense research in regard to disturbances in Ca^{2+} homeostasis observed in the epilepsy and neurodegenerative diseases (Steinbeck *et al.*, Exp Neurol 2011).

The aim of this study is to determine if, in addition to ORAI1, there are neuronal specific channels or receptors, which interact with STIM proteins during SOCE. The potential PM partners of STIMs, VGCC, glutamate receptors and Na^{+}-Ca^{2+} exchanger, were selectively inactivated by chemicals in order to assess their role in SOCE in cortical neurons prepared from 19-day-old embryonic Wistar rat brains. After 16 days of culture, single-cell Ca^{2+} levels in neurons were recorded using the ratiometric Ca^{2+} indicator dye Fura-2AM in the presence of different inhibitors such as nimodipine (VGCC), MK-801 (NMDAR), MCCG (mGluR), bepridil (exchanger). In some experiments neurons were treated with thapsigargin to deplete the ER stores following the Ca^{2+} re-addition to assess SOCE. The difference between Ca^{2+} response after treatment of neurons with inhibitors and response without them showed whether and how much Ca^{2+} influx is sensitive to the blockers of potential STIMs partners. The discovery of the new proteins interacting with STIM proteins will allow a better understanding of the mechanisms of SOCE.

This work was supported by funds from a National Science Centre (2011/01/D/NZ3/02051, JGB).

|A24|

Influence of P2X7R antagonist on glia activation in the early time point of EAE

Grygorowicz T.[1], Lenart J.[2], Lenkiewicz A.[1], Struzynska L.[1]

[1]Laboratory of Pathoneurochemistry, Department of Neurochemistry, Mossakowski Medical Research Centre, Polish Academy of Sciences, Warsaw, Poland
[2]Laboratory of Pharmaconeurochemistry, Department of Neurochemistry, Mossakowski Medical Research Centre, Polish Academy of Sciences, Warsaw, Poland

Multiple sclerosis (MS) is an autoimmune, neurodegenerative disease which is the most frequently the reason of disabilities of young adults, and is a very serious problem for contemporary medicine.

Progressively developing plaques of demyelination with oligodendrocyte and axonal death are observed during the course of MS. Within the central nervous system astroglia and microglia are important players in inflammation. Responding to the inflammatory signal, they become activated, change their morphology, release cytokines and up-regulate marker-proteins such as GFAP and Iba1, respectively. Both of these cell populations express purinergic receptor P2X7 which is likely involved in mechanisms connected with proinflammatory cytokine (IL-1b) release and cell death.

Experimental autoimmune encephalomyelitis (EAE) is a commonly used model of MS. EAE is evoked by injection of vaccine containing complete Freund's adjuvant, homogenate of guinea pigs' spinal cord and inactivated *Mycobacterium tuberculosis*. Animals, female Lewis rats, develop neurological symptoms similar to those observed in humans during MS.

The aim of this study was to investigate whether blocking of P2X7R by its selective antagonist BBG (Brilliant Blue G) influences the expression of astroglia and microglia specific proteins during the course of EAE.

In the inductive phase of EAE (4th day post immunization, 4 dpi) we observed an early activation of both astroglia and microglia, which was connected with overexpression of GFAP and Iba1, respectively. Overexpression of markers was also present at the peak of the disease (10 dpi). To elucidate the involvement of P2X7R in the mechanisms of glia activation during EAE, we examined brain tissue of EAE rats treated with BBG (50 mg/kg of body weight) starting from day 0 pi to day 6 pi. The immunofluorescent staining of brain specimens at 4 and 10 dpi, revealed decreased astroglia activation.

The activation of astroglia measured by fluorescence intensity showed that the immunoreactivity of GFAP in EAE group was 7-fold higher than that in EAE + BBG group at 4 dpi. At the peak of the disease the immune reactivity was 2-fold higher in EAE group than in EAE + BBG group. These results were confirmed by Western Blot analysis and qPCR.

Microglia activation in EAE group started at 4 dpi and proceed to the peak of the disease. In EAE + BBG group activated microglial cells were not observed before the peak of the disease. Intensity of the immunoreactivity in EAE group was 2-fold higher than in EAE + BBG group at 4 dpi. These results were also confirmed by Western Blot analysis and qPCR.

We may conclude that administration of BBG during the course of EAE results in the decreased reactivity of glial cells pointing out that P2X7R is actively involved in the mechanisms of cell activation during the disease.

Supported by grant no: 2012/05/N/NZ4/02191.

|A25|

Paracrine effect on energy metabolism of cholinergic SN56 cells in cytotoxic conditions

Gul-Hinc S., Ronowska A., Bielarczyk H., Szutowicz A.

Department of Laboratory Medicine, Medical University of Gdansk, Gdansk, Poland

Microglial cells, through the proinflammatory mediators are key elements initiating inflammatory reactions in the brain. They are linked with pathomechanism of Alzheimer's and other neurodegenerative diseases. Prolonged study of microglial cells have shown their neuroprotective, as well as neurotoxic effects on cholinergic neurons. The aim of this work was to investigate modifying effects of microglia on cholinergic neuronal SN56 cells subjected to common neurotoxic signals. One of this factors is zinc. Chronic exposure of differentiated (DC) SN56 cells to 0.150 mM Zn caused inhibition of pyruvate dehydrogenase (PDH) and aconitase activity (50%), decrease of acetyl-CoA level (30%), as well as loss of cell viability (60%). This results are consistent with our earlier findings (Ronowska *et al.* 2007). To investigate the paracrine effect of microglial cells on cholinergic SN56 we used conditioned medium of microglial cells. We reveal that conditioned medium of microglial cells has no effect on the survival of SN56 cholinergic cells, as well as activities of studied enzymes. Despite of that, conditioned medium of microglial cells partially prevented Zn-induced loss of DC viability to 20%, as well as PDH and aconitase activity, and acetyl-CoA level. These data demonstrate that neuroprotective effects of conditioned medium of microglial cells in Zn-challenged cholinergic neurons were linked with alterations in their acetyl-CoA metabolism. To clarify the molecular mechanism of this paracrine interactions more research is needed.

Supported by projects: GUMed ST-57, MN-15.

|A26|

Lowered expression of gliosis-associated markers in aging rats fed a high-fat diet

Gzielo-Jurek K.[1], Setkowicz Z.[1], Kielbinski M.[1], Ploszaj J.[1], Janeczko K.[1], Gazdzinski S.[2]

[1]Department of Neuroanatomy, Jagiellonian University, Cracow, Poland
[2]Military Institute of Aviation Medicine, Warsaw, Poland

Introduction: Obesity is strongly associated with insulin resistance and type 2 diabetes, hypertension, dyslipidemia. Together with abdominal obesity, these symptoms are recognized as a condition called metabolic syndrome (MS). MS is recognized as one of the main causes of avoidable mortality and morbidity in developed countries. In Poland it affects up to 25% of the population. In addition to the cardiovascular risks associated with MS, it is being increasingly recognized as a potential source of neurological disease, especially in aging patients. Obesity or MS are associated with loss of brain-derived neurotrophic factor (BDNF) signaling, oxidative stress, blood-brain barrier dysfunction and chronic inflammation. Here, we used rats fed a high-fat diet (HFD), consisting of 40% fat, 40% sugar and 10% fiber. The animals were maintained on either HFD or normal chow for a year, to simulate obesity-associated effects in the aging brain. We then studied glial activation by immunohistochemical (IHC) staining for astrocytic marker GFAP and microglial protein Iba-1.

Material and methods: Male Wistar rats were assigned randomly to HFD or normal diet (ND) groups at age of 45-50 days, then placed in single cages with constant access to the type of food assigned. The experimental animals were then maintained on their respective diets for a year, followed by sacrifice and perfusion fixation with 4% formalin in PBS. Brains were processed into 30 µm slices with a vibratome, and IHC for GFAP and Iba-1 were performed. The resulting slides were then photographed under a 4x objective. Panoramic images of whole stained hippocampi were assembled with Microsoft ICE. Next, an unsupervised local thresholding algorithm based on the Bernsen method, implemented in ImageJ, was used to measure the immunoreactive area fraction in the hippocampal formation. The resulting data were compared by Student's *t*-test.

Results: Somewhat surprisingly, we have found a significant ($p < 0.005$) reduction in immunopositive area fraction for both markers in animals from the HFD group. This is in accordance with the results of behavioral and magnetic resonance studies in the same population of animals, performed recently by our research group. In these studies, animals fed a HFD for 12 months exhibited better

spatial learning in the radial arm maze paradigm in comparison to controls. Similarly, the levels of *N*-acetylo-aspartate, loss of which is generally associated with aging-related changes and dementia, was higher in the HFD group. Further morphometric studies of astrocytes and microglial cells are underway, aimed at elucidating the nature of the effects of HFD in aging rats.

This work was supported by NCN 2011/03/B/NZ4/03771.

|A27|

Neuroprotective effects of undecylenic acid (UDA) against hydrogen peroxide-, staurosporine- and doxorubicin-induced cell damage in human neuroblastoma SH-SY5Y cells

Jantas D.[1], Piotrowski M.[2], Lason W.[1]

[1]Departament of Experimental Neuroendocrinology, Institute of Pharmacology, Polish Academy of Sciences, Cracow, Poland
[2]Jerzy Haber Institute of Catalysis and Surface Chemistry, Polish Academy of Sciences, Cracow, Poland

Undecylenic acid (UDA), a naturally occurring an 11-carbon unsaturated fatty acid has been used from several years as an economical antifungal agent and nutritional supplement. Recently, an additional clinical utility of UDA has been proposed as a promising component of nanocarriers for the oral delivery of proteins and peptides. Moreover, the potential usefulness of UDA as neuroprotective drug has been suggested, based on the ability of this agent to inhibit μ-calpain activity. In order to provide more evidence on neuroprotective potential of UDA, we tested this compound against oxidative stress (hydrogen peroxide)- and pro-apoptotic factors (staurosporine and doxorubicin)-evoked cell damage in human neuroblastoma SH-SY5Y cells. The data showed that UDA (1-40 μM) decreased the hydrogen peroxide-induced cell damage as confirmed by MTT reduction and LDH release assays. Moreover, the protection mediated by UDA in that model was connected with attenuation of hydrogen peroxide-mediated necrotic (PI staining) and apoptotic (caspase-3 activation) changes. Using Western blot analysis we demonstrated that UDA attenuated the hydrogen peroxide-stimulated increase in 145 kDa and 120 kDa of α, β spectrin II products, specifically cleaved by calpains and caspases, respectively. Next, we showed that UDA partially protected SH-SY5Y cells against the staurosporine- and doxorubicin-evoked cell death, however this effect was not connected with its influence on caspase-3 activity. Further studies at the St model of cell injury revealed that UDA decreased the St-induced mitochondria-cytosolic translocation of AIF (Apoptosis Inducing Factor) which is responsible for caspase-3 independent execution of apoptotic cell death. Finally, we demonstrated that inhibitor of PI3-K/Akt (LY294002) but not MAPK/ERK1/2 (U0126) pathway blocked the protection mediated by UDA in all tested models of neuronal cell injury. The data showed neuroprotective effects of UDA in various models of SH-SY5Y cell injury with the involvement of activation of pro-survival PI3-K/Akt pathway in that effect. Moreover, both caspase-3-dependent and -independent mechanisms could be involved in the mechanism of UDA-mediated protection in SH-SY5Y cells.

|A28|

Altered arginine metabolism in cells transfected with human wild type amyloid precursor protein (APP)

Jesko H.[1], Wilkaniec A.[1], Cieslik M.[1], Hilgier W.[2], Gassowska M.[1], Strosznajder J.B.[1], Lukiw W.J.[3], Adamczyk A.[1]

[1]Department of Cellular Signalling, Medical Research Centre, Polish Academy of Sciences, Warsaw, Poland
[2]Department of Neurotoxicology, Medical Research Centre, Polish Academy of Sciences, Warsaw, Poland
[3]Neuroscience Center of Excellence and Departments of Neurology and Ophthalmology, Louisiana State University Health Sciences Center, New Orleans, USA

Amyloid-beta (Aβ) peptide, the product of Aβ precursor protein (APP) proteolysis plays a central role in Alzheimer's disease (AD). Recent evidence suggests that alteration of urea cycle enzymes might be also involved in AD pathology. Our previous results showed that Aβ is associated with the induction of oxidative/nitrosative stress and stimulation of arginine metabolism by Nitric Oxide (NO) synthase (NOS). Although urea cycle is associated with the citrulline-NO pathway, the impact of Aβ on arginine degradation by its enzymes is unknown. Therefore, in the present study we investigated the expression of genes involved in the urea cycle in rat pheochromocytoma (PC12) cells overexpressing human wild type APP (*APPwt*). We compared gene expression levels of neuronal, endothelial and inducible *NOS* isoforms (*NNOS*, *ENOS*, *INOS*), urea cycle enzymes and corresponding amino acids in control PC12 and APPwt cells. Expression of each *NOS* isoform and urea cycle enzymes: Arginase-1 (*ARG1*) and Arginase-2 (*ARG2*),

Ornithine carbamoylotransferase (*OTC*), Argininosuccinate synthase (*ASS*), Arginosuccinate Lyase (*ASL*) and Ornithine Decarboxylase 1 (*ODC1*) was measured using quantitative Real-Time RT-PCR. Determination of amino acids arginine, ornithine and citrulline were carried out by high performance liquid chromatography (HPLC). Moreover, we investigated the changes in miRNAs responsible for modulation of gene expression of urea cycle in AD brains. Our data demonstrated that the overexpression of human wild-type *APP* in PC12 cells resulted in elevation of intracellular and secreted Aβ. The expression of urea cycle genes is disturbed both in *APPwt*-transfected PC12 cells and in AD brains. The expression of *ARG1* and *ARG2* enzymes which are responsible for the lysis of arginine to ornithine and urea was significantly reduced in APPwt cells by about three- and two-fold, respectively. *ODC1*, which catalyzes the decarboxylation of ornithine to form putrescine was reduced in APPwt cells by 36%. The expression of *ASS* that catalyzes the condensation of citrulline and aspartate to form argininosuccinate was also down-regulated in APPwt cells by 24% without changes in *ASL* gene expression. Our results indicated that arginine, the substrate for both NO synthesis and urea cycle, was unchanged in APPwt cells comparing to control. However, citrulline and ornithine were found to be significantly elevated in APPwt cells by 22% and 14%, respectively. We then investigated how the expression of *NOS* isoforms changed in each cell lines. Real-time PCR analysis revealed significant elevation of *NNOS* and *ENOS* mRNA by about six-fold and 50%, respectively in APPwt cells comparing to control, whereas *iNOS* was not detectable. In addition, we have found elevated level of miRNA-9 and -128a in AD brains that might modulate the expression of *ASS* and *NOS*, respectively. These results indicated that Aβ peptide is involved in the urea cycle modification in PC12 cells. We conclude that this peptide might have important role in AD pathomechanism via alteration of the arginine metabolism by NOS and urea cycle enzymes.

Supported from IMDIK statutory theme 17.

|A29|

TLR2 and TLR4 antagonists act like analgesics and potentiate opioids effectiveness under neuropathic pain

Jurga A.M., Rojewska E., Kolosowska N., Popiolek-Barczyk K., Makuch W., Przewlocka B., Mika J.

Department of Pain Pharmacology, Institute of Pharmacology, Polish Academy of Sciences, Cracow, Poland

Neuropathic pain is one of a current major clinical problems since its pathogenesis is still not known. It may appear as a consequence of nervous system damage or as a co-symptom of many diseases. There is rising amount of hypotheses indicating toll like receptors (TLRs) to play a role in neuropathic pain development and that TLR-dependent glial activation reduce opioids analgesia. The goal of our experiments was to evaluate the contribution of TLR2 and TLR4 in modulation and maintenance of neuropathic pain and their ability to amplify the morphine and buprenorphine effectiveness in neuropathic pain model. Experiments were performed on Wistar male rats and consisted of biochemical analysis (Western blot, qPCR) of the lumbar ipsilateral spinal cord tissue and behavioral tests (von Frey's for tactile allodynia, cold plate for thermal hyperalgesia). Neuropathic pain was developed using Bennett's model (chronic constriction injury (CCI) to the sciatic nerve). TLR antagonists were administered once per day for 7 days after CCI: LPS-RS (TLR4&TLR2 antagonist) and LPS-RS Ultrapure (TLR4 specific antagonist) – allodynia and hyperalgesia were measured 1-3 hours after drug administration on day 2 and 7 after CCI. Opioids (morphine or buprenorphine) were injected once on day 7, after CCI and 60 min after morning antagonists administration. All experiments were carried out according to the recommendations of International Association for the Study of Pain (Zimmermann *et al.* 1983) and the NIH Guide for Care and Use of Laboratory Animals and were approved by the Local Bioethics Committee (Cracow, Poland). Biochemical analysis shows on day 7 after CCI the strong up-regulation of TLR2 and TLR4 mRNA and protein levels as measured on the ipsilateral dorsal (L4-L6) spinal cord level as compare to the naïve rats. Repeated intrathecal administration of LPS-RS and LPS-RS Ultrapure attenuated allodynia and hyperalgesia as measured by von Frey and cold plate tests. Additionally, we examined if chronic administration of TLR receptor antagonists influence opioids analgesia on 7th day. Our preliminary data suggest that both TLR2 and TLR4 indeed play significant role in neuropathic

pain development, since their levels are elevated in neuropathic pain conditions.

Grant OPUS 2011/03/B/NZ4/00042.

|A30|

Contribution of CCK_A receptors to cardiovascular and respiratory effects of cholecystokinin in anesthetized rats

Kaczynska K., Szereda-Przestaszewska M.

Laboratory of Respiratory Reflexes, Mossakowski Medical Research Centre, Polish Academy of Sciences, Warsaw, Poland

Cholecystokinin (CCK) is a neurotransmitter, neuromodulator and a gastrointestinal hormone present in the central and peripheral nerve terminals and in endocrine cells. Within the brain CCK is engaged in feeding/satiety, pain/analgesia, panic/anxiety and neurological disorders.

In the nodose ganglia, abounded with cell bodies of primary afferent fibers transmitting sensory information from the cardiorespiratory organs, mRNA for CCK_A and CCK_B receptors is expressed. Nucleus of the solitary tract, a key brainstem area for the integration of autonomic functions, receiving projections from afferents of the nodose ganglia, displays immunoreactivity for CCK and its receptors.

Therefore, we investigated a share of vagal input at infra- and supra-nodosal level and the contribution of CCK_A and CCK_B receptors to the cardiorespiratory responses produced by an intravenous injection of cholecystokinin in anesthetized rats.

Cholecystokinin administered intravenously at a dose of 50 µg/kg induced short-lived decline in tidal volume and respiratory rate resulting in depression of minute ventilation. Mid cervical vagotomy had no effect on CCK-evoked ventilatory changes, whereas supranodosal denervation abolished slowing down of the breathing. Cardiovascular response to the CCK challenge was characterized by a transient decrease, followed by an augmentation in the mean blood pressure (MAP) in the intact animals. Following vagotomy performed at both levels, the declining phase of MAP was abrogated. Blood pressure changes were associated with decreased heart rate present in all neural states. All cardiovascular and respiratory effects were antagonized by pretreatment with devazepide – CCK_A receptors' antagonist, whereas CI988 – an antagonist of CCK_B receptors, was ineffective.

In conclusion, our results indicate that CCK modulates slowing down of respiratory rhythm via CCK_A receptors located in the nodose ganglia, and depresses tidal volume via the central CCK_A dependent mechanism. CCK-evoked declining in blood pressure may be due to the activation of vagal afferents, whereas pressor responses seem to be possibly mediated by the activation of CCK_A receptors in the vasculature and/or central nervous system. Bradycardia was probably induced by the direct action of CCK on heart pacemaker cells.

|A31|

Involvement of 5-HT_{1A} receptors in mirtazapine and risperidone co-treatment effect on NA, DA and 5-HT extracellular level in the rat frontal cortex

Kaminska K.[1], Golembiowska K.[1], Rogoz Z.[1,2]

[1]Department of Pharmacology, Institute of Pharmacology, Polish Academy of Sciences, Cracow, Poland
[2]The Podhale State Higher Vocational School, Nowy Targ, Poland

Major depressive disorder (MDD) is a chronic mental illness with a life time prevalence of 5-12% in adult men and 9-26% of adult women. Although initial antidepressant (AD) therapy significantly reduces symptoms of depression in many patients, only 50-60% of persons with MDD respond to the treatment. Moreover, ca. 30-40% of MDD patients never achieve symptom resolution by means of a standard AD therapy. The problem of AD-resistant depression has been the subject of a number of thorough studies, with no apparent therapeutic success, though. Hence, there is a strong need for an alternative antidepressant treatment. Several clinical reports have postulated a beneficial effect of an additional low dose risperidone to ongoing treatment with ADs. Like other atypical antipsychotic drugs, risperidone is known to produce minimal extrapyramidal side-effects compared to classical antipsychotics. It has been proposed that risperidone in lower doses acts mainly by blocking 5-HT_{2A} serotonin receptors, while at higher doses it mostly blocks D_2 dopamine receptors. Moreover, it has been shown that mirtazapine, a noradrenergic and specific serotonergic AD is an agonist of 5-HT_{1A} receptor and an antagonist of the central α_2-auto- and hetero-adrenoreceptors. It also blocks 5-HT_2 and 5-HT_3 receptors and displays a very low affinity for DA receptors and a high affinity for histamine H_1 ones.

The aim of our study was to understand the mechanism of clinical efficacy of combination an antidepressant and an antipsychotic in drug-resistant depression.

We studied the effect of an AD (mirtazapine) and risperidone (an atypical antipsychotic) given separately or jointly, on the extracellular levels of dopamine (DA), serotonin (5-HT) and noradrenaline (NA) in rat frontal cortex. The animals were given single intraperitoneal injections of risperidone (1 mg/kg) and mirtazapine (10 and 20 mg/kg). The release of monoamines was investigated using a microdialysis in freely moving animals, and assayed by HPLC with coulochemical detection.

Mirtazapine dose-dependently increased the cortical extracellular levels of DA, 5-HT and NA. Similarly, risperidone increased the cortical extracellular levels of the monoamines studied. The combination of mirtazapine (20 mg/kg), or both doses of mirtazapine (10 and 20 mg/kg), with risperidone produced significantly stronger release of DA and NA, respectively (but not of 5-HT release) compared to the effect of administration of a single drug. The increase in the DA (but not NA) release induced by mirtazapine plus risperidone was partly blocked by the selective 5-HT_{1A} antagonist WAY 100635 (0.2 mg/kg).

The obtained results suggest that the ability of risperidone to augment the therapeutic efficacy of mirtazapine in treatment-resistant depression may be due, at least in part, to the potentiation of mirtazapine-induced increases in cortical DA and NE. Furthermore, among other mechanisms, 5-HT_{1A} receptors may play some role in this action.

This study was financially supported by statutory funds of the Institute of Pharmacology, Polish Academy of Sciences, Cracow, Poland.

|A32|

Brain swelling after pilocarpine-induced epilepsy: effect of cerebral malformation in rats

Kielbinski M.[1], Gzielo-Jurek K.[1], Setkowicz Z.[1], Banasik T.[2], Ploszaj J.[1], Weglarz W.[2], Janeczko K.[1]

[1]Department of Neuroanatomy, Jagiellonian University, Cracow
[2]Laboratory of In Vivo Imaging, Institute of Nuclear Physics, Polish Academy of Sciences, Cracow

Brain edema and gliosis accompany neuronal loss as the main effects of epileptic seizures, both in patients and in animal models, such as pilocarpine administration.

Cerebral malformations in humans are strongly associated with intractable epilepsy, especially in pediatric patients. The most prevalent of these is the focal cortical dysplasia (FCD), a cryptogenic malformation of brain development resulting in loss of cortical lamination, formation of cortical and subcortical ectopias, disrupted white matter and other abnormalities. Animal models aimed at simulation of these phenomena rely on controlled physical or pharmacological disruption of neurodevelopment. The onset of this disruption, i.e. the day of gestation when the stimulus is applied, determines the pattern of changes and their severity.

Here, we used prenatal gamma irradiation at embryonic days E13, E15, E17 or E19 in comparison with untreated controls, to elucidate the effects of irradiation-induced dysplasia on the volume of different brain structures. We have previously shown that the presence of dysplastic changes interacts with epileptogenic factors affecting seizure susceptibility and the expression of glial and neuronal markers. We hypothesize that after pilocarpine injection – a widely studied model of epileptic seizures – different patterns of dysplasia would differentially affect the resulting changes in brain volume.

Animals irradiated with a dose of 1 Gy at E13 (N = 11), E15 (N = 9), E17 (N = 9) or E19 (N = 8), as well as normal controls (N = 10) were given pilocarpine (250 mg/kg) at P60. After 72 h the animals were sacrificed, perfused transcardially with 10% formalin and the brains were removed. T2-weighed images taken with a 9.4 T magnetic resonance scanner were then obtained. Using a computer-assisted Cavalieri method, the volumes of the entire brain, hippocampus and brainstem structures (midbrain, pons and medulla oblongata) were estimated. Volumes were compared between groups to show differentially affected regions. Also, within each group, comparisons were made with age-matched untreated animals: irradiated at E13 (N = 12), E15 (N = 12), E17 (N = 12) or E19 (N = 12) and naïve controls (N = 14). ANOVA with HSD corrected for unequal N or Student's t-tests were used.

In both pilocarpine-treated and untreated animals, brain volume was reduced in a time-dependent manner, with animals irradiated earlier showing a more profound loss in brain volume. In animals after pilocarpine injection, hippocampal volume normalized to whole brain volume follows an opposite trend, with greatest effects in animals irradiated at E17 or E19. In addition, pair-wise comparison of naïve vs. pilocarpine treated rats revealed an attenuated effect of seizures on brain and hippocampal volume in animals irradiated at E19. This is consistent with the notion that dysplasia modifies the effects of pro-convulsive stimuli, with effects depending on the onset of disturbed neurogenesis.

Supported by National Center for Science (NCN) grants DEC-2012/05/N/NZ2/00641 and 2011/01/B/NZ4/00586.

|A33|

Neurochemical changes linked to antipsychotic-like phenotype of mGlu4 knockout mice

Kleczek N.[1,2], Slawinska A.[1], Marciniak M.[1], Wieronska J.[1], Pilc A.[1]

[1]Department of Neurobiology, Institute of Pharmacology, Polish Academy of Sciences, Cracow, Poland
[2]Department of Neurophysiology and Chronobiology, Institute of Zoology, Jagiellonian University, Cracow, Poland

Introduction: The metabotropic glutamate 4 (mGlu4) receptor has been proposed as an important target in the search of novel antipsychotic drugs. Several orthosteric and allosteric activators of that receptor were shown to possess antipsychotic effects in animal models of schizophrenia. In the present study we investigated the role of mGlu4 receptor in the pathophysiology of schizophrenia. We used mGlu4 knockout mice to see, if the lack of the receptor results in any behavioral changes in animal models of psychosis. Moreover, we investigated a possible neurochemical changes in the selected proteins known as the markers of psychosis, e.g. 5-HT1A receptor, GAD65 and GAD67 enzymes. The level of proteins was investigated in the stratum, hippocampus and prefrontal cortex.

Material and methods: Adult C57BL/6J mice with mGlu4 receptor knockout (mGlu4 KO) and wild type (WT) mice were used in this study. Mice with mGlu4 receptor knockout were generated in Institute of Pharmacology, Polish Academy of Sciences in Krakow. Animals were maintained under standard laboratory condition on 12-hour light/12-hour dark cycle at a room temperature of 19-22°C with free access to food and water. To investigate phenotype of mGlu4 KO we used behavioral models of selected symptoms of schizophrenia, such as DOI-induced head twitches and one-trial recognition task. Animals were treated with GABAB antagonist CGP 55845 (10 mg/kg, *i.p.*) or 5-HT1A antagonist, WAY 100635 (0.2 mg/kg, *s.c.*), 30 and 45 min before test, respectively. The relative mRNA expression of 5-HT1a receptor, GAD-65 and GAD-67 enzymes was measured with the use of quantitative Real-Time Reverse Transcriptase PCR.

Results: Knockout mice had a reduced response to psychostimulant in DOI-head twitches reflected by decreased number of episodes, as well as less sensitivity to MK-801-induced disruption in one-trial recognition task. The behavioral effect observed in mGlu4 knockouts in DOI-induced head twitches was reversed after administration of CGP 55845 and WAY 100635. In the mRNA studies the decreased level of 5-HT1A mRNA in the frontal cortex was observed, but not in the hippocampus or striatum. In contrast, the increases in GAD-65 and GAD-67 mRNA levels in frontal cortex were noticed. The level of GAD65 mRNA was also increased in the hippocampus, but neither of GADs were changed in the stratum.

Conclusions: The present study shows an antipsychotic-like phenotype of mGlu4 mutant mice which can be reversed by GABAB antagonist (CGP55845) or 5-HT1A antagonist (WAY100635). Furthermore, the changes in the mRNA level of selected proteins known to be important in schizophrenia are relevant to the phenotype observed in the behavioral studies and stays in line with human studies.

|A34|

Sildenafil, an inhibitor of phosphodiesterase 5 (PDE5), affects asymmetric behavior and monoamine metabolism in unilaterally 6-OHDA-lesioned rats treated chronically with L-DOPA

Kmiec I., Lenda T., Kaminska K., Czarnecka A., Lorenc-Koci E.

Department of Neuro-Psychopharmacology, Institute of Pharmacology, Polish Academy of Sciences, Cracow, Poland

The dopamine replacement therapy with L-DOPA still remains the most widely used treatment for Parkinson's disease (PD). However, over time, the effectiveness of the drug decreases, while motor complications, such as dyskinesia, develop. Therefore, the search for a new therapeutic approach that can provide benefit over L-DOPA therapy is still ongoing. Recently, attention of researchers has focused on the nitric oxide (NO) – soluble guanylyl cyclase (sGC) – cyclic GMP signaling pathways in the striatum as a new target for the treatment of PD.

The aim of the present study was to examine the effects of chronic *i.p.* treatment with the phosphodiesterase 5 (PDE5) inhibitor, sildenafil in combination with the widely used antiparkinsonian drug, L-DOPA on asymmetric behavior and monoamine metabolism in the striatum (STR) and substantia nigra (SN) of unilaterally 6-OHDA-lesioned rats. The experiments were performed on male Wistar rats injected unilaterally with 6-OHDA (8 µg/4 µl) into the medial forebrain bundle. Two weeks later, rats exhibiting more than 100 contralateral rotations per 1 h in the apomorphine (0.25 mg/kg) test, indicative on an extensive loss of the nigrostriatal neurons, were treated chronically

with sildenafil (2 mg/kg) and L-DOPA (12.5 mg/kg), alone or in combination, once daily for successive 14 days. Rotational behavior was also recorded immediately after the first and penultimate doses of the examined compounds. Rats were killed 1 h after the last doses of these drugs, their STR and SN were dissected on an ice-chilled plate and stored at –80°C until further procedures were applied. The tissue concentrations of dopamine (DA) and its metabolites were determined using an HPLC method.

Our results showed that sildenafil did not evoke contralateral rotations after acute or chronic treatment. In contrast, L-DOPA produced distinct contralateral rotations already visible 10 min after its first dose and lasting almost 100 min. Moreover, after chronic L-DOPA treatment their number was higher than after its acute injection. However, after combined acute administration of sildenafil and L-DOPA, the number of contralateral rotations was markedly higher while after chronic treatment lower than in the group receiving L-DOPA alone. Regarding DA concentration, chronic sildenafil administration affected the tissue DA level neither in the ipsi- nor contralateral STR and SN. Chronic treatment with L-DOPA alone significantly increased the tissue DA content only in the ipsi- and contralateral SN when compared to the corresponding side of the 6-OHDA-lesioned groups receiving sildenafil. However, chronic combined treatment with these compounds produced markedly higher increases in the tissue DA contents in the ipsilateral STR and SN than in the group of rats receiving L-DOPA alone.

The obtained results suggest that administration of a low dose of the PDE5 inhibitor, sildenafil jointly with L-DOPA modulates rotational behavior and tissue DA concentrations in the nigrostriatal system of unilaterally 6-OHDA-lesioned rats.

This work was supported by a grant from the National Science Centre of Poland, based on decision No. UMO-2011/01/B/NZ4/01581.

|A35|

The evidence for potential of human bone marrow mesenchymal stem cells to cross the blood-barrier after their intra-arterial transplantation

Koniusz S.[1], Andrzejewska A.[1], Janowski M.[1,2], Lukomska B.[1]

[1]NeuroRepair Department, Mossakowski Medical Research Centre, Polish Academy of Sciences, Warsaw, Poland
[2]Russel H. Morgan Department of Radiology and Radiological Science, Division of MR Research, The Johns Hopkins University School of Medicine, Baltimore, USA

Introduction: Mesenchymal stem cells (MSC) have recently emerged as promising candidates for cell-based therapy in neurological disorders. Based on differentiation potential of MSC initial studies focused on the regenerative capacity of these cells. However, over time it became clear that MSC mediated their positive effect rather through the production of trophic factors. The mechanisms of action used by MSC i.e. immunomodulation, cell protection, pre-reparation and stimulation of angiogenesis have been elucidated *in vitro* but the data from pre-clinical studies have been unclear. Furthermore, the potential for minimally invasive delivery of MSC therapy in term of clinical transplantation is of particular interest. Critical questions include MSC homing to ischemic tissues from peripheral blood and the efficiency of this process. The aim of the study was to analyze the presence, distribution and quantity of human bone marrow mesenchymal stem cells (hBM-MSCs) after their intra-arterial delivery in focal cerebral ischemic rats.

Material and methods: The experiments were performed in adult male Wistar rats. To induce rat brain injury ouabain – Na/K ATPase pump inhibitor have been chosen which brings metabolic and structural cell changes that mimic ischemic deep-brain, stroke-like lesion. For the surgical procedure rats were anesthetized and immobilized in a stereotactic apparatus, then a small burr hole was drilled in the cranium over the right hemisphere, the needle was lowered into the right striatum and 1 µl/50 nmol ouabain was injected. Two days after the ischemic insult, 5×10^5 hBM-MSC (Lonza) tagged with iron nanoparticles conjugated with rhodamine (Molday, BioPAL) were transplanted into the right internal carotid artery. After 1, 3, 7, 14, 21 and 28 days post-transplantation rats were sacrificed, the brains were removed and quickly frozen. Then immunocytochemical analysis of hBM-MSC present in the brain, cervical lymph nodes and spleen was performed using anti-human (CD44, STEM121 and Ku80) antibodies.

Results: The preliminary results of ongoing studies revealed the presence of transplanted cells in the rat brain. hBM-MSC injected intra-arterially were visible in the right hemisphere in the area between cortex and stratium of ouabain-injured rat brain near the ischemic lesion. The fluorescent signal of Molday particles and positive staining for human antigens were observed until 28 days of observation after hBM-MSC transplantation.

Conclusions: Intra-arterial delivery of hBM-MSC promotes their migration to ischemic sites of the brain where they may release paracrine factors for the local or systemic effect. The further studies of hBM-MSC presence in the lymphatic tissues as well as neurotrophic, neuroprotective and immunomodulating function of transplanted cells in focal cerebral ischemic disorders are in progress.

This work was support by KNOW 06 project: "The role of bone marrow mesenchymal stem cells in CNS repair of brain ischemia disorders".

|A36|

Influence of dopamine agonists on the harmaline-induced tremor measured by force plate actimeters

Kosmowska B., Glowacka U., Wardas J., Ossowska K.

Department of Neuro-Psychopharmacology, Institute of Pharmacology, Polish Academy of Sciences, Cracow, Poland

Harmaline is a β-carboline derivative which is commonly used for modelling one of the most frequent movement disorder, essential tremor (ET), in animals and screening potential tremorolytic drugs. Oscillation frequency of the harmaline-induced kinetic/postural tremor is 10-12 Hz in rats. It is generally accepted, that the primary cause of tremor induced by this compound is an abnormal synchronous activation of the olivo-cerebellar glutamatergic climbing fibres. This activation leads to increased glutamate release in the cerebellum and induction of complex spike activity of Purkinje cells of the cerebellar cortex. However, mechanisms underlying harmaline-induced tremor seem to involve also other neurotransmitter systems.

The aim of the present study was to examine the influence of the non-selective agonists of dopamine receptors: apomorphine (D_1-D_5) and pramipexole (D_2, D_3) on the harmaline-induced tremor in rats. Propranolol (the first-line treatment of ET) was used as a reference compound. Since tremor is difficult to quantify and distinguish from other motor abnormalities in animals, this behaviour was measured objectively by fully automated Force Plate Actimeters. To quantify the intensity of the tremor, the following parameters were measured: AP1 (power in the 0-8 Hz band), AP2 (power in the 9-15 Hz band) and tremor index (difference in power between the AP2 and AP1). In order to examine the locomotor activity, the total distance travelled by an animal was also measured. In some groups of animals the focused stereotypy or AP2/distance ratio was analysed additionally.

The generalised tremor induced by harmaline administered at a dose of 15 mg/kg *i.p*. was related to an increase in the AP2 parameter and the tremor index. Propranolol injected at a dose of 20 mg/kg *i.p*. reversed both the above effects of harmaline. Apomorphine administered at doses of 0.5 and 1 mg/kg *s.c*. further enhanced AP2 and at the lower dose also the tremor index elevated by harmaline. The increase in the AP2 was stronger than an enhancement of locomotor activity induced by apomorphine in the harmaline-treated animals. Pramipexole (0.1, 0.3 and 1.0 mg/kg *s.c*.) had no effect on tremor index, but at dose of 0.1 mg/kg significantly reduced AP2 parameter.

The present study suggests that apomorphine enhances the tremor induced by harmaline, and this effect is at least partly independent of hyperactivity induced by this dopamine agonist. In addition, the results after pramipexole administration revealed the contribution of D_2/D_3 receptors in regulation of tremor in harmaline model of ET.

The study was supported by Statutory Funds of the Department of Neuro-Psychopharmacology, Institute of Pharmacology, Polish Academy of Sciences, Cracow, Poland.

|A37|

Effects of different stressors on amygdalar monoamines

Krotewicz M.[1], Bajer M.[1], Krotewicz M.K.[2]

[1]Department of Neurobiology, Faculty of Biology and Environent Protection, University of Lodz, Lodz, Poland
[2]Departament of General and Colorectal Surgery, Medical University of Lodz, Lodz, Poland

The amygdala has attracted interest as concerns its implication in emotion – behaviour interactions. The amygdala complex receives innervation from the noradrenergic, serotonergic and dopaminergic pathways originating from the brain stem. The monoaminergic systems participate in the regulation of emotional behaviour. On the other hand, it was shown that different stressors have an impact

on monoaminergic neurotransmission. In order to compare the neurochemical effects of different stressors we exposed rats to the most popular anxiety tests. The anxiety tests are widely used to study behaviour of rats in the "stress" – inducing situation. In these different ethological procedures, animals are exposed to unknown environment differing in size, shape, lighting, time of exposure etc. The most popular anxiety tests for the study of exploration and emotionality in rodents have become the open field (OF) and the elevated plus-maze (EPM). The influence of various pharmacological agents on behaviour and physiological functions have been investigated in these tests. It should also be noted that the anxiety tests are used interchangeably in the investigation of anxiety mechanisms. In the present study we undertook a simultaneous examination of noradrenergic, serotonergic and dopaminergic systems activity in the amygdala of rats exposed to one of the three anxiety tests: open field (OF), elevated plus maze (EPM) and transitions test (TT). The experiments were performed at the same time on adult male Wistar rats, housed in groups under controlled conditions. The rats were individually subjected to one of the anxiety tests (OF, EPM or TT) and sacrificed by decapitation immediately after a test procedure. The concentration of noradrenaline, dopamine, serotonin and their metabolites were determined in the amygdala using high-performance liquid chromatography with electrochemical detection. The results of our study showed that stressogenic procedure of the used anxiety tests exerted influence on indices of the monoaminergic systems activity in the amygdala. Especially, the exposure of rats to the used tests (OF, EPM and TT) was accompanied by increase in serotonin turnover in the amygdala. The obtained data revealed that the exposition of rats on the stressogenic situation deeply increase serotonin metabolism in the amygdala region. It is likely that the elevation of serotonin turnover in this emotional brain region sensitize the serotonergic system on influence of serotonergic ligands. The presented results confirm our previous observation that the transition test (TT) is a good tool to study behavioural effects of anxiolytic agents acting on serotonergic system.

|A38|

Opioid receptors expression and PGP 9.5-positive epidermal nerve fiber density in psoriasis – relationship with itch

Kupczyk P.[1], Reich A.[2], Wysokinska E.[3], Gajda M.[4], Holysz M.[5], Hwang T.[6], Kobuszewska A.[2], Nowakowska B.[1,7], Drukala J.[8], Szepietowski J.C.[2]

[1]Laboratory of Immunogenetic and Tissues Immunology, Department of Clinical Immunology, Ludwik Hirszfeld Institute of Immunology and Experimental Therapy, Polish Academy of Sciences, Wroclaw, Poland
[2]Department of Dermatology, Venereology and Allergology, Wroclaw Medical University, Wroclaw, Poland
[3]Laboratory of Molecular Immunobiology of Cancer, Department of Experimental Oncology, Ludwik Hirszfeld Institute of Immunology and Experimental Therapy, Polish Academy of Sciences, Wroclaw, Poland
[4]Department of Histology, Jagiellonian University Medical College, Cracow, Poland
[5]Department of Biochemistry and Molecular Biology, Medical University of Poznan, Poznan, Poland
[6]Department of Pharmacology, Medical University of Minnessota, MN, USA
[7]Laboratory of Cellular and Tissues Engineery, Department of Cell Biology, Division of Biochemistry, Biophysics and Biotechnology, Jagiellonian University, Cracow, Poland
[8]Laboratory of Tissues Immunology, Medical Center of Ludwik Hirszfeld Institute of Immunology and Experimental Therapy, Polish Academy of Sciences, Wroclaw, Poland

Opioid receptors (OR): *OPRM1*/MOR, *OPRK1*/KOR, *OPRD1*/DOR, *OPRL1*/ORL are highly expressed in central nervous system (CNS) and to lesser degree outside the CNS in peripheral tissues like lungs, heart, vessel walls, immune cells and in the skin. OR in the skin participate in transmission of molecular signals from CNS and control keratinocyte differentiation, proliferation, and apoptosis. OR are also suggested as potential targets for peripheral pain and itch therapy.

However, molecular studies on itch in psoriasis gave inconclusive results. The most widely discussed theory mentioned downregulation of skin nervous system and imbalance of different classes of neurobiological pathways. OR theory suggested that *OPRM1*/MOR system is responsible for promotion, while *OPRK1*/KOR system for suppressing itch signals in the skin and CNS. To prove this suggestion, 20 psoriasis patients with and without itch underwent punch biopsies from non-lesional and lesional skin. The results of study of OR expression and epidermal nerve density were compared with the clinical parameters. Itch intensity have been assessed using VAS (Visual Analogue Scale), while severity of psoriasis with

PASI (Psoriasis Area and Severity Index). Control group consisted of skin samples obtained from 20 healthy volunteers. A multiplex real-time PCR with UPL probes were used to determine gene expression of *OPRM1/ACTB* and *OPRK1/ACTB* by relative quantification analysis. Protein expression evaluation was performed by indirect immunofluorescence on skin frozen sections using anti-MOR and anti-KOR antibodies labelled with secondary fluorochrome conjugated antibodies. Fluorescence intensity analysis was done using ImageJ.

OPRM1/MOR expression was similar in all groups, while *OPRK1* gene show decreased expression in lesional psoriatic skin compared to controls. A lower expression of *OPRK1* gene was noted in patients with itch compared to those without itch. KOR expression was not significantly different in lesional and non-lesional skin of patients without itch compared to control group. Lesional skin with itch showed significantly lower KOR expression compared to non-lesional one or control group. Epidermal innervations analysis show significantly higher PGP 9.5-positive nerve density in non-lesional and lesional skin compared to control and exhibited positive correlation with VAS and reverse with PASI.

Based on our results, we believe that imbalance of *OPRK1*/KOR and constant *OPRM1*/MOR expression with downregulation of cutaneous nervous system may be relevant neurobiological and molecular pathogenic factors in psoriatic itch.

|A39|

Activity and supercomplexes assembly of mitochondrial complex I and IV in striatum during process of functional compensation for deficits in dopaminergic system in rat

Kuter K.[1], Ossowska K.[1], Dencher N.[2]

[1]Department of Neuropsychopharmacology, Institute of Pharmacology, Polish Academy of Sciences, Cracow, Poland
[2]Physical Biochemistry, Department of Chemistry, Technische Universität Darmstadt, Darmstadt, Germany

Introduction: At the early stages of Parkinson's disease (PD) motor degeneration of dopaminergic system is masked by potent compensatory mechanisms. Mitochondrial oxidative phosphorylation complexes (Cx) I, III and IV form higher order structures – supercomplexes (SCxs) that improve their function by channeling substrates, stabilizing protein assemblies and reducing ROS formation. Compensatory processes could depend on increased energetic demands for surviving cells and intracellular adaptations in mitochondrial function and structure. Our aim was to investigate if functional compensation of motor deficit after selective degeneration of dopaminergic neurons would influence activity of mitochondrial Cx I and IV and cause adaptation in their SCx assembly.

Material and methods: We have prepared PD rat model of selective nigrostriatal dopaminergic system degeneration by intracerebral, stereotaxic injection of 3 μg/3 μl 6-hydroxydopamine into medial forebrain bundle. Animals showed decreased locomotor activity 3 days after the operation and this disability was functionally compensated after 4 weeks. Using solubilized crude mitochondrial membrane fraction from striatum we performed in-gel enzymatic activity measurements of complex I and IV, after blue-native electrophoresis.

Results: Cx I amount of SCxs and individual Cx I_1, as well as performance of SCxs, (but not I_1) decreased at both time-points after operation, to the same degree. At the same time specific activities were mostly not changed. There were no significant changes in Cx IV amounts but performance of Cx IV within SCxs was decreased – mostly after 4 weeks ($I_1III_2IV_3$, $I_1III_2IV_2$). Also, specific activity of SCxs was decreased only 4 weeks after toxin injection, correlating with functional compensation in behavior. No changes were detected in Cx IV individual or dimeric form.

Conclusions: The decrease in specific activity of Cx IV in form of SCxs indicated its role in compensatory mechanisms.

The study was supported by the Statutory Funds of the Institute of Pharmacology, PAS, Cracow, Poland and Technische Universität Darmstadt, Germany, DAAD scholarship to KK.

|A40|

Gender differences in the neurochemical response of trigeminal ganglion neurons to peripheral inflammation in mice

Kuzawinska O., Lis K., Cudna A., Balkowiec-Iskra E.

Department of Experimental and Clinical Pharmacology, Medical University of Warsaw, Warsaw, Poland

The trigeminal system, with first-order neurons in the trigeminal ganglion (TG), provides sensory innervation to craniofacial tissues, many of which are associated with

chronic pain conditions, such as trigeminal neuralgias, migraines and temporomandibular joint (TMJ) disorders. Our previous studies showed that inflammatory reaction in the area of TG nociceptive endings (induced by tooth injury) affects neurochemical properties of TG ganglia, causing increase in concentration of both the neurotrophin brain-derived neurotrophic factor (BDNF) and well-established modulator of TG pain reaction – calcitonin gene-related peptide (CGRP). Moreover, our *in vitro* data showed that among three proinflammatory cytokines examined (IL-1, IL-6, TNF), only TNF was capable of influencing TG ganglia properties. In the present study, we have employed CFA-induced TG inflammation model to begin investigating the underlying molecular mechanisms of the inflammation-induced changes in trigeminal neurons properties.

A model of oro-facial inflammation was obtained by local injection of 30 µl of CFA to the mice left whisker pad. Controls were injected with the same volume of saline. Seven and 14 days after CFA injection mice were euthanized by spinal cord dislocation. Both TG ganglia were removed for quantitative PCR analysis. To study the effect of peripheral inflammatory reaction evoked by CFA administration on TG function we measured the expression of BDNF, CGRP and three proinflammatory cytokines – IL-1β, IL-6 and TNF, separately in the left and the right trigeminal ganglia, both in male and female mice, 7 and 14 days after induction of inflammation.

Our results indicate that response of TG ganglia to peripheral inflammatory reaction is gender-dependent, what may explain differences in frequency and severity of trigeminal nerve-associated disorders observed between women and men.

TG neurons in female mice showed increased expression of CGRPa, this neuropeptide may act as the main mediator of trigeminal signaling during migraine.

This project has been supported by the Polish National Science Center, based on the Decision No. DEC-2012/05/B/NZ4/02385.

Research subject implemented with CePT infrastructure financed by the European Union – the European Regional Development Fund within the Operational Programme "Innovative economy for 2007-2013".

|A41|

Maraviroc modulates neuropathic pain by the CCR5 and CCR2 chemokine receptors

Kwiatkowski K., Rojewska E., Makuch W., Mika J.

Department of Pain Pharmacology, Institute of Pharmacology, Polish Academy of Sciences, Cracow, Poland

Neuropathic pain develops as a result of pathological lesions within the nervous system. Recently were identified pronociceptive properties of chemokines and chemokine receptors. It was documented that the expression of CCR5 receptor is increased as a result of nerve injury, and it seems to be crucial for hyperalgesia and allodynia development. CCR5 is mostly expressed by microglial cells. What is more, previous research demonstrated that CCR5 and CCR2 chemokine receptors can link up in heterodimers. In order to understand the potential role of CCR5 and CCR2 in neuropathic pain, the aim of our studies was to examine the influence of selective antagonist of CCR5 receptor (maraviroc) on hyperalgesia and allodynia under neuropathy. Additionally we measured expression of CCR5, CCR2 and glial cell markers in neuropathic pain model. All experiments were carried out according to IASP rules (Zimmermann 1983). According to Yaksh and Rudy (1976) Wistar rats were implanted with intrathecal (i.th.) catheters. After seven days we performed chronic constriction injury (CCI) of the sciatic nerve according to Bennett and Xie (1988). On day 3 and 7 after CCI two behavioral tests were conducted to measure hyperalgesia (cold plate test) and allodynia (von Frey test). qRT-PCR was used to measure CCR5, CCR2, C1q and GFAP mRNA levels in spinal cord and dorsal root ganglia (DRG) in vehicle- and maraviroc-treated CCI-exposed rats. We provided evidence that chronic (once a day) i.th. administration of maraviroc attenuated the neuropathic pain symptoms on day 3 and 7 in CCI-exposed rats. qRT-PCR analysis indicate that maraviroc decreased activation of C1q-positive cells in spinal cord and DRG as measured on day 7 after CCI. Additionally we validated at the same time point that expression of CCR5 and CCR2 receptors is increased in spinal cord as well as in DRG after sciatic nerve injury. Interestingly, those changes are diminished by maraviroc chronic administration. Our results suggest that modulation of CCR5 and CCR2 by maraviroc might be a potential novel therapeutic approach for neuropathic pain treatment.

Supported by NCN2011/03/B/NZ4/00042 and statutory founds.

|A42|

Chronic treatment with a nitric oxide donor, molsidomine and L-DOPA, alone or in combination, differently affect cGMP concentration in the striatum of unilaterally 6-OHDA-lesioned rats

Lenda T., Kmiec I., Kaminska K., Czarnecka A., Konieczny J., Lorenc-Koci E.

Department of Neuropsychopharmacology, Institute of Pharmacology, Polish Academy of Sciences, Cracow, Poland

It is well-known that dopamine (DA) modulates the synthesis of second messengers: cyclic adenosine monophosphate (cAMP) and cyclic guanosine monophosphate (cGMP). DA acting via striatal DA D1 receptor stimulation, activates adenylate cyclase (AC) and initiates cAMP synthesis while via DA D2 receptor stimulation inhibits this reaction. Moreover, DA-mediated stimulation of DA D1 receptors localized on the striatal nNOS-containing interneurons initiates NO synthesis while stimulation DA D2 heteroreceptors evokes opposite effects. Hence, DA-induced initiation of NO synthesis and then NO-mediated activation of soluble guanylyl cyclse (sGC) lead to the increased cGMP production. The cGMP formation is tightly regulated not only by enzymes contributing to its synthesis but also by an enzyme involved in its degradation. In the DA-deafferented rat striatum 6-8 weeks after lesion, the cGMP level was significantly decreased while cAMP increased. Chronic treatment with L-DOPA differently affected the cAMP and cGMP levels in the striatum (STR) of dyskinetic and non-dyskinetic rats. In dyskinetic rats, the nucleotide levels dramatically decreased in the ipsi- and contralateral STR. In non-dyskinetic rats, cAMP increased while cGMP decreased only in the contralateral STR.

The aim of the present study was to examine the effects of chronic treatment with the nitric oxide donor molsidomie and L-DOPA, alone and in combination, on the cGMP concentration in the STR of unilaterally 6-OHDA-lesioned rats.

The experiments were performed on male Wistar rats injected unilaterally with 6-OHDA (8 µg/4 µl) into the medial forebrain bundle (MFB). Control, sham-operated rats received vehicle instead of 6-OHDA. Two weeks later, 6-OHDA-lesioned rats exhibiting more than 100 contralateral rotations per 1 h in the apomorphine (0.25 mg/kg) test, indicative on an extensive loss of the nigrostriatal neurons, were treated chronically with molsidomine (2 mg/kg *i.p.*) and L-DOPA (25 mg/kg *i.p.*), once daily for successive 14 days. The concentration of cGMP in the ipsi- and contralateral STR was determined 1hour after the last drug doses.

Our data show that 4 weeks after unilateral injection of 6-OHDA into the MFB, the cGMP concentrations in the ipsi- and contralateral STR were significantly increased compared to the corresponding sides of the sham-operated group receiving *i.p.* vehicle. Chronic treatment of unilaterally 6-OHDA-lesioned rats with molsidomine alone caused further increases in the cGMP levels on both sides of the STR vs. 6-OHDA-lesioned group treated i.p. with vehicle. However, chronic administration of L-DOPA alone to these rats enhanced the cGMP concentration in the contralateral STR while combined injection of molsidomine + L-DOPA increased significantly its level in the ipsilateral STR compared to the corresponding sides of 6-OHDA-lesioned group receiving *i.p.* vehicle.

The obtained results suggest that chronically administered molsidomine, can affect the occurrence of dyskinesias by modulating the striatal levels of cGMP.

This work was supported by a grant from the National Science Centre of Poland, based on decision No. UMO-2011/01/B/NZ4/01581.

|A43|

Shifted activation of NF-κB transcription factor in various cell subpopulations in rat model of cerebral ischemic stroke

Lietzau G.[1], Kowianski P.[1,2], Karwacki Z.[3], Dziewiatkowski J.[1], Domaradzka-Pytel B.[1], Morys J.[1]

[1]Department of Anatomy and Neurobiology, Medical University of Gdansk, Gdansk, Poland
[2]Department of Health Sciences, Pomeranian University of Slupsk, Slupsk, Poland
[3]Department of Neuroanesthesiology, Medical University of Gdansk, Gdansk, Poland

Introduction: NF-κB plays a regulatory function in the CNS during development and in various pathological conditions. Dual, antagonistic role of NF-κB in cerebral stroke is related with diverse composition of the complexes of this transcription factor. NF-κB dimers containing RelA/p65 subunit exacerbate brain damage by inducing pro-inflammatory and pro-apoptotic genes, whereas c-Rel-containing dimers promote cell survival by inducing anti-apoptotic gene transcription. While NF-κB presence in neuronal nuclei was confirmed by numerous studies, its activation in glial cells still remains the subject of discussion.

Aim: The aim of this study was answering the following questions: 1) in which cell subpopulations and when activation of RelA/p65 and c-Rel subunits of NF-κB occurs

in the CNS after permanent cerebral ischemia?, 2) are there any changes in the DNA-NF-κB binding activity during the first 24 hours of ischemic stroke?

Material and methods: Permanent middle cerebral artery occlusion (pMCAO) was performed in 40 middle-aged (72 weeks old) male Wistar rats. Animals were randomly assigned to 4 experimental groups with different post-ischemic survival period: 3 h, 6 h, 16 h and 24 h. Activation of NF-κB was assessed by immunohistochemistry and immunoblotting. EMSA was performed to analyze the DNA binding activity of NF-κB.

Results: After pMCAO activation of both subunits of NF-κB was observed in neurons, astrocytes and microglia, but not in oligodendroglial cell lineage. Activation of "neuroprotective" c-Rel subunit occurred during the first 3 h, and was observed mainly in neurons. During the whole study period, an increased expression of RelA/p65 was found in the damaged tissue. Activation of this subunit in neurons was present in all experimental groups, however – in astroglia and microglia it was observed predominantly at 16 and 24 h after pMCAO. Substantial loss in the number of neurons during the first 24 hours of stroke was also present. In our study, transient decrease in NF-κB-DNA binding activity at 6 h, and subsequent increase – at 16 h and 24 h were detected.

Conclusions: Regulatory function ofNF-κB transcription factor in the acute ischemic stroke is related with its presence in the various cellular subpopulations of the CNS. Prevalence of RelA/p65 over c-Rel subunit explains the dominance of pro-apoptotic action of NF-κB in this pathological process. Changes in NF-κB-DNA binding activity may result fromthe increased cell death of RelA/p65- and c-Rel-immunoreactive neurons during the first hours of ischemic insult and delayed activation of RelA/p65-containing dimers in astrocytes and microglial cells, that occurs no sooner than 16 hours after ischemia induction.

|A44|

Prenatal exposure to 4-para-nonylphenol disrupts estrogen receptor α, but not estrogen receptor β and retinoid X receptor signaling in mouse embryonic neuronal cells

Litwa E., Rzemieniec J., Wnuk A., Lason W., Kajta M.

Institute of Pharmacology Polish Academy of Sciences, Department of Experimental Neuroendocrinology, Cracow, Poland

Nonylphenol (NP) belongs to a wide group of endocrine disrupting chemicals present in plastic wrappings, bottles, and textile paints. Endocrine disrupting chemicals are known to mimic, antagonize or modify the endogenous hormonal activity and cause deleterious effects on living organisms. Due to the structural similarity, nonylphenol is able to imitate the natural hormone 17-beta-estradiol by competing for the binding site of the estrogen. Although half life of NP in humans is very short, humans are continuously exposed to nonylphenol, especially by food intake. Recent data demonstrated that it accumulates in the brain in much higher concentrations than in other tissues. There is a growing body of evidence that exposure to endocrine disruptors during pregnancy or perinataly, impairs mental development of infants and children. However, mechanisms of action of nonylphenol on the brain tissue at early stages of neural development need to be clarified. In the present study we investigated the impact of prenatal exposure to nonylphenol on estrogen receptors (ERα, ERβ) and retinoid X receptor (RXR) signaling in mouse hippocampal cells. CD1 Swiss Albino pregnant mice were exposed to nonylphenol from 6th to 16th gestation days. Hippocampal cells from control and NP-treated mouse embryos were cultured according to the standard procedures, and subjected either to NP or its solvent at 7 day *in vitro*. Hippocampal cell cultures derived from control and NP-treated mouse embryos expressed mRNAs and proteins for ERα, ERβ, and RXR, as detected by real time-PCR and specific ELISAs. Addition of nonylphenol (5 μM) to the cultures stimulated mRNA expression of the receptors, except for ERα mRNA that remained unchanged in the cultures of hippocampal cells from NP-treated embryos. Nonylphenol (5.10 μM) also induced caspase-3 activity in hippocampal cultures and enhanced it up to approximately 170% of the control, independently of prenatal treatment of hippocampal tissue. In both types of hippocampal cultures, ERβ and RXR antagonists, PHTPP and HX 531, attenuated the NP-induced effect. However, ERα antagonist MPP inhibited the NP-evoked caspase-3 activity only in cultures derived from NP-treated embryos. These data suggest that prenatal exposure of hippocampal tissue to NP disrupts ERα, but not ERβ and RXR signaling pathways, mainly by affecting ERα mRNA expression and anti-apoptotic capacity of the receptor.

This work was supported by the Polish National Center of Science, grant no. 2011/01/N/NZ4/04950.

|A45|

Effects of mGluR5 positive and negative allosteric modulators on brain damage evoked by hypoxia-ischemia in neonatal rats

Makarewicz D.[1], Slomka M.[1], Danysz W.[2], Lazarewicz J.W.[1]

[1]Department of Neurochemistry, Mossakowski Medical Research Centre, Polish Academy of Sciences, Warsaw, Poland
[2]Merz Pharmaceuticals GmbH, Frankfurt am Main, Germany

In the present study, we tested the hypothesis that the level of brain development determines the effectiveness of functional coupling between metabotropic glutamate receptor 5 (mGluR5) and *N*-methyl-*D*-aspartate receptors (NMDARs) in terms of neuroprotection. We examined the effects of negative and positive allosteric modulators of mGlu5 receptors (fenobam and ADX47273, respectively) on brain damage induced by hypoxia-ischemia (H-I) in 7-day-old rats. The test drugs were administered intraperitoneally 10 min after H-I. Rectal body temperature was measured for 2.5 h, and the weight of both hemispheres was determined 14 days after the insult. In the vehicle-treated groups, H-I reduced the weight of the ipsilateral (ischemic) hemisphere by approximately 33%. Fenobam (10 mg/kg) had no significant effect on brain damage or the weight of the contralateral (control) hemisphere. In contrast, fenobam (20 mg/kg) potentiated ischemic brain damage by 57.4%. ADX47273 (5, 10, and 30 mg/kg) had no significant effect on ischemic brain damage and did not interfere with the weight of the contralateral hemisphere. In all of the experimental groups, we detected no significant changes in rectal temperature. In conclusion, in 7-day-old rats, the bidirectional modulation of mGluR5 by fenobam (10 mg/kg) and ADX47273 (all doses tested) did not result in significant changes in H-I-evoked brain damage, supporting the hypothesis that the coupling of mGluR5 and NMDARs is a phenomenon that depends on brain development and is not fully operational in 7-day-old rat pups.

|A46|

Initial characterization of neurotrimin (Ntm) gene deficient mice

Mazitov T., Innos J., Vasar E.

Institute of Biomedicine and Translational Medicine, University of Tartu, Estonia

Introduction: Neurotrimin protein belongs to the IgLON family of proteins with Lsamp, Obcam, and Kilon. All these molecules are quite similar, highly glycosylated membrane proteins, characterised by three Ig domains and GPI anchor. They act as heterodimers forming protein complexes that stimulate and inhibit neurite outgrowth and guide axons. On the organism level, members of the IgLON family have been implicated in psychiatric disorders, obesity and certain types of cancer. The goal of our research group is to characterize the IgLON family as a whole by means of both, model organisms (knockout mice) and molecular methods. We have provided a thorough characterization of the phenotype of Lsamp-deficient mice and have now extended our research to include Ntm-deficient mice.

Material and methods: Neurotrimin (Ntm) gene deficient homozygous and heterozygous male and female mice and their wild-type littermates were tested in a battery of behavioral tests. Also some preliminary pharmacological experiments were performed to test for possible changes in major monoaminergic systems.

Results: First, we tested the animals for vision, hearing and olfaction and found that they have normal sensory abilities. We also tested Ntm-deficient mice in three anxiety tests (hyponeophagia, plus maze and light/dark box) and in the locomotor activity test (motility box) and found that their behavior does not differ from that of their wild-type littermates. However, we observed statistically significant differences in one of the learning and memory tests, the active avoidance test. Ntm-deficient mice learn slower than their wild-type and heterozygous littermates, probably exhibiting a learning impairment. Differences were also evident in pharmacological pilot studies with ethanol and amphetamine. Ntm-deficient mice were more sensitive to the sedative effect of ethanol, as it took much longer for them to regain the righting reflex after i.p. injection of 4 g/kg of ethanol. Furthermore, the locomotor stimulating effect of 5 mg/kg of amphetamine was weaker in Ntm-deficient mice than in wild type animals.

Conclusions: In this study, the basic phenotyping of neurotrimin (Ntm) gene knockout male and female mice was performed. These mice display normal sensory abilities, normal locomotor activity and normal anxiety level.

However, they have a learning impairment and altered sensitivity to ethanol and amphetamine, probably reflecting changes in the activity of major monoaminergic systems. It is remarkable that Lsamp deficient mice have a similar pharmacological phenotype, which is not surprising, however, because Ntm and Lsamp are close interaction partners and form heterodimers together. The study underlines the importance of studying all the members of the IgLON family of proteins together.

Poster session II

|B1|

Osteopontin gene and clinical course of multiple sclerosis in a Polish population

Michalowska-Wender G.[1,2,3], Biernacka-Lukanty J.[1,3], Michalak S.[2,3,4], Raczak B.[1,3], Wender M.[2]

[1]Laboratory of Neurogenetics, Department of Neurology, University of Medical Sciences, Poznan, Poland
[2]Neuroimmunological Unit, Medical Research Center, Polish Academy of Sciences, Poznan, Poland
[3]Department of Neurology, University of Medical Sciences, Poznan, Poland
[4]Department Neurochemistry and Neuropathology, University of Medical Sciences, Poznan, Poland

Osteopontin (OPN) is a key cytokine involved in T-cell activation in multiple sclerosis (MS), and is therefore called an early T-cell activation gene. Studies performed in various geographical regions have demonstrated significant differences. In this study we analysed whether the OPN gene has an effect on MS occurrence and clinical course in a Polish population. Our study material consisted of 100 MS patients compared with control material. The clinical course was evaluated by the EDSS score. After extraction of DNA from peripheral blood cells, genotype and allele frequencies in exon 6 and 7 were examined using specific primers by a standard PCR reaction. The distribution of variables was tested with the D'Agostino-Pearson test. Then the statistical analysis based on one-way ANOVA, Mann-Whitney test and logistic regression was performed using a licensed version of MedCalc software.

The genotype distribution and allele frequencies were not similar between patients and controls but differences were not statistically significant. The heterozygous C/T genotype in position 8090 was detected in 21.6% of patients and in 10% of control material. Our results are negative with respect to the impact of the osteopontin gene on susceptibility to MS in Poland. Genetic polymorphism of OPN was established to be associated with MS in Japanese patients. It seems therefore that the haplotype structure may differ from one population to another. However, we have identified the 8090 T/T 9250 C/C osteopontin genotype associated with higher levels of disability in MS patients. Age is an independent factor influencing disability measures. Based on one-way ANOVA testing, the clinically significant genotypes were identified. The EDSS score was higher (3.0; 2.0-4.0, median; interquartile range) in 8090 T/T + 9250 C/C patients than in 8090 C/C + 9250 C/C MS patients (1.75; 1.5-2.0) (p = 0.0120). The disability in 8090 C/C + 9250 C/T MS patients was higher (EDSS = 3.75; 2.5-4.5) than in 8090 C/C + 9250 C/C MS patients (1.75; 1.5-2.0) (p = 0.0137). In logistic regression analysis of the effect of variables on EDSS scoring in the model, including sex, age and genotype categories, age was found to be independent factor influencing disability (p = 0.0140). No differences in age between genotype categories were found.

|B2|

L-histidine administration increases brain carnosine concentration in rats with thioacetamide-induced acute liver failure: a contribution to increased antioxidant capacity (TAC)?

Milewski K., Hilgier W., Albrecht J., Zielinska M.

Department of Neurotoxicology, Mossakowski Medical Research Centre, Polish Academy of Sciences, Warsaw, Poland

Hepatic encephalopathy (HE), a consequence of acute or chronic liver failure, is a complex neuropsychiatric disorder where oxidative/nitrosative stress (ONS) plays a decisive pathogenic role. ONS imposed on astrocytes causes their swelling which is the primary cause of cerebral edema, increased intracranial pressure herniation, and direct cause of death in acute HE. Existing evidence suggest that systemic administration of L-histidine (His) may be a potentially useful therapeutic agent for the brain edema associated with HE (Rama Rao 2007). The effect of His was primarily ascribed to inhibition of excessive Gln transport to mitochondria (the "Trojan Horse" hypothesis). However, His is known for its antioxidant action; a study from our laboratory has shown that His also prevent reduction of glutathione content in brain mitochondria of TAA rats (Ruszkiewicz 2013) and increases the total antioxidant capacity (TAC) of the brain (Ruszkiewicz and Albrecht 2014). One other *in vitro* study demonstrated reduced mitochondrial permeability transition (mPT) and oxidative stress in ammonia-exposed astrocytes pretreated with His (Rao 2010). We speculated that the action of His may be due to the action of its metabolites. Of these, histamine is a component of and thought to be related with inflammation, one of accompanying events in HE progression. Carnosine, a dipeptide may be associated with wide range of neuroprotective properties (Trombley 2000). It was also indicated that carnosine prevents TAA induced liver injury in rats (Mehmetcic 2007). Here we investigated the effects of acute HE on the rat blood and brain content of hista-

mine and carnosine. HE was induced using the thioacetamide model (300 mg TAA/kg 3 times *i.p*. in 24 h intervals). His was administrated *i.p*. 2 h before TAA (100 mg/kg). Brains and blood were collected 24 h after last injection.

Systemic administration of His had no lasting effect on its concentration in cerebral cortex and in blood plasma either in control and TAA rats, neither did it affect the concentration of histamine in there, countering its putative role in potentiating systemic inflammation in TAA rats. In contrast, the brain level of carnosine was significantly elevated after His treatment in both control and HE rats, suggesting that carnosine may be responsible for some beneficial effects of His administration in the setting of HE. Studies to verify this hypothesis are under way in our laboratory.

Supported by the National Science Centre grant No 2013/09/B/NZ4/00536.

|B3|

Antidepressant-like properties of 1,2,3,4-tetrahydroisoquinoline and its methyl derivative in animal models of depression

Mozdzen E., Michaluk J., Wasik A., Romanska I., Antkiewicz-Michaluk L.

Department of Neurochemistry, Institute of Pharmacology, Polish Academy of Sciences, Cracow, Poland

Depression is a serious disorder in today's society, with estimate of lifetime prevalence as high as 21% of the general population in some developed countries. As defined by the American Psychiatric Association, depression is a heterogeneous disorder often manifested with symptoms at the psychological, behavioral and physiological levels. As with all diseases, approximations of both the disorder and the actions of corrective medications in laboratory animals are essential for the development of effective therapies. Most of the currently used antidepressant drugs are monoamine based, affecting the inhibition of re-uptake or metabolism of noradrenaline (NA), serotonin (5-HT), or dopamine (DA), because they play a key role in central nervous system (CNS) in pathophysiology of depression.

The present study is aimed to investigate the potential antidepressant properties of an endogenous amine 1,2,3,4-tetrahydroisoquinoline (TIQ) and its methyl derivative, 1-methyl-1,2,3,4-tetrahydroisoquinoline (1-MeTIQ). The experiments were carried out on male C57BL6J mice (25 ± 2 g) (Charles River Laboratories, Sulzfeld, Germany). The antidepressant-like activity of tested compounds was evaluated in the behavioral and neurochemical analysis. In the behavioral study, the forced swim test (FST) and tail suspension test (TST) were used as widely used rodent models sensitive to the effects of acute antidepressant treatments. Additionally, the motor function of mice was checked in the locomotor activity test after investigated drugs administration. TIQ and 1-MeTIQ were administrated in three different doses: 10, 25 or 50 mg/kg *i.p*. Imipramine (15 or 30 mg/kg *i.p*.) was used as a reference drug. Control mice were treated with saline. In the neurochemical *ex vivo* study, the levels of NA, 5-HT, DA and their metabolites, the rate of monoamines metabolism and their neuronal activity in different mice brain structures were determined by HPLC methodology with electrochemical detection. All procedures were approved by the Ethical Committee of the Institute of Pharmacology, Polish Academy of Sciences in Cracow.

The results of these studies have shown that TIQ and 1-MeTIQ administrated systematically to mice produced antidepressant-like effect in the FST. They significantly decreased the immobility time ($p < 0.01$), stronger than imipramine and did not affect the locomotor activity in mice. Additionally, TIQs increased the rate of NA metabolism, enhanced the factor of DA re-uptake inhibition with simultaneously decrease in the rate of 5-HT metabolism in mice brain structures. The results obtained indicate that TIQ and 1-MeTIQ possess a potential antidepressant activity in mice, suggesting their possible mechanism of action based mainly on activation of monoaminergic system – inhibition of MAO-dependent oxidation of monoamines and increase in their concentrations in different brain structures. In that light, both tested compounds may be effective for the depression therapy in a clinical setting.

These studies were financed by the project Interdisciplinary PhD Studies "Mol-Med".

|B4|

The actions of 5-methoxy-diisopropyltryptamine ('foxy') in rat prefrontal cortex and striatum

Noworyta-Sokolowska K.

Department of Pharmacology, Institute of Pharmacology, Polish Academy of Sciences, Cracow, Poland

5-methoxy-diisopropyltryptamine (5-MeO-DIPT, 'foxy') is one of the most popular 'club drug' in the United States, Canada, Japan and Europe. It has been noted in case reports that 5-MeO-DIPT induces visual and auditory hal-

lucinations, insomnia, emotional expression similarly to psylocin and psylocibin. That contributed to recognition these drug as a hallucinogen, however its mechanism of action in the brain is not fully understood. A comparison of the chemical structure of 5-MeO-DIPT shows structural similarities with serotonin (5-HT) and 3,4-methylenedioxymethamphetamine (MDMA). That suggests its possible influence on monoamine systems such as dopamine (DA) and 5-HT as a main mechanism of action of these drug. Moreover, hallucinations noted after 'foxy' treatment indicate on possible influence on glutamate (GLU) system.

The aim of the study was to examine the extracellular level of DA, 5-HT, γ-aminobutyric acid (GABA) and GLU after 5-MeO-DIPT administration in freely moving rats.

All experiments were performed in a strict accordance with the Polish legal regulations concerning experiments on animals (Dz. U. 05.33.289). Determination of extracellular levels of DA, 5-HT, GABA and GLU on Wistar-Han male rats (280-300 g) was carried out using microdialysis technique. The probe implantation in the frontal cortex (AP +2.8, DL +0.8, V –5.7) and in the corpus striatum (AP +1.8, DL +2.8, V –7.0) took place 24 h before experiments. Dialysate fractions were analyzed by High Performance Liquid Chromatography (HPLC) with electrochemical detection. The chromatographic data was processed by Chromeleon v. 6.80 (Dionex, USA) software.

Single intraperitoneal administration of 5-MeO-DIPT given at a dose of 20 or 10 × 2 mg/kg produced increase in DA and 5-HT release in the rat striatum and the frontal cortex. At the same time increase in GLU and GABA extracellular level was observed in the frontal cortex. However, transient increase in GLU release in rat striatum was followed by decrease in its level for the rest of experimental time. A slight but significant decrease in GABA extracellular level was noted in the striatum. An intriguing behaviour such as head shaking, salivation, walking backward, convulsions during first hour after 5-MeO-DIPT administration was observed as well as playing piano, tickles movement, tremor and muscle weakens were seen throughout the study.

Observed increase in DA and 5-HT extracellular level with concomitant decrease in metabolite extracellular level indicates on inhibition of DA and 5-HT transporters located on DA or 5-HT nerve terminals. Increase in extracellular GLU level may cause behavioural symptoms such as convulsions and head shakings and may also indicate on possible hallucinogenic drug action.

Supported by grant from National Centre of Science (NCN) no 2013/09/B/NZ7/04104.

|B5|

Paraquat induces changes in activity and supercomplexes assembly of mitochondrial complex I and mitochondria membranes fluidity in SH-SY5Y cells

Olech L.[1], Leskiewicz M.[2], Basta-Kaim A.[2], Dencher N.[3], Kuter K.[1]

[1]Department of Neuropsychopharmacology, Institute of Pharmacology, Polish Academy of Sciences, Cracow, Poland
[2]Department of Experimental Neuroendocrinology, Institute of Pharmacology, Polish Academy of Sciences, Cracow, Poland
[3]Physical Biochemistry, Department of Chemistry, Technische Universität Darmstadt, Darmstadt, Germany

Introduction: Paraquat (PQ) is a herbicide which enhances risk of developing Parkinson's disease (PD). It increases the level of reactive oxygen species (ROS) in cells via the redox cycling performed by many oxidoreductases. Previous studies showed decreased activity of respiratory complexes (Cxs) I and III by PQ. In the inner mitochondrial membrane Cxs form higher order structures named supercomplexes (SCxs), what has crucial effect to its functioning.

Aim: Our aim was to investigate the influence of PQ on activity of mitochondrial Cx I assembled in SCxs and as individual form in a model of neuron-like cells.

Material and methods: Differentiated SH-SY5Y cells (10 μM retinoic acid in DMEM with 10% FBS for 7 days) were treated with 600 μM PQ for 24 hours. Vitality (by MTT test), mortality (by LDH test) and endogenous ROS level (using H_2DCFDA) at this time point were analyzed. Cells were also incubated next 24 hours with fresh medium without PQ. Mitochondria were isolated directly after incubation with PQ as well as after additional time with withdrawal of toxin. After mitochondria solubilization blue-native electrophoresis with further in-gel enzymatic activity measurements of Cx I were performed. Mitochondrial membranes fluidity was measured using fluorescence anisotropy method.

Results: Incubation of cells with PQ caused decrease in vitality and had no influence on mortality. PQ elevated level of endogenous ROS. A significant decrease in activity of Cx I was observed in the three highest molecular weight SCxs. Withdrawal of PQ led to progressive loss in activity of Cx I in the same SCxs and further decreased the activity of complex I in lower mass SCxs. In this time point a slightly increased fluidity of mitochondrial membranes was also observed.

Conclusions: Elevated ROS level may be related to decrease in activity of Cx I in the highest molecular weight

SCxs. PQ caused progressive perturbation in mitochondria even after withdrawal of toxin.

The study was supported by the Statutory Funds of the Institute of Pharmacology, PAS, Kraków, Poland and Technische Universität Darmstadt and DAAD.

|B6|

Proteasome inhibitor abrogates the neuroprotective effect of hyperbaric oxygen preconditioning in experimental global cerebral ischemia

Ostrowski R.P., Stepien K., Pucko E., Wojda R., Matyja E.

Department of Experimental and Clinical Neuropathology, Mossakowski Medical Research Centre, Polish Academy of Sciences, Warsaw, Poland

Hyperbaric oxygen preconditioning (HBO-PC) has been known to provide neuroprotection against cerebral ischemia. However, it is not known whether HBO-PC is effective against severe global brain ischemia, induced by bilateral common carotid artery (CCA) occlusion and profound systemic hypotension due to exsanguinations (modified two vessel occlusion cerebral ischemic model; 2VO). Moreover, the role of proteasome in the mechanisms of HBO-PC has not been as yet investigated.

The aim of this study was to investigate whether brain injury that results from carotid occlusion and deep hypotension is reduced with HBO preconditioning, and to determine the involvement of proteasome in the preconditioning mechanism.

The experiments were performed on 48 male Wistar rats within body weight range of 280-350 g, allocated to the following groups: naive control, sham, rats with 2VO untreated (2VO group), rats with 2VO preconditioned with HBO (HBO-PC group) and rats with 2VO and the proteasome inhibitor MG132, injected *i.p.* at a dose of 1 mg/kg, at 30 min prior to every session of HBO-PC (MG132 group). HBO-PC procedure used 100% oxygen at 2.5 ATA 1 hr daily for 5 consecutive days with the last session at 24 hrs before ischemia. The ischemia was induced under ketamine and xylazine anesthesia by drawing blood from femoral artery to decrease mean arterial blood pressure to 30-35 mm Hg, followed by CCA bilateral occlusion for 5 min. Rats were examined for sensorimotor and T-maze performance deficits and the mortality was calculated. They were euthanized at 24 hrs for WB or at 7 days for brain histology.

After ischemia (2VO group), the number of surviving neurons in CA1 zone of the hippocampus was equivalent to only 5.7% of CA1 neurons in the sham control. However, in the HBO-PC group, the number of well preserved neurons was as high as 20.8% of that in the sham control. When the group preconditioned with HBO also received MG132, the number of surviving neurons equaled 2.7% of control. HBO-PC tended to reduce mortality (25% vs. 38% amongst untreated), although insignificantly. In the MG132 group, 45% of mortality was noted. HBO-PC resulted in 63.9% average T-maze scores as compared to 27.8% in the unpreconditioned rats after ischemia. The proteasome inhibitor combined with HBO-PC reduced the score to 33.3%. On Western blot, the preliminary results showed an increased level of apoptotic protein Bim (BCL-2-interacting mediator of cell death) in the brain after ischemia, while it was reduced in the brains of animals preconditioned with HBO. MG132 reversed the HBO-PC-induced decrease in brain levels of Bim.

In conclusion, the HBO-PC-induced brain protection against severe ischemic brain insult appears to be proteasome-dependent. In order to further verify the underlying mechanism, future studies will examine ubiquitin-ligases and proteasomes leading in concert to a depletion of pro-apoptotic proteins upon HBO-PC.

The authors want to thank Małgorzata Pożdzik, MSc for the excellent technical assistance.

|B7|

Mutated human beta-amyloid precursor protein gene (*APP-sw*) causes aberrant autophagy in NGF-differentiated neural PC-12 rat pheochromocytoma cells

Pajak B.[1], Kania E.[1], Orzechowski A.[1,2]

[1]Electron Microscopy Platform, Mossakowski Medical Research Centre, Polish Academy of Sciences, Warsaw, Poland
[2]Department of Physiological Sciences, Faculty of Veterinary Medicine, Warsaw University of Life Sciences – SGGW, Warsaw, Poland

Pheochromocytoma PC-12 cells are immune to physiological stimuli directed to evoke programmed cell death. Besides, metabolic inhibitors are incapable to sensitize PC-12 cells to extrinsic or intrinsic apoptosis unless they are used in toxic concentrations. Surprisingly, these cells become receptive to cell deletion after human *APP-sw* gene expression. PC-12 cells were nucleofected with a plas-

mid containing amyloid beta precursor protein wild type APP(-wt), or swedish mutation APP(-sw) together with resistance genes to antibiotics (gentamicin and ampicillin) expressed under green fluorescent protein (GFP) gene promoter. Next, cells were subjected to 48 h differentiation programme (4% FBS + 2% HS + NGF in DMEM) followed by 48 h treatment with selected substances dissolved in 0.1% BSA + NGF in DMEM. Afterwards, cell cultures were subjected to molecular analysis. Presence of transgene and gene activity in nucleofected cells was evaluated by PCR and Western blot analysis, respectively. Transfected neural rat PC-12 cells were examined to asses cytotoxicity of normal APP processing product beta-amyloid via MTT and Neutral Red assay. We observed reduced cell viability in *GFP* vector + *APP-sw*-nucleofected cells (drop by 36%) but not in *GFP* vector–, or *GFP* vector+ *APP-wt*-nucleofected cells. Lower viability was accompanied by higher expression of Aβ 1-16 and elevated secretion of Aβ 1-40 (in average 53.58 pg/mL). At the ultrastructural level autophagy-like process was demonstrated to occur in *APP-sw*-nucleofected cells with numerous autophagosomes and multivesicular bodies but without autolysosomes. Human *APP-sw* gene is harmful to PC-12 cells and cells are additionally driven to incomplete autophagy-like process. When stimulated by TRAIL or nystatin, CLU protein expression accompanies early phase of autophagy.

This research was funded by National Science Centre (Poland), Grant No. UMO-2011/03/B/NZ7/02328.

|B8|

Mysterious neuropeptides: phoenixin and spexin. Are they really promising from the clinical viewpoint?

Palasz A., Rojczyk-Golebiewska E., Wiaderkiewicz R.

Department of Histology, Medical University of Silesia, Katowice, Poland

Recently, a lot of new regulatory peptides has been identified and described. Newly discovered and still very mysterious neuropeptides such as phoenixin and spexin appear to be a uniquely intriguing factors. Extremely poorly studied neuropeptide; phoenixin (PNX) has almost the same pattern of hypothalamic immunoreactivity as better known nesfatin-1. This intriguing endogenous factor may control the reproductive hormone secretion by the modulation of the pituitary GnRH receptor expression. Probably, phoenixin sensitize the pituitary to releasing factors, rather than directly promote the exocytosis of secretory vesicles to endocrine cells. Immunohistochemical studies revealed PNX positive cells in the rat hypothalamus, dorsal horn, spinal trigeminal tract, nucleus of the solitary tract and even in the trigeminal and nodose ganglia. It was also observed that exogenously administered PNX may preferentially suppress visceral as opposed to thermal pain. Recent reports suggest that the mechanism of signal transduction activated by PNX is MAPK/ERK pathway. Phoenixin may play significant role in reproduction and energy homeostasis at the level of the hypothalamic centres. Recent data may also implicate phoenixin in reproductive or metabolic disorders. Spexin which was identified through bioinformatics search strategy, a novel gene containing spexin has been named NPQ. These peptides have no homologies to other proteins. The rat spexin differs from the human and mouse molecules only by one amino acid at the C-terminal domain. In the brain, many spexin-positive neurons were visible, while neuroglia was usually negative. The hippocampal neurons showed moderate immunoreactivity as well as cerebellar Purkinje cells and brain stem neurons. Spexin seems to have multiple physiological functions in mammals. Studies using goldfish revealed the involvement of SPX in reproduction and food-intake regulation. Treatment of animals with SPX decreased the secretion of LH and suppressed appetite. Recent findings also demonstrates the central control of SPX in cardiovascular/renal function and nociception. Spexin may be a novel factor involved in weight regulation, with potential for obesity therapy.

|B9|

Mitochondria dysfunction and oxidative stress in neurodegenerative process influenced by the designer drug of abuse – *N*-benzylpiperazine

Persona K.[1], Polus A.[2], Goralska J.[2], Gruca A.[2], Dembinska-Kiec A.[2], Piekoszewski W.[1]

[1]Jagiellonian University, Faculty of Chemistry, Department of Analytical Chemistry, Cracow, Poland
[2]Jagiellonian University – Medical College, Department of Clinical Biochemistry, Chair of Clinical Biochemistry, Cracow, Poland

"Designer drugs of abuse" is a common name for substances advertised as "legal alternative to illegal compounds". Despite of the introduction of prohibition in trade of medicinal products which mimic the effects of ille-

gal drugs, the problem of "legal highs" is still significant. Knowledge about the effects of action of such substances is scarce and mainly derived from the description of cases form toxicological wards. One of model compounds from the group of designer drugs of abuse is *N*-benzylpiperazine (BZP) – a psychoactive agent for the central nervous system with stimulating and sympaticomimetic properties. The mechanism of action of BZP is compared to the one of MDMA, while the effects are defined as 10-times weaker than the effects of d-amphetamine.

The aim of the study was to evaluate the impact of BZP on brain cells apoptosis including the potential role of mitochondria, the formation of oxidative stress, and disruption of cells energy state in presumptive neurodegenerative properties of this drug.

Experiments were performed using a line of human glial tumor cells (LN-18) incubated with BZP for 24 h. The choice of doses of BZP in the range of 10 mg/mL to 300 mg/mL were made through evaluation of LDH released into the culture medium as well as through consideration of the concentration of drug in the biological material taken from BZP users. Analysis of parameters associated with mitochondrial dysfunction and oxidative stress formation, such as: changes in mitochondrial membrane potential ($\Delta\psi_m$) and reactive oxygen species (ROS) were measured with the use of flow cytometry technique (FACS), whereas changes in ATP level were examined using luminescent method. The activity of caspases: 3, 8, 9 was analyzed in fluorescence measurements. Increase of oxidative DNA damage was evaluated by ELISA test through determination of DNA oxidative damage marker: 8-OHdG.

The conducted research demonstrated statistically significant changes in increased mitochondrial membrane potential and increased ROS production, along with decreased ATP level. Increased changes in activation of caspase-3 which are a confirmation of cell apoptosis undergoing under the influence of BZP were observed, however no statistically significant changes in activation of caspase-8 and -9 were stated. Elevated ROS generation resulted in oxidative DNA structure changes, which was confirmed by increased levels of 8-OHdG in the cells.

The results indicate that BZP at concentrations comparable to the ones detected in biological material taken from people taking this drug can induce apoptosis in glial cells by affecting the mitochondrial dysfunction and resulting in the oxidative stress generation. The results may also indicate neurodegenerative properties of BZP.

K. Persona acknowledges financial support from the Interdisciplinary PhD Studies project "Molecular sciences for medicine" (co-financed by the European Social Fund within the Human Capital Operational Programme).

K. Persona received funds to prepare her doctoral dissertation from the National Science Centre in the framework of a doctoral scholarship funding (ETIUDA) based on the decision no. DEC-2014/12/NZ7/00262.

|B10|

Identification and classification of transcriptional variants and non-coding RNAs induced by antidepressants in the mouse striatum

Piechota M.[1], Golda S.[1], Jantas D.[2], Przewlocki R.[1,3], Korostynski M.[1]

[1]Department of Molecular Neuropharmacology, Institute of Pharmacology, Polish Academy of Sciences, Cracow, Poland
[2]Department of Experimental Neuroendocrinology, Institute of Pharmacology, Polish Academy of Sciences, Cracow, Poland
[3]Department of Neurobiology and Neuropsychology, IPS, Jagiellonian University, Cracow, Poland

The therapeutic effects of antidepressants are mediated by neuroplastic changes in the brain systems controlling drive and motivation. Despite well-known pharmacological actions of antidepressants, we are still far from having a clear picture of the molecular programs initiated by these drugs. We used next-generation sequencing and bioinformatics approach to build a genome-wide inventory of protein coding and non-coding transcripts altered by antidepressants. Genome expression was analyzed in mouse striatum 4 hours after the administration of mianserine (20 mg/kg, *i.p.*) or tranylcypromine (20 mg/kg, *i.p.*) treatment. We identified 153 gene transcripts of various biotypes regulated (FDR < 0.1%) in response to antidepressants. These transcripts are expressed in five different patterns and are enriched in protein coding variants (77%). Expression of different types of drug inducible transcriptional variants was verified using qPCR, including retained intron (*Clk1*), alternative TSS (*Mctp1*), small RNA (*Mir1983*) or long non-coding RNA (*Neat1*). We also indicated that two key gene regulatory systems are active in separate cellular compartments of the striatum, CREB1/SRF in neurons and GR/CTCF in glia. The results suggest that critical step of molecular regulation of neuroplasticity takes place on the level of transcriptional units rather than genes. This regulation may constitute a transcriptional trigger for development of long-lasting effects of antidepressants in the brain.

This work was supported by POIG De-Me-Ter 3.1 and NCN grant 2011/03/D/NZ3/01686.

|B11|

The role of CXCL9 and CXCL12 in nociceptive transmission under diabetes

Pilat D., Zychowska M., Rojewska E., Mika J.

Department of Pain Pharmacology, Institute of Pharmacology, Polish Academy of Sciences, Cracow, Poland

Neuropathic pain is one of the most common late complications of diabetes. It is known that neuronal mechanisms can be modulated by pronociceptive mediators released by non-neuronal cells which become activated in the spinal cord during diabetes. However, the signals that mediate the spread of nociceptive signaling remain to be established. Chemokines seems to be crucial for mediating inflammation, although their role in nociceptive processes still needs to be evaluated. Both CXCL9 and CXCL12 are thought to mediate inflammatory processes in people suffering from diabetes, taking into account that both chemokines have increased plasma levels in patients. The role of those chemokines under diabetic neuropathic pain is unknown. The aim of our study was to determine whether in the mice model of diabetic neuropathy there is a change in the level of CXCL9 and CXCL12, and that intrathecal administration of these chemokines does affect nociceptive processes in naive mice. Male Albino-Swiss mice were rendered diabetic by an intraperitoneal injection of streptozotocin (STZ). The experiments were carried out 7 days after the injection of streptozotocin. To analyze if CXCL9 and CXCL12 may be involved in nociceptive transmission, we used RT-qPCR and antibody array techniques. Additionally these chemokines were administrated by an intrathecal injection to the naive mice. Behavioral tests conducted to measure hyperalgesia (cold plate test) and allodynia (von Frey test) were carried out 1, 4 and 24 hours after the injection. All experiments were carried out according to IASP rules (Zimmermann 1983). We have demonstrated that a single streptozotocin injection in mice can induce significant neuropathic pain along with an increase in plasma glucose levels. Seven days after the administration of STZ, an upregulation of CXCL9 and downregulation of CXCL12 mRNA were observed and measured by RT-qPCR. In parallel we observed an upregulation of protein level of both chemokines, as measured by an antibody array. The intrathecal administration of CXCL9 and CXCL12 showed its pronociceptive properties such as allodynia and hyperalgesia. In summary, we provided evidence for a development of allodynia and hyperalgesia following the administration of CXCL9 and CXCL12 in a naive mice. Therefore, we suggest that both studied chemokines, which are upregulated in diabetic neuropathy, are one of the reasons of pain development.

This work was supported by statutory founds and NCN grants 2012/05/N/NZ4/02416 and 2011/03/B/NZ4/00042.

|B12|

Parthenolide down-regulates pronociceptive factors (IL-1beta, IL-18 and iNOS) and enhances morphine effectiveness under neuropathic pain

Piotrowska A., Popiolek-Barczyk K., Kolosowska N., Makuch W., Rojewska E., Pilat D., Mika J.

Department of Pain Pharmacology, Institute of Pharmacology, Polish Academy of Sciences, Cracow, Poland

Neuropathic pain is caused by damage of the nervous system. This type of pain is resistant to conventional analgesics, including the effects of morphine, what comprises on a serious clinical problem. Treatment of neuropathic pain remains a challenge and requires combination therapy, because of not fully understood pathomechanism, as well as many components involved in nociceptive transmission. The goal of our studies was to determine the influence of parthenolide (PTL; an inhibitor of the NF-κB) on neuropathic pain development and changes in pronociceptive factors. Moreover, it was interesting to examine a possible influence of PTL administration on effectiveness of morphine in rat model of neuropathic pain. Research was carried out on Wistar rats implanted with intrathecal (*i.t.*) catheters. Neuropathic pain was developed using Bennett's model (chronic constriction injury (CCI) to the sciatic nerve). PTL (5 µg/5 µl) was dissolved in 50% DMSO and preemptively administered *i.t.* 16 h and 1 h before CCI and then once daily for 7 days. Two behavioral tests were conducted to measure allodynia (von Frey test) and hyperalgesia (cold plate test). Morphine was injected once, on day 7 after CCI and 60 min after morning PTL administration. Experiments were carried out according to IASP recommendations and were approved by the local Bioethics Committee. Behavioral studies have shown that chronic *i.t.* administration of PTL attenuated the allodynia and hyperalgesia on days 3, 5 and 7 after CCI. Western blot results demonstrated down-regulation of pronociceptive cytokines: IL-1beta, IL-18 and iNOS, parallel to down-regulation of p38MAPK as measured on day 7 after chronic PTL administration. Chronic treatment of PTL enhanced morphine analgesia, which was proven

by von Frey and cold plate tests. In summary, these results suggest that PTL reduces neuropathic pain by modulating the signaling pathways regulated by p38MAPK and by down-regulation of the expression of pronociceptive factors produced by the microglia cells. PTL is especially promising because it is already used in human therapy; our work provides the first evidence for its analgesic potency and beneficial properties on morphine effectiveness during neuropathic pain.

This work was supported by grant OPUS NCN 2011/03/B/NZ4/00042, and statutory funds. K. Popiolek-Barczyk is a Ph.D. student and has a scholarship from the KNOW sponsored by the Ministry of Science and Higher Education, Poland.

|B13|

The neuroprotective role of PKCβII in ischemia-reperfusion injury

Poleszak O., Beresewicz M., Kruszynska D., Zablocka B.

Molecular Biology Unit, Medical Research Centre, Polish Academy of Sciences, Warsaw, Poland

Protein kinase C β (PKCβ) is a serine/threonine kinase whose role in neuronal cells survival/ protection needs further investigation. Previous studies revealed that ischemic injury induce a rapid and long lasting increase of PKCβ in mitochondrial fraction but mainly in ischemia-resistant part of hippocampus, what may bespeak neuroprotection. Hence, here we set out to determine the role of PKCβ isozymes βI and βII in two models of brain ischemia (i) *in vitro* in rat organotypic hippocampal cultures subjected to excitotoxic injury which mimics ischemic injury and (ii) *in vivo* – transient brain ischemia in gerbils. Therefore we tested: (i) the effect of ischemic injury on the amount of both PKCβ isozymes and activity of PKCβII in mitochondria isolated from ischemia-vulnerable (CA1) and ischemia resistant (CA2-4, DG) hippocampal regions, (ii) the effect of inhibition of PKCβ isozymes in organotypic hippocampal cultures subjected to excitotoxic injury and (iii) by pull down chromatography followed by mass spectrometry the potential PKCβII mitochondrial partners to elucidate PKCβII-mediated neuroprotective mechanisms. In our studies we have observed that transient ischemic episode induces a significant elevation of PKCβII protein level and activity in ischemia-resistant part of hippocampus in mitochondrial fraction. Moreover, exclusive inhibition of PKCβII is sufficient to obtain 100% of damage in hippocampal organotypic slices. Thus results suggest that it is rather PKCβII than PKCβI which may be a key element responsible for neuroprotection. To elucidate the mechanisms of PKCβII-mediated neuroprotection its mitochondrial partners were identified. The analysis recognised a number of proteins belonging to mitochondrial inner and outer membrane as well as mitochondrial matrix. They are involved in regulation of different metabolic pathways such as fatty acid oxidation, glucose metabolism, electron transport chain and others. Using phophosite database (http://www.phophosite.org) we verified that most of identified PKCβII-partners have putative PKC phosphorylation sites indicating that regulation of these metabolic pathways by PKCβII phosphorylation may lead to PKCβII-mediated neuroprotection. The functional significance of the PKCβ phosphorylation is being studied.

The project is supported by NSC grant 2012/05/B/NZ/00415 and KNOW-MMRC project.

|B14|

Morphology of synapses and expression of selected proteins involved in synaptic transmission in the mouse azoxymethane model of hepatic encephalopathy

Popek M.[1], Frontczak-Baniewicz M.[2], Zablocka B.[3], Albrecht J.[1], Zielinska M.[1]

[1]Department of Neurotoxicology, Mossakowski Medical Research Centre, Polish Academy of Sciences, Warsaw, Poland
[2]Electron Microscopy Unit, Mossakowski Medical Research Centre, Polish Academy of Sciences, Warsaw, Poland
[3]Molecular Biology Unit, Mossakowski Medical Research Centre, Polish Academy of Sciences, Warsaw, Poland

Hepatic encephalopathy (HE) is characterized by imbalance between excitatory and inhibitory neurotransmission in disfavor of the former which becomes potentiated on transition from acute to chronic stages of the disease. The established view is that ammonia, a key neurotoxin, primarily affects astrocytes, leaving neurons relatively spared. However, impairment of the expression and/or function of specific astrocytic proteins (e.g.: glutamate transporters GLT-1, GLAST, Na-K-Cl co-transporter or potassium channel Kir4.1 or trombospondin-1) results in synaptic dysfunction, mainly involving the NMDA class of Glu receptors. However, there is limited body of evidence concerning the morphology of the synapses in HE-affected brain, particularly the impact of HE on the activity of pro-

teins involved in the NMDA receptor function, trafficking, or composition.

In the present study we used C57Bl6 mice subjected to a hepatotoxic insult (azoxymethane (AOM) administered *i.p*. at 100 mg/kg of body weight) as an experimental model of acute liver failure. We commenced with examining synaptic ultrastructure in cerebral cortex of AOM mice. Next, we compared the subunit composition of NMDA receptor in control and AOM mice, by measuring the expression of the two key subunits, NR1 and NR2A. In order to assess the synaptic hardware, mRNA and/or protein levels of postsynaptic density protein 95 (PSD-95), protein kinase C zeta (PKCζ) and PKMζ, an independent fragment of catalytic domain of PKCζ were quantified using real-time and Western blot analysis.

Cerebral cortex of AOM mice was characterized by the presence of increased numbers of enlarged synapses showing abundance of synaptic vesicles in the presynaptic zone. The expression of NR1, a major NMDA receptor subunit in a mice cerebral cortex was slightly increased, whereas NR2A subunit remained unchanged in AOM model. The amount of PSD-95, the protein involved in anchoring of NMDA receptor subunits, was increased by ~40% compared to control. The expression of PKCξ involved in the synaptic events was increased by ~30% and ~40% at the mRNA and protein level, respectively. However, expression of PKMξ, a protein with a unique role in LTP maintenance, was unchanged. Of note, PKCξ protein level was reduced by ~20% in P2 membrane fraction and elevated by ~30% in S2 cytosolic fraction in AOM mice, suggesting impaired trafficking of PKCξ to the plasma membrane. While implications of the above described changes for neurotransmission remain to be analyzed in further detail, this report is to our knowledge the first to demonstrate that changes in the synaptic hardware which may have direct bearing on its functioning, including LTP, do occur in the acute stage of HE.

Supported by the Polish-Norwegian grant "CORE", Grant Number: Pol-Nor/196190/26/2013 and the Leading National Research Centre (KNOW).

|B15|

Expression and the level of selected apoptotic proteins and *Trp53* mutations in PS/APP mice

Postrach I.[1], Rozycka A.[2], Strugala A.[3], Oczkowska A.[1], Florczak-Wyspianska J.[4], Dezor M.[1], Jagodzinski P.P.[2], Kozubski W.[4], Dorszewska J.[1]

[1]Laboratory of Neurobiology, Department of Neurology, Poznan University of Medical Sciences, Poznan, Poland
[2]Department of Biochemistry and Molecular Biology, Poznan University of Medical Sciences, Poznan, Poland
[3]Department of Molecular and Systems Biology, Institute of Bioorganic Chemistry, Polish Academy of Sciences, Poznan, Poland
[4]Chair and Department of Neurology, Poznan University of Medical Sciences, Poznan, Poland

Alzheimer's disease (AD) is the most common, incurable and progressive neurodegenerative disease. There is a number of factors involved in the pathogenesis of AD, i.e. amyloid precursor protein (*APP*) gene. Mutations in the *APP* gene contribute to the familial AD (FAD), by changes in the processing of this gene resulting in increase of β-amyloid (Aβ) level. In double transgenic mouse model of AD, mutation of APP695 is associated with early-onset of FAD. In aged transgenic mice show elevated level of Aβ, which may cause the generation of free radicals. Free radicals may oxidize macromolecules in cells, such as DNA. 8-Oxoguanine DNA glycosylase 1 (OGG1) is a main DNA repair enzyme that excises 8-oxo-2'-deoxyguanosine from DNA. DNA damage may induce apoptosis in a wild-type p53-expressing cell. Bcl-2 is an anti-apoptotic protein, which prevents caspase-3 activation by Bax proten. Regulation of Bcl-2 family gene expression is not completely understood in AD.

The aim of the study was the analysis of *Trp53* gene mutations and expression, and analysis of p53, OGG1, tumor necrosis factor alpha (TNF-alpha), Bax and Bcl-2 protein levels in Alzheimer's disease model PS/APP and control mice.

The studies were performed on female double transgenic PS/APP of B6.Cg-Tg(APP695)3DBo Tg(PSEN1dE9) S9Dbo/J stain (Jackson Lab., USA; about 8-months old) and young adults (8-12-weeks old) and aged-match control C57BL/6J stain mice. Brains of the animals were isolated and divided into three structures: cerebral gray matter (GM), subcortical white matter (WM) and cerebellum (C). The analysis of *Trp53* mutations was performed by using DNA sequencing and expression of this gene was carried out with use of RT-PCR and the level of p53 protein and other analysed apoptotic proteins was performed by Western blotting.

Our studies showed that the frequency of mutations was almost fourfold higher in PS/APP mice (A929T, A857G; 44%), compared to controls (T854G, G859A; 14%). However, it was shown that the expression of *Trp53* gene increased only in GM and C of PS/APP mice ($p < 0.05$) as compared to aged-match controls. Moreover, in GM and WM of PS/APP mice without *Trp53* mutations occurred a tendency to increase p53 protein levels together with elevated *Trp53* gene expression. Simultaneously, in PS/APP mice the presence of *Trp53* mutations did not lead to changes in expression and levels of Bax, Bcl-2, OGG1 and TNF-alpha proteins. In PS/APP mice we showed the tendency to decreased ratio of Bax:Bcl-2.

It seems that mutations of *Trp53* gene may lead to changes in expression especially of this gene and levels of p53 protein in PS/APP mice.

|B16|

Comparison of the neuroprotective potential of neuropeptide Y (13-36) and ACPT-I in spontaneously hypertensive rats subjected to transient focal cerebral ischemia using functional tests

Przykaza L.[1], Domin H.[2], Boguszewski P.[3], Smialowska M.[2], Kozniewska E.[1]

[1]Laboratory of Experimental Neurosurgery, Department of Neurosurgery, M. Mossakowski Medical Research Centre Polish Academy of Sciences, Warsaw, Poland
[2]Department of Neurobiology, Institute of Pharmacology, Polish Academy of Sciences, Krakow, Poland
[3]Laboratory of Limbic System, Nencki Institute of Experimental Biology Polish Academy of Sciences, Warsaw, Poland

The aim of this study was to evaluate and compare neuroprotective potential of neuropeptide Y (13-36) (NPY_{13-36}) and (1S,3R,4S)-1-aminocyclopentane-1,2,4-tricarboxylic acid (ACPT-I) against ischemic brain damage in spontaneously hypertensive rats (SHR), using functional tests and macroscopic morphological evaluation of brain infarction volume. NPY_{13-36} is a specific agonist of presynaptic neuronal Y2 receptors. Numerous previous studies have shown that activation of Y2 receptors inhibits glutamate release and protects against excitotoxicity in vitro and *in vivo*. ACPT-I is an unspecific agonist of group III metabotropic glutamate receptors (mGluR), which are known also to decrease excitatory transmission. ACPT-I has been shown to suppress seizure activity in animal epilepsy models and to protect neurons against kainate-induced excitotoxicity *in vitro* and *in vivo*.

Although there is a theoretical basis for a neuroprotective effect of both compounds against ischemic brain damage and a decrease in the size of ischemic infarct after inhibition of glutamate release has been demonstrated, no data is available evaluating post-ischemic functional state after treatment with either NPY_{13-36} or ACPT-I. Forty one male SHRs, weighing 270-300 g, were used for this study. Transient focal cerebral ischemia was induced for 90 min by the intraluminal occlusion of the right middle cerebral artery (MCA). Microflow (LDF) in the brain cortex supplied by this artery was continuously monitored with a help of a laser-Doppler flowmeter starting before the occlusion of the vessel. NPY_{13-36} (10 µg) or vehicle were administered into the right lateral ventricle either 30 min after MCA occlusion or 30 min after reperfusion. ACPT-I (30 mg/kg) or vehicle were administered intraperitoneally in separate groups of rats according to the same paradigm. Behavioral tests (CatWalk, open field and forelimb placing) were performed before ischemia and 72 hours after reperfusion. The area of infarction was evaluated after the completion of behavioral tests on brain tissue slices stained with 2,3,5-triphenyltetrazolium chloride (TTC) using a computer based image analysis system. Both NPY_{13-36} and ACPT-I significantly diminished volume of infarction and improved selected gait parameters even when administered during reperfusion. The forelimb placing reflex was improved, however, only when neuroprotective compounds where administered 30 min after MCA occlusion. Moreover, ACPT-I occurred to be more efficient in improving rats mobility in the open field. Thus, these results suggest that ACPT-I exerts better protection than NPY_{13-36} in this model of ischemia.

The study was supported by grant No. N N401 091037 from MS&HE.

|B17|

Genes associated with minocycline efficacy in neuropathic pain

Rojewska E.[1], Korostynski M.[2], Przewlocki R.[2], Przewlocka B.[1], Mika J.[1]

[1]Department of Pain Pharmacology, Institute of Pharmacology, Polish Academy of Sciences, Cracow, Poland
[2]Department of Molecular Neuropharmacology, Institute of Pharmacology, Polish Academy of Sciences, Cracow, Poland

Microarray analysis give us an opportunity to exam the molecular mechanisms of neuropathy and to find a new targets for neuropathic pain treatment. Last studies show multiple endogenous factors, which are involved in the chronic

pain development. It is known that the neuroimmune interactions play important role in this process and they may be one of the reasons for the loss of efficacy for many analgesics. Our previous data indicated the importance of spinal microglia activation-related genes in the development of neuropathic pain and their participation in the persistence of its symptoms. Repeated minocycline (30 mg/kg, *i.p.*) was shown to relieve neuropathic pain symptoms by inhibiting the spinal microglia activation and, in consequence, reduced release of numerous cytokines. The genes associated with minocycline efficacy under neuropathy should provide insight into the etiology of pain. Therefore, the aim of the our study was to determine, at the spinal cord level, which of the genes that were changed after sciatic nerve injury are modulated by minocycline. The microarray experiments helped us to identify numerous transcripts that are important for the development of neuropathy and may be possible targets for drug therapy. The DNA microarray method allowed us to choose 93 transcripts (transcription pattern T) from 22 500 studied transcripts, due to their abundance level changes after sciatic nerve injury, as well as 39 transcripts that were modulated by repeated administration of minocycline. To further research we have selected two gene expression patterns T1 and T2. The first transcription pattern T1consisted of 10 transcripts with mRNA abundance levels rising after the injury and minocycline inhibit the effect of the injury; and the T2 transcription pattern have 6 transcripts with mRNA abundance levels dropping following CCI and minocycline reverses the effect. Additionally, we studied changes in selected gene expression by RT-PCR. In summary, our gene analysis offers the first step towards future research into genes that can be modulated and may be good targets for effective and safe therapies for the treatment of neuropathic pain.

Supported by statutory founds and NCN grant 2011/03/B/NZ4/00042.

|B18|

Anti-ischemic effects of 3,3'-diindolylmethane in mouse hippocampal cells at early developmental stages

Rzemieniec J., Litwa E., Wnuk A., Lason W., Kajta M.

Department of Experimental Neuroendocrinology, Institute of Pharmacology, Polish Academy of Sciences, Cracow, Poland

Cerebral ischemia is a condition in which insufficient blood flow results in poor oxygen and glucose supply to the brain, thus causing brain damage or stroke. During the neonatal period of life, ischemia appears as a major risk factor of cerebral palsy, seizures and cognitive impairments. Ischemic episodes have been increasingly recognized in children, but diagnosis and management is difficult because of diversity of underlying risk factors and the absence of a uniform treatment approach. 3,3'-diindolylmethane (DIM) is a plant-derived, acid-catalyzed condensation product of indole-3-carbinol that exhibits property of selective aryl hydrocarbon receptor modulator, and shows anti-carcinogenic capacity by inducing apoptosis in various cancer cells. Recent studies also indicated neuroprotective potential of DIM against brain inflammation and neurodegenerative diseases. The aim of present study was to evaluate neuroprotective effect of DIM in mouse hippocampal cells exposed to ischemia at early developmental stages. In this study, ischemic conditions were mimicked by exposure of embryonic hippocampal cells in primary cultures at 2, 7 and 12 days *in vitro* to 6 h lasting oxygen and glucose deprivation (OGD). Caspase-3 activity and lactate dehydrogenase (LDH) release were measured at 18 h of reoxygenation. In this study paradigm, OGD induced LDH release in mouse hippocampal cultures and increased its level by 23, 165 and 40% at 2, 7 and 12 days *in vitro*, respectively. OGD also caused about 30% enhancement in caspase-3 activity, but only in neuronal cells at later studied days *in vitro*. DIM used in wide concentration range (0.01-10 mM) inhibited the ischemia-induced LDH release in mouse neuronal cells at all analyzed stages. In addition, DIM in concentrations of 0.01 and 10 mM reduced the OGD-induced caspase-3 activity in 7 and 12 days old hippocampal cultures. This study demonstrated strong protective and anti-apoptotic effects of DIM in neuronal cells exposed to ischemia/OGD at early developmental stages. According to our data, the selective aryl hydrocarbon receptor modulator may represent novel therapeutic approach against ischemic brain injury.

This study was supported by the Polish National Center of Science grant No. 2011/01/N/NZ3/04786.

|B19|

Induction of oxidative stress in rat brain after repeated oral exposure to silver nanoparticles

Skalska J.[1], Frontczak-Baniewicz M.[2], Lenkiewicz A.[1], Struzynska L.[1]

[1]Laboratory of Pathoneurochemistry, Department of Neurochemistry, Mossakowski Medical Research Centre, Polish Academy of Sciences, Warsaw, Poland
[2]Electron Microscopy Platform, Mossakowski Medical Research Centre, Polish Academy of Sciences, Warsaw, Poland

The unique physical, chemical and biological properties of silver nanoparticles (AgNPs) have led to their extensive use in many industrial applications, including food industry, textile engineering and silver-based consumer products (e.g. cosmetics, cleansers, medical devices).

However, silver nanoparticles can interact with many substances in the human body due to their high reactivity, which might result in unknown hazards. Presently, only a few studies are dedicated for investigating their toxic potential. Most of them have been conducted using *in vitro* models.

The aim of the present study was to investigate whether commercially available small-sized silver nanoparticles induce oxidative stress in male adult rats and to compare their effect with the effect caused by silver ions.

Animals were exposed to oral application of 10 ± 4 nm AgNPs or silver ions in concentration 0.2 mg/kg for 14 days. Using transmission electron microscopy (TEM), nanosized granules were detected in the brain of exposed rats. To assess oxidative stress in the brain homogenates from exposed animals, ROS level and membrane peroxidation were measured. Additionally, the influence of AgNPs and silver ions on antioxidant enzymes activity (catalase, superoxide dismutase, glutathione peroxidase) was evaluated. Despite this, the ratio of reduced to oxidized glutathione was investigated, so was the level of protein glutathionylation. Our results show, that exposition to AgNPs or silver ions resulted in increase in ROS level, lipid peroxidation and antioxidant enzymes activity in the brain homogenates, whereas the ratio of reduced to oxidized glutathione significantly decreased.

These results indicate, that the induction of oxidative stress under condition of AgNPs or silver ions exposure, is almost certainly one of the mechanisms of their neurotoxicity.

|B20|

Prenatal stress enhances the production of pro-inflammatory cytokines: studies in hippocampal organotypic cultures

Slusarczyk J., Trojan E., Glombik K., Basta-Kaim A.

Departament of Experimental Neuroendocrinology, Institute of Pharmacology, Polish Academy of Sciences, Cracow, Poland

Inflammatory processes may be one of the most important causes of the development and progression of affective disorders. Due to a cytokine theory of depression changes in production of cytokines may play the role in the etiology of these disease. It has been observed that IFN-γ, IL-1 or IL-2 administration may lead to manifestation of symptoms and behavioral changes resembling those observed in major depression in humans. On the other hand, stress is a very important factor investigated in context of mood disorders. Exposure to stressful events, especially in the critical time of development as prenatal or early postnatal period, influences brain homeostasis by affecting the nervous, endocrine and immune systems and may lead to disturbances in the neurodevelopment in adulthood.

In our studies, we determined the effect of prenatal stress procedure – an animal model of depression – on the cytokine levels in hippocampal slice cultures. This *ex vivo* procedure allows preservation of natural connections between the immune, nervous and endocrine systems, cytoarchitecture and functional neuronal-glial interactions. The hippocampus was chosen for the study due to its role in the pathogenesis of depression.

Pregnant Sprague-Dawley rats were subjected daily to three (at 9.00, 12.00, 17.00 o'clock) stress sessions from 14th day of pregnancy until delivery. Control pregnant females were left undisturbed in their home cages. Hippocampal slice cultures were prepared from 7-8 day old rats, according to the method previously described by Stoppini *et al*. (1991) with slight modifications. Hippocampi, isolated from control and prenatally stressed animals were sectioned into 350 µm transverse slices, separated and then transferred onto porous membrane inserts of 6-well culture plates. Each well contained 1 ml culture medium composed of 50% DMEM; 25% HBSS; 25% Horse Serum; 5 mg/ml glucose; amfotericin B; penicillin–streptomycin). Cultures were initiated in a regular, 25% horse serum-containing medium which was gradually replaced by a serum-free, defined-solution-based medium. Cultures were maintained for 7-9 days under standard conditions. The levels of cytokines (TNF-α, IL-1β, IL-6) in supernatants were quantified by specific ELISA kits.

Prenatal stress procedure enhanced the release of IL-1β and TNF-α in hippocampal slices. Moreover, we observed an increased production of IL-6 in hippocampal organotypic cultures obtained from animals after prenatal stress procedure.

Our results, using the organotypic cultures, show that prenatal stress may have an important influence on hippocampus, the brain structure, which plays a key role in the pathogenesis of depressive disorders. Increased inflammatory status after stress may affects these structure especially the neuron-glia interaction.

This work was supported by grant no. 2013/09/B/NZ7/04096.

|B21|

Comparison of pronociceptive system's activity in two neuropathic pain models in mice

Starnowska J., Rojewska E., Mika J., Przewlocka B.

Department of Pain Pharmacology, Institute of Pharmacology, Polish Academy of Sciences, Cracow, Poland

Neuropathic pain may be caused by various conditions that result in nerve damage, including traumatic injury or disease, like diabetes. Typical painful symptoms, such as hyperalgesia (enhanced response to painful stimuli) and allodynia (painful response to neutral stimuli), are thought to be related to constant over-activation of pronociceptive system. Identification of biochemical components that comprise on escalated nociceptive mechanisms may help in finding an efficient remedy premised on re-balancing pronociceptive system's functions. In our study we compared two mice neuropathic pain models that refer to the common clinical neuropathy causes: Bennett's chronic constriction injury model (CCI) with sciatic nerve damage, and streptozotocin-induced diabetic neuropathy. Male CD-1 Albino Swiss mice were tested at 7th, 14th, 21st and 28th day after CCI surgery or streptozotocin (STZ) intraperitoneal administration to assess allodynia and hyperalgesia development, with usage of von Frey and cold plate tests, respectively. Also the glucose level in animals' blood was measured to assess diabetes development. All animals that have not developed neuropathy after nerve injury were excluded from the study as well as animals with no diabetes in STZ model. The curve of allodynia and hyperalgesia development is different for these two models. While hyperalgesia and allodynia intensity is similar on day 7 in both models, it differentiates markedly on day 14 and on day 28. In the latter time point much weaker effects are obtained in a model of CCI and, in contrast, stronger in the STZ model. This proves that neuropathy symptoms in diabetes build up over time, while symptoms in CCI model have opposite tendency. At every time point aforementioned probes of spinal cord tissue were taken to be further analyzed with qRT-PCR method for the activity of pronociceptive systems by analysis of the changes in kappa opioid, B2, and/or MC4 receptors which activation produced pronociceptive effect mediated by endogenous peptides, such as dynorphin, bradykinin and/or alpha MSH. Such analysis is to identify peptides and biochemical routes that are crucial in neuropathic pain development and maintenance. Further studies may test the possibilities of modulating the activity of pronociceptive peptides with their receptors' blockage, with an outlook to develop novel neuropathic pain therapies.

The work was supported by grant Maestro NCN 2012/06/A/NZ4/00028. J. Starnowska is a Ph.D. student and has a scholarship from the KNOW funds sponsored by Ministry of Science and Higher Education, Poland.

|B22|

Morphological features of astrocytic reaction after transcient cerebral ischemia in the rat

Steliga A.[1], Lietzau G.[2], Waskow M.[1], Karwacki Z.[3], Wojcik S.[2], Klejbor I.[1,2], Morys J.[2], Kowianski P.[1,2]

[1]Department of Health Sciences, Pomeranian University of Slupsk, Słupsk, Poland
[2]Department of Anatomy and Neurobiology, Medical University of Gdansk, Gdansk, Poland
[3]Department of Neuroanesthesiology, Medical University of Gdansk, Gdansk, Poland

Introduction: Cerebral ischemia is one of the most powerful pathological stimuli triggering reaction of glial cells, known as reactive astrogliosis. Fundamental features of this reaction depend on type, duration and severity of the pathological stimulus, as well as affected region in the brain [1]. Astrocytes are one of the most important cell populations of the central nervous system, generating the response to the damaging factor. Astrocytic reaction to ischemic stroke is predominantly related with restriction and isolation of the damaged tissue from the intact brain's structures, as well as ability to restore the other damaged cell populations.

Aim: The assessment of selected morphological features of reactive astrocytes, indicating their potential for division,

proliferation and reduction of tissue damage consequences was performed in the rat model of ischemic stroke.

Material and methods: Forty adult male Wistar rats were used in this study. Transient focal cerebral ischemia was evoked by placement of the surgical thread into the internal carotid artery and 1 hr occlusion of the middle cerebral artery. The postoperative survival period was up to 6 weeks. Immunocytochemical stainings for GFAP, Ki-67, and Pax6 were performed, with subsequent confocal microscopic study.

Results: Both studied transcription factors, namely Ki-67 and Pax6 were found in GFAP-immunorecative (ir) astrocytes, localized within the damaged brain. The intensity of double-labeling for the studied factors increased gradually after the first week of reperfusion. Intense hypertrophic reaction developed. An increased GFAP-ir of the astrocytic fibers surrounding the lesion was observed.

Conclusions: Reassuming, our results concerning astroglial reaction indicate regaining of the morphological features, characteristic for the earlier developmental stages, by this cell lineage, as well as development of proliferative and division capacities in response to transient ischemia. The intense and multidirectional nature of the astrocytic response should be taken into account in future studies on the ischemic stroke.

References

1. Steliga A, Waśkow M, Karwacki Z, Wójcik S, Lietzau G, Klejbor I, Kowiański P. Transcription factor Pax6 is expressed by astroglia after transient brain ischemia in the rat model. Folia Neuropathol 2013; 51: 203-213.

|B23|

Sensitivity of glioma cell lines to modified isotiourea derivative (ZKK-3) under anoxia conditions

Stepien K.[1], Ostrowski R.P.[1], Pucko E.B.[1], Kazimierczuk Z.[2], Matyja E.[1]

[1]Department of Experimental and Clinical Neuropathology, Mossakowski Medical Research Centre, Polish Academy of Sciences, Warsaw, Poland
[2]Institute of Chemistry, Warsaw Life Sciences University, Warsaw, Poland

Introduction: Gliomas are the most common primary brain tumours. Despite the improvement of the surgical techniques, radio- and chemotherapy, the treatment of malignant gliomas remains non effective. Hypoxia is thought to play the major role in treatment failure of glial tumours. The aim of this study was to examine how an anoxic gas application impacts on the growth and proliferation of glioma-derived cell lines treated with selected cytostatic agent with potential anti-tumour properties.

Material and methods: The experiment was performed on human glioblastoma T98G cell line (WHO grade IV), cell line derived from low-grade paediatric brain tumour – subependymal giant cell astrocytoma (SEGA, WHO grade I) and normal human astrocytes (HA). For the experiment, the modified isothiourea derivative, N,N'-dimethyl-S-(2,3,4,5,6-pentabromobenzyl)-isothiouronium bromide (ZKK-3), was chosen. Cells were cultured in a medium supplemented with ZKK-3 (25 and 50 μM) or without the tested agent. Cells were divided into two experimental groups. One of them was subjected to 24 hours oxygen deprivation after ZKK-3 application, while the second one was additionally exposed to 18 hours of anoxia pretreatment (N_2/CO_2 gas mixture with 95% N_2 and 5% CO_2). Control cultures were maintained in normoxic conditions. The viability of cells was assessed using Trypan blue dye exclusion. Cell proliferation was evaluated by hemocytometer and Multisizer 3 Beckman Coulter.

Results: Oxygen deprivation caused the decrease of viability of SEGA neoplastic cells and normal human astrocytes. However, there was no significant alteration in the number of cultured T98G cells between cells exposed to 24 hours of anoxia and those maintained in normoxic conditions. The reduction of T98G cell lines proliferation rate was observed only while 18 hours of anoxic gas pretreatment was applied. The anoxic conditions resulted in considerable decrease of sensitivity of T98G glioma cells to the low concentration of ZKK-3, especially in the group pretreated with anoxia. For 50 μM of tested compound, the impact of anoxia on T98G cell line viability was not observed.

Conclusions: Reduction of anti-tumour properties of ZKK-3 related with oxygen deprivation condition, observed for lowconcentration of tested agent, was probably associated with the drug resistance effect. However, the 24h-anoxia was insufficient to induce drug resistance at high 50 μM concentration of tested compound. It might suggest, that limited access to the oxygen slows down the metabolism of astroglial cells due to anaerobic respiration. This phenomenon probably results in decrease of proliferation rate in anoxia-treated cell lines. The results spotted in anoxia-treated T98G and SEGA cell line suggest that the survivability of neoplastic cells upon anoxia conditions might depend on tumour type/grading.

The research was supported by the KNOW-MMRC project and partially by the Foundation for the Development of Diagnostic and Therapy.

|B24|

An analysis of the relationship between anxiety and social rank

Strzelczuk M.[1], Krotewicz M.[1], Bajer M.[1], Krotewicz M.K.[2]

[1]Department of Neurobiology, Faculty of Biology and Environmental Protection, University of Lodz, Lodz, Poland
[2]Department of General and Colorectal Surgery, Medical University of Lodz, Lodz, Poland

Social rank limits social space for conspecifics. This phenomenon occurs in human and non-human forms of social community. Social rank means that the individuals high in the social rank have more social opportunities compared to those low in the social hierarchy. Several studies revealed that maintenance of social position is stressogenic and altered action of physiological systems. In our previous studies we observed that the brain noradrenergic system is implicated in the control of social rank studied in a social competition test what indicates that social rank have important consequences for the hypothalamo-pituitary-adrenocortical (HPA) system activity of the conspecifics. It is known that the brain noradrenergic neurons activity is closely related to the control of the HPA system. The obtained data showed that the maintenance of the low social position was correlated with enhance of noradrenaline release. It indicates that the low position in social stratification was due to anxiety induced by the presence of a high ranking animal, winner of a competitive situation. One of the hypothesis suggests that the formation of social rank resulted in the increase of anxiety in low ranking people. Moreover, the anxiety and observed in subordinate people anhedonia lead to mood disorders and other pathologies. The present study was designed to examine 1) anxiety indices of conspecifics holding different social position and 2) correlations between social indices measured in the social competition test and concentration of corticosterone (CORT) in the blood plasma of rats. In the presented experiments two social competition models were used, with or without food deprivation. The statistical analysis of behavioural indices registered during anxiety test showed a lack of differences related to social stratification. However, visible differences were revealed in temporal dynamics of measured behavioural indices in relation to social position. Competition between conspecifics was associated with differences in CORT concentration accordingly to social rank of rats. Additionally, the analysis of social indices showed a positive correlation between CORT concentration and index of vertical behaviour of dominants.

|B25|

Effects of glutamate receptors antagonists on morphological and biochemical changes in the myelin of EAE rats

Sulkowski G.[1], Dabrowska-Bouta B.[1], Frontczak-Baniewicz M.[2], Struzynska L.[1]

[1]Laboratory of Pathoneurochemistry, Department of Neurochemistry, Mossakowski Medical Research Centre, Polish Academy of Sciences, Warsaw, Poland
[2]Electron Microscopy Platform, Mossakowski Medical Research Centre, Polish Academy of Sciences, Warsaw, Poland

Experimental autoimmune encephalomyelitis (EAE) is an animal model useful in investigations of the pathomechanisms of multiple sclerosis (MS). MS is an inflammatory demyelinating disease of the central nervous system (CNS) that often affects young adults between 20-40 years of age. A characteristic sign of the disease is the damage and loss of oligodendrocytes and myelin sheaths in the white matter of the spinal cord and brain. So far the etiology of MS is unknown. However, presumably one of the mechanisms involved in the disease, might be excitotoxicity. The elevation of glutamate in cerebro-spinal fluid as well as changes in the expression of glutamate receptors (iGluRs and mGluRs) and excitatory amino acids transporters (EAATs) were observed in brains of MS patients/EAE animals. We tested the effect of glutamatergic receptors antagonists: NMDARs – amantadine and memantine and mGluRs G I – LY 367385 and MPEP, on the neurological condition of EAE rats and biochemical and morphological changes observed in brain's myelin during EAE course in rat brains. The electron microscopy studies showed disturbances in myelin ordered layers in EAE rats. A significant changes in the structure of oligodendrocytes, activation and proliferation of microglia and astroglia were also observed. Moreover, we investigated the levels of mRNA for characteristic myelin protein (myelin markers) such as: MOG, MAG, PLP, and CNP-ase, by real time PCR technique in EAE rats and after treatment with glutamate receptors antagonists. The therapy with some of glutamate receptors antagonists (amantadine and memantine) has shown protective effects in EAE rats. The results suggest that disturbances in progressive brain damage in EAE and mechanisms of myelin degradation may be associated with glutamate excitotoxicity.

This work was supported by the Polish MNiSW grant N N401 620038.

|B26|

Oligodendrocyte progenitors provide trophic support for ischemically injured nervous tissue

Sypecka J., Strojek L., Winiarska H., Sarnowska A.

NeuroRepair Department, Mossakowski Medical Research Centre, Polish Academy of Sciences, Warsaw, Poland

The main role of oligodendrocytes is to myelinate nerve fibers in the central nervous system. However their high importance for the functioning of nervous tissue is suspected to go beyond the process of myelinogenesis. To address this issue, we designed a study aimed at determining potential neuroprotective properties of oligodendrocytes and their progenitors. For this purpose, rat organotypic hippocampal slices were exposed to a brief oxygen and glucose deprivation (OGD) which allows mimicking an ischemic injury in vitro. Immediately after the OGD procedure, the hippocampal slices were co-cultured together with differentiating oligodendroglial progenitors derived from neonatal rat brains. The cell survival and proliferation rate in the injured slices were estimated by immunohistochemical methods. After confirming the beneficial influence of the neighboring oligodendrocytes on the injured tissue, a set of molecular and biochemical experiments was carried out with aim of determining the mechanism(s) of the observed profound neuroprotective effect. The obtained results revealed that the oligodendrocyte-derived BDNF is the major factor promoting neuron survival in OGD-subjected hippocampal slices, while SCF strongly promote the cell proliferation. Among the newly-born cells, neuroblasts and microglia could be found most frequently, pointing to both the neuroprotective and neuroimmunomodulatory role of differentiating oligodendrocytes. In conclusion, the presented study revealed that oligodendrocytes are able to secret BDNF and other active factors, thus providing trophic support for the other neural cells. The presented study confirms the hypothesis concerning the complex functions of oligodendrocytes in the nervous tissue.

Supported by grant 0345/B/P01/2010/38.

|B27|

The influence of recombinant α-synuclein protein injection on the expression of selected inflammatory factors in the murine brain

Sznejder-Pacholek A., Joniec-Maciejak I., Wawer A., Schwenkgrub J., Mirowska-Guzel D.

Department of Experimental and Clinical Pharmacology, Medical University of Warsaw, Warsaw, Poland

The studies exploring possible reasons of the neurodegeneration in Parkinson's disease are still far from conclusion. However, it has been already confirmed that α-synuclein protein (ASN), together with other proteins, is the principal component of Lewy pathology and influences strongly the pathogenesis of Parkinson's disease. It was observed that the increased level of ASN protein caused the microglia response. Microglial activation leads to the increased expression of inflammatory genes in the central nervous system (CNS), and the infiltration of peripheral immune cells into the CNS. Recent evidence suggests that reactive microglia cells may actively participate in the damage of dopaminergic neurons. Therefore, we examined the potential role of recombinant monomer of ASN in the inflammatory reaction in murine model of PD, hoping that clarification of the exact role of ASN in the inflammation will help us to understand the molecular mechanism of injuries of dopaminergic cells. ASN was bilaterally administered into substantia nigra (SN) or striatum (ST). We investigated the effect of high ASN monomer concentrations on microglia response: ionized calcium-binding adapter molecule 1 (IBA1) expression by western blot method, as well as some pro-inflammatory cytokines expression (interleukin: IL-6, IL-12) by Real-Time PCR and the lymphocytes T (CD3+, CD8+, CD4+) infiltration in the ST and SN of mice. The infiltration of the lymphocytes was measured by immunohistochemical method. We observed an increase of activated microglia cells (IBA1), a strong infiltration of lymphocytes T (CD8+ and CD4+) and higher level of mRNA for pro-inflammatory cytokines (IL-6, IL-12) after bilateral injection of ASN.

Our study provided more evidence for the involvement of ASN in the inflammatory response in the CNS. However, further studies are required to reveal the detailed mechanism of the influence of ASN in neuro-inflammation in course of Parkinson's disease.

|B28|

Impact of triclosan on aryl hydrocarbon receptor-induced neurotoxicity and apoptosis in mouse neocortical neurons

Szychowski K.A., Wojtowicz A.K.

Department of Animal Biotechnology, Agricultural University of Cracow, Cracow, Poland

Triclosan (TCS) is an antimicrobial agent used extensively in personal care and sanitizing products, such as soaps, toothpaste, and hair products. Over the past half century TCS has been incorporated into ever growing numbers of medical products as well as in household items, such as plastic cutting boards, sports equipment, textiles and furniture. The TCS has been detected in water and sediments and also in human workplace and private houses dust in wide range of concentrations. A number of studies has shown presence of TCS in different human tissue such as blood, adipose tissue, liver, brain, breast milk and in urine. There are limited studies evaluating the toxicity of TCS and data concerning bioaccumulation of TCS in living organisms are inconsistent. Some evidence indicate that TCS can be cumulated in human nails but previous studies have demonstrated that TCS is also metabolized to sulfate and glucuronide by the liver and extracted in methylated form in urine. It is well known that TCS has a similar chemical structure to dioxin and in the presence of sunlight may be transformed to produce up to four dioxin compounds such as 2,8-DCDD, 2,3,7-TCDD, 1,2,8-TriCDD, and 1,2,3,8-TCDD. Aryl hydrocarbon receptor (AhR) is involved in the cell response to the numerous xenobiotics especially to dioxin. It has been demonstrated that this receptor is involved in regulation of genes expression which control growth and differentiation of neurons, and plays a key role in their metabolism and adaptation. The apoptosis dependent on the activation of AhR has been observed in primary cells cultures of the neocortex, hippocampus and cerebellum. The aim of the present study was to investigate the involvement of AhR in the cytotoxic and proapoptotic effects of TCS in mouse neocortical neurons. The cultures of neocortical neurons were prepared from Swiss mouse embryos on 15/16 day of gestation. The cells were cultured in phenol red-free Neurobasal medium with B27 and glutamine. On 7th day *in vitro* AhR siRNA was applied to neurons for 12 h at 50 nM in antibiotic-free medium containing the siRNA transfection reagent interferin. After silencing process the experimental cell culture groups were treated with AhR agonist β-naphthoflavone (βNF) and TCS for 24 h. After silencing procedure and exposure to βNF or TCS the release of the lactate dehydrogenase (LDH) in the culture medium and caspase-3 activity in cells was measured.

Our preliminary data demonstrated that in the presence of βNF as well as TCS the increase in neuronal apoptosis and LDH release into the culture medium were observed. In neurons undergoing silencing procedure in the presence of βNF no significant changes in cytotoxicity or induction of apoptosis were observed. Additionally, the cytotoxic as well as proapoptotic effect of TCS was partially reduced after silencing process. In summary, the presented study demonstrated that AhR is involved in TCS mechanism of action.

Support by statutory funds of Agricultural University in Cracow DS 3242/14.

|B29|

The impact of olanzapine on the dehydrogenase lactate release in cortical organotypic cultures – study in an animal model of schizophrenia

Trojan E., Slusarczyk J., Glombik K., Kurek A., Basta-Kaim A.

Departament of Experimental Neuroendocrinology, Institute of Pharmacology, Polish Aacademy of Sciences, Cracow, Poland

Introduction: Schizophrenia is a common and disabling psychiatric brain disorder of neurodevelopmental origin, in which both genetic and environmental factors appear to play an important role. Many data from epidemiological and clinical studies indicate that viral or bacterial infection during pregnancy may enhance the risk of schizophrenia in adulthood. Therefore among the animal models used to study the etiology of schizophrenia, the systemic administration of the bacterial endotoxin lipopolysaccharide (LPS) during pregnancy is often applied.

Aim: The aim of this study was to assess the effect of prenatal LPS administration on the lactate dehydrogenase (LDH) activity in cortical organotypic cultures in both – basal and inflammatory conditions. Moreover, we determined the role of antipsychotic drug – olanzapine administration on the above mentioned parameter and the possible mechanism of this drug action in cortical organotypic cultures obtained from control and prenatally LPS treated offspring.

Material and methods: Female Sprague-Dawley rats were paired with syngenic males. Pregnancy was confirmed

the next morning. LPS (at the dose of 1 mg/kg, Serotype 026:B6) was injected sc every second day from the 7th day of pregnancy till delivery. The cortical organotypic cultures were prepared from the brains isolated from 6-7 day old offspring. All biochemical analyses were performed after culture stabilization. The activity of lactate dehydrogenase was measured in the medium by colorimetric LDH assay. The tests were performed in cortical organotypic cultures obtained from control and prenatally LPS -treated newborns in both basal conditions and following additional endotoxin (100 ng/ml) stimulation. In the next set of experiments the influence of olanzapine (at a dose of 5 μM) or/and selective phosphatidyloinositol 3-kinase (PI3K) inhibitor – wortmannin (at the dose of 10 μM) – administration was evaluated.

Results: Our data demonstrated that prenatal LPS administration during last two weeks of pregnancy increased LDH release from the cortical organotypic cultures. Moreover in the cortical cultures obtained from pups prenatally treated with LPS the potentiation of LDH release after acute LPS treatment with comparison to cultures of controls was observed. On the other hand acute administration ofolanzapine resulted in a decrease of cell mortality. The involvement of PI3K/Akt pathway in the olanzapine action was confirmed by the use of wortmannin, an inhibitor of phosphatydylinositol 3-kinase which attenuated the protective olanzapine action.

Conclusions: This study provided evidence of the protective effect of olanzapine in cortical organotypic cultures in animal model of schizophrenia based on prenatal LPS administration. Furthermore, it may be postulated that inhibitory impact of this drug on the LDH release is mainly connected with enhancement of PI3k pathway.

This study was supported by statutory funds Institute of Pharmacology PAS.

|B30|

Increased concentration of a-synuclein alters metabolism and transport of dopamine in mice

Wawer A.[1], Sznejder-Pacholek A.[1], Joniec-Maciejak I.[1], Schwenkgrub J.[1], Mirowska-Guzel D.[1,2]

[1]Department of Experimental and Clinical Pharmacology, Medical University, Warsaw, Poland
[2]Institute of Psychiatry and Neurology, Warsaw, Poland

Parkinson's disease (PD) is the second most common progressive neurodegenerative disorder after Alzheimer's disease. It is characterized by two major processes: a progressive loss of dopaminergic neurons and an accumulation of intraneuronal Lewy bodies containing misfolded fibrillar a-synuclein (ASN). Neurodegeneration occurs mainly in substantia nigra (SN), accompanied by a decreased concentration of dopamine (DA) and its metabolites in striatum (ST). Various etiological triggers have been linked to PD, including genetic mutations and environmental toxins, but the pathway that leads to neurodegeneration remains unknown.

The aim of our study was to examine the influence of recombinant monomers of ASN on dopaminergic system activity. 1-year-old male C57Bl mice were used in this study. ASN was bilateraly administered into SN or ST. Animals were sacrificed at 4 weeks following ASN administration.

To evaluate the influence of the ASN on the neurodegeneration concentrations of striatal DA and its metabolites were measured by high performance liquid chromatography (HPLC). The expression of dopamine transporter (DAT) was measured by western blot method.

We observed changes in dopamine metabolism after ASN monomers administration. Our study also showed statistically significant influence of ASN on dopamine reuptake via DAT.

Further research must be conducted to better understand the crucial role of ASN in the neurodegenerative process in PD.

|B31|

Adipokines and other factors connected with dementia

Wehr H., Bednarska-Makaruk M., Graban A.

Department of Genetics and I Department of Neurology, Institute of Psychiatry and Neurology, Warsaw, Poland

Several circulating factors manifesting activity in neurochemical events were determined in persons with dementia and compared with control subjects. The whole group comprised 327 persons: 207 females and 120 males, aged 72.7 ± 8.7 years. 68 of them were diagnosed as probable Alzheimer's disease (AD), 33 as dementia of vascular origin (VaD), 47 as mixed dementia (MD), 83 as mild cognitive impairment (MCI) and 96 were controls without cognitive impairment (C). The levels of several adipokines: adiponectin, leptin, resistin and of the brain derived neurotrophic factor (BDNF) and interleukin-6 (IL-6) were determined in blood serum.

As connection of dementia with carbohydrate metabolism disturbances is observed, therefore glucose levels, glucose tolerance and insulin levels were also determined.

Statistically significant higher adiponectin and IL-6 levels, as compared with controls and glucose intolerance, were stated in MD and higher resistin levels and glucose intolerance in VaD. Therefore these preliminary results suggest the existence of disturbances in such forms of dementia which are connected with vascular pathology.

|B32|

Purinergic P2 receptors activation mediates neuroblastoma SH-SY5Y cell death evoked by extracellular α-synuclein

Wilkaniec A., Cieslik M., Gassowska M., Lenkiewicz A.M., Czapski G.A., Adamczyk A.

Department of Cellular Signaling, Mossakowski Medical Research Centre, Polish Academy of Sciences, Warsaw, Poland

The purinergic P2 receptors for adenosine 5'-triphosphate (ATP) are abundantly present in the central nervous system and play important roles in neurotransmission, neuromodulation, as well as in glial cells function. P2 receptors belong to two structurally distinct families, the G protein-coupled P2Y receptors and the ligand gated ion channels – P2X receptors. Recently, extracellular ATP and specific purinergic receptor subtypes have been shown to be involved in neurodegenerative disorders including Parkinson's and Alzheimer's diseases. However, till now the mechanisms underlying the disturbances in ATP-mediated neurotransmission are not well established. Recent studies indicated that in neurodegenerative disorders, α-synuclein (ASN) has been released and taken up by cells that may facilitate its progressive pathological spreading in the brain. Our own *in vitro* studies support the idea of transcellular spread of secreted ASN and showed its significant cytotoxic effect when applied extracellularly. Therefore, the aim of this study was to examine the role of purinergic P2 receptors and ATP in the neurotoxicity induced by extracellular ASN.

The experiments were performed in human SH-SY5Y neuroblastoma cells differentiated with the all-trans retinoic acid (ATRA) using immunochemical, spectrophotometric, radiochemical and spectrofluorometric methods. Our study showed that SH-SY5Y cells express P2X4, 5, 7 and P2Y1 receptors. We have investigated the effect of ASN on gene expression and protein level of all these receptors, but we did not observe any significant changes. However, exposure of SH-SY5Y cells to ASN (10 μM) induced significant increase in cytosolic calcium load, that was mainly caused by the activation of extracellular Ca^{2+} influx. The stimulation of P2 receptors by ATP (5 mM) was found to trigger the similar but more pronounced effect than ASN. Furthermore, we found that ASN-evoked Ca^{2+} influx was partially eliminated by the selective purinergic P2 receptors antagonist, PPADS (200 μM). In order to clarify the molecular mechanisms mediating the activation of P2 receptors, we examined the effect of ASN on extracellular ATP concentration and found that ASN promoted the release of ATP from SH-SY5Y cells. Moreover, both exogenous ASN and ATP induced significant increase in SH-SY5Y neuroblastoma cells death by about 50%. The toxic effect of these compounds was significantly prevented by PPADS, indicating that activation of P2 receptors is involved in cytotoxicity evoked by extracellular ASN in the human neuroblastoma SHSY-5Y cell line. Taken together, these results raise the possibility that the P2 signaling pathway could be a therapeutic target for treating neurodegenerative disorders.

Supported by NCN grant 2013/09/D/NZ3/01359.

|B33|

Impact of retinoid X receptor on the apoptotic and toxic effects of dichlorodiphenyldichloroethylene (DDE) in mouse embryonic neuronal cells

Wnuk A., Rzemieniec J., Litwa E., Lason W., Kajta M.

Department of Experimental Neuroendocrinology, Institute of Pharmacology, Polish Academy of Sciences, Cracow, Poland

One of the most toxic compounds is dichlorodiphenyldichloroethylene (DDE) which is metabolite of the pesticide dichlorodiphenyltrichloroethane (DDT). DDE may easily cross the skin and blood-brain barrier. It accumulates in human organisms, especially in adipose and brain tissues. Recent epidemiological data exhibited the association between exposure to pesticides and increased ratio of neural degeneration. Enhanced level of DDE was detected in brain and blood samples of people suffering from Alzheimer's disease. Available data suggest that DDE induces apoptosis in bird and murine neurons. Although neurotoxic effects of DDE have been demonstrated, the role of retinoid X receptor (RXR) in apoptotic and toxic actions of DDE needs to be clarified. This study aimed to provide evidence on involvement of RXR in DDE-induced

apoptosis and neurotoxicity in mouse neuronal cells in primary cultures.

Our study demonstrated that DDE (10 and 100 µM) activated caspase-3 in the mouse neuronal cell cultures, which was found within 6 hours after the treatment and accompanied by significant increase in lactate dehydrogenase-release (LDH) at 6 and 24 h of experiment. These effects were not tissue-specific, i.e. hippocampal, neocortical and cerebellar cells responded to DDE in similar way. In addition, the apoptotic and neurotoxic effects of DDE were followed by approximately 2-fold increase in RXR protein level, as evidenced by ELISA and Western blot analyses. DDE-induced stimulation of RXR-signaling was verified using selective antagonist HX531and specific siRNA. HX531 inhibited the effects evoked by DDE and reduced both caspase-3 and LDH release. Furthermore, in RXR siRNA-transfected cells DDE did not retain its apoptotic and toxic potency, thus suggesting a crucial role of the receptor in propagation of DDE-induced apoptosis and neurotoxicity.

This work was supported by the Operating Program of Innovative Economy 2007-2013, grant No. POIG.01.01.02-12-004/09.

|B34|

Contribution of tachykinin NK_1 and µ-opioid receptors to cardio-respiratory effects of the analgesic chimeric peptide in anaesthetized rats

Wojciechowski P.[1], Szereda-Przestaszewska M.[1], Lipkowski A.W.[2]

[1]Laboratory of Respiratory Reflexes, Department of Experimental Pharmacology, Warsaw, Poland
[2]Department of Neuropeptides, Mossakowski Medical Research Centre, Polish Academy of Sciences, Warsaw, Poland

Clinical use of opioid analgesics is limited by a variety of side effects such as respiratory arrest, arterial hypotension, drug tolerance and dependence. Therefore, many attempts are being made to create an effective analgesic that is free fromabove-mentioned side effects. Recently synthesized peptide – AWL3106 – is composed of two pharmacophores: µ opioid receptor agonist – dermorphin, and tachykinin NK_1 receptor agonist – substance P_{7-11}. This novel peptide shows strong analgesic activity of 5 and 30 folds the potency of morphine after intravenous and intrathecal administration, respectively.

The purpose of the present study was to show the contribution of each pharmacophore to cardio-respiratory pattern evoked by AWL3106.

Cardiorespiratory parameters were measured in 27 anaesthetized spontaneously breathingrats. Animals were treated with an intravenous injection of AWL3016 (0.3 µmol/kg) in the following scheme:

– in control conditions (n = 9) and after blockade of opioid receptors with naloxone (2 mg/kg) (n = 9),
– following simultaneous blockade of opioid (naloxone) and tachykinin NK_1 receptors with SR140333 (2 µmol/kg, n = 9).

Control intravenous injection of AWL3106 induced an apnoea of mean duration of 5.1 ± 0.7 s ensued by breathing of 19% reduced frequency (f) and 22% augmented tidal volume (V_T) with no signs of ventilatory depression, as well as 59% fall in mean arterial pressure (MAP) measured 2 min post drug.

Naloxone injected 2 min prior to AWL3106 challenge prevented the occurrence of apnoea as well as significantly reduced the maximal fall in breathing rate and an increase in tidal volume compared to the control injection. Minute ventilation still remained unaffected. Opioid receptor blockade failed to prevent the decrease in MAP. Subsequent blockade of NK_1 receptors resulted in suppression of all cardiorespiratory effects induced by AWL3106.

The present study showed that activity of opioid pharmacophore was essential to induce apnoea, whereas simultaneous activation of opioid and tachykinin receptors with AWL3106 affected both components of respiratory pattern (V_T and f). Arterial hypotension was associated mainly with activation of tachykinin NK_1 receptors.

|B35|

Neurochemical changes underlying modified swim test as an animal model of negative symptoms of schizophrenia

Wozniak M., Wieronska J., Pilc A.

Institute of Pharmacology, Polish Academy of Sciences, Cracow, Poland

Modified swim test has been recently introduced as an animal model of negative symptoms of schizophrenia, especially the blunted effect. The model is based on the repeated treatment with antagonist of NMDA receptor – MK-801 (0.4 mg/kg, one a day for 13 days) which increases the immobility in the modified swim test 24 h after the final injection

of chosen compound. These behavioral deficit was reversed by the atypical antipsychotic risperidone (0.1 and 0.2 mg/kg), as well as by agonist of 5-HT_{1A} receptors – (RS) 8-OH-DPAT (0.01; 0.025 mg/kg). We also studied the activity of two positive allosteric modulators of $GABA_B$ receptor: CGP7930 (1; 2.5; 5 mg/kg) and GS39783 (0.5; 1; 2 mg/kg) in the same model. The compounds were active at the doses of 5 mg/kg and 0.5 and 1 mg/kg, respectively. In the second part of the present study, with the use of western blotting analysis, we also investigated the changes in 5-HT_{1A} receptor and GAD65 and GAD67 level in PFC and hippocampus of MK-801-treated mice, as those proteins can be regarded as the markers of the psychosis. The increases in 5-HT1A receptor level was observed both in the PFC and hippocampus, while decrease in GAD65 protein was observed in the hippocampus only. No changes were observed for GAD67 receptor level in either structure investigated. Our findings support the hypothesis that the changes in 5-HT1A receptor and/or GABA level may contribute to the pathophysiology of schizophrenia.

|B36|

Role of the Ras in regulation of BNIP3 expression in glioblastoma cells

Wysokinska E., Kalas W., Pawlak A., Ziolo E., Strzadala L.

Ludwik Hirszfeld Institute of Immunology and Experimental Therapy, Polish Academy of Sciences, Wroclaw, Poland

It has been demonstrated that anticancer treatments are able to induce autophagy in cancer cells. The role of autophagy in cancer is not clear, as autophagy may promote cancer cell survival or became the mechanism of growth restriction. In glioma cells this process can be induced byanticancer agents such as arsenic trioxide, ceramide, temozolomide, quercetin or radiation.

Ras proteins, frequently mutated in human cancers, function as molecular switches regulating pathways responsible for proliferation and cell survival. Ras family proteins were shown to play a role in the autophagy process. For example, HRas is able to induce autophagy through ERK signaling pathway in human colorectal, breast and cervical cancer. In other models Ras induces autophagy by upregulating Atg5 or Noxa and MEK/ERK pathway. Bcl-2/adenovirus E1B-19 kDa-interacting protein 3 (BNIP3), likewise Ras protein, is responsible for the fate of cancer cells. BNIP3 is an important mediator of cell survival and a member of the Bcl-2 family of proteins that regulate programmed cell death and autophagy.

In our previous studies, we for the first time demonstrated correlation between Ras, BNIP3 and process of autophagy in human colorectal cancer cell line (DLD-1). We have showed the primary role of KRas in the regulation of BNIP3 protein expression, establishing a link between the expression of oncogenic HRas and upregulation of BNIP3 and their control of autophagy in cancer cells. Additionaly we found that upregulation of BNIP3 in DLD-1 cells results in KRas-dependent resistance to 5-Fluorouracil.

Glioblastomas are the most aggressive form of brain tumor that show resistance to treatment with various chemotherapeutic agents and BNIP3 was shown to promote its survival and adaptation to hypoxia by autophagy. The purpose of our studies is to elucidate the role of Ras and BNIP3 in induction of autophagy in U373MG glioma cell line. Here we present the data on regulation of BNIP3 expression by Ras in glioblastoma cells in normoxia and hypoxia. We believe that these studies will reveal the new opportunities for treatment of glioblastoma.

References

1. Swiderek E, Kalas W, Wysokinska E, Pawlak A, Rak J, Strzadala L. The interplay between epigenetic silencing, oncogenic KRas and HIF-1 regulatory pathways in control of BNIP3 expression in human colorectal cancer cells. Biochem Biophys Res Commun 2013; 441: 707-712.
2. Kalas W, Swiderek E, Rapak A, Kopij M, Rak JW, Strzadala L. H-ras up-regulates expression of BNIP3. Anticancer Res 2011; 31: 2869-75

This work was supported by grant of NCN no. 2011/01/NZ4/00938.

|B37|

Effect of clonidine on kynurenic acid production in rat brain cortex

Zakrocka I., Turski W.A., Kocki T.

Department of Experimental and Clinical Pharmacology, Medical University of Lublin

Clonidine is a central acting antihypertensive agent. Its mechanism of action is connected with activation of presynaptic α2-adrenoreceptors and imidazoline receptors in the central nervous system. Clonidine may have also influence on glutamatergic neurotransmission, by attenuating effects caused by NMDA or AMPA receptors activation. Kynurenic acid (KYNA) is the only known endogenous antagonist of excitatory amino acid receptors and of

α7 nicotinic receptors. Cerebral synthesis of KYNA from its bioprecursor L-kynurenine is catalyzed by aminotransferases localized preferentially within astrocytes. In the brain, two distinct kynurenine aminotransferases, KAT I and KAT II, are responsible for the formation of KYNA. KYNA was shown to display potent neuroprotective properties and its impaired production was implicated in the neurodegenerative diseases. Additionally, it was recently reported that KYNA could play a role in regulation of blood pressure. A significant reduction of blood pressure in animal model of hypertension has been achieved by local intracerebral administration of KYNA.

The aim of this study was to evaluate the effect of clonidine on the formation of KYNA in brain cortex in rat.

Experiments were carried out on brain cortex obtained from male Wistar rats. The effect of clonidine on kynurenic acid concentration was evaluated on cortical slices after 2 hours of incubation in different concentrations of tested drug. To determine kynurenine aminotransferases (KATs) I and II activities cortical tissue was homogenized and dialyzed for 12 hours. Homogenates were incubated for 2 hours with tested compound. Supernatant was applied on the cation-exchange resin (Dowex 50 W+). Eluted kynurenic acid was subjected to the HPLC and quantified fluorimetrically. The experiments were conducted at least three times to achieve comparable results. Experimental procedures have been approved by the Local Ethical Committee in Lublin and are in agreement with European Communities Council Directive on the use of animals in experimental studies.

Clonidine at the concentration of 1, 3 and 5 mM decreased KYNA production in the brain cortical slices to 80% ($p < 0.05$), 70% ($p < 0.001$) and 40% ($p < 0.001$) of control, respectively. whereas at the concentration of 0.5, 0.1 and 0.01 mM was ineffective. Clonidine at the concentration of 0.01-5 mM did not affect the activity of KAT's.

The data presented here indicate that clonidine might decrease cortical level of kynurenic acid and thus suggests the novel mechanism of action of clonidine.

Supported by the grant for young scientists from Ministry of Science and Higher Education, MNmb515/2013.

|B38|

Influence of losartan on kynurenic acid production in the rat brain cortex

Zakrocka I., Turski W.A., Kocki T.

Department of Experimental and Clinical Pharmacology, Medical University of Lublin, Lublin, Poland

A renin–angiotensin–aldosteron (RAA) system is an important regulator of body homeostasis. It is thought to regulate not only water – electrolyte metabolism, including the regulation of thirst, blood pressure maintenance, vasopressin release, but it is responsible for controlling thermoregulation, learning, memory, emotions, reproduction and sexual behaviors as well. Among angiotensin receptors, the most prominent role in pharmacotherapy possesses receptor type 1 (AT-1), RAA was also implicated in the development of neurodegenerative disorders. It was reported that activation of RAA in the brain may have important role in animal seizure models. Recent studies indicate that substances interfering with concentration and pharmacodynamic properties of angiotensin are proven to have neuroprotective effect, especially to ischemic nervous tissue, improving patient's prognosis after vascular brain damage.

Kynurenic acid (KYNA) is the only known endogenous antagonist of excitatory amino acid receptors and of α7 nicotinic receptors. Brain KYNA displays high affinity towards the glycine site of N-methyl-D-aspartate (NMDA) receptor complex. The cerebral synthesis of KYNA from its bioprecursor L-kynurenine is catalyzed by two distinct kynurenine aminotransferases (KAT I and KAT II). The disturbances of KYNA production have been linked to the occurrence of epilepsy, Huntington's disease, Alzheimer's disease, schizophrenia, AIDS-related dementia and others. The anticonvulsant and neuroprotective role of KYNA in vivo and in vitro is well documented.

In this study we aimed to analyze whether losartan, an AT_1 – receptor antagonist, might modify KYNA production in brain cortex of a rat.

In cortical slices losartan at the concentration of 0.5, 1, 3 and 5 mM decreased KYNA synthesis to 61% ($p < 0.05$); 17% ($p < 0.001$) 6% ($p < 0.001$) and 5% ($p < 0.001$) of control value, respectively. The activity of KAT I was decreased by losartan at the concentration of 0.01; 0.1; 0.5; 1 and 3 mM to 45% ($p < 0.01$); 13% ($p < 0.001$); 12% ($p < 0.001$); 6% ($p < 0.001$); 3% ($p < 0.001$) of control value, respectively. The activity of KAT II was diminished by losartan at the concentration of 0,01; 0,1; 0,5; 1 and 3 mM to 74% ($p < 0.01$); 9% ($p < 0.001$); 6% ($p < 0.001$); 2% ($p < 0.001$); 1% ($p < 0.001$) of control, respectively.

Our data suggest that losartan might decrease kynurenic acid production in the rat brain cortex, most probably via influence on KAT's activity.

Supported by the grant from National Science Centre (NCN) PRELUDIUM 4 No UMO-2012/07/N/NZ4/02088.

|B39|

The role of oxidative stress in cytotoxicity evoked by tetrabromobisphenol a in primary cultures of rat cerebellar granule cells

Zieminska E., Lenart J., Lazarewicz J.W.

Department of Neurochemistry, Mossakowski Medical Research Centre, Polish Academy of Sciences, Warsaw, Poland

Tetrabromobisphenol A (TBBPA) and other brominated flame retardants (BRF) are additives to industrial products reducing their combustibility. It was found that TBBPA leaks to environment and contaminates samples collected from humans and wildlife. Recent papers showed cytotoxic effects of BRFs, however relatively few studies addressed the subject of TBBPA neurotoxicity and its mechanisms. Although there are indications that TPPBA-induced excitotoxicity, influx of extracellular Ca^{2+} and particularly its release from intracellular stores play a key role in the mechanism of TPPBA neurotoxicity, there is also data suggesting a primary role of oxidative stress in this process. The aim of this study was to evaluate the latter hypothesis. Experiments were performed using the primary cultures of rat cerebellar granule cells (CGC) at 7th day *in vitro*. To evaluate TBBPA neurotoxicity, the cells were exposed for 30 min to this BFR, and neuronal viability was assessed after 24 h, using fluorescence microscope and propidium iodide staining. During or after 30 min incubation with TBBPA in Locke medium, we estimated selected parameters of oxidative stress including reactive oxygen species (ROS) production and changes in mitochondrial membrane potential by measuring DCF and rhodamine fluorescence, respectively. Moreover, the intracellular glutathione (GSH) level was assessed using fluorescence kit, SOD level with Western blot and catalase activity using absorbance kit. Free radical scavengers GSH, vitamin C or N-acetyl cysteine (NAC), NMDA receptor antagonist MK801 and ryanodine with bastadin 10 inhibiting intracellular Ca^{2+} release *via* ryanodine receptors as well as a megachannel antagonist cyclosporine A (CsA) were used as pharmacological tools to test different mechanisms contributing to oxidative stress and cytotoxicity. Viability of cells 24 h after 30-min incubation with 25 μM TBBPA decreased to 30% compared to control, while application of all the substances tested, except CsA, increased their survival to 60-80%. Incubation with 25 μM TBBPA increased ROS production by about 50% and significantly decreased the mitochondrial potential. Application of 1 mM GSH completely prevented the former effect but did not affect depolarization of mitochondria. Administration of 7.5 to 25 μM TBBPA dose dependently decreased intracellular GSH level to 40%, and catalase activity to 60% of the control. Application of ROS scavengers, bastadin with ryanodine and MK801 partially prevented these effects. In turn SOD-1 level increased in dose depend manner but SOD-2 declined after TBBPA administration compare to the control. Results of the presented experiments indicate that oxidative stress reflected by changes in ROS production, GSH/SOD level and catalase activity, plays a significant role in TBBPA cytotoxicity in CGC in concert with excitotoxicity and calcium imbalance, but not with activation of megachannels.

Supported by the NCN grant 2012/05/B/NZ7/03225.

|B40|

Bastadin 12 is a new tool useful in the study of mechanisms of intracellular calcium release evoked by thapsigargin and Tetrabromobisphenol A

Zieminska E.[1], Stafiej A.[1], Toczylowska B.[2,3], Lazarewicz J.W.[1]

[1]Department of Neurochemistry, Mossakowski Medical Research Centre, Polish Academy of Sciences, Warsaw, Poland
[2]Institute of Biochemistry and Biophysics, Polish Academy of Sciences, Warsaw, Poland
[3]Nalecz Institute of Biocybernetics and Biomedical Engineering, Polish Academy of Sciences, Warsaw, Poland

Thapsigargin (Th) is the established Ca^{2+} releaser from intracellular ER stores. Studies of others using mainly skeletal SR membranes demonstrated that Th-induced Ca^{2+} efflux from SR can be inhibited by simultaneous administration of ryanodine (Ry) and the macrocyclic brominated thyrosine derivative bastadin 5 (Ba5) at micromolar concentrations but not by these compounds applied separately. These results have been interpreted as unmasking by Th of Ry-insensitive leak conformation of ryanodine receptors (RyR) which are converted by Ba5 into Ry-sensitive conformation. We previously confirmed these properties of Ba5

using the rat cerebellar granule cell (CGC) in primary cultures. The effects of other bastadin derivative Ba12 on Ca^{2+} homeostasis were never systematically studied. Tetrabromobisphenol A (TBBPA) is a commonly used brominated flame retardant with the recognized neuro- and cytotoxic properties. It has been suggested that release of Ca^{2+} from the intracellular stores mediates TBBPA cytotoxicity. In the present experiments, using CGC and the fluorescent intracellular Ca^{2+} probe fluo-3, we evaluated usefulness of the synthetic Ba12 as a tool that could replace Ba5 in the comparative study characterizing intracellular Ca^{2+} release evoked by thapsigargin and TBBPA. The results demonstrated that 200 nM Th as well as 30 μM Ba12 applied alone induces increase in the intracellular Ca^{2+} level in CGC, while 2.5 and 10 μM Ba12 did not interfere with basal Ca^{2+} concentration. Both 2.5 μM Ba12 or 200 μM Ry administered separately only partially reduced the release of Ca^{2+} induced by Th, whereas these compounds in combination completely inhibited this effect. Ca^{2+} transients in CGC evoked by the muscarinic receptor agonist, 100 μM oxotremorine-M, were significantly inhibited by antagonist of IP3 receptors 100 μM 2-APB, but not by Ba12 and Ry given either separately or together. TBBPA (5, 10 and 25 μM) concentration-dependently increased intracellular Ca^{2+} level in CGC. Administration of Ba12 in combination with Ry completely blocked the increase in intracellular Ca^{2+} concentration evoked by 10 μM TBBPA, while these compounds applied separately were ineffective. In conclusion, these results show that Ba12 can replace Ba5 in testing sensitivity to Ry of Ca^{2+} release from the intracellular stores of cultured neurons and in identifying leak conformation of RyR. They are also consistent with the hypothesis that TBBPA and Th induce release of intracellular Ca^{2+} through a common mechanism involving leak conformation of RyR.

Supported by the Polish National Science Centre grant # 2012/05/B/NZ7/03225.

|B41|

The neuroprotective effect of histone deacetylase inhibitor – sodium butyrate after experimental neonatal hypoxia-ischemia

Ziemka-Nalecz M., Jaworska J., Sypecka J., Zalewska T.

NeuroRepair Department, Mossakowski Medical Research Centre, Polish Academy of Sciences, Warsaw, Poland

Birth asphyxia remains a frequent cause of perinatal morbidity and mortality. During perinatal hypoxic-ischemic (HI) brain injury neuronal cells are damaged and lose their functions or die. In the past few years, it has become clear that brain ischemia stimulates neural stem cell proliferation and differentiation in the cerebral neurogenic area – the dentate gyrus (DG) of the hippocampus, which is frequently injured after the perinatal HI. Induction of neural progenitors after HI insult may represent an endogenous mechanism for brain regeneration. Mounting evidence indicates that histone deacetylase inhibitors (HDACi) exert stimulation of endogenous neurogenesis in adult brain. Our aim in this study was to examine the influence of HDACi – Sodium Butyrate (SB) on the generation of neurons and oligodendrocytes in immature brain subjected to hypoxia-ischemia. Furthermore, we tried to elucidate the mechanisms of action of Sodium Butyrate. We utilized an established model of hypoxia-ischemia induced in rats of postnatal day 7 (PND7). After ligation of the left common carotid artery the animals were exposed to hypoxia (7.6% oxygen for 60 min). Sham-operated rats were used as controls. SB (300 mg/kg) was injected subcutaneously for 5 consecutive days starting immediately after HI. To estimate the proliferation profile and phenotype of newborn cells, animals were injected with BrdU (50 mg/kg). 3-14 days after HI the presence of BrdU-positive cells was seen in both hemispheres (ipsi- and contra-lateral) with the strongest proliferation level occurring 3-6 days after the injury. To confirm that BrdU-positive cells represent newly generated neuroblasts and oligodendrocyte progenitors, we used double staining BrdU/DCX and NG2/BrdU, respectively. We found that administration of SB stimulates the generation of neuroblasts and progenitors of oligodendrocytes, and leads to reduced volume of brain lesion caused by HI insult. We also evaluated if neuroprotective effect was associated with increasing acetylation of histon H3 and with changes in the expression of some proteins which control apoptosis.

Supported by NSC grant 2012/05/B/NZ3/00436.

|B42|

Lesions of noradrenergic neurons with DSP-4 inhibit cell proliferation in the dentate gyrus of the hippocampus but do not damage the progenitor cells in adult mice

Zietek M., Swiergiel A.H.

Department of Animal and Human Physiology, University of Gdansk, Gdansk, Poland

DSP-4 is a highly selective neurotoxin of central and peripheral noradrenergic neurons. DSP-4 strongly inter-

acts with the noradrenaline uptake mechanism at the level of the neuronal membrane and permanent degeneration of noradrenergic terminals, though the precise mechanism of its action has not yet been fully elucidated. Several investigators reported that the neurotoxic effects of DSP-4 are more extensive in the region innervated by axons of the locus coeruleus (LC). Moreover, noradrenergic cells from the LC degenerate in Parkinson's disease. We assessed the number of proliferating cells in the dentate gyrus of the hippocampus of adult mice after damage to the projection from the LC as a result of a single administration of DSP-4.

Male Swiss mice (6-7 weeks) were divided into two groups that were examined 4 and 16 days after the administration of DSP-4. In the first group, the brains were dissected four days after a single injection of DSP-4 (50 mg/kg, 0.1 ml, *i.p.*, $n = 4$) or saline (0.1 ml, $n = 8$) and investigated by immunohistochemistry. Cell proliferation was determined, using 5-bromo-2'-deoxyuridine, which is combined with the newly synthesized DNA. The brains of the second group of animals, sixteen days after the administration of DSP-4 (50 mg/kg, 0.1 ml, *i.p.*, $n = 4$) or saline (0.1 ml, $n = 8$), were also analyzed immunohistochemically. The immunohistochemical studies in group I showed significant differences between the experimental and the control animals. Four days after administration of DSP-4 we observed decreased number of proliferating cells in the experimental groups in all examined section as compared to the control groups. In group II, 16 days after administration of DSP-4 an increased number of proliferating cells was found in all experimental groups compared to controls. Unfortunately, no statistically significant differences were confirmed. The results suggest that the lesion of noradrenergic neurons caused by DSP-4 does not damage the progenitor cells which produce granule neurons in the hippocampus.

|B43|

Neuronal and glial progenitors obtained from human iPS cells on 3D modified collagen scaffolds – the tool for the neurodevelopmental and neurotoxicity studies

Zychowicz M.[1], Pietrucha K.[2], Podobinska M.[1], Augustyniak J.[1], Winiarska H.[1], Buzanska L.[1]

[1]NeuoRepair Department, Mossakowski Medical Research Centre, Polish Academy of Sciences, Warsaw, Poland
[2]Lodz University of Technology, Lodz, Poland

Since the induced pluripotent stem cells (iPSC) can be obtained from the adults, the regenerative medicine can be supported by new tools comprising autologous iPS-derived cells. The neurodegenerative diseases are in the scope of current research based on the iPS cells technology, while biomaterials combined with the iPS derived cells can have a great potential to fulfill the demands of neuroregeneration of CNS.

Here we describe the possibility of neural commitment and differentiation of iPS as well as HUCB-NSC cells seeded onto the chemically modified collagen scaffolds in order to establish and standardize the *in vitro* "biomimetic" culture system.

Shape-sponge scaffolds were prepared from the porcine collagen dispersion using a lyophilization technique. This process produces a highly three-dimensional (3D) porous scaffold. Due to relatively weak mechanical and thermal properties the collagen sponges were cross-linked using carbodiimide. This way is preferable for modification due to that "zero length" cross-linking chemical catalyst non-incorporation within structure of matrix, and scaffolds exhibit no cytotoxicity.

The iPS cells obtained by non integrative, virus free methods were expanded in the feeder free culture and differentiated toward neural linage. The obtained neural stem cells, as well as more differentiated neuronal/glial cell population, were seeded on the collagen modified scaffolds. The RT PCR data have revealed gradual disappearance of pluripotency markers (*Oct4, Sox2, Nanog*) during the differentiation process and acquiring the neural markers, such as *Nestin, Pax6, GFAP, Map-2, Neurogenin.*

The undifferentiated, pluripotent stem cells seeded on the chemically modified, collagen scaffolds revealed limited viability and did not differentiate spontaneously. In contrast iPSC derived neural stem cells and more differentiated neural progenitors survived, adhered in a well-defined flattened manner, and after a few days co-culture on the scaffolds expressed neuronal (Nestin, Beta-Tubulin III,

MAP-2, Doublecortin) and glial (A2B5, NG2, PDGFRa, GFAP) markers.

Moreover, the modified collagen scaffold can serve as a stem cell niche surrogate and can be used for toxicology studies. The HUCB-NSC cells seeded on these scaffolds were more resistant to the methylmercure treatment compare to the two dimensional culture conditions.

Our results indicate that collagen-based 3D microenvironment preferentially support neurally committed cells as compared to induced pluripotent stem cell, and may serve as an in vitro platform for further medical, pharmacological and toxicological applications.

The work is supported by statutory funds to MMRC and National Science Centre via Grant No DEC-2011/03/B/ST8/05867 and EIT+ BioMed 5.4 Project.

|B44|

The role of CXCL1 and CXCL5 in in nociceptive transmission in a mouse model of diabetic neuropathy

Zychowska M., Rojewska E., Pilat D., Mika J.

Department of Pain Pharmacology, Institute of Pharmacology, Polish Academy of Sciences, Cracow, Poland

Diabetic neuropathy is the most common complication of diabetes mellitus, however its mechanism is still poorly understood. It seems that the chemokines may play a key role. It was shown that increased serum levels of CXCL1 and CXCL5 are linked to obesity, hyperglycemia, and impaired islets of Langerhans function. The goal of our study was to examine how the level of two chemokines CXCL1 and CXCL5 varies in the course of diabetic neuropathy and how their administration influences nociceptive transmission. All experiments were performed on Albino Swiss mice. Diabetes type 1 model was obtained by single intraperitoneal injection of streptozotocin (STZ; 200 mg/kg; *i.p.*). To verify the development of hyperglycemia, the blood glucose concentration and body weight were measured. In order to evaluate allodynia and hyperalgesia, von Frey test and cold plate tests, respectively, were used. The changes in mRNA amount and protein level of CXCL1 and CXCL5 in lumbar spinal cord were estimated by qRT-PCR and Antibody Array technic, respectively. The influence of single intrathecal (*i.t.*) administration of CXCL1 and CXCL5 on nociceptive threshold were measured using the tail flick, von Frey and cold plate tests, after 1, 4 and 24 hours. Both chemokines were administrated in doses 10 ng, 100 ng and 500 ng/5 ml. The experiments were carried out according to the Institute's Animal Research Bioethics Committee and in accordance with IASP rules (Zimmermann, 1983). We observed that the STZ injection in mice increased plasma glucose and decreased body weight, along with inducing significant allodynia and hyperalgesia measured seven days after administration. No changes of CXCL1 and CXCL5 mRNA level were observed, in contrast upregulation of both at protein level was detected at day seven after STZ-treatment. The *i.t.* administration of CXCL1 and CXCL5 shown their pronociceptive properties. Furthermore, both contributed to the development of allodynia and hyperalgesia, however after 24 h only mechanical allodynia was still observed. Summing up, these findings indicate that CXCL1 and CXCL5 play an important role in the diabetic neuropathic pain development, which requires further research.

Supported by the NCN-grants 2012/05/N/NZ4/02416, 2011/03/B/NZ4/00042 and statutory funds. Magdalena Zychowska, a Ph.D. student, is a scholarship holder from the KNOW sponsored by Ministry of Science and Higher Education, Republic of Poland.

|B45|

LPS injections in young rats affect reactive gliosis following seizures evoked in adulthood

Kosonowska E., Kielbinski M., Gzielo-Jurek K., Janeczko K., Setkowicz Z.

Department of Neuroanatomy, Institute of Zoology, Jagiellonian University, Cracow, Poland

Aims: An increased activity of the immune system during an ongoing inflammatory process has adverse effects on the nervous system – it disturbs homeostasis of neural tissue and hence causes activation of two types of glial cells (reactive gliosis): astrocytes and microglial cells. Considering recent scientific reports, prior inflammation may change susceptibility to epileptic seizures. However, there is still not enough studies which indicate which cells and processes it can activate. Lipopolysaccharide (LPS) injection results in a massive antimicrobial defense reaction with an acute excessive activation of microglia. Some studies suggested that activated microglia may play a neuroprotective role by facilitating reparatory and regenerative processes. However microglia may also ini-

tiate and exacerbate neuropathological changes through secreting proinflammatory and cytotoxic molecules. Astrocytes may contribute to brain damage in a similar way but they also produce neuroprotective molecules and exert its neuroprotective actions on the neighbouring neurons. This issues could be important in case of studying the effects of systemic inflammation on seizure susceptibility. The aim of this study was to examine the long term effect of systemic inflammation induced on different postnatal developmental stages on activation of glial cells (astrocytes and microglial cells) in different experimental groups (with or without induction of status epilepticus).

Methods: LPS solution was injected intraperitoneally (2 mg/kg b.w.) to Wistar rats on postnatal day 6 or 30. When became two-month-old, the rats which survived inflammation were injected with pilocarpine to evoke status epilepticus and sacrificed 3 days thereafter. Brain sections were then processed for GFAP and Iba-1 immunohistochemistry to evaluate the area of reactive gliosis in the hippocampus using ImageJ software (*Area Fraction measurement*).

Results & Conclusions: Unexpectedly, the obtained results showed that status epilepticus induced in the adult rats evoked statistically significant reductions of Iba-1- and GFAP-immunopositive areas within the hippocampal formation. However, peritoneal LPS injections performed on the postnatal day 6 could prevent such seizure-induced decreases both in Iba-1 and GPAP tissue immunoreactivity. Following LPS injections on the postnatal day 30 significant decreases were limited to GFAP immunoreactivity only. The detected changes appear to reflect modification in reactive morphological transformation of their cellular substrates, i.e. astroglia and microglia involved in formation of seizure-genic gliosis in the hippocampal formation. Therefore, further detailed investigations are needed to elucidate relations between the reactive phenomena and effects of LPS proinflammatory stimulation at early stages of postnatal development on glial responses to seizures evoked in adulthood.

Supported by NCS GRANT: UMO-2012/05/B/NZ4/02406.

|B46|

The high cervical spinal cord injury and unilateral phrenic nerve ligation strongly reduce sGC/cGMP signaling in lower respiratory pathway followed by the failure of EMG activity in diaphragm

Lukacova N.[1], Hricova L.[1], Gedrova S.[1] , Galik J.[1], Pavel J.[1], Sulla I.[1], Stropkovska A.[1], Zavodska M.[1], Oroszova Z.[1], Chalimoniuk M.[2], Langfort J.[2]

[1]Institute of Neurobiology, Slovak Academy of Sciences, Kosice, Slovakia
[2]Mossakowski Medical Research Centre, Polish Academy of Sciences, Warsaw, Poland

The high cervical spinal cord injury leads very often to the interruption of descending bulbospinal respiratory pathway, one of the vital pathways in CNS, which begins in brainstem, innervates phrenic motor neurons located at the C3-C6 cervical level and controls the diaphragm. Such injury leads to breathing rhythm abnormalities and life-threatening weakness of respiratory function. We previously demonstrated NO/soluble guanylyl cyclase (sGC) signalization in upper bulbospinal respiratory pathway. This study is focused on sGC/cGMP signalization in lower respiratory pathway after i) unilateral SCI performed at C2-C3 level, and ii) unilateral phrenic nerve ligation. The phrenic motoneurons within the phrenic nucleus in cervical spinal cord have been identified with retrograde tracer Fluorogold (FG). Two days after FG injection into hemidiaphragm, the ipsilateral phrenic motoneuronal pool was labeled within C3-C5 segments, with the greatest density found at C4 level. The increased intensity of sGCβ1staining was detected 8 days after phrenic nerve ligation in phrenic motoneurons (C3-C5 segments) on the side of the injury. In addition, the phrenic nerve ligation strongly reduced the level of sGCβ1 in efferent respiratory pathway (diaphragmatic nerve) just below the nerve ligation, what correlates with the alterations of cGMP level in diaphragm. Although we found strong reduction of the cGMP level in both the contra- and ipsilateral hemidiaphragm, the decrease was much stronger on the side of the ligation. The unilateral interruption of the high cervical spinal cord had less impact on the cGMP synthesis in the diaphragm (mostly on contralateral side). It seems that the phrenic nerve activity was after cervical hemisection limited, but not so dramatically than after the phrenic nerve ligation. We assume that pre-phrenic interneurons located between the brainstem and the spinal cord may amplify the phrenic output after high cervical hemisection on contralateral

side. Moreover, the results clearly show remarkable unilateral silencing of the EMG activity after the phrenic nerve ligation and/or C2-C3 hemisection.

Supported by VEGA Grants No. 2/0173/14, 2/0191/13, 2/0187/13 and CE-NOREG SAS.

Editorial note:
The abstracts are printed in the form accepted by the Scientific Programme Committee of the Symposium.

Instructions to Authors

This instruction is based upon *Uniform Requirements for Manuscripts Submitted to Biomedical Reviews* (the complete document appears in N Engl J Med 1997; 336, 309-315).

Aims and scope

Folia Neuropathologica is an official journal of the Mossakowski Medical Research Centre Polish Academy of Sciences and the Polish Association of Neuropathologists. The journal publishes original articles and reviews that deal with all aspects of clinical and experimental neuropathology and related fields of neuroscience research. The scope of journal includes surgical and experimental pathomorphology, ultrastructure, immunohistochemistry, biochemistry and molecular biology of the nervous tissue. Papers on surgical neuropathology and neuroimaging are also welcome. The reports in other fields relevant to the understanding of human neuropathology might be considered.

Ethical consideration

Papers describing animal experiments can be accepted for publication only if the experiment conforms to the legal requirements in Poland as well as with the European Communities Council Directive of November 24, 1986 or the National Institute of Health Guide (National Institute of Health Publications No. 80-23, Revised 1978) for the care and use of Laboratory Animals for experimental procedure. Authors must provide a full description of their anesthetics and surgical procedures. Papers describing experiments on human subjects must include a statement that experiments were performed with the understanding and consent of each subject, with the approval of the appropriate local ethics committee.

Submission of manuscripts

Articles should be written in English. All new manuscripts should be submitted through the online submission at http://panel2.termedia.pl/fn
For authors unable to submit their manuscript online, please contact with Prof. E. Matyja, Editor-in-Chief of *Folia Neuropathologica*, ematyja@imdik.pan.pl
The Editorial Board reserves the right to reject a paper without reviewers' opinion if the content or the form of the paper does not meet minimum acceptance criteria or if the subject of the paper is beyond the aims and scope of the journal.

Legal aspects

In sending the manuscript the author(s) confirm(s) that (s)he has (they have) not previously submitted it to another journal (except for abstracts of no more than 400 words) or published it elsewhere. The author(s) also agree(s), if and when the manuscript is accepted for publication, to automatic and free transfer of copyright to the Publisher allowing for the publication and distribution of the material submitted in all available forms and fields of exploitation. The author(s) accept(s) that the manuscript will not be published elsewhere in any language without the written consent of the copyright holder, i.e. the Publisher.
All manuscripts submitted should be accompanied by an authors' statement including signed confirmation of the above and confirming that this publication has been approved by all co-authors (if any), as well as by the responsible authorities at the institution where the work has been carried out. The authors' statement should be signed by ALL co-authors. Additionally, the author(s) confirm(s) that (s)he is (they are) familiar with and will observe the "Instruction to Authors" included in *Folia Neuropathologica* and also that all sources of financial support have been fully disclosed. Materials previously published should be accompanied by written consent for reprinting from the relevant Publishers. In the case of photographs of identifiable persons, their written consent should also be provided. Any potential conflict of interest will be dealt with by the local court specific to the Publisher. Legal relations between the Publisher and the author(s) are in accordance with Polish law and with international conventions binding on Poland.
Authors agree to waive their royalties.

Anonymous review

All manuscripts will be subject to a process of anonymous editorial review.

Preparation of manuscripts

Articles must be written in English, with British spelling used consistently throughout. Authors not entirely familiar with English are advised to correct the style by professional language editors or native English speakers.

- The length of original article should not exceed 20 printed pages including text, illustrations, tables, and references.
- Manuscripts should be typed using 12pts.font, double-spaced, and fully corrected. Allow a margin at least 2.5 cm at the top, bottom and left side of the page. Text should not be justified.

- The title page should contain: the author's full names, title of the paper, all authors' affiliations, full name and address of the communicating author (including e-mail address and fax number), running title (not exceed 40 characters including spaces).
- The abstract should not exceed 350 words. A list of 3–10 key words is recommended below the abstract.
- The manuscript body should be organized in a standard form with separate sections: Introduction, Material and Methods, Results, Discussion, and References. Review articles should be divided into sections and subsections as appropriate without numbering.
- Do not underline in the text. Avoid footnotes.
- All dimensions and measurements must be specified in the metric system.
- The source of any drug and special reagent should be identified.
- Particular attention needs to be paid to the selection of appropriate analysis of data and the results of statistical test should be incorporated in the results section.
- The nomenclature used should conform to the current edition of the Nomina Anatomica or Nomina Anatomica Veterinaria.
- Acknowledgements should be made in a separate sheet following Discussion and before References. These should contain a list of dedications, acknowledgements, and funding sources.
- Legends of figures and tables should be typed on separate pages.
- The editor reserves the right to make corrections.

Tables

- Tables numbered in Roman numerals require a brief but descriptive heading.
- The major divisions of the table should be indicated by horizontal rules.
- Explanatory matter should be included in footnotes, indicated in the body of the table in order of their appearance.
- Tables must not duplicate material in the text or in illustration.

Illustrations

All figures should be supplied electronically at resolution 300dpi in all standard formats (tiff, jpg, Adobe Photoshop, Corel Draw, and EPS). Name your figure files with "Fig" and the figure number, e.g., Fig1.tif

- The maximum figure size is 84 mm or 174 mm for use in a single or double column width, respectively.
- When possible, group several illustrations on one block for reproduction. Like all other figures, block should be prepared within a rectangular frame to fit within a single or double column width of 84 and 174 mm, respectively, and a maximum page height of 226 mm.
- Each figure should include scale magnification bar; do not use magnification factors in the figure legends.
- All figures, whether photographs, graphs or diagrams, should be numbered using Arabic numerals and cited in the text in consecutive numerical order
- **Immunohistochemical study requires color illustrations of very good quality. The papers with white and black immunohistochemistry will not be accepted.**
- **The expense of color illustrations must be borne by the authors.** The cost of color print for every successive 8 pages is 200 euro irrespective of the number of color pages, i.e., the price remains the same whether there is one or eight pages.

The Publisher makes out the bill to the communicating Author.

References

The list of references (written on a separate page) should include only those publications that are cited in the text. Avoid citation of academic books, manuals and atlases. References may be arranged alphabetically and numbered consecutively. References should be given in square brackets with no space between the comma and the consecutive number, e.g. [3,4,6-12].

References should be written as follows:

Journal papers: initials and names of all authors, full title of paper, journal abbreviation (according to Index Medicus), year of publication, volume (in Arabic numerals), first and last page (example below):

1. Valverde F. The organization of area 18 in the monkey. Anat Embryol 1978; 154: 305-334.
2. Uray NJ, Gona AG. Calbindin immunoreactivity in the auricular lobe and interauricular granular band of the cerebellum in bullfrogs. Brain Behav Evol 1999; 53: 10-19.

Book and monographs: initials and names of all authors, full title, edition, publisher, place, year (examples below):

1. Pollack RS. Tumor surgery of the head and neck. Karger, Basel 1975.
2. Amaral DG, Price JL, Pitkanen A, Carmichael ST. Anatomical organization of the primate amygdaloid complex. In: Aggleton JP (ed.). The amygdala. Wiley-Liss, New York 1992; pp. 1-66.

Reference to articles that are accepted for publication may be cited as „in press" or Epub.

Proofs

Corrections to the proofs should be restricted to printer's errors only; other alterations will be charged to the authors. In order to maintain rapid publication, proofs should be returned within 48 hours, preferably by e-mail, fax or courier mail. If the Publisher receives no response from the authors after 10 days, it will be assumed that there are no errors to correct and the article will be published.

Subscription information

The journal is published in one volume per year consisting of four numbers. The annual subscription price is 160 PLN for Institutions from Poland and 80 PLN for individual subscribers from Poland and 140 Euro for foreign Institutions and 70 Euro for foreign individual subscribers.
Payment should be made to:
Termedia sp. z o.o., ul. Kleeberga 8, 61-615 Poznań
BZ WBK III O/Poznań PL 61 1090 1359 0000 0000 3505 2645
SWIFT: WBKPPLPP

The publisher must be notified of a cancellation of a subscription not later than two months before the end of the calendar year. After that date the subscription is automatically prolonged for another year.
Publishing, Subscription and Advertising Office:
TERMEDIA Publishing House
ul. Kleeberga 2
61-615 Poznań, Poland
phone/fax +48 61 822 77 81
e-mail: termedia@termedia.pl
http://www.folianeuro.termedia.pl

Folia Neuropathologica

AUTHOR'S STATEMENT

Title of the article

.....

.....

.....

The author(s) hereby confirm(s) that:

☐ The above-mentioned work has not previously been published and that it has not been submitted to the Publishers of any other journal (with the exception of abstracts not exceeding 400 words).

☐ All co-authors named and the relevant authorities of the scientific institutions at which the work has been carried out are familiar with the contents of this work and have agreed to its publication.

☐ In sending the manuscript together with illustrations and tables agree(s) to automatic and free transfer of copyright to the Publisher allowing for the publication and distribution of the material submitted in all available forms and fields of exploitation, without limits of territory or language, provided that the material is accepted for publication. At the same time the author(s) accept(s) that the submitted work will not be published elsewhere and in whatever language without the earlier written permission of the copyright holder, i.e. the Publisher.

☐ (S)he (they) agree to waive his(her)(their) royalties (fees).

☐ (S)he (they) empower(s) the Publisher to make any necessary editorial changes to the submitted manuscript.

☐ All sources of funding of the work have been fully disclosed.

☐ The manuscript has been prepared in accordance with the Publisher's requirements.

☐ (S)he (they) is (are) familiar with the regulations governing the acceptance of works as published in *Folia Neuropathologica* and agree(s) to follow them.

☐ (S)he (they) agree to accept appropriate invoice from the Publisher in case colour illustrations are implemented.

Date *Signatures of **all authors***

The covering letter formula can be found at: www.folianeuro.termedia.pl
-The covering letter should be sent to Associate Editor:

Milena Laure-Kamionowska
-Editorial Office of Folia Neuropathologica
Mossakowski Medical Research Centre, Polish Academy of Sciences
Poland Medical Research Centre
ul. Pawinskiego 5
02-106 Warszawa, Poland

CONTENTS